REPORT NO.
UCB/EERC-81/07
JUNE 1981

EARTHQUAKE ENGINEERING RESEARCH CENTER

THE SEISMIC RESISTANT DESIGN OF R/C COUPLED STRUCTURAL WALLS

by

A.E. AKTAN
V.V. BERTERO

Report to the National Science Foundation

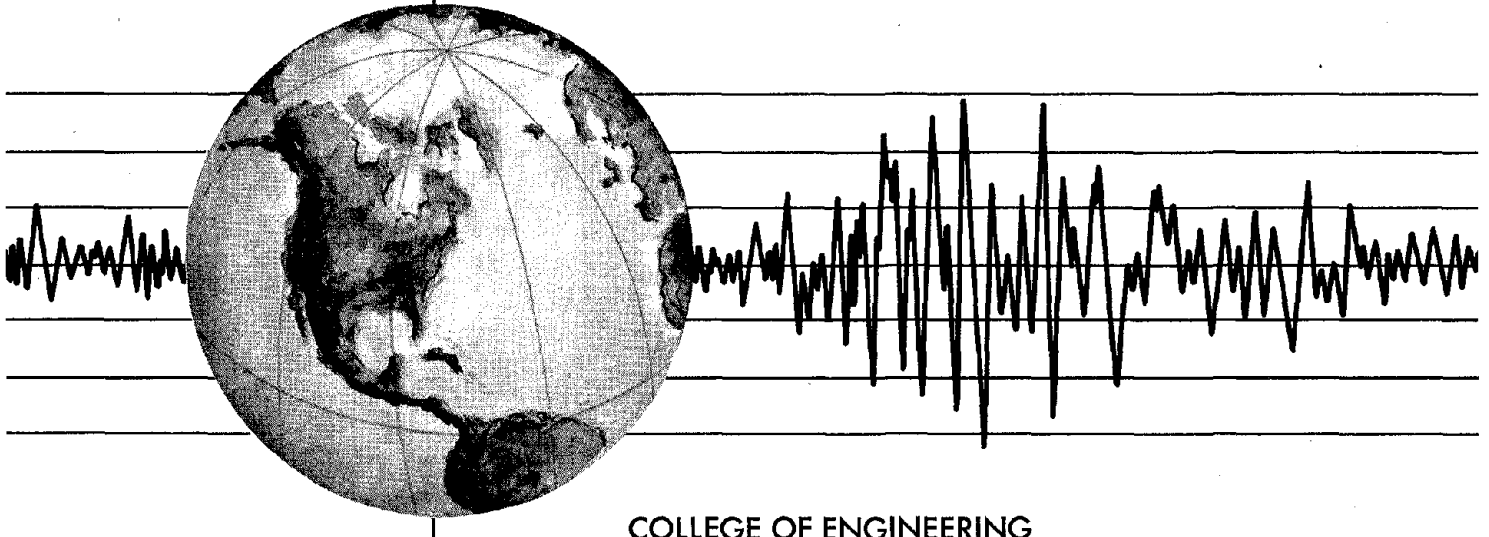

COLLEGE OF ENGINEERING

UNIVERSITY OF CALIFORNIA · Berkeley, California

For sale by the National Technical Information Service, U.S. Department of Commerce, Springfield, Virginia 22161.

See back of report for up to date listing of EERC reports.

DISCLAIMER

50272-101

REPORT DOCUMENTATION PAGE	1. REPORT NO. NSF/CEE-81040	2.	3. Recipient's Accession No. PB82 113358

4. Title and Subtitle
The Seismic Resistant Design of R/C Coupled Structural Walls

5. Report Date
June 1981

6. U281004

7. Author(s)
A. E. Aktan and V. V. Bertero

8. Performing Organization Rept. No.
UCB/EERC-81/07

9. Performing Organization Name and Address
Earthquake Engineering Research Center
University of California, Berkeley
Richmond Field Station
47th Street and Hoffman Boulevard
Richmond, Calif. 94804

10. Project/Task/Work Unit No.

11. Contract(C) or Grant(G) No.
(C)
(G) PFR-790894

12. Sponsoring Organization Name and Address
National Science Foundation
1800 G Street, N.W.
Washington, D.C. 20550

13. Type of Report & Period Covered

14.

15. Supplementary Notes

16. Abstract (Limit: 200 words)

This is the first in a series of progress reports which summarize the recent developments and findings of ongoing research on "The Seismic Resistant Design of R/C Coupled Structural Walls" at the University of California, Berkeley.

Integrated analytical and experimental research on the seismic response of R/C structura wall-frame structures has been conducted at U.C. Berkeley for the past decade. Recently considerable efforts have been devoted to the study of the seismic behavior of coupled structural walls and their behavior in wall-frame structural systems. This report documents the progress of that study.

A survey of existing analytical and experimental work regarding the seismic response of R/C wall and coupled wall-frame systems, as well as relevant documented post-earthquake studies on these systems, are presented in the first part of this report. As assessment of the states of the art and practice regarding the design of building structures incorporating these systems is included.

Studies and design and fabrication of the required testing facility necessary for conducting the experimental investigation of seismic behavior of a 1/3-scale model of a 4 1/2-story coupled wall subassemblage belonging to a 15-story prototype structure, are described in the main portion of this report. Analytical studies of the seismic responses of the prototype buildings are summarized briefly.

17. Document Analysis a. Descriptors

b. Identifiers/Open-Ended Terms

c. COSATI Field/Group

18. Availability Statement	19. Security Class (This Report)	21. No. of Pages
Release Unlimited		240
	20. Security Class (This Page)	22. Price

(See ANSI-Z39.18) See Instructions on Reverse

OPTIONAL FORM 272 (4-77)
(Formerly NTIS-35)
Department of Commerce

THE SEISMIC RESISTANT DESIGN

OF R/C COUPLED STRUCTURAL WALLS

by

A. E. Aktan
Associate Research Engineer
Department of Civil Engineering
University of California, Berkeley

V. V. Bertero
Professor of Civil Engineering
University of California, Berkeley

Report to Sponsor:
National Science Foundation

Report No. UCB/EERC-81/07
Earthquake Engineering Research Center
College of Engineering
University of California
Berkeley, California

June 1981

ABSTRACT

This is the first in a series of progress reports which summarize the recent developments and findings of ongoing research on "The Seismic Resistant Design of R/C Coupled Structural Walls" at the University of California, Berkeley.

Integrated analytical and experimental research on the seismic response of R/C structural wall-frame structures has been conducted at U.C. Berkeley for the past decade. Recently considerable efforts have been devoted to the study of the seismic behavior of coupled structural walls and their behavior in wall-frame structural systems. This report documents the progress of that study.

A survey of existing analytical and experimental work regarding the seismic response of R/C wall and coupled wall-frame systems, as well as relevant documented post-earthquake studies on these systems, are presented in the first part of this progress report. An assessment of the states of the art and practice regarding the design of building structures incorporating these systems is included.

Studies and design and fabrication of the required testing facility necessary for conducting the experimental investigation of seismic behavior of a 1/3-scale model of a 4 1/2-story coupled wall subassemblage belonging to a 15-story prototype structure, are described in the main portion of this progress report. Analytical studies of the seismic responses of the prototype buildings are summarized only briefly as these studies are being published in a separate EERC report.

A second progress report will follow documenting the results

obtained in the first series of experiments conducted on a 1/3-scale model subassemblage. The progress achieved in the analytical studies of this integrated analytical and experimental research of seismic response of R/C wall-frame systems will also be presented.

ACKNOWLEDGEMENTS

The studies reported herein on the seismic resistant design of R/C coupled structural walls were conducted as part of the work supported by the National Science Foundation, currently under Grant No. PFR-790894. This grant supports a research program on "Seismic Behavior of Structural Components," of which a subproject, No. 0-22002, is devoted to studies of R/C wall-frame structural systems. Any opinions, discussions, findings, conclusions and recommendations are those of the authors and do not necessarily reflect the views of the National Science Foundation.

The authors are indebted to Development Engineers B. Lotz and D. Clyde, and to Development Technician W. MacCracken, as well as other members of the SESM and EERC Laboratory technical staff who contributed their efforts to many phases of the research described herein.

The participation of research assistants M. Habib, M. Piazza, and A. Ozselcuk on various phases of the research is acknowledged. Analytical studies were carried out using the computer facilities of both the Lawrence Berkeley Laboratory and the Department of Computer Sciences of the Berkeley campus. The experimental work is being conducted at the Structures Laboratory at the Richmond Field Station, as well as the Structures Laboratory at Davis Hall, Berkeley. Finally the writers gratefully acknowledge the assistance of S. Gardner in editing this report, T. Avery for typing, and D. Ullman and R. Steele for preparing the illustrations.

TABLE OF CONTENTS

LIST OF TABLES

LIST OF FIGURES

SEISMIC RESISTANT DESIGN OF R/C COUPLED STRUCTURAL WALLS

1. Introduction

1.1 General

Current earthquake-resistant design philosophy requires that the structure be able to resist minor ground shaking without damage and to resist moderate ground shaking with no structural damage but with some allowable minor nonstructural damage. The design philosophy acknowledges that structural damage will be caused by strong ground shaking, but the damage should not be to the extent that lives are endangered [1.30]. In accordance with this philosophy, the demands on the structure which correspond to different ground shaking levels have to be assessed in terms of force, distortion, and energy dissipation demands upon individual elements of the structure. It is also necessary to assess if the supplies provided by the structural members are sufficient to meet such demands.

The present design philosophy focus is on damage control, as opposed to the earthquake-resistant design concept of previous decades characterized by an emphasis on ductility. Research advances in earthquake engineering [1.10, 1.24] have enabled the profession to seek more comprehensive solutions to earthquake-resistant design problems than just ductility. Consequently, the structural systems of medium-high-to-tall buildings now frequently incorporate reinforced concrete structural walls. It has been observed in past earthquakes that structural walls, when properly detailed and constructed, provide buildings with excellent damage control.

One particular structural wall system which shows great potential for efficient seismic-resistant design as demanded by current design philosophy, is the coupled structural wall. Two or more structural walls, coupled by connecting beam and slab systems, possess significantly higher stiffness than if they were not coupled. This stiffness furnishes an improved damage control property.

The redundancy and potential energy dissipation capacity which can be provided by properly designing the coupling girders may be used to advantage to "tune" the system to provide a natural strong column-weak beam type of response. This type of response is especially desired because each coupling girder can provide two sources (plastic hinges) of energy dissipation, thus a large amount of energy dissipation can be achieved without the accompanying large drift problems. In many DMRSF systems, a strong column-weak beam design inadvertantly responds as a soft-story system when nonstructural elements constrain energy dissipation to a few floors.

Coupled-structural walls are not as affected by nonstructural elements, an inherent advantage over the DMRSF system. It has been demonstrated that it is possible to design and construct coupling girders with significant deformation and energy dissipation capacity. Similarly, isolated walls have been shown to possess favorable inelastic response characteristics, provided that the phenomenon of "web-crushing," (a form of sudden shear-compression failure of the wall panel) sliding shear, and instability can be postponed until sufficient inelastic distortion can take place. Even after web crushing, barbell shaped walls with effectively confined edge members were

observed to be capable of offering considerable lateral resistance and energy dissipation capacity working as a "soft story" system.

The state of the art in R/C structural wall-frame building design governing seismic effects has advanced considerably as a result of intensive research carried out by major institutions in the U.S. and throughout the world. Although a significant amount of data is available on the response of individual components of coupled wall systems, information on the overall system response of coupled wall-frame structures is inadequate to formulate proper guidelines on seismic-resistant design of these structures. Therefore, research should continue to be conducted on structural systems incorporating structural walls, particularly coupled walls.

The state of the practice as represented by current code has yet to recognize the data generated on the response of wall-frame and coupled-wall-frame systems during the last decade, and to incorporate such findings in its provisions. Although there have been efforts toward this, existing U.S. code provisions for the design of tall reinforced concrete structural wall-frame systems (coupled or isolated), incorporate some provisions of questionable soundness, as well as inconsistencies and shortcomings. These questionable provisions may result in frame-coupled wall system design with undesirable ultimate-limit-state response characteristics.

Research on the seismic response of isolated and coupled wall-frame structures has been underway in Berkeley for the past decade. Information on major findings on the response of isolated wall-frame structures and individual components of these systems has been reported in the course of ongoing research [1.17, 1.43, 1.44].

This report's basic objective is to summarize developments and major findings of work in progress at this institution on integrated analytical and experimental research of coupled wall-frame structures. As a consequence of the emphasis given recently to this research, particularly the experimental phase, this report will be augmented as new information on the behavior of these structures is generated. The research will be presented in two main chapters. Chapter 1 provides adetailed survey of previous experimental work on isolated and coupled wall-frame systems and the individual components of these systems, including post-earthquake observations. Also included is a brief survey of recent relevant analytical work that was carried out on these structures. Chapter 1 is concluded by an investigation of the state of the art and code in the design of tall R/C wall/coupled wall-frame systems, and specific information on the objectives and scope of ongoing research in Berkeley on the response of these structures.

Chapter 2 lists preliminary analytical and experimental work conducted at Berkeley during past years in order to lay the foundation for a long-range research program aimed at better understanding of the seismic behavior of medium-high-to-tall R/C structural coupled wall-frame structural systems.

1.2 Review of Past Research on Reinforced Concrete Shear Walls

1.2.1 Post-Earthquake Investigations

1.2.1.1 General

Post-earthquake investigations have been a major source of information on earthquake engineering for structural engineers. Research on earthquake-resistant structures has been carried out parallel to post-earthquake studies since the 1940s. Knowledge acquired from the study

of moderate to destructive earthquakes, especially during the past three decades, has contributed significantly to advances in the understanding of structural response under ground excitation, and consequently to the improvement of seismic code provisions.

The relatively well-documented earthquakes of Chile (1960), Agadir, Morocco (1960), Skopje, Yugoslavia (1963), Niigata, Japan (1964), Anchorage, Alaska (1964), Caracas, Venezuela (1967), Tokachi Oki, Japan (1968), San Fernando, California (1971), Managua, Nicaragua (1972), Oita, Japan (1971), Guatemala City, Guatemala (1976), and Sendai, Japan (1978) have been instrumental in improving existing code provisions as well as formulating new ones regarding structural systems, effect of soil conditions, lateral force coefficients and distribution, member design and detailing, and control of damage by limiting interstory drift.

A review of post-earthquake investigations on the behavior of moderately tall- to tall-reinforced concrete structures incorporating shear walls is presented in the following section.

1.2.1.2 The 1963 Skopje, Yugoslavia, Earthquake [1.3, 1.35]

A number of medium-height reinforced concrete structures were extensively damaged or collapsed in the Skopje earthquake. Of these, the ten-story Quay Towers, the fourteen-story Trade Union Building, and the fourteen-story Karpos Tower were relevant structures incorporating unreinforced concrete bearing walls. Some of the walls in the lower stories of the Trade Union Building were reinforced. This was the only structure reported to have insignificant structural damage after the earthquake. Strong motion records were not obtained and, to the best of the writers' knowledge, there were no subsequent analytical evaluations

of the damage reported in the literature.

1.2.1.3 The 1964 Anchorage, Alaska, Earthquake [1.3, 1.46]

A significant number of relevant structures built during 1950-1960 were extensively damaged during the earthquake. The eight-story Hill Building, with two reinforced concrete central core units connected by beams and a steel frame, survived with relatively less extensive damage. The stiffer core unit had damage at the foundation level and a local shear failure between the first and second floors along a weak plane caused by irregular openings. Beams connecting the core units were damaged on the second and third floors. Upper story beams and core had less damage. The failure was attributed to a layer of sub-standard concrete at the foundation level of the stiffer core unit.

The Mt. McKinley and 1200L Apartment Buildings were almost identical as to construction, orientation, and damage. They were both 14-story structures with central core units and pierced facade shear walls along their peripheries. The only difference between these structures was in the first story of one of the facade walls. The damage patterns of these structures were remarkably consistent.

Significant damage was observed on the facade walls pierced by a large number of regular openings. The connecting beams, most of which had a depth-to-length ratio larger than one, had diagonal shear failure up to the twelfth floor. On the narrower sides, both structures had two stiff walls on each side of a flexible wall, all connected by deep beams. One of the stiffer walls had a complete fracture at the third-story level, while no visible damage was observed on the other wall.

The connecting beams were observed to be most severely damaged on the fifth-floor level, with damage becoming progressively less in both directions.

The Mt. McKinley Building was subjected to forced vibration tests and subsequent analytical evaluations after the earthquake. The distribution of coupling beam damage along the height of the structure was in accordance with the relative magnitudes of the computed forces. The wall fractures in both structures were attributed to the existence of improper construction joints in the fractured locations and to the small amount of horizontal and vertical reinforcement.

The Penney Building was a five-story structure, nearly square on plan, with predominant lateral stiffness along one side only. Built in 1962, it collapsed partially and was demolished after the earthquake. Torsional effects were computed to cause highest unit stress on the second story as the shear walls varied in amount and distribution along the height of the structure. Correspondingly, wall failure occurred at the second-floor level.

The six-story Four Seasons Apartment House collapse was perhaps the most spectacular failure involving shear walls. The structure had two interior cores and peripheral steel columns. Post-tensioned prestressed lift slabs were used. The basic cause of the collapse of this building was the failure of the two cores which were attributed to the poor splicing of the main bars at the first-story level.

1.2.1.4 The 1967 Caracas, Venezuela, Earthquake[1.3, 1.34, 1.14]

There were four cases of complete collapse of medium-height structures in the Caracas earthquake, these were the twelve-story

Mijagual Apartment Building, the twelve-story Neveri Apartment Building, the ten-story Palace Corvin Building, and the ten-story San Jose Building. The Palace Corvin had a reinforced concrete core which accounted for less than 15 percent of the lateral stiffness. The frames, however, were not connected to this core. The other three structures that collapsed did not incorporate reinforced concrete shear walls.

Of a significant number of structures which were extensively damaged, several with central reinforced concrete core units were observed. The ten-story H-shaped apartment building, Amalfi, had a central core unit on the side of which a vertical crack through the height of the structure appeared after the earthquake. The columns at the corners of the structure were observed to be damaged. The building was repaired after the nonstructural partitions of the first four stories, which were badly damaged, were removed.

The Atlantic Oil Building, an eight-story structure with a reinforced concrete central core unit, which was terminated at the fifth floor to be continued by tile walls, had extensive damage at this floor. The twelve-story Plaza I, consisting of two separate towers with reinforced concrete shear walls in both directions, had no structural or nonstructural damage. The Bahia del Mar, a twelve-story building with a tall first story, incorporated a rigid central reinforced concrete core unit which was terminated at the fifth floor. Damage was significant at the vicinity of this floor.

1.2.1.5 The 1971 San Fernando, California, Earthquake [1.19, 1.23]

A significant number of strong-motion records were obtained for this earthquake, enabling a realistic appraisal of the induced forces. A number of the damaged structures incorporated reinforced concrete

shear walls. Several tall structures with shear walls had no damage despite significant recorded acceleration magnitudes. Of the few collapses that occurred, the Olive View Hospital had shear walls, but these were terminated before the ground floor where failure took place.

The Indian Hills Medical Center was a seven-story structure with a reinforced concrete frame. It was rectangular in plan, with a projection at one of the longer faces, and four shear walls were used in each direction of the building for lateral strength. Floor slabs were made of lightweight aggregate, while the other members were made using normal weight aggregate. The walls had edge members. Beams ran along the narrow direction only. There were no accelerometers in the immediate vicinity of the building. Base accelerations on the order of 0.4 g were estimated. Some of the shear walls were damaged by cracks along the horizontal construction joints at floorlines. This was attributed to the intrusion of lesser strength floor concrete into the joint during construction. In addition to the diagonal wall cracking at the first floor, the edge member was separated from the wall at the base of this floor. More damage involving the slabs and the frame members was also observed. Repairs amounted to 9 percent of the original cost of the building.

The Holy Cross Hospital, another seven-story structure located next to the Indian Hills Medical Center, had a complex lateral load resisting system. The shape of the plan of the structure was a cross. Shear walls, some terminated below the second floor, in conjunction with four core units distributed within the building, were relied on for seismic resistance. Different qualities of concrete were used for the walls, the slabs, and joists. Because of poor construction

technique, the vertical elements had a layer of concrete of lesser strength along the heights of the floor systems.

The Holy Cross Hospital had more extensive damage than the Indian Hills Medical Center; rehabilitation costs were estimated to be 48 percent of the value prior to the earthquake. The damage consisted of severe diaphragm cracking at the discontinuities of the shear walls along the height of the building as well as several modes of wall failure. The wall-floor joints exhibited damage where the lesser strength floor concrete had intruded into the wall concrete. Most of the walls had serious damage over the doors which perforated the walls. The walls were not provided with sufficient shear reinforcement above these door openings. These regions were also penetrated by ducts. Walls below the fourth-floor level had extensive X-cracking, with reinforcing steel exposed at numerous locations. The structure columns exhibited a number of failures related to significant lateral drifts, this despite the walls and core units.

The Museum for Antique Cars, a five-story reinforced concrete building, was under construction when the earthquake occurred. The building had solid facade walls all around a rectangular perimeter. The floor system consists of 8 in. two-way reinforced concrete slabs supported on beams, which in turn, are supported on columns. In the exterior walls the beams and columns are cast integrally with the walls. While the walls and columns are cast of normal-weight concrete, the slabs and beams, even those cast integrally with the walls, are cast of lightweight concrete. This resulted in weak construction joints on the wall at the floor levels, particularly at the first-story level, where significant damage was observed after the earthquake. The wall

fractured around the building along the first-floor level, i.e., at the beam-wall joints. These joints were later repaired by developing keys across the joints.

The Antique Car Museum, Olive View Hospital, Indian Hills Medical Center, and Holy Cross Hospital were four of the relevant structures incorporating shear walls which were structurally damaged. These structures were all subjected to severe ground motion, and damages to the walls resulted from inadequate conceptual design and possibly poor construction. A large number of high-rise buildings, most of which were instrumented, were subjected to ground accelerations of smaller magnitude; a number of these were subsequently analytically studied.

Of the structures studied, the Certified Life Building, built according to the 1964 Los Angeles City Code provisions, was a fourteen-story reinforced concrete shear wall building with shear walls running in one direction of the building and a central core unit continuous throughout the height of the structure. This was the only structure with continuous shear walls investigated in the major Los Angeles area subsequent to the earthquake. The three strong-motion accelerographs at the ground-floor level, sixth-floor level and roof, recorded maximum accelerations of .26 g, 0.39 g and .395 g along the transverse direction of the building. There was no observed structural damage, and the nonstructural damage was minor enough to be repaired as part of the normal building maintenance. Studies of other buildings with different structural systems subjected to similar excitation in the Los Angeles area, revealed many cases of extensive nonstructural damage.

An important aspect of this last structure was that the core consisted of two basic U-units coupled by girders with a depth/length ratio of approximately 0.5. No girder failure or serviceability problem was noticed, despite dynamic story shears and overturning moments of roughly twice the code values estimated to have occurred (from analysis of the recorded acceleration histories).

1.2.1.6 The 1972 Managua, Nicaragua, Earthquake[1.16, 1.47]

A single strong-motion record was obtained in this earthquake. Studies indicated the stronger horizontal component to contain at least as much damage potential as the N-S component of the 1940 El Centro record, with a maximum acceleration of 0.38 g. The ground acceleration magnitudes in the downtown area where the investigated modern medium-tall to tall buildings were situated, were estimated, through analyses of seismoscope records, to be higher than those recorded by the strong-motion accelerograph.

Detailed damage appraisals and analytical studies were carried out on a number of relevant buildings, some with reinforced concrete shear walls. It was observed that none of the shear wall structures had more than moderate damage, while many moment-resisting frame structures exhibited severe damage, and some collapsed.

The Edificio Administrativo ENALUF Building, with basement, ground floor, and six additional floors of smaller plan dimensions, had two central reinforced concrete core units and a frame for lateral resistance. The building is rectangular in plan, with typical floor construction consisting of precast, pretensioned joists, and a lightweight reinforced concrete slab. The vertical elements were cast in place, the cores being internally framed by cast-in-place slab and beam construction.

The building was designed with the ACI 318-63 and SEAOC 1966 codes. The main damage, in the form of crushing, occurred locally at one corner of one of the cores at the foundation level, where the concrete section was weakened by large indentations on both sides of the core made for telephone ducts, metal boxes and piping. The girders connecting the two core units hinged at the ends with concrete spalling at the connections. Some diaphragm cracking was observed throughout the building as well as some diagonal cracking on the cores. The overall performance of the structure was concluded to be satisfactory with only minor cosmetic damage. Subsequent period measurements were carried out. Comparing theoretical virgin, and measured post-damage periods, drifts exceeding twice the elastic limit were estimated. The structure and the whole building were easily and economically rehabilitated.

The Teatro Nacional Ruben Dario was completed in 1969 with steel facade columns and a reinforced concrete shear wall frame system at the interior. The shear walls at the stage area were the equivalent of a twelve-story tall building (40 m). Although subsequent analysis and vibration studies indicated drifts exceeding the elastic limit, only minor cosmetic damage was observed. The mass associated with this structure was insignificant, as there were no intermediate slabs and the roof consisted of a steel truss system.

The Banco de America Building had one of the most favorable responses to the earthquake. A reinforced concrete coupled shear wall building of seventeen stories (225 ft in elevation), it was built in accordance with the 1964 U.B.C. provisions and was square in plan with two symmetry axes. Four central core units were tied to each other by two connecting girders at the floor levels. There were T-shaped

facade columns along the periphery, connected to the cores by a flat slab. The core walls suffered only hairline diagonal cracks between floor levels. The tie beams exhibited a uniform damage between the third and the seventeenth floors. These beams were constructed with duct openings under the slab. Concrete under the openings dropped out, exposing the beam bars. This also led to slab damage (shear fracture) around the top of the duct openings. The tie beams, which did not have the duct openings, appeared to have flexural yield at the wall connections. There was slight or minor nonstructural damage.

The Banco Central Building, a fifteen-story reinforced concrete frame structure with walls at one end, adjacent to the Banco de America Building, suffered extensive nonstructural and some structural damage. A comparison of the responses of the two structures has helped to reinforce the current earthquake-resistant design philosophy -- an insistence on damage (drift) control in conjunction with energy dissipation.

1.2.1.7 The 1976 Guatemala City, Guatemala, Earthquake [1.18, 1.29, 1.36]

No strong-motion records were obtained during the Guatemala City earthquake. Seismoscope readings were deconvoluted to indicate maximum accelerations in the order of 0.4 g at the ground floor of a building. Aftershocks, recorded by strong-motion instruments, indicated ground acceleration magnitudes in the order of 0.2 g. Documentation of structural damage is extremely limited. A number of medium-height reinforced concrete structures were involved in strong ground motion. A brief survey of the observed post-earthquake condition of these buildings follows.

The fifteen-story (plus two basements) Camara de Industria Building had four core units at each corner, with a rear portion relying on a shear wall in one direction. The floor system consisted of joists and haunched beams connecting the core units. There is no record of damage to the cores. The beams had shear cracks throughout the height of the structure at the ends of the haunches. The joists were also reported to exhibit widespread damage.

The Edificio Médico incorporated two rigid central core units and columns, all tied together by a two-way joist slab system. This eleven-story structure was observed to suffer widespread cracking of the joist floor system in the first three floors, in conjunction with slight nonstructural damage.

The Condominio Reforma (Fiasa) Building was thirteen-stories tall with one basement, and was designed according to the provisions of the 1966 SEAOC Code. Square and symmetric in plan, the building had four external reinforced concrete shear walls and an internal core as its structural system, in addition to columns at the corners. The square center core constituted a couple shear wall system in one direction of the building. The external walls were connected to the core by one-way slab systems. The coupled wall system comprising the central core was the only structural element with observed damage. The coupling beams had slight cracking at and above the middle stories. Hairline diagonal cracks were observed on the walls. Nonstructural damage was noted on masonry walls around the core wall in the form of cracking.

The Condominium Convista Building, fifteen-stories tall, had a mixed structural system consisting of massive coupled shear walls and a

substantial moment-resisting frame. There were no axes of symmetry. The performance, however, was excellent, with no observed structural damage and only minor separation, which was easily repaired, between nonstructural masonry walls and the structural members.

The response of modern frame structures of moderate height in Guatemala City was observed to be successful in terms of surviving the earthquake with no collapse. A comparison with the stiffer structures, however, indicated large permanent deformations and significant damage to nonstructural elements. Frames which incorporated waffle slabs in conjunction with columns fared especially badly. Two other structures of the shear wall type, the Banco de Guatemala with a shear wall core system designed for the full lateral load, and the Edificio El Cortijo, relying on shear walls for lateral resistance, were not reported to have suffered any form of damage.

1.2.1.8 The 1978 Sendai, Japan, Earthquake [1.13, 1.15]

This earthquake is formally designated as the Miyagi-Ken-Oki, June 12, 1978, earthquake. Sendai is a large, modern city with a number of ten- to twenty-story structures in the downtown area, within the Miyagi Prefecture. A number of strong-motion records were obtained in Sendai, indicating ground acceleration intensity of 0.25 g to 0.4 g.

A majority of the medium-height structures in Sendai utilized a steel frame system. Another typical construction incorporated structural steel sections in conjunction with standard reinforcing steel in concrete members, termed a steel-reinforced concrete system. These structural systems were braced with reinforced concrete shear walls in certain cases. A previous earthquake of lesser intensity had occurred in Sendai on February 20, 1978. Most of the minor damage, observed after the

earthquake in June, was first reported to have appeared after the earthquake in February but became more apparent in June.

The Sumimoto Life Insurance Building, an eighteen-story steel frame with a central reinforced concrete core unit and transverse reinforced concrete shear walls on the exterior four corners -- all continuous -- was instrumented. No damage was reported apart from minor cracking in the interior core, as well as along some construction joints in the stairwells. The maximum recorded acceleration at the ground floor in the June earthquake was 0.26 g, with the corresponding eighteenth-floor acceleration of 0.56 g.

The engineering faculty building of Tohoku University, a nine-story reinforced concrete framed building with shear walls, was another instrumented structure. Peak base accelerations of 0.17 g and 0.24 g in the February and June earthquakes were recorded. The corresponding peak response accelerations on the ninth floor were 0.37 g and 1.0 g in these earthquakes, respectively. The duration of intense response with top floor accelerations in excess of 0.25 g, was approximately 20 seconds during the June earthquake. The reported damage consisted of minor shear wall cracking and broken windows, which is a spectacular success considering the intensity of ground excitation and the two successive earthquakes.

A number of structures with excessive system damage as well as partial collapses, were reported for this earthquake. None of the major buildings with this degree of damage incorporated shear walls.

1.2.1.9 Concluding Remarks

The major documented earthquakes of the past twenty years were surveyed for post-earthquake damage to medium-tall to tall buildings

incorporating concrete shear walls. Damages, varying from complete collapse to insignificant minor cosmetic damage, were recorded. In the case of each building with major structural damage, gross design and/or detailing errors, poor quality control of materials, and/or poor construction were revealed.

The most frequent design errors were related to discontinuous shear walls. Discontinuity of walls in any level of the observed structures, especially in the first story, had catastrophic effects on the response of the structure. Although not included in the survey, the partial collapse of the Imperial County Services Building in the 1979 El Centro earthquake was caused by the same type of conceptual design error. Subsequent investigations of this structure are in progress.

Detailing errors include inadequate anchorage of the walls to the foundation, inadequate lap splicing in wall and edge member reinforcement at the floor levels, improper construction joints at the floor levels, and inadequate shear reinforcement of beams connecting the shear walls and duct openings in such beams. Detailing errors such as inadequate anchorage have led to complete collapse, while other errors have contributed to significant structural damage.

The impression emerging from the post-earthquake surveys in the later cases of Managua, Guatemala City, and Sendai has been especially favorable in terms of structures relying on reinforced concrete shear walls for lateral resistance. A large number of medium-height structures up to 225 ft. (Banco De America, Managua), have withstood, with only insignificant cosmetic damage, severe earthquake excitation, which has resulted in many times the code prescribed lateral forces. Some of these structures incorporated coupled shear walls.

The common type of damage to well-designed shear walls appears to be cracking, with widths ranging from hairline to several millimeters. The coupling beams, if adequate shear reinforcement was provided, exhibited cracking and spalling at the ends, indicating yield, for a majority of the observed cases.

A qualitative comparison of the damage control capacities of the well-designed bare frame and frame-shear wall systems indicates the unquestionable superiority of the shear wall structure. In many cases involving post-elastic response, the repair time and cost for the shear wall structures were reported to be significantly less that that required for comparable frame structures. Perhaps the best evidence that professional engineers are beginning to recognize the superiority of shear walls for seismic-resistant construction is that most of the rehabilitation of damaged buildings, or retrofitting of existing buildings, is done by adding shear walls. Remaining problems are: the proper structural layout of shear walls, i.e., the adequate distribution in plan and height; the proper way of coupling; and the adequate combination of shear walls with ductile moment-resisting frame.

1.2.2 Previous Experimental Research on Isolated Structural Walls

1.2.2.1 General Remarks

Experimental research on the response of structural walls prior to 1970 was limited in quantity and covered only squat walls. A survey of this research with significant findings is provided by Park and Paulay [1.26]. With the notable improvement in the state of the art in the earthquake-resistant design of reinforced concrete buildings during the last decade, and the accompanying current design philosophy which demands damage control, research on the earthquake response of medium to tall

structural walls was initiated in a number of major institutions. Integrated analytical and experimental research on shear wall structures has been underway at the University of California, Berkeley; the Portland Cement Association (P.C.A.) Laboratories in Skokie, Illinois; the University of Illinois, Champaign-Urbana; the University of Christchurch, New Zealand; and at a number of other institutions. The experimental programs and major findings of this research are presented in the following sections.

1.2.2.2 Summary of Previous Experimental Research on Isolated Structural Walls

Experimental work on medium-tall to tall isolated structural walls in the last decade, particularly at the P.C.A. [1.25] and the University of California, Berkeley [1.17, 1.43, 1.44], has resulted in a more comprehensive understanding of the seismic behavior of these structural components. Dynamic response studies on small-scale models of frames coupled with walls at the University of Illinois, Champaign-Urbana [1.1], have led to a number of conclusions on frame-wall interaction during seismic excitation.

The experimental studies in the laboratories of the P.C.A. and Berkeley were conducted on one-third scale model subassemblages of isolated walls. The P.C.A. specimens were 6 ft. 3 in. wide, 15 ft.tall and 4 in. thick cantilevers with no intermediate beams or slabs, representing a one-third scale model of an element of a structural wall system. A series of 16 tests were reported [1.25]. The specimens were loaded horizontally by a concentrated force at the top. Monotonic and two different reversing load histories were applied during the tests. Constant vertical column loads were applied to seven of the

specimens, while to the rest of the specimens no axial force was applied. The variables studied in these experiments included: (1) shape of the cross-section -- rectangular, barbell or flanged; (2) amount of main flexural reinforcement in the edge members, which in turn affected the shear to moment ratio; (3) amount of hoop reinforcement in the edge members; (4) amount of horizontal shear reinforcement of the walls; (5) axial forces; (6) concrete strength; (7) load history; and (8) construction joints.

A series of eight specimens were constructed, tested, repaired and retested in Berkeley, resulting in a total of 18 tests which were presented in three reports [1.17, 1.43, 1.44]. All the specimens were one-third scale subassemblages of the first three stories of a prototype structural wall. Specimens had a first-story height of 4 ft. and subsequent story heights of 3 ft. each. Six of the specimens had barbell sections; the rest were rectangular. All had 3 in. thick slabs protruding at each floor level. Overall depths were 7 ft. 10 in. Those with barbell shapes had 10 in. square edge columns and 4 in. wall thickness, while the rectangular specimens had 4.5 in. wall thickness. The prototype structures for the barbell and rectangular walls were ten- and seven-stories high, respectively.

The specimens were initially loaded with equal axial forces on each of the edge columns representing the gravity forces. Although the total axial force was kept constant throughout the experiment, the relative values were varied to simulate the overturning moment effects. The overturning moment was itself varied in accordance with the variation of lateral load in such a manner that the moment-shear ratio was maintained constant. The main parameters of these studies included:

(1) loading history; (2) cross-section -- barbell and rectangular; (3) amount and arrangement of wall reinforcement; (4) magnitude of nominal shear stress; (5) methods of confining the edge columns; (6) construction joints and splices; and (7) effectiveness of repair and retrofitting techniques.

A preliminary assessment of the effects of the basic parameters governing isolated structural wall response was presented previously [1.12]. A more detailed assessment is provided below.

(1) Loading History: One monotonic and two cyclic load histories were applied at the P.C.A. tests. The first cyclic load history comprised three full cycles of load reversals at a certain load level, repeated for increasing load levels up to the first yield level of the wall. A large number of cycles at the full yield level of the wall were then carried out, increasing the displacements, until the failure of the specimen. The full yield level was defined as the force causing yield of all flexural reinforcement as observed from the force-deformation relations of the specimen. The second cyclic load history, which was synthesized from analytical earthquake response studies of walls, comprised a repetition of one full cycle with bounds under the yield level, followed by another full cycle at full yield. The attained deformations in both directions were increased until failure occurred.

There were basically two different load/deformation programs in the Berkeley tests. The so-called monotonic load program actually incorporated a number of unloadings and reloadings during the loading to the largest displacement that could be attained in one direction before failure was detected. This was followed by reversing the load in the other direction for a major one-half load cycle. The cyclic load program was applied by cycling the specimen with full deformation

reversals a number of times at progressively increasing displacement bounds.

A comparison of responses obtained for similar specimens under different load histories indicates that reversing loads affected the stiffness, strength, deformation capacity, and failure modes of the interstory specimens. Top level displacement ductilities on the order of 10 and 4 and interstory drift magnitudes of 5.5% and 3% were recorded for the monotonic and cyclic histories, respectively. Monotonic displacement ductilities of this magnitude (10), however, were observed to be accompanied by stability problems. As the displacement in the initial loading direction induced significantly large cracks, which remained open after unloading, an attempt to load the specimen in the other loading direction resulted in buckling of the main compression bars.

Cycling induced a degradation of the hysteretic behavior. The dissipated energy under cyclic load, however, surpassed the energy dissipation observed under monotonic loading. The deterioration caused by cyclic loading was mainly due to the loss in shear stiffness. An assessment of the effects of different cyclic loading histories indicates that the decay in shear stiffness is strongly dependent on the previous maximum deformation levels rather than on the cumulative deformations attained in previous cycles.

The overall behavior of the walls under both monotonic and cyclic load histories was very favorable, as significantly higher levels (in comparison to similar responses of ductile moment-resisting frames) of energy dissipation were realized before the appearance of stability problems. This was attributed to the post-yield deformation profile of the wall, where most of the drift was concentrated to the lower floor(s). The P-δ effect for the same maximum-interstory drift,

therefore, is less in a tall wall as compared to a tall frame. Despite the deterioration in the hysteretic behavior produced by cyclic loading, walls retained a significant portion of the envelope strength attained under monotonic loading (approximately 80 percent, in general).

(2) The effects of cross section: The barbell cross section was observed to be superior to the rectangular cross section as the latter was generally limited in deformation capacity through local, or overall, out-of-plane stability problems. The barbell shape was observed to be suitable for incorporating effectively confined edge members which acted as large dowels and restrained sliding shear of the wall panel. Loss of cover was not accompanied by a significant loss in the out-of-plane stiffness for barbell walls, which proved to be a significant factor in the premature failure of the rectangular walls.

On the other hand, the increased deformation and shear capacity of the barbell made this type of wall more susceptible to web crushing type of failure under large deformation reversals. However, even after web crushing, the effectively confined members provided sufficient redundancy to resist vertical loading without stability problems. The behavior of the wall after web crushing was noted to resemble that of a soft first-story frame with effectively confined short first-story columns.

The flanged shape was not observed to be superior to the barbell except for its inherently larger out-of-plane stiffness. From the detailing point of view, the flanged section poses problems in confinement and is susceptible to damage at the interface of web and flange. Observed ductilities and other hysteretic behavior patterns for flanged and barbell specimens were similar, which accounted for the fact that the flanged wall had a significantly lower yield displacement.

(3) Edge member confinement: Specimens with spiral and square hoop confinement as well as ordinary ties at the edge members were tested. Volumetric confinement percentages of 0.0135 - 0.018 were used for a majority of the specimens, while others were tested with ties resulting in 0.22 percent lateral reinforcement. Confining the boundary members was observed to improve inelastic performance significantly by restraining buckling of main flexural reinforcement, increasing the strain capacity and restraining the disintegration of core concrete, and increasing the shear capacity and stiffness of the edge members. The most effective form of confinement was observed to be with spiral reinforcement which provided the best restraint against bar buckling. Wall with edge member lateral reinforcement of 0.22 percent as compared to 1.35 percent had 22 percent less shear capacity. Measured maximum shear distortions for the specimen with unconfined edge members were 15 percent more than the comparable specimen with confined edge members. The unconfined specimens exhibited significantly less stiffness and energy dissipation.

(4) Amount and arrangement of wall reinforcement: The effects of the amount of wall reinforcement were a common parameter in both the P.C.A. and Berkeley tests. In the P.C.A. study, two specimens, identical in all respects except for the amount of wall steel, were tested under the same load history. The specimen containing 2.2 times the horizontal wall reinforcement had approximately the same strength, stiffness and endurance as the specimen with less shear reinforcement.

At Berkeley, two specimens, one with half the horizontal and vertical wall steel of the other, were tested under different load histories. More wall steel resulted in slightly more deformation capacity. It was noted that the decrease in wall reinforcement did not

affect the response characteristics in proportion to the decrease.

The arrangement of wall steel was noted to be a significant parameter by comparing the response of two specimens with the same amount of wall reinforcement, except that the bars in one specimen were arranged in a 45^{o} inclined mesh, rather than in the standard vertical and horizontal arrangement. This specimen was observed to have larger energy dissipation capacity due to larger deformation capacity and less stiffness degradation.

Spacing of the wall reinforcement was also noted to be a significant parameter in affecting the crack pattern of the walls. As the shear carrying mechanism and the failure mode were directly dependent on the crack pattern, the spacing of the wall reinforcement was noted to be a more significant variable than the amount of this reinforcement.

(5) Magnitude of nominal shear stress, concrete strength and axial forces: Different amounts of main flexural reinforcement in the edge members of the P.C.A. specimens (1.11 to 3.67 percent in general) resulted in different nominal shear stress magnitudes attained during the tests ($3.7\sqrt{f'_c}$ - $14.1\sqrt{f'_c}$. The nominal shear stresses were calculated using 0.8 ℓ_w as the effective depth of the cross section. Shear stress magnitudes of $13.4\sqrt{f'_c}$ were attained in the Berkeley tests.

The magnitude of the shear stress was observed to be the major parameter affecting hysteretic response and failure mechanisms of the specimens. Walls subjected to low shear stress developed horizontal flexural cracks in the boundary elements which eventually reached and propagated into the web, and practically throughout the whole panel, intersecting with other cracks and slicing the lower regions of the walls into several horizontal layers. Interlocking and dowel action

of the edge members were then the main shear carrying mechanisms due to the horizontal layering of the wall. These mechanisms were sufficient to develop the full flexural capacity, as all failures of this group of specimens were due to buckling of compression bars, or instability of the compression zone, or in the best case, fracture of tension bars.

In walls which developed high shear, the horizontal flexural crack at the edge member had an inclined crack propagation into the wall panel, resulting in relatively symmetric compression strut systems for each loading direction. When these walls were subjected to sufficiently large lateral displacements producing significant flexural yielding, all the compression struts focussed in a small corner zone at the base of the panel and the boundary (edge) member, and failure for all this group of specimens occurred through web crushing. Under vigorous cyclic loading the web crushing was accelerated due to the deterioration of crushing resistance of the concrete at the faces of intersecting cracks, developed because of loading and/or deformation reversals. This premature crushing led to the formation of a horizontal band near the wall foundation that extended across the width of the wall panel and in which the concrete had been crushed and spalled, and a mechanism of sliding shear had developed in the wall (being the main shear resistance offered by the dowel action of the two edge members).

As web crushing appeared to be the dominant factor in limiting inelastic deformation and endurance capacity of the walls under high shear reversals, this phenomenon was investigated in detail. Web crushing was observed to be interrelated to both the shear stress and loading history, as it was observed to occur only under cyclic loading and only after a number of loading reversals, whereas a significant spread is observed in the shear stress values under which this

phenomenon occurred. It was therefore concluded that the present code limitation of $10\sqrt{f'_c}$ for nominal shear stress did not eliminate the possibility of web crushing when large inelastic response involving reversals of deformation is expected.

The relation of concrete strength to web crushing was further investigated by testing two specimens differing only in concrete strength by a factor of 2.2. The specimen with the higher concrete strength developed a shear stress of $10.9\sqrt{f'_c}$, while this value was $13.8\sqrt{f'_c}$ for the other specimen, the ultimate force capacities differing by only a factor of 1.17. The changes in hysteretic characteristics, however, were far more substantial; the specimen with the higher concrete strength endured twice as many cycles under large deformation and dissipated approximately three times more energy before web crushing occurred. The attained displacement ductilities were approximately two and four for the lower and higher concrete strengths. The implication of these tests in that the concrete strength had a considerably more significant contribution to the deformation and energy dissipation capacities of the specimen as compared to its force capacity. This is natural since the force capacity of the specimen is controlled by flexure, where concrete strength does not have an appreciable influence. The concrete strength is observed to have appreciable influence, however, on delaying the numerous adverse effects of shear stress on the deformation and energy dissipation capacity. The specimen with higher concrete strength was under only $10.9\sqrt{f'_c}$ shear stress while the specimen with the smaller concrete strength was subjected to a shear stress of $13.8\sqrt{f'_c}$, which had far more detrimental effects to its hysteretic behavior.

Furthermore, the phenomenon of web crushing under deformation reversals cannot be related to a certain concrete strength or eliminated

by limiting the shear stress. To be realistic and conceptual, any limitations on stress and dimensions (web thickness vs. column dimensions, for stability considerations) should be related to the expected deformation levels and endurance requirements.

Another factor that was observed to affect the phenomenon of web crushing was the axial force. Axial force magnitudes on the order of 7 percent of the ultimate capacities of the edge members were observed to be significantly beneficial in the response. The specimen with constant axial load of this magnitude had approximately 30 percent more shear capacity, less pinching under reversals, more rotation capacity and approximately one-half shear distortion under similar rotations, as compared to the corresponding specimen with no axial load. The main beneficial effect of axial load of this magnitude was in increasing the shear capacity and stiffness of the edge columns. This, in turn, was instrumental in enacting better hysteretic characteristics and in increasing the shear capacity of the wall, as this was affected mainly by the shear capacities of the edge columns.

There is a lack of data on the effects of axial loads of higher magnitudes and, especially, large tensile forces. The Berkeley tests were conducted under column axial loads programmed to simulate the dead load and overturning moment effects as synthesized from analytical studies on the prototype and resolved into a couple. The axial loads, therefore, varied between realistic limits and they were representative of actual load levels. The failure mechanisms and hysteretic characteristics were not significantly different from those obtained in the P.C.A. tests.

(6) Construction joints: Construction joints fabricated according to existing construction practices performed satisfactorily. The same

was concluded for lap splices in vertical wall steel located in critical regions. Proper anchorage of the horizontal reinforcement into the confined core of the edge member and proper lapping of the longitudinal reinforcement of the edge member are more important than laps in vertical wall steel or construction joints. Since the edge members provided the main shear capacity and stiffness of the walls by acting as extremely effective dowels, once these were cracked, the construction joints were not observed to undergo significant horizontal shear slippage. This points to another significant advantage of the effectively confined edge members, since construction joints in walls without such edge members have been observed to be a main source of damage and of failure after earthquakes (Section 1.2.1).

(7) Repaired specimens: The effectiveness of various repair techniques was investigated by repairing and retesting the walls at different damage states. The techniques of epoxy injection, replacing crushed or cracked panels by new concrete, and detailing of the renewed panel, were studied.

A significant observation was made on repair techniques involving welding on grade 60 reinforcing bars. Even when all known precautions were taken during the welding operation (control of temperature, usage of the correct electrode, experienced welder) a welded connection resulted in a severely impaired elongation capacity of the bars at the connection. It was concluded that welding on a grade 60 reinforcing bar generally reduces the rupture strain so significantly that breakage usually occurs as soon as the bar yields.

In general, if the boundary members retained the integrity of core concrete, repairs that did not involve welding of main reinforcement were successful in restoring the capacity of the repaired specimens close to that of the virgin ones. Although none of such repaired specimens exhibited early loss of strength or endurance, the permanent strains that accumulate during initial testing should affect the endurance of the repaired specimens to a certain extent.

1.2.2.3 Conclusions

(1) The experimental and accompanying analytical studies of slender isolated structural wall response indicate basic differences between beam and wall behavior. Walls, although commonly modeled and conceptually appraised as similar to beam/columns, possess inherently different load carrying and failure mechanisms. The interactions between flexure, axial force, and shear, affect wall response differently than beam or column response.

The major reason for different behavior patterns of beam/columns and slender walls is the redundancy provided to the walls through effectively confined boundary members. The boundary members provide and maintain stiffness to the wall even after loss of their concrete cover; they restrain shear distortions in general and limit sliding shear failure by acting as extremely effective dowels. Boundary members provide a strong, ductile and stable compression zone and are instrumental in instituting a uniform crack distribution across the panels, which improves stress redistribution as well as damping characteristics. Boundary members improve endurance and energy dissipation capacity of the walls to the extent that the factor limiting deformation capacity becomes web crushing. Even after this phenomenon, the boundary members

provide sufficient redundancy to maintain vertical load carrying capacity and an appreciable amount of energy dissipation capacity. Furthermore, any damaged wall can be effectively repaired as long as the cores of the boundary members retain their integrity.

(2) The effects of different deformation mechanisms, mainly flexure, shear and bond (fixed-end rotation or rotation concentration at the foundation level) on the total inelastic deformation of the walls, were not of the same order of importance as observed in beams. In the walls, shear deformations and fixed-end rotations constituted approximately 40 and 10 percent of the total top displacement under monotonic loading. During cyclic loading, the contribution of shear deformation increased to as much as 87 percent of the total top displacement. The corresponding roles of shear and fixed-end rotation deformation components are reversed in beams.

(3) All test specimens exhibited more flexural strength than the design strength. The maximum increase was on the order of 30 percent, attributed mainly to the strain hardening of flexural reinforcement. Similarly, significant increases in the actual shear capacities as compared to design shear values, on the order of 30 to 50 percent, were observed. This is due to a prevailing misconception in the evaluation of shear strength of walls with boundary members. Current code expressions for shear strength computation are based on beam behavior under monotonic loading. The relative contributions of confined edge members as dowels in compression and tension, panel steel, concrete strength, and the effects of force and deformation reversals, are not incorporated in estimation of the shear strength and deformation capacity of walls. Furthermore, limiting the nominal shear stress to a $\phi\ 10\sqrt{f'_c}$ although desirable,is not rational. First

because this limitation cannot eliminate the web crushing type of failure under deformation reversals,and, second, because considerably higher shear stress, on the order of $14\sqrt{f'_c}$, were attained in the tests.

(4) The observed behavior of slender walls with well-confined boundary members was extremely favorable as far as strength, stiffness, endurance, deformation capacity, and energy dissipation were concerned. Present seismic code provisions which prescribe a higher horizontal force factor (k factor) for buildings incorporating such walls, are questionable.

Another observed misconception in the current code provisions is related to the prescribed distribution of horizontal forces. As the shear design of members of ductile moment-resisting space frames is based on the ultimate flexural strength that can be developed in the member, the distribution of horizontal forces is not significant in preventing shear failure. However, the shear design of walls is not based on the flexural capacity, but on the design base shear, as obtained from the prescribed external forces. The present practices of increasing the load factor in shear design and limiting shear stress to $\phi\ 10\sqrt{f'_c}$ do not eliminate the possibility of shear failure because actual horizontal force distribution can be quite different than that assumed by code. The significance of the distribution of lateral forces in design is investigated in subsequent sections of this report.

1.2.3 Previous Experimental Studies of Connecting Girders of Coupled Shear Walls

1.2.3.1 General

There is ample literature on the cyclic load behavior of reinforced concrete beams which are slender (moment arm to effective depth ratio of 3.5 or more) and/or under low shear (nominal shear stress less

than $6\sqrt{f'_c}$). Many of the existing beam tests were carried out to study the behavior of beam elements of ductile moment-resisting space frames (DMRSF). Accordingly, the dimensions, longitudinal and shear reinforcements and loading programs were modelled after the observed characteristics of such beams.

Recent studies on the coupling beams of reinforced concrete shear walls have demonstrated that the general dimensional characteristics, shear stress and deformation, energy dissipation and endurance demands of these elements are quite different from the conventional DMRSF elements [1.12, 1.27]. The coupling beams are generally (1) deep (moment arm to effective depth ratios of one or less were observed to be common); (2) under shear stresses considerably larger than those of DMRSF beams (nominal shear stress magnitudes of $6\sqrt{f'_c}$ and more are frequently encountered); (3) subjected to significantly large inelastic end rotation demands (40×10^{-3} rads. and up to 90×10^{-3} rads. were observed[1.27] ; and (4) subjected to a significantly large number of yield excursions or inelastic rotation reversals (effects of higher modes of vibration were observed to cause a larger number of force reversals in the connecting beams than the walls [1.22]).

The basic parameters affecting the behavior of coupling beams and main conclusions of research on these elements carried out in Berkeley [1.11, 1.21], by the P.C.A.[1.7], Canterbury [1.28] and a number of other institutions [1.22, 1.33. 1.45], are summarized in the following sections.

1.2.3.2 Parameters Affecting the Behavior of Reinforced Concrete Coupling Elements of Coupled Structural Walls

(1) Moment arm to effective depth ratio (a/d ratio): Although, in general, a wide range of a/d ratios may be encountered for coupling beams,

the stiffness demand from these beams for "efficient coupling" usually results in a/d ratios of less than 2. Tests in Canterbury, New Zealand, incorporated specimens with a/d ratios less than unity [1.28], while the Berkeley specimens had a/d ratios of approximately 3 [1.11], and the P.C.A. specimens had 1.4 and 2.8 for the a/d ratio [1.7]. More recent tests, carried out in Canterbury, New Zealand, investigating "slab coupling" on specimens with a/d ratios greater than 3, were reported [1.39].

In general, the a/d ratio defines the relative contributions of the beam and arch actions to the shear resistance of reinforced concrete beams. The arch action contributes significantly to the shear capacity of beams with a/d ratios of less than 3. It was observed by Paulay [1.28] that the behavior of beams which had a/d ratios approaching unity was considerably different from more slender beams under deformation reversals. Both the compression and tension reinforcement in the deep beams were observed to be in tension as a result of diagonal cracking. Continued deformation reversals induced significant residual tensile strains throughout the depth of the beam leading to the "sliding shear" type of failure. Furthermore, diagonal cracking resulted in the loss of shear stiffness which contributes more to the total stiffness of such beams than the flexural stiffness. Consequently, inelastic deformation reversals of deep beams with conventional reinforcement was accompanied by a severe drop in stiffness and prompt loss of strength and, consequently, of energy dissipation through sliding shear.

Tests on "slab coupling" in the same institution [1.39] have resulted in a number of conclusions on the effectiveness of such coupling and behavior patterns of coupling elements which are short but also

slender so that the a/d ratios approach 4.

One important conclusion reached after reversed loading tests with an extremely severe loading program (over 30 full cycles, with displacement ductilities approaching 10 at the later cycles) was that the elements exhibited severe stiffness degradation starting with the early cycles. Stiffnesses of 10 percent of the initial elastic stiffness were characteristic after a number of load reversals. This was associated with torsional effects encountered due to the slenderness of the coupling elements.

The effective width of the slab that can be relied on to couple structural walls was observed to be significantly smaller than that given by a number of previous analytical studies. For modeling purposes, a slab width equal to the clear distance between the two coupling walls was suggested. For estimating the stiffness of this coupling element, using 20 percent of the gross uncracked moment of inertia was suggested.

The concentration of shearing stress at the edge of the wall and slab led to punching shear problems. This would be characteristic in cases where the width of the coupling element is much larger than the width of the wall and special detailing would be necessary at the interface. One test of the series was carried out by incorporating a shallow beam in conjunction with the slab and perpendicular to the wall at the wall edge. The a/d ratio for this specimen was on the order of 1.5. This specimen exhibited an uncommon horizontal shear failure in the beam which limited the imposed deformations during the test. It was concluded that continued research on beam and slab coupling was necessary.

In conclusion, the a/d ratio of connecting elements appears to be a major parameter affecting the failure mechanism of the element in general. Closely associated with this parameter is the shear stress and the arrangement of the longitudinal and transverse reinforcement and detailing at the interface of the wall.

(2) The nominal shear stress: The maximum nominal shear stress realized in the coupling element under deformation reversals is another significant parameter affecting the hysteretic characteristics and failure mechanisms of these elements.

The maximum shear stress is a function of the a/d ratio, the flexural reinforcement ratio and detailing, and the yield strength and strain hardening characteristics of the flexural reinforcement. The smaller the a/d ratio, the larger the shear stress, since the arch action contributes to the shear capacity in addition to the standard beam mechanism in resisting shear [1.26]. The larger the flexural reinforcement ratio and the yield strength, the larger the shear stress, since the shear force that can be developed in a flexural member is directly related to the flexural capacity of the member through statics.

Previous studies have demonstrated that beams under load reversals, designed according to the present seismic code for the high seismic risk regions, failed in a flexural mode for shear stress magnitudes of $3\sqrt{f'_c}$ or less. Buckling of compression reinforcement was the typical failure mechanism. The Bauschinger effect in steel and "closing of the crack" are the main sources of degradation in hysteresis.

Shear stress magnitudes between $3\sqrt{f'_c}$ - $3.5\sqrt{f'_c}$ induce flexural-shear failures. Shear emerges as the reason behind the pinching and decay of hysteresis. Shear stresses of magnitudes $3.5\sqrt{f'_c}$ - $6\sqrt{f'_c}$ start to induce the "sliding shear" type of failure and limit energy dissipation through severe decay of stiffness. Effective confinement to restrain the disintegration of the core can prolong shear capacity and energy dissipation capability under deformation reversals. However, providing a sufficient amount of transverse reinforcement is not adequate to preserve stable hysteretic characteristics under cyclic load at large deformation levels.

Shear stress magnitudes of larger than $6\sqrt{f'_c}$ are detrimental in hysteretic response. Conventional reinforcement arrangements are not successful in restraining sliding shear failure which can occur after a few deformation reversals. One possible remedy for the detrimental effects of high shear is to limit the flexural capacity of the cross section and thus to keep the possible maximum shear stress that can develop to a tolerable level [1.9]. If two consecutive hinges develop along a beam, the shear is limited by the flexural strength at the plastic hinges. The designer, however, may not be able to take advantage of this possibility due to other restraints.

The second possible remedy for the effects of shear is to resort to using reinforcing patterns that are different from the conventional ones.

(3) Arrangement of flexural and shear reinforcement: A number of different reinforcing schemes for beams with small a/d ratio (less than 3) and/or high shear (over $3\sqrt{f'_c}$) were suggested and tested under load/deformation reversals [1.11, 1.33, 1.28]. These are summarized below.

(a) Intermediate longitudinal bars [1.33] -- Using intermediate longitudinal bars as shear reinforcement was observed to improve the hysteretic response of beams subjected to shear stress magnitudes between $3\sqrt{f'_c}$ and $6\sqrt{f'_c}$. Hysteresis was stabilized and endurance was improved with two intermediate layers of longitudinal bars in addition to the ACI 318-71 specified lateral reinforcement. These bars formed an improved cage to maintain the integrity of the core. Beams with shear stress lower than $3\sqrt{f'_c}$ performed satisfactorily with only the code specified ties, while beams with shear stress magnitudes of over $6\sqrt{f'_c}$ did not perform well, regardless of intermediate longitudinal bars and ties.

(b) 45^0 diagonal bars -- Tests of beams with 45^0 inclined diagonal bracing bars were carried out at Berkeley [1.11] and by the P.C.A. [1.7]. The a/d ratios of the specimens were 3 and 1.4, respectively. In the Berkeley specimen, the diagonal bars were placed in addition to the existing longitudinal reinforcement and double ties, and were capable of resisting the entire shear. The diagonal bars were especially restrained by close double ties at the regions where they were bent. This beam performed exceptionally well even under shear stress levels of $6.2\sqrt{f'_c}$. Pinching in the force-displacement hysteresis was literally eliminated under a vigorous cyclic program with progressively increasing displacement bounds.

The comparable beam with only longitudinal reinforcement and double ties did not perform as well under the same load program. Shear stress magnitudes of $5.8\sqrt{f'_c}$ were attained for this beam, which resulted in pinching and severe loss of strength under cycling at deformation levels approximately 5 times that of yield.

In the P.C.A. specimens, one and two of the longitudinal bars at top and bottom were bent 45^{o} at the hinging region of the beam. No special effort was made to restrain these bars at their bending points; the same tie spacing was provided along the beam. These specimens behaved even worse than the comparable longitudinally reinforced beams, due to the loss of support for the diagonal bars at the bent locations. The stirrups provided could not restrain the diagonal bars where they were bent at the top and bottom of the beam. Shear stress magnitudes of $7\sqrt{f'_c}$ - $9\sqrt{f'_c}$ were realized for these specimens which exhibited severe pinching and loss of strength.

The assessment of the results of the Berkeley and P.C.A. tests on this reinforcing scheme indicates that this type of reinforcing requires uncommon attention to detailing and workmanship to be effective. As the conventionally reinforced counterparts of these specimens were not totally satisfactory, and, as another, simpler reinforcing scheme of installing full-length diagonal reinforcement was proved exceptionally successful, particularly for beams having a/d ratios smaller than two, the use of 45^{o} diagonal reinforcement may not be justified for these types of coupling beams.

(c) Full-length diagonal reinforcement -- Full-length diagonal reinforcement as the main moment and shear carrying mechanism was first tested by Paulay [1.28] and was demonstrated to be successful in eliminating sliding shear in beams of a/d ratio less than one. Later this reinforcement, which is equivalent to embedding a steel truss in concrete, was shown to be effective for more slender beams, even for a/d ratios of 3.33 [1.2]. Beams with such reinforcement and a/d ratios of 1.4 and 2.8 were tested by the P.C.A. [1.7] and were observed to maintain stable hysteresis at shear stress magnitudes of $10.9\sqrt{f'_c}$.

In the tests carried out by Paulay, prototype coupling beams with 12 in. and 30 in. cross sectional dimensions and 3 ft overall length were reinforced with conventional longitudinal bars or full-length diagonal struts. Each of these struts was formed by a bundle of reinforcing bars. The a/d ratio for the beams was 0.7. The conventionally reinforced beam failed after one post-yield cycle due to sliding shear. The specimen with full-length diagonal bars was designed assuming that a truss mechanism, formed by the diagonal bars, would carry the total shear. The theoretical ultimate load was realized and the beam sustained a large number of load cycles at significant deformation levels with ideally stable hysteresis. End rotations close to 0.1 radians were attained for this beam.

It was concluded that the success of full-length diagonal reinforcement was dependent on restraining the buckling of compression bars of the truss. Adequate spiral or hoop reinforcement around the bundle of bars forming the legs of this truss was suggested for this purpose. Adequate concrete cover on the sides to restrain out-of-plane stability of the reinforcement was also observed to be a critical factor in developing the full capacity of the reinforcement.

Tests carried out by the P.C.A. [1.7] on full-length diagonal reinforcement utilized specimens with 4 in. by 6.67 in. cross sections and full span lengths of 16.67 in. or 33.33 in. The a/d ratios of the 1/3-scale model specimens were 1.4 and 2.8, respectively.

The beams were reinforced by hoop reinforcement capable of resisting the total expected shear. The diagonal bars were designed by the truss analogy as suggested by Paulay [1.28]. The test program was exceptionally severe, comprised of a succession of three full cycles of deformation followed by another three cycles, with increasing

deformation bounds for each set of cycles. Both beams behaved exceptionally well with no pinching of hysteresis or loss of strength until the bars buckled and subsequently fractured within the beam-wall interface where no hoops were provided. Shear stress intensities of $10.9\sqrt{f'_c}$ and $5.3\sqrt{f'_c}$ were realized for the short and longer beams, respectively.

Comparable beams with conventional longitudinal reinforcement developed shear stress of $10.3\sqrt{f'_c}$ and $3.5\sqrt{f'_c}$ for short and longer beams, respectively. These beams exhibited severe pinching and loss of strength, which was more critical in the response of the shorter beam. Both of these beams failed through sliding shear in spite of the hoops that did not yield under the maximum shear.

Studies carried out at the Middle East Technical University [1.2] had the objective of testing the effectiveness of full-length diagonal reinforcement in more slender beams where this type of reinforcement may be used in conjunction with conventional longitudinal reinforcement. Test specimens had 9.8 in. by 19.6 in. cross sectional dimensions and a/d ratios of 3.33. Two test specimens had the same number of either diagonal or longitudinal bars, while two others had different ratios of diagonal and longitudinal bars, the total reinforcement remaining the same. All the beams were designed for the same strength, which was found by superposing the contribution of diagonal bars, computed as a truss, and the contribution of the longitudinal bars as a reinforced concrete beam. The total compression or tension steel ratios were one-half of the balanced, individually. Lateral ties in accordance with the ACI 318-77 were provided to all specimens. The loading program was comprised of four full loading cycles at a displacement of approximately three times the average yield

displacement followed by four cycles at five times the average yield displacement.

The specimen with only longitudinal steel attained a shear stress of $4\sqrt{f'_c}$ and failed through a flexural shear mechanism (resulting in sliding shear), exhibiting severe pinching and a 30 percent drop in strength. The diagonally reinforced specimen did not exhibit as much strain hardening and attained a shear stress magnitude of $3.5\sqrt{f'_c}$. The hysteretic characteristics were excellent, similar to those of a steel coupon under cycling stress. All specimens developed their computed ultimate strength, indicating that the contributions of longitudinal and diagonal bars may be superposed for an estimate of the total strength when both types of reinforcement are used together.

Although, for beams that are as slender and under shear stress magnitudes of less than $6\sqrt{f'_c}$, adequate hysteresis can be obtained by increasing the confinement reinforcement, these tests indicate that full-length diagonal reinforcement can also be used with less dependence on ties and still yield extremely favorable hysteretic characteristics. In certain applications, diagonal reinforcement may be easier to assemble than extremely close multiple-tie reinforcement, also enabling a better quality control in the placement of concrete. Use of this reinforcement in slender beams resulted in less deformation hardening than the one with longitudinal steel, due mainly to local buckling effects within the cracks at the interface of the beam and wall. However, the shell concrete did not spall, and the overall damage to the beam was considerably less in the case of the diagonal reinforcement.

A significant requirement in utilizing the full advantages of diagonal reinforcement was observed to be adequate anchorage of the bars in the walls. Since these bars are strained more uniformly along

the length of the beam as compared to longitudinal bars, the overall elongation of the beam may be significant. Even in the case of proper end anchorage of the diagonal bars, growth of the beam due to local slippage was observed.

1.2.3.3 Conclusions

The seismic demands from coupling elements of coupled structural walls are especially severe, in terms of inelastic end rotation magnitudes and number of post-yield deformation reversals. These elements, therefore, require special attention to detailing, especially when the a/d ratio is smaller than 3 and the expected ultimate shear stresses are on the order of $6\sqrt{f'_c}$. The most successful scheme for such beams is to arrange the main flexural reinforcement in a diagonal manner, forming a steel truss mechanism within the beam. Such an arrangement was observed to enhance hysteretic characteristics of slender horizontal beams, with a/d ratios as large as 3.33 (when used in conjunction with regular reinforcement), and may be the only successful solution in the case of deep beams with smaller a/d ratios. The critical region in the use of this detailing scheme is the beam and wall interface, where buckling of compression bars within a large crack should be restrained by effective confinement. For significantly deep beams, out-of-plane buckling of these bars due to insufficient side cover was also observed as a problem. These problems, however, can be handled through careful design and detailing.

Use of extremely slender coupling elements, such as slabs, was also observed to pose critical problems. The punching shear effects at the interface of wall and slab, as well as the loss of stiffness due to torsional effects, were observed to be significant problems.

Moreover, the stiffness provided by slab coupling was not observed as sufficient to consider the walls as coupled structural walls.

1.2.4 Review of Experimental Research on Coupled Structural Walls

1.2.4.1 General Remarks

Experimental data on the seismic response of coupled walls is extremely limited. Two tests on 1/4-scale 7-story coupled walls were carried out at the University of Canterbury, New Zealand. The basic parameter in these tests was the arrangement of reinforcement in the coupling beams [1.32]. Preliminary results of two tests on a 1/3-scale 6-story coupled wall model were reported by the P.C.A. [1.4]. The basic parameters in these tests were the strength and stiffness of the connecting beams. A series of "earthquake simulator" tests on the response of coupled structural walls has been underway at the University of Illinois at Urbana-Champaign. Four approximately 1/12-scale 10-story models and six 6-story models with the same scale were tested in this institution [1.5, 1.20].

Apart from these investigations, to the writers' knowledge there has been no comprehensive experimental study on the seismic response of reinforced concrete coupled structural walls.

1.2.4.2 The University of Canterbury Tests [1.32]

The test specimens represented a 1/4-scale model of a chosen 7-story prototype, with a symmetrical, 2-wall, coupled system. The overall aspect ratio (h/D) of the system was 3.43. The connecting beams were extremely stiff for this aspect ratio, with a/d ratios of 0.65. This topology was claimed to be typical of New Zealand practice. The specimens had wall sections of 4 in. by 24 in. and a total height of 18 ft, with beam dimensions of 3 in. by 12 in. and clear length of

1 ft 3 in.

The walls did not have confined edge members; they contained ten #5 bars on the outer, and two #5 bars on the interior faces as main flexural reinforcement at the base. The beams had two #3 bars, top and bottom, in one of the specimens. These bars were arranged in a diagonal fashion in the other specimen. The two walls were prestressed along the center line by cables, representing the dead load, to a stress of 260 psi, which was kept constant during the tests.

The specimens were loaded at three points, resulting in a triangular load distribution in accordance with local code provisions. The old Japanese system of incorporating a dummy specimen to maintain base fixity through symmetry was utilized. Four load cycles below yield were followed by a number of fully reversing load cycles at the ultimate load capacity of the system. The ultimate load capacities of the specimens were observed to be approximately 20 percent larger than the computed values, which was attributed to the strain hardening of the main wall reinforcement.

In the specimen with conventionally reinforced coupling beams, first beam yield started at approximately 45 percent of the observed ultimate load. About half of the beams (at the lower stories) yielded by 50 percent of the observed ultimate load. The other beams yielded at later load stages. The initial (cracked) loading stiffness of the system was maintained exceptionally well until the first yield in the walls (tension wall). The increase in load capacity after first wall yield was 35 percent; however, the stiffness of the system was almost completely lost during this last increment of the lateral load. The average stiffness of the system was approximately twice the computed uncoupled stiffness of the walls, based on cracked sections. It was also

approximately one-third of the computed coupled stiffness, based on uncracked gross cross sectional properties.

The force-displacement hysteresis of the specimen with conventionally reinforced beams exhibited a slight pinching and approximately 20 percent loss in load capacity during the fourth large displacement reversal. Displacements approximately three times the yield displacement were attained for both loading directions during the large deformation reversals. Although the hysteresis obtained for this wall was observed to be "inferior" compared to the hysteresis demonstrated by the second specimen, it appears to be adequate in terms of stiffness, strength, energy dissipation, and endurance.

The axial force components of the walls were estimated to provide 70 percent of the total overturning moment capacity. As a consequence of this major contribution, the hysteretic characteristics of the system are affected by the hysteretic characteristics of the beams considerably. This is apparent from the low stiffness around the zero load region (for load ranges $\pm$ 20 percent of ultimate) followed by a stiffness similar to the initial loading stiffness, up to approximately 80 percent of the ultimate load. The beams were observed to exhibit a "sliding shear" behavior which reflected on the hysteretic characteristics of the system.

The second-floor beam was observed to be the critical beam. Rotations on the order of 0.085 radians, corresponding to a rotational ductility of 12, were recorded for this beam. During the final load cycle in which complete plastification of the system occurred, beams between the second and sixth floors had similar rotations. During this cycle, the elongation in the second floor beam reached 0.16 inches (strain of 1%).

An extremely significant aspect of coupled wall behavior, the portion of the total shear resisted by the tension and compression walls, was unfortunately not investigated through experimental observations and measurements. Failure of the wall was initiated by crushing of concrete in the compression corner of the tension wall, followed by severe shear slip at the base of this wall, with reinforcement at the damaged corner buckling in the direction of the slip. The compression wall, however, maintained approximately 75 percent of the ultimate load capacity at a very large deformation at the top of the wall of 14 in., even after failure of the tension wall. It was concluded that the dowel capacity of the failed tension wall contributed to the remaining shear capacity, to some extent, at the final stages of loading. Whether the failure of the tension wall can be considered as web crushing or as a standard compression failure, is not very clear. The report mentions that the cover concrete "spalled off".

The specimen with diagonally reinforced beams was able to sustain one more large displacement cycle than the first specimen. The appearance of the force-displacement hysteresis of this structure implies significantly better overall hysteretic characteristics. No pinching is apparent, and the energy dissipated through cycling within ultimate force bounds increases with cycling, with no loss of load capacity. This specimen developed approximately 1.2 times the computed ultimate strength, similar to the first specimen. The first beam yield commenced at 33 percent of the observed ultimate load. First yielding in the wall occurred at approximately 63 percent of the ultimate load. The stiffness did not deteriorate as rapidly after the first yield in the wall as in the first specimen, and the overall deformation hardening characteristics appear to be better. The average (yield) stiffness of the coupled wall system

was approximately one-half of the stiffness based on uncracked gross cross sectional properties. Displacements approximately 10 times the first yield displacement (or 5 times the "effective yield" obtained by intersecting an average secant and the strain hardening branch) were attained in both loading directions with no decrease in the load capacity.

The failure of the second specimen occurred through instability of the compression wall. This wall kinked and buckled in the out-of-plane direction at its base due to an initial form error.

The diagonally reinforced coupling beams were concluded to be extremely effective in maintaining strength, stiffness, and energy dissipation of the structure during large deformation reversals. As in the first test specimen, the second-story beam, was the most stressed beam during low deformation cycles. Unlike the first test specimen, however, the first-floor beam was observed to be subjected to the largest rotations during high deformation cycles, with rotational ductilities approaching 16 (maximum rotation 0.05 radians). Another difference in beam response in the two tests is observed in the distribution of beam deformations along the height of the structure. In the first test specimen, the beams above the second floor had similar end rotations during the large deformation reversals. The beams of the second specimen exhibited end rotation magnitudes varying almost linearly from 0.05 to 0.025 radians along the height of the structure, the largest value attained for the first-floor beam, during the final deformation cycle. This may indicate that the first-floor beam maintained its strength until the termination of the test due to instability of the compression wall. A photograph of the specimen taken after the test does not indicate much distress in this beam.

The growth of the diagonally reinforced beams surpassed the elongations recorded for the conventionally reinforced beams. Second- and third-floor beams had elongations of 0.55 inches, corresponding to a strain of 3.7 percent.

The main conclusions derived from these tests can be summarized as follows:

(1) The detailing of the connecting beams influenced the overall force-deformation relations and hysteretic characteristics of the coupled wall systems to the extent that the observed hysteretic characteristics of the system were reflections of those of the beam. Such an influence, however, should not be generalized to all coupled wall topologies. The test specimens resembled slender perforated cantilever beams, with an overall aspect ratio of 3.43 and coupling beam span to depth ratios of 1.25. Furthermore, the coupling beam strengths were such that 70 pecent of the total overturning resistance was provided by the coupling action. Both the stiffness and strength characteristics of the coupling beams relative to the walls are major parameters, resulting in the beam response governing the overall structural response.

(2) The conventionally designed beams of the first specimen developed nominal shear stresses of $6.5\sqrt{f'_c}$ and failed in sliding shear. The behavior of this system, which may still be considered as adequate for certain earthquake demands, was significantly inferior to the second system with diagonally reinforced beams. The second specimen dissipated approximately twice the energy dissipated by the first specimen under a similar deformation history. Furthermore, the resulting damage to the beams of the second specimen was considerably less.

(3) Both specimens behaved in a flexural mode. This was evident from the contribution of bending deformations to the top displacement.

Near the ultimate load, this contribution was approximately 80 percent. For different structure vs. beam aspect ratios, different modes of behavior should be expected. The nominal ultimate shear stress in the walls, assuming equal shear contribution and using 0.8 d_w as effective depth, was $5.71\sqrt{f'_c}$ for each wall. In U.S. practice, values up to "$\phi 10\sqrt{f'_c}$" ($7.5\sqrt{f'_c}$) are permitted by the code.

(4) The walls were rectangular in cross section with no confined edge members. Horizontal wall steel was arranged as simple stirrups bounding the complete wall cross section. Furthermore, the flexural steel at the interior wall faces was one-fifth of the steel at the exterior faces, complying with the results of elastic analysis. As the beams of the first specimen lost strength through cycling, the demand for reinforcement at the inner wall faces increased. Furthermore, the absence of confined edge members resulted in a severe degradation of concrete at the wall hinging regions. All these factors contributed to the early failure of the tension wall of specimen 1. The capability of the compression wall of maintaining 75 percent of the ultimate shear after the failure of the tension wall is remarkable. This is another indication that the shear strength of concrete walls is not correctly estimated by existing approaches.

The inherently small out-of-plane stiffness of the rectangular cross section is further demonstrated by the stability failure of the second specimen.

(5) Throughout the tests of both specimens, a significant amount of shear transfer from the tension wall to the compression wall was observed. Although this transfer was not quantitatively assessed, the compression wall was estimated to resist 75 percent of the shear at large deformations. This transfer has extremely significant implications because, for coupled

shear walls designed for a higher shear to moment ratio, the compression wall may not tolerate the increased shear demand, failing in brittle shear-compression. A correct assessment of the actual shear capacities of walls under different magnitudes of axial forces is therefore absolutely necessary to determine the permissible shear in isolated and especially in coupled shear walls. As the shear capacity of a wall depends not only on the strength of the materials but more significantly on deformation levels and history, such an assessment should incorporate expected deformation levels and number of inelastic deformation excursions.

1.2.4.3 Tests of a Six-Story Coupled Wall

Preliminary findings on two tests of a six-story coupled wall specimen were reported by the P.C.A. [1.4]. The specimen had two symmetric rectangular walls 4 in. thick, 6 ft 3 in. wide and 18 ft tall. The clear span of the connecting beams was 16.67 in. The specimen was not modeled after a prototype, but was assumed to represent a 1/3-scale model of a coupled wall system, with story heights of 3 ft in the model.

The connecting beam dimensions in the first test were 6.67 in. deep and 4 in. wide. After the first test, these were repaired into larger sized beams of 8 in. depth and 10 in. width. The overall aspect (height/width) ratio of the system was 1.33, with coupling beam span to depth ratios of 2.5 and 2 for the original and repaired beams, respectively. The strength and stiffness of these beams were considered to represent two extremes in the coupling strength and stiffness for the two walls. The design shears for the weaker and stronger beams were $5.8\sqrt{f'_c}$ and $9.8\sqrt{f'_c}$, respectively. The measured contributions of coupling action to the total ultimate base moment were 10 percent and 30 percent in the two tests. The beams for both of the specimens were provided

with web reinforcement corresponding to the design shear stress, based on the computed maximum strength of the beams, without considering the code capacity reduction factor or the actual strain hardening of the reinforcing steel.

The walls had confined boundary members, each one having 4 percent longitudinal reinforcement. Horizontal steel in the walls was sufficient to resist a calculated ultimate shear force corresponding to a mechanism consisting of yield at the ends of the coupling beams (but no strain hardening) and 1.25 times the flexural ultimate strength of the walls at the base. The specimens were provided at each floor level with a floor slab stub 2 1/2 in. thick and 7 ft 4 in. wide. Each of the specimens tested was loaded laterally at the top slab level with concentrated forces applied equally to both walls. No axial forces were applied to the specimen.

The loading program for the first specimen consisted of three load reversals below the yield level of the coupling beams, followed by three reversals with sufficient intensity to yield all the coupling beams and both walls at the bases. This loading program was repeated on the repaired specimen and followed by eight more load reversals, four of which were of sufficient intensity to induce yielding of the strengthened beams between the third and sixth floors. The last four cycles yielded the remaining beams and developed the ultimate capacity of the walls.

Following are some of the main observations and conclusions from these tests:

(1) The flexible coupling beams in the first test resulted in a coupling action which provided only 10 percent of the base moment

capacity. This system behaved in a similar manner to two isolated walls, loaded side by side, after 25 percent of the ultimate load of the system was reached. Comparing the stiffness and strength characteristics of one of the piers of the coupled system to a comparable isolated wall tested previously [1.6], the initial stiffness of the coupled wall is approximately three times the stiffness of the isolated wall. After cracking and yield in a majority of the coupling beams, which occurred at 25 percent of the "system" yield load, the stiffness of the coupled wall is very close to the stiffness of the isolated wall. The maximum load applied at the top of each of the walls of the coupled system is approximately 5 percent larger than the ultimate load of the isolated wall.

The sequence of yield in the coupling beams was top beam, third-, fourth-, fifth- and second-floor beams, consecutively. These beams yielded within 30 percent of the system yield load. The first-floor beam yielded within 10 percent of the system yield load. Three load cycles at the full yield load of the system resulted in extensive damage to all the beams. A significant separation between the walls at the openings is reported, which was an indication of the "growth" of the coupling beams, accentuating their deterioration. At the end of this test, the walls exhibited widespread cracking, especially in the first three stories, with horizontal finely spaced flexural cracks on the boundary members and inclined cracks on the panels. The maximum nominal shear stress attained was $4.4\sqrt{f'_c}$ for the first test.

(2) The stiffer and stronger beams in the second test resulted in a coupling of 30 percent at the ultimate load. The overall stiffness and strength of each of the individual walls of this system were approximately 30 percent more than the stiffness and strength of a

comparable isolated wall, according to tests carried out previously on similar isolated walls. The sequence of yield in the beams was the fourth-, fifth-, third-, sixth-, second- and first-floor beams. Beam yield started at approximately 70 percent of the ultimate load and was concluded just prior to the failure load.

The specimen endured eight full load cycles at the ultimate load, corresponding to the yield of all the beams but the first-story beam. During the eighth cycle, web crushing of the compression wall occurred after yielding of the remaining first-story beam. The compression wall was subjected to 42 percent of its balanced axial load at the yield of all the beams. The tension wall exhausted 63 percent of its pure tensile yield capacity due to the beam shear forces at the yield of all the beams. The top deflection of the compression wall was 3.8 in. at web crushing. The comparable isolated wall had a maximum top deflection of 6 in., while failing through sliding shear. The maximum load applied to the coupled wall system at web crushing correspond to a nominal shear stress of $6.8\sqrt{f'_c}$ on each wall, based on 0.8 times the depth of the wall. The shear transfer from the tension wall should have increased the shear of the compression wall to a level substantially higher than $6.8\sqrt{f'_c}$.

The walls exhibited significant lateral expansion during the test because of lateral growth caused by the diagonal crack pattern.

(3) The most significant assessment on the results of the two tests is the adverse results of "over-coupling" walls under significant shear stress. Although even the extreme coupling of the test specimen contributed to only 30 percent of the base ultimate moment capacity as compared to 70 percent in the New Zealand tests, this was sufficient to limit the deformation capacity of the system significantly. Compared

with the test results on the isolated wall, the deformation capacity of the coupled system was only 63 percent of the isolated wall. The strength increase of each wall due to coupling, on the other hand, was only approximately 30 percent.

It appears that a "reserve" shear capacity is required in the shear design of the walls of a coupled wall system. This "reserve" shear capacity should be related to the strength of the coupling beams. Because of the shear transfer from the tension to the compression wall, a significant reduction in the deformation capacity may be caused by premature web crushing in the compression wall. Unless the walls have sufficient reserve shear capacity for expected transfers, or unless the gravity force magnitude is sufficient to overcome the uplift in the tension wall, strong coupling or even just light coupling may be detrimental to the seismic behavior of the system. The effects of the gravity forces (dead and live) were neglected in these tests. These effects appear to be extremely significant in influencing shear strength.

These conclusions increase the significance of the problem of assessing the actual shear capacity of an isolated wall when subjected to variable axial forces and to large deformation reversals. Without conceptual and reliable means of predicting the "true" shear capacity, a realistic coupled wall design is difficult unless large overstrength in shear is supplied.

1.2.4.4 The Earthquake Simulator Tests on Small Coupled Shear Wall Models

Four 1/12-scale, 10-story coupled wall systems [1.5] and six 1/12-scale, 6-story coupled wall systems [1.20] were tested on the earthquake simulator at the University of Illinois at Urbana-Champaign. One of

the six-story specimens was tested under static loading [1.20]. In addition to the analytical objectives of generating data for subsequent analytical investigations and verifying whether the observed structural responses justify the applicability of simple analysis and design schemes, a number of design parameters were studied.

The major design parameter in the first series of tests was the strength of the coupling beams. The overall aspect ratio of the walls was 5, while the span to depth ratio of the beams was 2.67. The specimens were designed with the "substitute structure" approach where the elements of the real structural members are modeled as linear elements with comprehensively computed flexural stiffnesses reduced by a "damage ratio" equivalent in concept to a "ductility ratio". In the design, damage ratios of 1 and 2 for the walls and the beams, respectively, were incorporated. An estimate of the viscous damping characteristics of the substitute structure was synthesized from the estimated hysteretic damping characteristics of the individual members. The resulting structural model, with distorted member stiffnesses and damping, was analyzed by the modal analysis technique utilizing a design spectrum for a maximum ground acceleration of 0.5 g. The members of the test specimen were then designed for the member forces obtained for the substitute structure.

To study the effects of increased beam strength, the beams of a test specimen were detailed with twice the reinforcement of the first three specimens. The four test structures were excited on the earthquake simulator by a series of compressed ground acceleration records of increasing damage potential. All the test structures survived the "design" base motion exceptionally well. Successive earthquakes of spectrum intensitites of approximately two and three times the design earthquake

resulted in extensive damage to the structures. Some of the main conclusions of the study are as follows:

(1) Significant reduction in the natural frequencies of all test structures, on the order of 50 percent or more, were observed as soon as the initial large deformation excursion occurred.

(2) For all test structures the displacement wave forms were similar to the structure base moment wave form. The displacement wave forms of different stories had maxima occuring at the same time.

(3) The apparent centroids of the lateral forces on the test structures corresponding to maximum base moment were located at 0.7 H or higher, where H is the height of the structure from the base.

(4) The damage in the first three specimens was concentrated at the ends of the connecting beams, particularly between levels three and six, after the tests. Spalling of the concrete on the exterior edges of the piers were observed. The fourth specimen with twice the flexural reinforcement in the beams had critical damage at the bases of the walls. For all test structures the nominal shear stress (total base shear divided by gross area of both piers) did not exceed $4\sqrt{f'_c}$.

In the second series of tests five 6-story coupled wall specimens of 1/12-scale were tested on the earthquake simulator. An additional specimen was tested under static loading. The major design parameters in these tests were the effects of beam strength and stiffness on the structural response. These specimens had an overall aspect ratio of 3.22 with span to depth ratios of the beams being either 1.67 or 2.5. The dynamic tests of the specimens were carried out in a manner similar to that of the first series of tests on 10-story coupled walls. The specimen with stiffer and stronger beams (span/depth ratio of 1.67, beam flexural steel ratio of 2.2 percent) failed by developing the full axial

tension capacity of the tension wall and the full flexural capacity of the compression wall.

The second group of specimens (span/depth ratio of 2.5 and beam flexural steel ratios of 1 percent) failed by developing hinges at the ends of all the beams and flexural yielding of the walls.

The third group of specimens was similar to the second group except that these specimens contained one-half the flexural reinforcement in the beams. Failure mechanisms were similar to the second group of specimens. Some of the conclusions of this study are as follows:

(1) The measured initial stiffnesses of the test structures were slightly less than the stiffnesses computed comprehensively by assuming cracked beams and cracked lower walls. The frequencies measured at the beginning of a test decreased to roughly one-half of these values at the end of a test.

(2) The maximum top level deflection observed during the test runs with a maximum base acceleration of 1 g was from 2.7 to 4.6 times the deflection calculated using a response spectrum and modal analysis and a completely uncracked structure.

(3) The relative contributions of higher modes to the base shear and moment increased with decrease in strength and stiffness of the connecting beams.

(4) The hysteretic relations for the connecting beams had a major effect on the overall hysteretic relation for the structure.

1.2.5 Analytical Research on R/C Coupled Structural Walls

A large number of investigations were carried out for linear analysis of coupled wall systems. The relevant studies in this context are noted by Park and Paulay [1.26]. A systematic effort to model and analyze these systems in the inelastic range was observed during recent years, which will be briefly reviewed in this section.

Santhakumar [1.32] has listed previous efforts on the analysis of reinforced concrete coupled wall systems and proposed a finite difference formulation for the elasto-plastic analysis of these systems, as part of his dissertation in Canterbury, New Zealand.

Mahin and Bertero [1.22] developed a computer code and analyzed a number of structures subjected to earthquake excitation. Using an equivalent plane frame idealization, they carried out nonlinear time history analyses of the Banco De America building in Managua and formulated a number of conclusions regarding the nonlinear response of its coupled wall system. One of the main conclusions regarded the influence of the coupling girders on the seismic response of the system; the time-histories of internal forces of most of these girders were observed to reflect a strong second mode response, which increased the number of shear reversals and yield excursions.

Takayanagi [1.37] at Urbana, studied the dynamic responses of two small scale ten-story coupled walls, which were tested on the shaking table [1.5] previously. The analytically generated data could, therefore, be checked by the experimental results. This enabled an assessment of the analytical modelling. Walls and the coupling beams were represented by one-dimensional line elements. Flexural beam elements were assumed to develop concentrated inelastic hinges at their

ends while the column (wall) elements were divided into a number of "subelements" in order to simulate the propagation of inelasticity for these members. Flexural, shear and axial nonlinearities, axial-flexural and flexural-shear interactions were also incorporated for the wall members. This permitted the study of the effects of these nonlinearities and interactions on the stiffness redistribution of moments and forces in the coupled walls. Different hysteresis characteristics were assumed for each action. A number of conclusions regarding the effects of these nonlinearities and interactions on the static and dynamic responses of coupled walls were reached as a result of monotonic quasi-static and dynamic analyses which were carried out.

The static analysis led to the following conclusions:

(1) The incorporation of inelastic axial deformations (stiffness) resulted in an approximately 15 percent reduction in the computed lateral stiffness. The same stiffness reduction was also simulated when a 60 percent reduction in the linear axial stiffness was considered in the analysis.

(2) The base shear redistribution was observed to start with cracking of the tension wall. The tension wall contributed to only 28 percent of the total base shear until yielding of the walls commenced. After yielding of both walls, the proportion of the shear in the tension wall was observed to increase again.

(3) The contribution of coupling action to the base moment resistance was observed to reduce from 71 percent to 55 percent as walls and beams cracked, beams yielded, and wall yielding was initiated.

The effects of hysteretic pinching and strength decay of the connecting beams on the dynamic response of the system were among the investigated variables. It was observed that these effects caused approximately 25 percent larger displacements and 10 percent lower wall shears.

No effect of these variables was observed on maximum moments.

A general nonlinear time-history analysis code, DRAIN-2D developed by Kanaan and Powell* at Berkeley, was adapted by a number of researchers to analyze frame-wall systems. Takayanagi, who continued his efforts at the P.C.A. [1.38], implemented a beam element in DRAIN-2D which had inelastic shear and flexural springs at each end, side by side. The effects of the change in axial force on the stiffness of these springs, however, were not incorporated. Analysis of a 20-story wall-frame system did not indicate a significant contribution of the shear-yield mechanism in the form that it was implemented in the analytical model.

Saatcioglu et al. [1.31], at the P.C.A., developed a degrading stiffness column element and implemented this in DRAIN-2D to represent the wall elements in modelling the coupled walls. Effects of a varying axial force on flexural yield level and post-yield stiffness were incorporated. Additional springs at the member ends represented shear yielding and decay, in addition to flexural inelasticity.

The incorporation of the effects of changes in axial force on flexural stiffness were observed to have significant effects in the seismic forces of the walls. In the case of strong coupling elements, the shear force in the compression wall was observed to increase as much as 50 percent when this effect was considered.

In a continuing study at M.I.T. on the seismic response of large panel precast concrete buildings [1.8], the program DRAIN-2D was used to carry out parametric studies of precast walls coupled by connectors. Some of this study's findings may be considered as applicable to the response of monolithicaly constructed reinforced concrete coupled shear walls. The walls were assumed to remain linear in this study while the connectors were modelled as nonlinear elements. Two

---

* See Ref. [2.6] in List of References, Chapter 2.

dimensionless parameters were devised to represent the topology of coupled wall systems. These parameters represented the overall geometry of the system and the ratio of coupling to wall stiffness.

After a parametric study including these geometric parameters, the strength of the coupling elements, earthquake motions and assumptions on hysteresis, a number of conclusions were reached regarding optimum connector stiffness and strength vs wall stiffness and strength.

The following conclusions are considered pertinent to the reported study.

The selection of the coupling stiffness at the threshold of the insensitive range - (i.e., - when any further increase in the coupling stiffness would not result in a proportional increase in the overall system stiffness), was suggested as the best choice for both serviceability and ultimate state responses.

The most important parameter governing the effectiveness of hysteretic damping for the coupled systems that were studied was observed to be the relative coupling strength. The optimum coupling strength leading to the best energy dissipation characteristics was evaluated to be a function of the stiffness characteristics of the wall configuration. Inelasticity of the coupling medium was observed to reduce linear base force demands in the order of 50% during response to an artificial ground motion, which was compatible with the design spectra of ATC-3 [1.40].

Work on precast walls with ductile connection schemes for earthquake resistance is continuing at M.I.T.

1.3 Research Needs in the Design of Wall-Frame Structures

A study of previous analytical and experimental research on medium-height to tall wall-frame and coupled wall-frame systems indicate a number of areas which require further investigation for a thorough understanding of the behavior and development of better guidelines for conceptual design of these systems. Some of these problem areas are relevant for both wall and coupled wall-frame structures while others are specifically related to coupled wall-frame structures. A brief discussion of these problem areas on wall-frame systems, considering both the state of the art and the state of the practice as represented by present seismic code regulations [1.40, 1.42],follows.

1.3.1 Topological Distinctions

At present, there is no existing guideline to distinguish between isolated walls in parallel, coupled walls, and isolated walls that are perforated. It has been observed that the response of different types of wall systems was significantly affected by the topological characteristics of the system.

An illustration is given in Fig. 1.1 where the prototypes are compared of coupled wall structures studied experimentally by several institutions. The significant differences in researchers' conceptions of a "medium-height to tall-coupled structural wall" are observed. The extreme differences in the topologies of these systems naturally result in different conclusions and design guidelines. There is a need to establish topological guidelines to define and to distinguish between isolated walls, coupled walls, and perforated walls. Depending on the designers' choice of these systems, different design guidelines should be followed. As an example, a well-confined interior edge member may

not be required in the case of a perforated wall, however, such a wall would require a different reinforcement detailing around the openings as compared to coupled walls. Another example would be design guidelines on the strength of the coupling members. To require the same contribution from the coupling action in the design of both coupled wall and perforated wall systems may lead to undesirable response characteristics for the coupled wall systems.

The state of the practice as reflected by current regulations [1.40, 1.42], contains no reference to coupled or perforated wall systems. Research is required, and the findings should be incorporated in codes, on assessing topological indexes which can distinguish between the different behavior patterns of isolated, coupled and perforated wall-frame systems. At present, codes impose height limitations for structural systems incorporating walls. Regardless of the type of wall considered -- isolated or coupled -- any building higher than 160 ft in Seismic Zone 4 is required by UBC [1.41, 1.42] to incorporate a frame capable of resisting at least 25 percent of the total lateral force for the building. Although more favorable to wall systems, ATC-3 [1.40] imposes similar height limitations for structural systems incorporating walls. Such height limitations should distinguish between the different types of structural walls-isolated or coupled, because of the significant differences in observed response characteristics.

1.3.2 Intensity of Earthquake Force

The intensity of the earthquake force is based on the structural system and building period (in addition to other factors), according to both the UBC [1.42] and ATC-3 [1.40] provisions. Both codes permit the computation of building period by an empirical expression based on

the height and base dimension of the structure only, i.e., the mechanical characteristics of the structural system is not incorporated explicitly in the computation of the period. The other major variable affecting the intensity of the seismic force is the structural system. While UBC [1.41, 1.42] prescribes a higher force coefficient for systems incorporating walls, ATC-3 [1.40] prescribes a higher force coefficient for the comparable frame system. In assessing earthquake force, neither distinguishes between the different types of wall systems. An evaluation of existing experimental data does not justify: (1) higher seismic force than frame wall systems; and (2) same seismic force for all types of wall systems.

1.3.3 Distribution of Earthquake Force along the Height of the Building

Code regulations [1.40, 1.41, 1.42] do not incorporate the different deformation characteristics of the wall-frame, coupled wall-frame, wall or frame systems in the distribution of force along the height of the building. Provisions regarding the distribution are different for UBC [1.41, 1.42] and ATC-3 [1.40] and both base the force distribution on the mass distribution only, disregarding the stiffness distribution over the height of the structure. This is equivalent to neglecting any wall-frame or wall-to-wall interactions in establishing the distribution of the lateral force. The actual distribution of lateral force may not be very important in the design of ductile moment resisting space frames since the shear capacity of the members of these frames are based on the actual ultimate plastic moment capacities at both ends of the members. This distribution, on the other hand, is relevant when the design of any type of wall system is considered, as the design moment to shear ratio at the base of the walls is based on this distribution. Any error in the distribution

may result in an underdesign in shear with respect to the flexural strength, leading to the possibility of early shear failure (diagonal shear failure or web crushing and sliding shear) before sufficient inelastic dissipation of energy by flexural yielding may take place.

1.3.4 Design Internal Forces of the Wall Systems

The design internal forces of the wall systems are established through linear (nominal) analysis with respect to the following provisions according to UBC [1.41, 1.42]: (1) Frames and walls shall resist the total force in accordance with their relative rigidities considering interaction, (2) Shear walls, acting independently of the frame, shall resist the total required lateral force, (3) The frame shall resist at least 25 percent of the total required lateral force. The ATC-3 [1.40] provisions include conditions (1) and (3) only. Consequently, the design shear, flexure and axial force for the wall system is obtained by analysis using a force distribution which, as discussed in 1.3.3, is not representative of the actual stiffness characteristics of the structure. Furthermore, the design forces computed with respect to condition (2) of UBC [1.41, 1.42] which usually control the design of the walls, do not incorporate interaction at all.

To reduce the possibility of early shear failure of walls, UBC provisions incorporate higher force and strength reduction factors for design against shear as compared to the design for axial-flexural behavior. ATC-3, however, incorporates the same force factor, while using a higher capacity reduction factor, in shear design as compared to the axial-flexural design. There is no guarantee, however that wall systems designed with either of these provisions (UBC, ATC-3) will not suffer shear failure before sufficient energy dissipation is realized through

inelastic distortion. The maximum shear and maximum axial force-flexure might occur at different times at the base of a wall system during earthquake excitation. For "impulsive" types of excitation, however, the times of occurrence of the maximum internal forces may be very close. Exhaustive research is urgently required to assess the possible values of maximum shear force associated with a certain design axial-flexural strength at the base of a wall system. Still another complication, in the conceptual design of wall systems, is the actual shear strength of a wall, as discussed subsequently.

1.3.5 Shear Design of the Wall Systems

The code [1.40, 1.41, 1.42] provisions regarding the shear design of walls do not incorporate the recent advances in the state of the art concerning information on the behavior and failure mechanisms of slender walls with effectively confined edge members. Code provisions are based on behavior of monotonically loaded beams. Conceptually shear design should incorporate the different shear resistance mechanisms, particularly the contribution of the edge members, in function of the expected maximum deformation levels and the level of axial force in accordance with the observed significance of these variables in the actual shear capacity of the walls. The present code approach of limiting the maximum shear strength in order to eliminate shear failure does not safeguard against shear failure, as the type of shear failure observed in tests of walls with confined edge members was found to be the "web crushing" type of failure. Web crushing was observed to depend upon the intensity; level of moment and shear and axial force, and their interaction; concrete strength; arrangement and spacing of web steel; number of load reversals; and the maximum level of deformation. Consequently, simply

limiting shear stress without incorporating the other variables cannot effectively safeguard against shear failure. Further research on the phenomenon of web crushing and subsequent incorporation in the code provisions on shear design of the research findings, is urgently required.

1.3.6 Problem Areas of Coupled Wall-Frame Systems

1.3.6.1 Analysis

The analysis of R/C coupled wall-frame systems is the topic of many published papers. Most of these papers have dealt with the linear analysis of these systems. The basic problem in such analysis is the mathematical modelling of the wall and connecting beam components. Laminar analysis, frame analysis, and finite element analysis, as well as elasto-plastic limit analysis techniques, have been proposed [1.32].

The main difference between a frame or an isolated wall-frame structure and a coupled wall-frame structure is the particularly high level of axial force in the coupled walls at the ultimate limit state. Especially because of present recommendations and code regulations [1.40, 1.41, 1.42], when high coupling girder stiffnesses are selected, the resulting flexural demands are also high as a consequence of linear analysis required by the code. The design, therefore, results in large flexural capacities for the girders. These girders develop large shear forces which contribute to significant tension and compression at the base.

At the ultimate limit state, the axial forces in the walls may be so large that the stiffness of the tension wall may be a small fraction of the stiffness of the compression wall. Consequently, the shear and flexure in the compression wall would be many times higher. This pattern of behavior may not be detected if linear analysis only is

carried out. A check of the ultimate limit state behavior by carrying out limit analysis should be implemented in the code for coupled wall structures. Overloading the compression wall should be avoided for desirable ultimate limit state behavior. As modern earthquake resistant design philosophy demands that: (1) stiffness; (2) strength; (3) stability; and (4) energy dissipation be distinct considerations in design, choosing high stiffnesses for coupling girders should not automatically result in large flexural strength for these girders.

The state of the art enjoins that research be conducted for a realistic simulation of the nonlinear earthquake response of coupled wall-frame structures. Areas requiring substantial research are: representation of the predominantly shear type of distortion of the inelastic wall components; the changes in flexural, shear, and axial stiffnesses due to fluctuating axial force; migration of the neutral axes of the wall components and the consequential effects of this on coupling girder demands; the spread of inelasticity, decay of hysteresis due to the effects of degrading bond and shear in the coupling girder and walls, and the effects of flexibility of the foundation. The problem of the three-dimensional coupled wall-frame interaction is especially accentuated because of the need for unusually significant force redistribution during inelastic response. A conceptual and tested mathematical model that would be capable of simulating such force redistributions between members is urgently required.

1.3.6.2 Proportioning

Research is urgently required to establish guidelines for initial proportioning and final design of the coupled wall systems. Both the states of the art and of practice (code) are quite advanced in the proportioning of frames and slab systems with established guidelines.

In the case of the coupled wall-frame systems, however, assessment of the optimum stiffness and strength of the coupling members with respect to the wall members remain as an unresolved problem. It was mentioned, previously, that the choice of coupling girder and wall dimensions may lead to isolated walls (along the same plane) a perforated wall or coupled walls. The behavior of each of these systems is different, hence, the final design considerations must also be different.

The present trend in establishing coupling girder stiffness is to base this stiffness on the overall stiffness of the coupled wall. It has been observed that there exists a threshold for coupling stiffness after which the overall stiffness of the coupled wall system does not increase considerably [1.8]. It appears suitable to choose such a coupling girder stiffness for high overall stiffness as an initial design iteration. However, when the strength of the coupling girders and the variation in this strength over the height of the structure are considered, it can be seen that research is needed to establish guidelines regarding these problems. These guidelines will have to be based on the topology of the structure, as discussed earlier. In general, the coupling girder strengths for a coupled wall system should be determined based on the maximum desirable compression and on the maximum tolerable resulting tension that can be developed in the walls at the ultimate limit state. It appears advisable to avoid any net tension force so that the compression wall may not be burdened by excessive shear and flexural transfer from the tension wall. It is also desirable that the walls not be under excessive compression so that part of the unconfined concrete of the wall panel is not crushed, particularly under the axial-flexural action on the wall. The state of the practice (code) is especially critical concerning the design of

coupled wall systems. The significant differences between the demands in the coupling beams and those in the regular frame beams should be recognized and incorporated in the code.

1.4 Objectives and Scope of Research

The objectives and scope of research on tall reinforced concrete coupled structural wall-frame structures at U.C. Berkeley proceeds from the assessment of the states of the art and practice (code) on the design of these structures as reported in Section 1.3. Since 1975 integrated analytical and experimental research on this subject has been in progress -- objectives of this analytical research are summarized as follows:

1.4.1 Design of Experiment

The foremost objective of these analytical studies has been to generate data to plan and conduct experimental research on the mechanical behavior, with particular emphasis on the hysteretic behavior, of coupled wall systems. Selection and design of prototype structures, design of the test facility, selection of the basic experimental parameters, design of the instrumentation and data acquisition systems were all carried out based on analytically generated data. Establishment of the major experimental parameters to be investigated and of loading histories is based on analytical research carried out under this context.

1.4.2 Magnitude and Distribution of Seismic Forces

The analytical phase of research also aims to generate information on realistic seismic force magnitudes and distributions during the earthquake response of frame-coupled wall structures. The basic variables affecting distribution, structural topology; main response or limit

states (serviceability, damageability and collapse); and the ground acceleration record will be considered.

1.4.3 Development of Models

An objective of the analytical studies is to seek improvements to the present modelling techniques in conjunction with available computer codes.

1.4.4 Conceptual Design

In view of the states of the art and code on the design of coupled wall systems, a major and ultimate objective of the analytical studies, in conjunction with the findings of the experimental studies, is to develop a conceptual design process for the medium-height to tall frame-wall structures. This process is expected to involve provisions on system and structural layout selection; initial proportioning of components; magnitude and distribution of lateral force, analysis, flexural-axial, and shear design; and detailing of the components and their joints and supports.

Some of these stated objectives have been already achieved and are incorporated in this interim report. Detailed results of continuing experimental work will be in successive reports and subsequent progress will be included in the final report. A listing of the experimental objectives of the research follows.

1.4.5 Shear Resistance Mechanisms

One experimental objective is related to obtaining better identification and quantitative information on the shear resisting mechanisms of barbell shaped walls with effectively confined edge columns.

A test frame which is suitable to test replicas of the edge members of the coupled wall specimens has been designed and built. Edge column

segments will be loaded with representative axial force and lateral shear histories to obtain information on the actual shear, and shear-flexural capacity of these members in function of their axial forces.

Another study area in this context is the web crushing phenomenon. This phenomenon will be studied during the tests of the coupled wall subassemblages by extensive internal and external instrumentation of the critical regions of the wall panels. The experimental findings from both the edge member and panel shear capacity studies will be assessed and complemented by analytical studies.

1.4.6 Proportioning

The effects of different coupling stiffness and strength as related to the wall stiffness and strength will be studied. The consequence of different detailing patterns for coupling members is planned as a variable in the experimental investigation.

1.4.7 Redistribution

Shear and moment redistribution will be assessed quantitatively during model testing by means of special force transducers in the coupling elements. The effects of coupling on the amount of redistribution will be studied.

1.4.8 Foundation Flexibility

The effects of foundation flexibility on the overall response of the coupled wall systems is another experimental objective to be complemented by analytical studies.

REFERENCES

1.1 Abrams, D. P., Sozen, M. A., "Experimental Study of Frame-Wall Interaction in Reinforced Concrete Structures Subjected to Strong Ground Motions," Civil Engineering Studies, SRS No. 460, University of Illinois at Urbana-Champaign, May 1979.

1.2 Aktan, A. E., "Earthquake Response of Beams Reinforced by Straight and Full Length Diagonal Bars," Faculty of Engineering, Department of Civil Engineering, Middle East Technical University, Ankara, Turkey, September 1978.

1.3 American Iron and Steel Institute, Earthquakes, 1975.

1.4 Aristizabal-Ochoa, J. D., Shiu, K. N., and Corley, W. G., "Effects of Beam Strength and Stiffness on Coupled Wall Behavior," Proceedings of the Second U.S. National Conference on Earthquake Engineering, Stanford University, Stanford, California, August 22-24, 1979, pp. 323-332.

1.5 Aristizabal-Ochoa, J.D., and Sozen, M. A., "Behavior of Ten-Story Reinforced Concrete Walls Subjected to Earthquake Motions," Civil Engineering Studies, SRS No. 431, University of Illinois, Urbana-Champaign, October 1976.

1.6 Aristizabal-Ochoa, J. K., et al., "Earthquake Resistant Structural Walls - Tests of Coupled Wall Systems," Report to NSF, under preparation, Portland Cement Association, Skokie, Illinois.

1.7 Barney, G. B., et al., "Earthquake Resistant Structural Walls - Tests of Coupling Beams," Report to NSF (RANN), submitted by Portland Cement Association, Research and Development, Construction Technology Laboratories, January 1978.

1.8 Becker, J. M. and Mueller, P., "Seismic Response of Large Panel Precast Concrete Buildings," Advanced Design Concepts Seminar, PCI Convention, October 14-18, 1979, Dallas, Texas.

1.9 Bertero, V. V., "Seismic Behavior of Structural Concrete Linear Elements (Beams, Columns) and their Connections," State-of-the-Art Report, AICAP-CEB Symposium on Structural Concrete under Seismic Actions, Rome, May 1979, Bulletin D'information No. 131, C.E.B., April 1979.

1.10 Bertero, V. V., (Organizer), "Earthquake-Resistant Reinforced Concrete Building Construction," Proceedings of a Workshop Held at the University of California, Berkeley, California, July 11-15, 1977 (In 3 Volumes).

1.11 Bertero, V. V., Popov, E. P., and Wang, T. Y., "Hysteretic Behavior of Reinforced Concrete Flexural Members with Special Web Reinforcement," Report No. UCB/EERC 74-9, Earthquake Engineering Research Center, University of California, Berkeley, 1974.

1.12 Bertero, V. V., "Seismic Behavior of R/C Wall Structural Systems," Paper presented at the VIth World Conference on Earthquake Engineering, Istanbul, Turkey, 1980.

1.13 Building Research Institute, "Report on the Damage by 1978 off Miyagi Prefecture Earthquake," Report No. 86, February 1979 (in Japanese).

1.14 Comision Presidencial para el Estudio del Sismo, "Secunda Fase del Estudio del Sismo Ocurrido en Caracas el 29 de julio de 1967," Ministerio de Obras Publicas, Caracas, Venezuela, 1978, Vols. A and B.

1.15 Earthquake Engineering Research Institute, "Reconnaissance Report, Miyagi-Ken-Oki, Japan, Earthquake, June 12, 1978," Berkeley, California, December 1978.

1.16 Earthquake Engineering Research Institute, "Managua, Nicaragua, Earthquake of December 23, 1972," Conference Proceedings, San Francisco, California, November 29-30, 1973, Vol. II.

1.17 Iliya, R., and Bertero, V. V., "Effects of Amount and Arrangement of Wall-Panel Reinforcement on Hysteretic Behavior of Reinforced Concrete Walls," Report No. UCB/EERC 80-04, Earthquake Engineering Research Center, University of California, Berkeley, 1980.

1.18 International Symposium on the February 4th, 1976, Guatemala Earthquake and the Reconstruction Process, Proceedings, Guatemala, May 1978, 2 Vols.

1.19 Jennings, Paul C., Editor, "Engineering Features of the San Fernando Earthquake, February 9, 1971," Report No. EERL 71-02, Earthquake Engineering Research Laboratory, California Institute of Technology, Pasadena, California, June 1971.

1.20 Lybas, J. M., and Sozen, M. A., "Effect of Beam Strength and Stiffness on Dynamic Behavior of Reinforced Concrete Coupled Walls," Civil Engineering Studies, SRS No. 444, University of Illinois, Urbana-Champaign, July 1977.

1.21 Ma, S.-Y. M., Popov, E. P., and Bertero, V. V., "Experimental and Analytical Studies on the Hysteresis Behavior of Reinforced Concrete Rectangular and T-Beams," Report No. UCB/EERC 76-2, Earthquake Engineering Research Center, University of California, Berkeley, 1976.

1.22 Mahin, S. A., and Bertero, V. V., "An Evaluation of Some Methods for Predicting Seismic Behavior of Reinforced Concrete Buildings," Report No. UCB/EERC 75-15, Earthquake Engineering Research Center, University of California, Berkeley, 1975.

1.23 Murphy, Leonard M., Scientific Coordinator, "San Fernando, California, Earthquake of February 9, 1971," U.S. Dept. of Commerce, 1973, Vol. I, Parts A and B.

1.24 Newmark, N. M., and Rosenblueth, E., "Fundamentals of Earthquake Engineering," Prentice Hall, Inc., 1971.

1.25 Oesterle, R. G., et al., "Earthquake Resistant Structural Walls - Tests of Isolated Walls - Phase II," Report to NSF submitted by Construction Technology Laboratories, P.C.A., October 1979.

1.26 Park, R., and Paulay, T., Reinforced Concrete Structures, John Wiley & Sons, Inc., 1975.

1.27 Paulay, T., "Coupling Beams of Reinforced Concrete Shear Walls," Proceedings of a Workshop on Earthquake Resistant Reinforced Concrete Building Construction (V. V. Bertero, Organizer), July 11-15, University of California, Berkeley, Vol. III - Technical Papers, pp. 1452-1462.

1.28 Paulay, T., and Binney, J. R., "Diagonally Reinforced Coupling Beams of Shear Walls," Publication SP-42, Shear in Reinforced Concrete, ACI, Detroit, Michigan, 1975.

1.29 Portillo Arriola, Rodolfo, Coordinator, "15 Estructuras Formales, Su Comportamiento durante el Terremoto del 4 de febrero de 1976 en Guatemala," Facultad de Arquitectura de la Universidad de San Carlos, Guatemala.

1.30 Recommended Lateral Force Requirements and Commentary, Seismology Committee, Structural Engineers Association of California, 1975.

1.31 Saatcioglu, M., Derecho, A.T. and Corley, W. G., "Coupled Walls in Earthquake-Resistant Buildings, Report to NSF, by Construction Technology Laboratories, Portland Cement Association, Skopie, Illinois, June 1980.

1.32 Santhakumar, A. R., "Ductility of Coupled Shear Walls," Thesis presented for the degree of Doctor of Philosophy in Civil Engineering, in the University of Canterbury, Christchurch, New Zealand, October 1974.

1.33 Scribner, C. F., and Wight, J. K., "Delaying Shear Strength Decay in Reinforced Concrete Flexural Members under Large Load Reversals," Report UMEE 78 R2, Department of Civil Engineering, University of Michigan, May 1978.

1.34 Sozen, M.A., "Engineering Report on the Caracas Earthquake of 92 July, 1967," National Academy of Sciences, 1968.

1.35 Sozen, M. A., "Structural Damage Caused by the Skopjie Earthquake of 1963," Report to the Committee on Masonry and Reinforced Concrete of the American Society of Civil Engineers and the American Concrete Institute, University of Illinois, Urbana, Illinois, January 1964.

1.36 Sozen, M. A., and Roesset, J., "Structural Damage Caused by the 1976 Guatemala Earthquake," Civil Engineering Studies, SRS No. 426, University of Illinois, Urbana-Champaign, Illinois, March 1976.

1.37 Takayanagi, T. and Schnobrich, W.C., "Computed Behavior of Reinforced Concrete Coupled Shear Walls," SRS Report No. 434, University of Illinois at Urbana-Champaign, December 1976.

1.38 Takayanagi, T., Derecho, A. T., and Corley, W. G., "Analysis of Inelastic Shear Deformation Effects in Reinforced Concrete Structural Wall Systems," CSCE-ASCE-ACI-CEB, International Symposium on "Nonlinear Design of Concrete Structures," University of Waterloo, Waterloo, Ontario, August 7-9, 1979.

1.39 Taylor, R. G., "The Nonlinear Seismic Response of Tall Shear Wall Structures," Research Report 77-12, Department of Civil Engineering, University of Canterbury, Christchurch, New Zealand, November 1977.

1.40 Tentative provisions for the Development of Seismic Regulations for Buildings prepared by the Applied Technology Council (ATC 3-06), 1978.

1.41 Uniform Building Code, 1973 Edition, International Conference of Building Officials, Whittier, California.

1.42 Uniform Building Code, 1979 Edition, International Conference of Building Officials, Whittier, California.

1.43 Vallenas, J. M., Bertero, V. V., and Popov, E. P., "Hysteretic Behavior of Reinforced Concrete Structural Walls," Report No. UCB/EERC-79/20, Earthquake Engineering Research Center, University of California, Berkeley, 1973.

1.44 Wang, T. Y., Bertero, V. V., and Popov, E. P., "Hysteretic Behavior of Reinforced Concrete Frames Walls," Report No. UCB/EERC 75-23, Earthquake Engineering Research Center, University of California, Berkeley, 1975.

1.45 Wight, J. K., and Sozen, M. A., "Strength Decay of R/C Columns under Shear Reversals," Journal of the Structural Division, ASCE, Vol. 101, No. ST 5, May 1975.

1.46 Wood, Fergus J., Editor-in-Chief, "The Prince William Sound, Alaska, Earthquake of 1964 and Aftershocks," U.S. Dept. of Commerce, 1967, Vol. II.

1.47 Wright, Richard N., and Kramer, Samuel, "Building Performance in the 1972 Managua Earthquake," NBS Technical Note 807, U.S. Dept. of Commerce, November 1973.

2. PRELIMINARY WORK FOR EXPERIMENTAL RESEARCH

2.1 General

To achieve the experimental phase of the research on seismic behavior of R/C coupled structural walls, the preliminary work presented in this chapter was undertaken. This work was initiated in 1975 and will be briefly summarized here. An intermediate in-house report on this work was produced by Li [2.7].

The main objectives of the preliminary studies were to investigate possible quasi-static testing schemes for R/C coupled structural wall specimens, to select the scheme most feasible in view of a large number of considerations and constraints, and to design the appropriate test facility. These investigations were carried out by incorporating a number of possible prototype structures.

Since generally it is the medium-tall to tall structures (6-7 floors and up) that are commonly designed with structural walls, and since the story height for such structures varies between 9- and 12 ft, testing of a large scale (min. 1/3) complete structural system was not possible with existing facilities. Because a prime constraint was to maintain a sufficiently large scale to reproduce important detailing and use of deformed bars, it was decided to test a subassemblage of the lower stories of a number of selected prototype structures.

The careful assessment of possible force and geometric conditions which the missing sections of the structure would impose during response, and the representation of these eliminated parts, prove to be the main difficulties in testing such a subassemblage. However, carefully planned subassemblage testing, successful in earlier studies [2.5, 2.18, 2.19] makes large scale model study economically feasible.

Previous analytical and experimental studies on coupled structural wall systems (Chapter 1), indicate that inelastic deformations (critical regions), are generally confined to the ends of the coupling beams and the bases of the walls. One criterion in the selection of a subassemblage for test purposes, is to include the critical regions of the structural system (or sub-system), as in the case of the coupled wall system isolated from the total structure in the test subassemblage. Another significant criterion is the scale, in conjunction with the dimensions of the prototype system, which determines the dimensions of any subassemblage and its compatibility with available test space. A scale of one-third was determined to be the appropriate scale where regular deformed reinforcing bars were used as the main reinforcement in the model. This scale also permitted the use of a realistic gradation of concrete.

A 4-story, 3-bay coupled wall subassemblage was determined to be the typical model, in accordance with: a scale of one-third, available test space, and dimensions of prototype coupled wall systems which had been studied. Such a subassemblage does not include all the regions of inelasticity which occur at the ends of all the coupling beams of the structure. However, the first four beams provide a sufficient number of beam specimens for a study of beam behavior and its effects on the overall behavior of the structure. Previous analytical and experimental studies [2.2, 2.14] have indicated that, in general, beams at the second and upper floors develop plastic hinges almost simultaneously and are subjected to similar demands. The second-, third- and fourth-floor beams of the subassemblage, therefore, provide a sufficient number of beam specimens with behaviors representative of the expected behavior of upper floor beams not included in the subassemblage.

Testing a subassemblage is equivalent in concept to studying a free body of a structure. Similar to the "free body" problems in statics, the force and geometric boundary conditions, as well as the loading conditions of the subassemblage, should be reproduced in order to be faithful to the complete structure, i.e., the prototype. It is, therefore, implied that the model subassemblage will be after a prototype structure.

Although examples in model testing without any established prototype structure are common [2.2, 2.10], relating the model to a specific prototype may be required if, (1) A subassemblage is being tested, (2) Consequences of certain design provisions (detailing problems incorporating bond, anchorage, splicing, etc.), are sought. Such provisions may not be directly applied to the design of a model without interpretation on the design of a prototype. In addition to the above, if analytical time-history analyses of the model are to be carried out, it is usually more credible to study the prototype and interpret the results on the model. If the model is subjected to earthquake effects, analytically, the length scale of the model should be incorporated in a time scale adjustment of the recorded ground motion. The consequences of this adjustment on the nonlinear response of a R/C model are not explicit. On the other hand, analytical response time-history studies of the model without the time scale adjustment of recorded ground motion may have credibility problems.

A number of possible prototype structures were investigated for the initial test specimen and for the test facility design. A 15-story office building was selected for a complete prototype study -- details are presented in the next section.

2.2 The Prototype Structure

2.2.1 General

The 15-story prototype selected for the first test series will have a "dual" structural system, with two symmetric coupled walls and eight frames along the N-S direction, and four frames (two of them incorporating walls), along the E-W direction. The typical floor plan and elevation are shown in Fig. 2.1.

According to the Uniform Building Codes [2.16, 2.17], buildings more than 160 feet in height are required to have ductile moment resisting space frames capable of resisting not less than 25 percent of the required seismic forces for the structure as a whole. To use a horizontal force factor "K" of "0.8" in establishing the earthquake loading of this structure (along the N-S direction), the ductile moment resisting space frame and shear walls should be designed with the following criteria (Table No. 23-I, UBC [2.16, 2.17]):

(1) The frames and shear walls shall resist the total lateral force in accordance with their relative rigidities considering the interaction of the shear walls and frames.

(2) The shear walls, acting independently of the ductile moment resisting space frame, shall resist the total required lateral forces.

(3) The ductile moment resisting space frame shall have the capacity to resist not less than 25 percent of the required lateral force.

Different structural systems in zones of lesser seismic risk are accepted by the UBC if higher horizontal force coefficients are used. However, in Zone 3 (UBC-73) or Zone 4 (UBC-79), a structural system incorporating walls over 160 ft in height can only be designed in accordance with the criteria prescribed in conjunction with the horizontal force factor of 0.80.

A preliminary design of the floor system with respect to serviceability requirements of the UBC-73 resulted in a 6 in. slab thickness and 24 by 15 in. beams in both directions. The frame columns and wall edge members were proportioned initially against the gravity and code lateral loading. The two identical coupled wall systems along the N-S direction are the subjects of this study. There are no established guidelines to proportion and the walls and the coupling beams.

The wall thickness is an important parameter contributing to the shear strength as well as the deformation capacity of a wall. Tests on isolated walls have indicated that web crushing was the basic mechanism through which walls with confined edge members reached their deformation capacities [2.10]. Thickness of the wall, therefore, is a design variable requiring careful assessment. The thickness of 12 in. was based on the minimum thickness requirements of UBC [2.16, 2.17] for stability purposes. This thickness resulted in a shear stress of 5.6 $\sqrt{f'_c}$ under factored earthquake base shear prescribed by UBC-73 [2.16].

Proportioning the coupling beams is a task of significant consideration. Elastic analysis in conjunction with code prescribed lateral loading is generally used to design the coupling beams. Consequently, the stiffer these beams, the larger the computed flexural demands, which results in a flexurally strong beam design. Thus, proportioning the coupling beams for increased stiffness also produces increased flexural strength, which could lead to undesirable behavior of the walls.

There are different approaches to the initial proportioning of the coupling beams. One approach concentrates on the "stiffness" aspect of the design and relates the coupling beam dimensions to the overall stiffness of the coupled wall system [2.3]. This overall stiffness may

be expressed as a percentage of the stiffness of a hypothetical "solid" wall where the openings are assumed not to exist. In this manner, the dimensions of the coupling girders may be related to the stiffness of the coupled wall system expressed as a percentage of the stiffness of a hypothetical solid wall. The pertinent computations are shown in Appendix 2.1 and the results are illustrated in Fig. 2.2, indicating that it is possible to attain 79 percent of a solid wall stiffness with coupling beam dimensions of 24 x 48 in.. Any increase in the coupling beam dimensions does not result in a substantial increase in the coupled wall stiffness.

A second consideration in choosing coupling girder sizes should be its a/d ratio. The smaller the a/d ratio the more difficult it becomes to maintain desirable hysteretic characteristics by conventional reinforcement detailing. The a/d ratio corresponding to the 24 x 48 in. section dimensions is 1.87. If the section were chosen as 30 by 52 in., to yield 84 percent of the corresponding solid wall stiffness, the a/d ratio would be 1.70.

For the coupling girders of the prototype, section dimensions of 24 x 48 in. were thus selected. The resulting percentage of the stiffness of a corresponding solid wall, 79 percent, is in fact an unrealistic figure because it is based on linear (uncracked) behavior. Experimental studies [2.14] have shown that the actual effective stiffness of a coupled wall is considerably less than the stiffness computed by assuming uncracked gross section dimensions. The 79 percent figure is only a relative quantity for comparing the effects of various girder dimensions.

Although it is not required by any existing code provision, the preliminary proportioning of the wall and coupling girders should also

be checked for the expected ultimate limit state behavior before concluding the design. Since the coupling beams are proportioned for stiffness and then designed for flexural demands based on nominal (linear) analysis, the large flexural capacities incorporated in these beams lead to large shear forces. These shear forces accumulate and constitute the coupling axial forces at the base of the walls. The coupling forces are maximum when all beams yield and reach ultimate capacities at both ends. The maximum tension and compression that can be developed at the base of the walls should be checked on the failure envelope of the wall cross sections (axial load-bending moment interaction diagram for limit state). If the tension is sufficient to cause a substantial reduction in the (shear and flexural) stiffness of the tension wall, this is an indication that significant shear and moment redistributions from this wall to the compression wall may be required. Furthermore, the development of tensile cracks in the wall may lead to significant reduction in shear resistance of the wall.

If the compression axial force (due to coupling and gravity forces) in the compression wall is close to the balanced load level for this wall, the compression wall may not have the required deformational capacity, i.e., the overall required ductility. If such assessments lead to an unfavorable appraisal of the wall behavior at the ultimate limit state, the detailing of reinforcement of the coupling girders (amount of reinforcement and grade of reinforcement), and in some cases, the selected girder dimensions, should be revised.

Another problem in proportioning the coupling girders with stiffness considerations only, is the restricted available curvature capacity of a stiff section (with respect to a smaller section with similar reinforcement percentage). As the coupling girders are subjected to rotation demands far exceeding a frame girder with similar dimensions, the available rotation (or curvature) capacity of the girder, which is proportioned for stiffness and designed for demands based on linear analysis, may not be

sufficient for the expected deformation levels of the structure at the ultimate limit state. This may lead to rupture of the reinforcing bars of the girders before the walls attain their capacity at the base.

The optimum balance between stiffness, strength and deformational capacities of the coupling beams is an important parameter affecting the behavior of coupled walls and will be studied.

2.2.2 Design of the Prototype

After an initial proportioning of the coupled wall system including beam dimensions, the prototype was designed according to both the 1973 and 1979-UBC provisions. There are significant differences in these provisions in the computation of base shear, the distribution of lateral forces and the shear design force factor. Details of the computations are given in Appendix 2.2. The resulting design base shears are 774 kips for the 1973-UBC provisions and 999 kips for the 1979-UBC provisions. Distribution according to the lateral forces of both these code provisions is given in Table 2.1.

The coupled wall system was analyzed under the code prescribed lateral loadings using the linear analysis program, TABS [2.20]. Results of these analyses are given in Table 2.2 and 2.3. The coupling girders were designed in three groups or as indicated in this table. Design computations for the walls and the girders are given in Appendix 2.2, and the resulting member details are shown in Figs. 2.3 - 2.7. The nominal strength of the materials was 4000 psi for concrete and 60 ksi for steel.

An important aspect in design is the detailing of the edge members of the walls. Linear analysis in conjunction with code prescribed loadings result in considerably smaller demands for the interior edge columns than for the exterior edge columns. As the coupling beams are

subjected to inelastic rotation reversals and start losing their flexural capacity (decay), the interior edge columns are computed to pick up increasing forces. In the limit state, when the beams lose all flexural capacity at both ends, the interior edge columns have been observed to have demands identical to the exterior edge columns. Furthermore, once the wall panel starts to fail, the existing interior edge members become even more important in avoiding brittle failure. In view of the importance of well-confined strong edge columns on the ultimate limit state behavior of the walls, it was decided to detail interior edge columns similar to the exterior edge columns. The premature interior edge column failure observed in New Zealand tests [2.14] is another factor in favor of similar detailing of interior and exterior edge columns of the coupled walls. Whether the interior columns do need similar detailing as the exterior columns is one of the parameters which will be investigated further.

An important consideration in design is the detailing of the coupling beams. Three types of connecting beams were designed for both 1973 and 1979-UBC provisions, as shown in Table 2.3. More than one alternative is presented for the detailing of each type of beam. In some of these alternatives, #12 bars are used for main reinforcement. Although a #12 bar is not manufactured, this will correspond to a #4 bar in a 1/3-scale model which is available. This was the reason for using #12 bars.

Note that in the detailing of the web reinforcement it was intended to provide, if possible, a lateral restraint to each longitudinal bar. This resulted in the need to provide considerably more lateral reinforcement than required by the shear demand. Restraining <u>each one</u> of the individual flexural bars at each tie application is <u>not</u> a code requirement. If the <u>same</u> number of flexural bars at top and bottom is used, the detailing of the web reinforcement is facilitated.

Anchorage of beam bars is a prime concern in the design. Although

details for this anchorage were not prepared for the prototype, they were drafted for the 1/3-scale model, as presented and explained in Section 2.3. The best anchorage for these bars can be maintained by continuing the bar into the wall, rather than bending them in the edge members of the wall. As the wall thickness is generally less than the beam thickness, it is not possible to continue all the beam bars unless the wall is thickened at the beam level.

Such detailing has been common in Japanese practice and is claimed to have significant advantages, not only for the anchorage of the beam bars, but also to redistribute stress in the wall panel and possibly to help delay web crushing. For this reason, a test with such detailing is also contemplated as a part of the planned experimental program.

During the design of the prototype, the main differences in the 1973- and 1979-UBC provisions regarding the design of structures incorporating shear walls were observed to be in: (1) magnitude of the "E" load, (2) the distribution of the "E" load, and (3) the force factor in computing the design shear force of the walls.

The total base shear, moment to shear ratio of prescribed "E" loading at the base and the design shear force of one coupled wall, were respectively: 774 kips, 68% of height, 1275 kips according to the 1973-UBC provisions; and, 999 kips, 71% of height, 1179 kips according to the 1979-UBC provisions. Consequently, the flexural reinforcement of the average coupling girder is 28 percent larger and the main flexural reinforcement of the walls is 50 percent larger in the 1979-UBC designed system than in the 1973-UBC designed system. Furthermore, the wall shear reinforcement in the 1979-UBC designed system is 17 percent less than in the 1973-UBC designed system.

The differences between the relevant provisions of the 1973 and 1979-UBCs are extremely significant, as indicated by the corresponding differences in outcomes. The increase in the flexural steel of the walls and the beams are especially consequential in the ultimate limit state response of the walls.

Assuming that the desirable ultimate limit state mechanism (where plastic hinges form at the ends of all the beams and the bases of the walls) is realized for both 1973-UBC and 1979-UBC designed systems, the shear accompanying this mechanism is computed to be 30 percent larger in the 1979-UBC designed system. Since the deformation capacity of the walls is limited by the crushing of the panel, which in turn is affected by the amount of shear stress, the 1979-UBC designed wall should be expected to have less deformation capacity than the 1973-UBC designed wall. Furthermore, the wall axial forces in the 1979-UBC designed wall will be larger due to the increased flexural reinforcement of the beams. This is another factor that will constrain the deformation capacity of the 1979-UBC designed wall as compared to the 1973-UBC designed wall.

The desirable ultimate limit state mechanism may not be realized at all. In certain cases, the tension wall may fail through tension, with insignificant plastic moment capacity, depending on the level of axial force that may be developed due to the coupling action. The deformation capacity of such a wall would be much less. Another factor which could impair the ultimate limit state deformation of a coupled wall system, is premature failure or severe degradation in the connecting beams before the walls reach ultimate capacity. A critical assessment of the 1973-UBC and the 1979-UBC provisions regarding the analysis and design of reinforced concrete systems incorporating coupled walls indicates that: (1) there are

significant shortcomings in both of these codes, (2) 1973-UBC provisions result in a coupled wall with a larger deformation capacity than the 1979-UBC provisions. The latter, however, results in a wall which has approximately 30 percent more flexural capacity.

A number of questionable specifications related to the UBC provisions on the analysis and design of tall, reinforced concrete structures incorporating walls were listed in the previous chapter. This list will be briefly repeated as several shortcomings were consequential in the resulting prototype design. Some of the observed deficiencies in the code were compensated for during the design by improving the code prescribed detailing. These are indicated in Appendix 2.2. Certain questionable specifications in design provisions, however, were deliberately incorporated into the final design, since a chief objective of the research was to investigate the soundness of the code provisions.

(1) The code provisions, defining the horizontal force coefficient for different structural systems, are not justified in prescribing higher force coefficients for all buildings with any type of wall system (Table 23-I) over those of the DMRSF's.

(2) The provisions requiring walls be designed to resist all the seismic lateral forces, and a DMRSF system, capable of withstanding at least 25 percent of the lateral load in all buildings (in Zone 3 or 4) over 160 ft in height, are questionable because they are not based on the real response of the structural system.

(3) The prescribed distribution of lateral force along the height is not realistic as it does not distinguish between the different deformation characteristics of frame, wall-frame, coupled wall-frame, and other systems.

(4) The shear force for which the walls shall be designed is not based on the actual flexural strength provided to the wall and on a realistic moment to shear ratio. To provide for a higher safety against shear failures, the load factor for shear design is prescribed higher than the load factor for flexural design. This higher load factor does not guarantee prevention of shear failure in the real structure, particularly in the case of 1979-UBC code in which this factor was decreased by 40 percent as compared to 1973-UBC.

(5) The shear design provisions are not based on recent experimental data on the shear strength and post-yield behavior of walls with effectively confined edge members. Present shear design provisions are similar to those obtained from observed behavior of beams under monotonic loading. The shear carrying mechanism of walls with confined edge members was observed to be different from that of beams under monotonic loading.

(6) There are no guidelines that will aid the designer in the proportioning of coupling girders. As linear analysis with the prescribed lateral loading is required to establish demands of these girders, stiffer girders attract more flexural strength. Consequently, the designer cannot design for stiffness and strength individually, but has to provide whatever strength is demanded by the selected stiffness. This does not necessarily result in better design.

(7) The designer is not required to check the ultimate limit state response of the wall. It is possible to design a structure that may not attain a desirable ultimate limit state mechanism. The wall axial loads at the ultimate limit state should be checked and assessed to determine whether the required shear and flexural strength can actually be developed under the possible existing axial forces. Code provisions that assure a ductile ultimate limit state mechanism for

coupled wall systems are lacking.

(8) The confinement requirements for coupling girders can be insufficient, particularly for short girders ($a/d \leq 2$). Because these girders can be subjected to significantly more critical demands than frame girders, (higher shear and larger number of deformation reversals) there should be special provisions for their design and detailing.

The 1973-UBC designed coupled wall system was selected as the one to be used in the first series of analytical and experimental studies, as it was assessed to possess more favorable ultimate limit state behavior. The 1979-UBC designed system, as well as an ATC 3-06 [2.15] designed system, are contemplated as possible subjects of subsequent analytical and experimental studies.

2.2.3 Ultimate (Maximum) Strength of the Prototype Coupled Wall System In Accordance with the 1973-UBC Provisions

The coupled wall system designed with 1973-UBC provisions was selected as the subject for the first series of analytical and experimental studies. Relative to the system designed with 1979-UBC provisions, this selected coupled wall system was assessed, in Section 2.2.2, as having more favorable ultimate limit state response characteristics.

The maximum strength of the 1973-UBC designed coupled wall system may be estimated by assuming that the ultimate limit state will be attained by developing a sufficient number of plastic hinges for a collapse mechanism, as shown in Fig. 2.8. This strength is required for two purposes: (1) to estimate the ultimate strength of the model, needed in order to design the experiments; and (2) to assess the consequences of the design carried out with respect to the 1973-UBC provisions. In general, it should also be assessed whether such a collapse mechanism can be attained, i.e., depending on the proportioning and reinforcement detailing of the members, the assumed collapse mechanism may not be realized, as it may be preceded with

premature failures in the coupling beams or the walls. To calculate the lateral load corresponding to the ultimate limit state mechanism shown in Fig. 2.8, (1) The moment to shear ratio, α, should be established, (2) The ultimate flexural capacities of the girders should be computed, and (3) The flexural capacities of the walls under the coupling axial forces and gravity loads have to be determined. Following these steps, statics may be applied to compute the collapse load.

The ultimate flexural capacities of the girders were obtained by using the program RCCOLA [2.8]. These beams were designed in three types, as explained in Appendix 2.2. The selected reinforcement detailing of each type of beam is shown in Figs. 2.4 - 2.6. The assumed material stress-strain characteristics for confined core concrete, shell concrete, and steel to obtain the moment-curvature responses of these beams are shown in Fig. 2.9. The assumed stress-strain characteristics for confined concrete may not be considered realistic as it is assumed that infinite strain can be developed with small stress. This explains why the moment curvature responses of all the types of beams indicate in the tables shown in Figs. 2.10-2.12, a termination of curvature capacity which was computed assuming the rupture of tension steel at a strain of 0.15. The use of the confined concrete stress-strain characteristics in Fig. 2.9 is justified when one considers that the objective in generating the moment-curvature responses for these beams was to obtain an overbound on the moment capacity (and hence shear, and hence wall axial forces) of the beams. The maximum shear forces that could develop at the ends of these girders was computed as 287 kips, 398 kips, and 532 kips for Type 1, 2 and 3 girders, respectively, based on the clear span of 168 in. for the girders, and neglecting gravity loading.

The uncertainty in these figures is significant due to possible

variations in the assumed strength of the materials. If the assumed ultimate strength of reinforcing steel was assumed as 90 ksi rather than 110 ksi, the resulting beam shear forces should be expected to decrease proportionally. Furthermore, zero axial force was assumed for the beams while the moment-curvature responses were generated; this is equivalent to assuming that the shear forces of both walls at the ultimate limit state are identical, which is not a realistic assumption. Actually, the tension wall should contribute less than the compression wall to the base shear, i.e., $V_1 < V_2$ in Fig. 2.8. Consequently, there should be axial forces in these beams, which would affect the computed flexural and shear capacities significantly.

The accumulated axial forces of the walls, N, due to the beam shears that result from the lateral force on the structure only (Fig. 2.8), are computed to be 6464 kips in the tension and compression walls. Incorporating the gravity load of 2270 kips, the tension and compression in the tension and compression walls are obtained as 4194 kips and 8734 kips, respectively.

These base axial forces are indicated on the axial force-flexure interaction diagrams (Fig. 2.13) of the cross section of one wall component, designed with respect to the 1973-UBC provisions. The section was shown in Fig. 2.3. The material stress-strain characteristics used in developing the interaction diagrams are shown in Fig. 2.9. The extreme envelope in Fig. 2.13 was obtained by picking the maximum moments indicated for an axial force on the corresponding moment-curvature response. As the confined concrete within the spiral was assumed to be capable of sustaining infinite strain (Fig. 2.9), the points below the balanced force on this envelope represent breaking of the main reinforcement. This

envelope, therefore, may be regarded as an overbound while the interaction diagram obtained for a maximum concrete strain of 0.004 may be regarded as a lower bound for section strength, for the specified material strengths in Fig. 2.9.

The compression in the compression wall, Fig. 2.13, is observed to exceed the balanced load, at the ultimate limit state. The tension in the tension wall is also observed to be significantly high. The average yield flexural rigidity (EI) (secant stiffness obtained for the yield moment and curvature) for the tension wall was obtained as 0.25×10^{10} kip-in. while this value was computed as 12.50×10^{10} kip-in. for the compression wall. Note: it is assumed that the tensile capacity of concrete is neglected; this is not true. The shear forces of these two walls should be expected to be significantly different, due to the fifty-fold difference in stiffness. The moment-curvature responses of the wall section for 8750 kips compression and 4200 kips tension are shown in Fig. 2.14.

The ultimate moment capacities of the tension and compression walls of the coupled wall were obtained as 0.6×10^6 kip-in. and 1.3×10^6 kip-in., respectively, from the extreme envelope in Fig. 2.13. The total base overturning moment of the coupled wall at the ultimate limit state can now be obtained as $0.6 \times 10^6 + 1.3 \times 10^6 + 6464 \times 450 = 4.8 \times 10^6$ kip-in., where the term 6464 kip x 450 in. = 2.9×10^6 kip-in. represents the contribution of coupling, which is 60 percent. The total base overturning moment corresponding to "1.4E" loading, was obtained as 1.6×10^6 kip-in., indicating that there is a flexural overstrength (or hidden strength) of three times the design flexural strength of the system. This is due to a large number of factors, the most significant of which is the strain hardening of reinforcing steel in the beams and

Another important factor is the conservative code assumption that the edge members alone are considered to resist all the overturning moment acting in the walls, i.e., the contribution of the vertical wall steel to flexural capacity is neglected.

The consequences of the 1973-UBC design provisions will be discussed in greater detail in subsequent chapters. A brief assessment of the design may follow from the axial force levels in the two walls at ultimate load, as indicated in Fig. 2.13. The axial force levels in both the tension and the compression walls are too high for favorable ultimate limit state behavior. The compression wall is subjected to more than its balanced force, significantly impairing the deformation capacity of this wall. In the tension wall the tension is so high that the wall has only one-fiftieth of the flexural stiffness of the compression wall. This implies that there will be a significant shear transfer from the tension wall to the compression wall which was not taken into consideration during the shear design of these walls.

The basic cause of the high level of axial force in these walls is the flexural strength of the coupling beams. As discussed in the previous section, design of these beams is based on linear analysis with code prescribed load. Hence, the stiffer the beams, the larger will be the flexural demand. An interesting observation here is the contribution of the coupling forces to the base overturning moment resistance. For the 1973-UBC designed walls, this contribution was computed as 60 percent. This percentage is less than the 67 percent suggested by the New Zealand researchers [2.11] for their particular coupled wall topology, as the criterion for the design of coupling girder strengths. Prescribing a 67 percent coupling force contribution to the base overturning moment as a design criterion does not ensure a desirable ultimate limit state behavior for all types of coupled wall topologies and wall cross sections. The coupling axial force in the tension wall should

not be permitted to overcome the gravity forces for a more balanced shear resistance contribution from a coupled wall system.

A design process which does not contain the shortcomings of the code design procedure is being developed and will be presented in subsequent volumes. Meanwhile, usage of a lower grade (Grade 40 as opposed to Grade 60) reinforcing steel in the coupling girders may be a remedy, as the ultimate strength to yield strength ratio for Grade 40 would be less than Grade 60. Another possible remedy to code provisions could be carrying out plastic analysis rather than elastic analysis for design purposes, with a restriction on the maximum tension that could occur in the tension wall at the ultimate limit state. Limiting the tension to zero, or, as an upper bound, to 10 percent of the ultimate tension capacity of the wall, may be a possible design alternative that could be consequential in assuring large deformation capacity without premature shear failure.

The ultimate base shear for the coupled wall system may be evaluated if an estimate on the bounds of α in Fig. 2.8 is made. Linear and nonlinear dynamic analyses of the prototype structure indicate possible values of α between 0.5 - 0.75 (Sections 2.2.4 and 2.2.5). As the ultimate base overturning moment was obtained as 4.8×10^6 kip-in., the bounds for the ultimate base shear may be estimated between 3000 to 4500 kips, approximately. The value of α corresponding to the "E" load distribution by the 1973-UBC provisions is 0.68. The value of base shear corresponding to an α value of 0.68 is 3268 kips.

In comparing this ultimate base shear by the factored design base shear of 2550 kips (Appendix 2.2), it is observed that the flexural overstrength in the design may lead to a shear force far exceeding the factored design shear force. Fortunately, there is an overstrength in shear as well, compared to the shear strength computed by code expressions.

This overstrength may or may not be sufficient to permit inelastic flexural deformations of the wall to the postulated ultimate limit state mechanism without prior shear failure.

2.2.4 Linear Dynamic Analyses of the Prototype

The prototype structure was analyzed using the modal spectral analysis option of TABS [2.20]. Acceleration spectra with 5 percent damping for the S00E component (0.33 g) of the 1940 El Centro ground acceleration record (Fig. 2.20) and the S16E component (0.4 g) of the ground motion at the base rock derived from the 1971 Pacoima Dam record were used in the analyses [2.9] (Fig. 2.20).

Basic objectives of the analyses were to generate data on the magnitude and distribution of earthquake forces on the prototype coupled wall system and to study the effects of frame-wall interaction in linear response. Data on EQ forces in linear response are required for an understanding of the upper bounds of the earthquake demands on the coupled walls. Furthermore, the frame-wall interaction problem is a significant, characteristic problem in the design of building systems incorporating structural walls. Although a significant number of previous analytical studies have been carried out on coupled walls, isolated from the rest of the structure (Section 1.2.5), a thorough investigation should include the effects of the frames on the response of the walls.

UBC provisions [2.16, 2.17] require frames to be incorporated in all building systems with walls, when the building is above 160 ft in height. It is required that these frames be capable of resisting at least 25 percent of the total base shear. Consequently, the frame-wall interaction is a common and significant problem which needs to be incorporated in research on structural walls. Conclusions reached from analytical or

experimental investigations on walls which are isolated from building systems may have to be subsequently modified to incorporate interaction.

In both linear and nonlinear analyses, the total building system is idealized into a plane frame-wall system, as shown in Fig. 2.15. The basic assumption implicit in this idealization is that the diaphragm system is axially infinitely stiff (all points at a certain elevation have identical lateral displacements), and flexurally infinitely flexible (different sag and uplift characteristics of the walls and the frames may be assumed not to affect each other). Also implicit is the assumption that the motion is occurring in one horizontal direction only.

The results of linear analyses are shown in Figs. 2.16 - 2.18 and Table 2.4. In these analyses, stiffness of the frame elements were based on uncracked gross section properties, while the stiffness of the coupled wall and coupling girder elements were based on cracked stiffnesses obtained from moment curvature responses. The main objective in using cracked stiffness for the walls, and, uncracked, thus relatively inflated stiffnesses for the frame elements, was to compensate for the misproportional reduction in the stiffness of the wall and frame elements with the onset of cracking. Former test results indicated large reductions in wall stiffness while the reduction in frame stiffnesses was generally considerably less with the onset of cracking [2.1].

Static analysis with the 1973-UBC "E" loading indicated that the frames contributed to the overall lateral stiffness by 40 percent, i.e., the lateral eight-floor displacement of the two coupled wall systems resisting the 1973-UBC "E" loading is 1.40 times the corresponding displacement of the total building (two coupled wall systems and eight frames) under the same load. The distribution of story shears for the static

analysis is shown in Fig. 2.16. The total base shear of the coupled wall is reduced by 18 percent from 774 kips to 655 kips when the interaction is considered. The moment to shear ratio at the base of the wall, resulting from the story shears in Fig. 2.16, is 68 percent of building height when the interaction is not considered, and is 57 percent of the height when the interaction is considered. The implication is that although the magnitude of the wall base shear is larger when the wall is assumed to resist the total earthquake forces individually, the distribution of seismic forces on the wall becomes more critical when the wall-frame interaction is considered. In other words, the shear associated with a unit bending moment at the base of the wall is 19 percent more when the interaction is considered. The design provisions of UBC [2.16, 2.17] should, therefore, be interpreted with caution when the shear design of the walls is being carried out, particularly if the walls are overdesigned against bending.

The story shear envelopes of the coupled wall system obtained through the SRSS approach are illustrated in Fig. 2.17 for El Centro and in Fig. 2.18 for the Derived Pacoima Dam analyses, considering the coupled walls individually and the total frame-wall system.

The fundamental period of the structure, when the coupled walls were assumed to resist the total earthquake effects (i.e., when the total mass of the structure was considered with just the two coupled wall systems in Fig. 2.1) was obtained as 1.20 seconds. The fundamental period was reduced to 0.99 seconds when the complete building was considered. The second and third periods of the isolated coupled wall model were 0.32 and 0.15 seconds, respectively. These periods were 0.28 seconds and 0.13 seconds when the complete building was considered.

The SRSS (Square Root of Sum of Squares) shear envelope distributions considering only the first three modes of the structure and the El Centro spectrum are shown in Fig. 2.17. It is observed that the story shears of the total building are significantly larger than when only the walls are considered to resist the EQ effects. Consequently, the story shears shared by the walls are larger when the interaction is considered. The increase in the base shear of the coupled walls is approximately 30 percent, as observed from Fig. 2.17*. The moment to shear ratio at the base of the coupled wall is decreased 17 percent from 0.7 H to 0.6 H when the interaction is considered. The 0.6 H figure is very close to the 0.57 H figure, obtained when interaction was considered in the static analysis with UBC-73 prescribed loading.

The results of dynamic analysis with the Derived Pacoima Dam record are shown in Fig. 2.18. Unlike the response to the El Centro record, the story shears of the coupled wall are less when the interaction is considered. The overall building base shear increased 5 percent when the interaction was considered, as compared to the case where only the walls resisted the EQ effects.

---

* The moment to shear ratios were computed from dynamic story shears in Fig. 2.17 and Fig. 2.18. These were computed by first obtaining an equivalent lateral force distribution which would produce the same dynamic story shear envelope. Then the overturning moment to base shear ratio corresponding to this equivalent lateral force distribution was obtained. Although the dynamic story shear envelope is based on a SRSS analysis, and hence may not represent the actual distribution of seismic force at a particular time instant, the moment to shear ratios for these distributions were computed and are assumed to be probable.

The walls' share of base shear, when the complete building system was considered, was 84 percent of the base shear of the total building. This figure was 83 percent for the El Centro analysis and 83 percent for static analysis, indicating that the frames' contribution to the total building base shear remained almost constant for static or different dynamic analyses. Similarly, the moment to shear ratio at the base of the coupled wall was between 68 - 71 percent of total building height when the interaction was not considered, for static and the two dynamic analyses. This figure was between 0.57 - 0.60 percent of height when the interaction was considered in these analyses. Consequently, the moment to shear ratio at the base of the walls and the relative contribution of walls and frames in resisting the total E/Q effects are affected by the static nature (i.e., - stiffness aspects) of the interaction only. On the other hand, the magnitude of the overall base shear demands, and the relative changes in these demands when the interaction is or is not considered, depends on the earthquake spectrum that was considered. The total base shear demands for one-half of the building are 6700 kips and 13700 kips for the El Centro (0.33 g) and Derived Pacoima Dam (0.4 g) spectra, respectively. The corresponding base shear demands of one set of coupled walls were 5700 kips and 11600 kips for these earthquakes, respectively. The coupled wall demands were 4450 kips and 13000 kips, respectively, when only the walls were assumed to resist the earthquake effects. As discussed earlier, the wall base shear demands due to El Centro went up 28 percent when the frame-wall interaction was considered. For Pacoima, the demand was decreased by 12 percent when the interaction was incorporated.

A summary of the computed linear demands at the base of the building

for code and dynamic analyses is given in Table 2.4. It is observed that the linear dynamic demands far exceed code demands. The UBC-73 "E" load analysis results should be adjusted by load factors of 2.8 for shear and 1.4 for BOM to obtain design demands. Even then, the dynamic shear demands for El Centro and Pacoima spectra are approximately two to six times larger than code demands.

The same conclusion is reached for the frames; there is a significant difference in the code and linear dynamic demands. The following criteria govern the design of frames in Dual systems [2.16, 2.17]:

"(i) The frames and shear walls shall resist the total lateral force in accordance with their relative rigidities, considering the interaction of the shear walls and frames

(ii) The ductile moment resisting space frame shall have the capacity to resist not less than 25 percent of the required lateral force."

The distribution of story shear demands by code and linear dynamic analysis for a typical frame are shown in Fig. 2.19. It is observed that criterion (ii) governs frame design from the base to the fourth floor; then criterion (i) governs the design.

The frame demands obtained by dynamic analysis are maximum at the sixth floor. At this floor, the El Centro analysis demand is 6 times and the Pacoima analysis demand is 13 times the code design demand, adjusted by the load factor of 1.4. Consequently, the linear dynamic demands versus design demands are larger for some of the floors of the frame than at the base of the coupled wall. This implies that these floors of the frames may have early inelasticity during serviceability earthquakes while the walls remain in the linear range.

The code requires frames as an insurance against collapse if the walls should fail through brittle failure. The presence of frames, however,

significantly increased demands due to El Centro, indicating that frames may lead to more adverse demands for the complete structure. To be able to design frames more efficiently, further investigation is needed of the requirement to incorporate frames in conjunction with walls in building systems over 160 ft in height.

2.2.5 Non-Linear Time-History Analyses of the Prototype

2.2.5.1 General

The time-history analyses of the prototype structure designed in accordance with the UBC-73 provisions (Fig. 2.1) were carried out as an initial step in the continuing analytical studies on tall R/C wall-frame buildings. The immediate objectives of these analyses were:

(1) To investigate the serviceability and damageability earthquake demands on the prototype buildings,

(2) To investigate the effects of the wall-frame interaction on these demands,

(3) To investigate the time-history of the internal forces of the wall as a basis in the determination of the loading program during experimental studies.

2.2.5.2 Ground Acceleration Records

The first 10 seconds of the S00E component of the 1940 El Centro accelerogram (Fig. 2.20) and the first 10 seconds of the S16E component of the "derived" 1971 Pacoima Dam accelerogram (Fig. 2.20) were used in the analysis. The original 1971 Pacoima Dam motion was synthesized [2.9] to arrive at a derived version of this record with the intention of representing the true bedrock motion, as the accelerometer was subsequently discovered not to be on firm rock. Moreover, it was again subsequently

discovered that the component directions were not S16E and S74W but different. For the purposes of analysis, the derived version was used of what was believed to be the S16E component of the original 1971 Pacoima Dam motion.

2.2.5.3 Mathematical Models

One set of coupled walls was loaded with one-half of the total mass of the building and was subjected to the two ground acceleration records. These analyses represented the UBC [2.16, 2.17] concept of walls resisting the earthquake effects individually. The basic intent in these analyses was to generate data for an assessment of the wall-frame interaction during different response phases of the prototype. Relatively more realistic and representative analyses were carried out by subjecting one-half of the symmetric building to the two base excitation records.

For reasons of economy, the four frames in the considered half of the building were lumped into a half frame, as indicated in Fig. 2.21. Each column of the idealized (mathematical) frame represented eight of the actual columns of the prototype; similarly each beam represented eight of the actual beams.

In both of these models (Fig. 2.21) mass corresponding to the weight of one-half of the total building was lumped at each floor level. These lumped masses were not assigned any rotational inertia.

The degrees of freedom considered were: (1) Lateral displacement at each floor level; (2) Vertical displacement; and (3) Rotations of each node. Consequently, there were 75 degrees of freedom in the isolated coupled wall and 150 degrees of freedom in the coupled wall-frame model.

A detailed discussion of the shortcomings and misrepresentations of these models is available in another report [2.12]. Only a brief listing and description of the modeling problems observed in using the computer code DRAIN-2D [2.6] in conjunction with the analysis of such coupled wall-frame systems, will be given here.

The wall and coupling girders were represented by one-dimensional topological models. The walls (and the columns) of the mathematical models in Fig. 2.21 were assigned the beam-column element option, while the connecting girders (and frame beams) were represented by R/C degrading beam elements of DRAIN-2D. Both types of elements simulate inelastic response and hysteresis through a concentrated hinge at each end.

(1) The 1-D modelling of the walls is highly questionable. The 1-D model and the associated deformation modes cannot represent the significant shear mode of behavior in both linear and, particularly, the nonlinear response ranges.

(2) Another shortcoming of 1-D representation of the wall components is in fixing the position of the wall neutral axis through the 1-D model. In reality, wall neutral axis changes location (migrates) during excitation. This migration, in turn, has considerable effect on the demands of the coupling girders as the length of the relatively rigid zone at the ends of the girders would change. Such occurrences cannot be modeled by 1-D representation of the wall elements.

(3) Modelling inelasticity through concentrated hinges at the ends of the members is contradictory to observed behavior of R/C elements. The spread of inelasticity is a significant characteristic of R/C, affecting the overall force-deformation relations considerably. Consequently,

lumping inelasticity at predetermined cross sections at member ends is a significantly questionable idealization, especially for the wall components.

(4) Axial inelasticity is not incorporated.

(5) Flexural inelasticity of the wall or column components is recognized when a pre-determined axial force-bending moment yield envelope is reached by the axial force and moment pairs at the ends of these elements. When the envelope (yield surface) is reached at either end of the member, the axial force-moment pair stay on the yield surface. Unloading from the yield surface is through the assigned linear flexural stiffness. Consequently, elasto-plastic hysteresis is realized for the plastic hinges at the ends of the beam-column members.

This process contains a significant shortcoming, which is the need to maintain a constant linear flexural stiffness for all axial force levels if the yield level is not realized at the ends of the member. As there are extreme differences in the flexural rigidities of the tension and compression walls, the corresponding linear flexural stiffnesses should reflect this difference. Unfortunately, the DRAIN-2D coding does not incorporate this effect. This "mis-representation" in the linear response phase affects the initial occurrence and sequence of plastic hinges and, therefore, the non-linear response phase.

(6) Another significant shortcoming that was realized in the DRAIN-2D coding is the inability to incorporate shear yield. As the shear stiffness and shear yield phenomena are as important as the flexural stiffness and flexural yield phenomena in the response of R/C wall components [2.10], their omission in the mathematical modelling is a significant shortcoming.

In DRAIN-2D, the effects of shear on flexural stiffness is incorporated by the standard modification of the appropriate terms of the member stiffness matrices. This, however, is suitable only for slender members where the effects of shear are of a lesser order than the effects of flexure on the overall behavior. The significant drawback in neglecting the phemonenon of shear-yield is in the high shear forces that are computed for the wall elements even after these develop plastic hinges. In reality, once a wall element yields, its shear capacity is also limited due to the "shear yield" phemonenon. Consequently, it cannot be expected to develop higher shears than its shear yield strength, as misleadingly computed by the program.

(7) Another drawback associated with the 1-D modelling of the wall components is the inability to incorporate the web crushing phenomenon. Furthermore, the model cannot distinguish between the demands of the exterior and the interior edge members.

(8) The R/C degrading beam element representation of the coupling girders is observed to be more appropriate than the one-dimensional beam-column element representation of the wall components. However, there are a number of shortcomings associated with this representation as well: concentrated hinges at the member ends, neglection of the effects of axial force on stiffness (these elements are assumed to have zero axial force), neglection of the effects of bond and shear in hysteresis (i.e., decay in hysteresis), are the observed shortcomings.

(9) It is possible to construct different models to represent the R/C coupled wall by using the available element library of DRAIN-2D. For example, the wall components may be represented by a number of beam-column and truss elements rather than a single element. These measures were not taken because of the significant costs in analysis. Modification of the

existing element library for better representation of the coupled-wall behavior is in progress.

(10) The representation of the four frames of the building in the form of a single half frame (Fig. 2.21) is questionable, as such an idealization results in an altered axial force history in the columns. Consequently, inelasticity in the columns would not be representative of the case if the complete frame topology (Fig. 2.1) were maintained. However, the model does reflect the overall lateral stiffness characteristics of the frames and is considered adequate in indicating any significant contribution of the frames in the magnitude and time-history of forces and deformations of the walls.

2.2.5.4 Data for Analyses: Member Properties, Gravity Loadings, Damping and Time Incrementation

The member properties used in the time-history analyses were obtained through moment curvature and moment-axial load interaction relations that were derived for the members by the computer code RCCOLA [2.8]. The wall, column, and frame beams' properties were assumed to be constant throughout the height of the building (Fig. 2.21). The coupling girders were designed in three types (Fig. 2.1) and their properties changed along the height according to the design. The inputs for the properties of the beam-column and R/C degrading beam elements are shown in Figs. 2.22 and 2.23.

The gravity loading for the total dead load and 40 percent of the live load was applied to the wall and frame nodes and retained during the dynamic analysis. This loading was computed with respect to the tributory loading areas of the vertical members. Forty percent of the live load was included in the mass computations also, assuming this to be a reactive load.

A mass proportional damping equivalent to 5 percent of the critical damping in conjunction with the fundamental period (0.99 secs. as computed from linear analysis) was used in the analyses.

The earthquake accelerograms were incremented in 0.05 seconds in the input. The integration time step was prescribed as 0.02 seconds. Short-trial analyses indicated very little change in analysis results carried out with integration time steps of 0.01 and 0.02 seconds.

2.2.5.5 Results of Analyses

Data on nonlinear structural response, generated by the analyses, are presented in detail in another report [2.12]. A limited review will be presented here, with emphasis on the response characteristics of the prototype building in order to derive loading histories and vertical-lateral load relations for the test specimens.

The time-histories of the displacement, shear force, bending moment, and axial force responses of the coupled wall-frame system subjected to the El Centro accelerogram are shown in Figs. 2.24 - 2.27. The shear forces and bending moments of the two individual walls of the coupled wall system are observed to remain identical. The axial forces are skew-symmetric with respect to the gravity forces.

Walls have remained linear during the response to El Centro; any inelasticity is confined to the coupling beams. The maximum drift was observed to be less than 0.3 percent. First yielding occurred at 1.94 seconds; at this time step beams of the fourth through tenth floors reached yield moment at their left ends. The maximum number of plastic hinges were attained at 2.02 seconds of response, when all beams except first, fifteenth and the fourteenth floor beams developed plastic hinges at both ends and the fifteenth and fourteenth floor beams had hinges at

one end only. The maximum inelastic rotation demand was from the fourth floor beam, and was 0.0026 radians. The frame beams at floors 6-14 yielded but the inelastic rotations were close to zero (0.0002 rads. max.).

The response of the structure to the El Centro ground motion may be appraised as an upper bound of the serviceability response, or as a lower bound of the damageability response, as defined by the S.E.A.O.C. recommendations [2.13]. The seismic force demands for this response are shown in Fig. 2.28 where the shear distributions of the coupled wall system at the times of maximum base shear and maximum base overturning moment are compared. A significant difference in the moment to shear ratio of the seismic forces is observed between these two cases. The value of α (overturning moment to shear ratio at the base as a factor of the total height) changed between 0.33 and 0.71. The ratio is 2.15, indicating that the 1973-UBC provisions, prescribing a force factor of 2.8 for the seismic force in shear design, as compared to a force factor of 1.4 in the case of the axial-flexural design, can barely make up for the difference in the distribution of seismic force at the times of maximum shear and axial-flexural demands. The code practice, as explained earlier, is to use the same seismic force distribution for both axial-flexural and shear designs.

The distributions of seismic story shears of the coupled wall system when the isolated coupled walls were analyzed under the same base motion, are presented in Fig. 2.29. Comparison with Fig. 2.28 indicates that incorporation of the wall-frame interaction increased the seismic demands, as was the case in linear analysis.* The moment to shear ratios for these analyses were obtained as 0.60 H and 0.40 H, for the cases of maximum overturning and maximum shear force at the base, respectively.

---

* The period of the walls acting alone was obtained as 1.20 sec, as given in 2.2.4. This period decreased to 0.99 sec when the frames were included in the model.

The difference is not as significant as when the interaction is considered (0.6 vs. 0.4 as compared to 0.71 vs. 0.33), indicating that the wall-frame interaction intensifies the difference between seismic force distributions at the times of maximum base overturning moment and base shear.

The time-history of the responses of the coupled wall-frame system subjected to the Derived Pacoima Dam ground motion is shown in Figs. 2.30 - 2.33. The time-histories of the shear and moment at the base of the individual walls of the coupled wall system indicate significant differences between the internal force histories of the individual walls.

The big acceleration pulse of the ground motion between the two and four seconds resulted in extensive damage to the system. At 2.98 seconds, a collapse mechanism is reached for the wall, as shown in Fig. 2.34. At 3.00 seconds, another column hinge as shown in Fig. 2.34, is observed on the 2nd floor of the tension column. As a consequence of the hinging pattern in Fig. 2.34, the tension wall released most of its shear, as required by the conditions of equilibrium.[2.12] This shear is picked up by the frame columns. This condition is not realistic as, in reality, the tension wall should be expected to retain a substantial amount of shear capacity [Sec. 1.2.2]. The use of 1-D elements (where yield is represented by concentrated plastic hinges at the ends) for the mathematical modelling of the wall have led to this unrealistic extreme in the release of shear to the frames.

The ground motion results in an unloading of the base hinges at 3.06 seconds. The loading of all plastic hinges between 3 and 3.06 seconds, which triggered the release of the shear of the tension wall

at the base, was a result of the main acceleration pulse of the ground motion. The effects of this pulse are similar to that of a laterally distributed force of monotonously increasing nature. The response of the structure to the Derived Pacoima Dam motion may be appraised as the upper bound of the damageability response, as a mechanism is caused for the wall by the earthquake. The frame columns remained linear, however, and the frame was observed to have satisfactorily performed as a restraint to the structure. The maximum drift attained was 0.9 percent. This drift should be compared with the 1.2 percent obtained when the isolated coupled wall system was analyzed, indicating the restraining effect of the frame on the structure.

The seismic force demands at the times of maximum base shear and base overturning moment are presented at Fig. 2.35. It is observed that the characteristics of the seismic force distribution at the times of maximum shear and moment are extremely different. At the time of maximum base overturning moment, which corresponds to the time of the maximum wall axial forces, there is a significant reduction in the first-story shear as a consequence of the release of shear in the tension wall upon hinging at the base and the second floor as discussed in the previous paragraphs.

The base overturning moment to shear ratio corresponding to the time of maximum overturning moment is larger than 1H due to the significant reduction of the shear at the base of the wall. This ratio was computed to be 0.34 H for the time of the maximum base shear. The difference in these ratios is significant and demonstrates the conceptual error in code design provisions which prescribe the <u>same</u> distribution for both shear and axial-flexural design of the walls.

Seismic force demands from the coupled wall when the coupled wall system, isolated from the structure, is subjected to the same ground motion, are shown in Fig. 2.36. Comparison with Fig. 2.35 indicates that the base shear demand from the wall alone increased when the frames were included in the analysis. The same pattern was observed for the El Centro responses as well. The seismic force attracted by the wall-frame system is significantly higher than the seismic force attracted by the wall system alone, due to the increased stiffness of the system.* Consequently, the shear shared by the wall, when the wall-frame system is considered, is observed to be larger than the shear in the wall when only the wall was subjected to excitation.

The increase in the maximum base shear when the frames were incorporated in the analysis is observed to be 11 percent for the El Centro response and 9 percent for the Pacoima response. These do not appear to be significant increases, however, for a wall that is at the verge of shear failure, a 10 percent increase in the base shear may be a very significant excess in demand. If the wall system has sufficient shear strength, the incorporation of the frames are observed to result in favorable changes in the earthquake response of the structure. The drifts, as well as the wall tensile forces, are reduced. The overturning moments do not change. More significantly, the frames reduce the shift in the center of oscillation of the structure, as is observed when the results of Figs. 2.30 and 2.37, where the displacement histories of the structure when the frames are and are not incorporated, respectively, are compared.

---

* The period of the walls acting alone was obtained as 1.20 sec, as given in 2.2.4. This period decreased to 0.99 sec when the frames were included in the model.

2.2.6 Assessment of the Design of the Prototype

The prototype structure, designed in accordance with the 1973-UBC provisions, was subjected to linear and nonlinear dynamic analyses, utilizing the 1940 El Centro (0.33 g) and 1971 Pacoima Dam (0.4 g) ground motions. These earthquakes were observed to represent the lower bound of the damageability and the ultimate limit state ground motions of the structure. The data generated on the demands from the structure in the cases of the damageability and the ultimate limit responses, will be compared with the supplies as provided through the design, to assess the success of the design that was carried out with respect to the 1973-UBC provisions.

2.2.6.1 Computation of Period

The Uniform Building Code prescribes the expression $0.5\ h_n/\sqrt{D}$ to compute the period. For the prototype, this results in a period of 1.15 seconds. Another expression, suggested by the code is:

$$T = 2\pi\sqrt{\Sigma\omega_i\delta_i^2 \div g\Sigma f_i\delta_i}\ .$$

To use this expression, a lateral force system, f_i, should be applied to the structure and the corresponding story displacements, δ_i, computed. ω_i represents the lumped weights and "g" is the gravitational acceleration. This procedure led to a period of 0.99 seconds for the complete structure, which corresponds to the value obtained from an eigenvalue analysis with the computer code, TABS [2.20]. An effective period can be computed from the time-history of the displacements in the case of nonlinear analysis. In this approach, the number of zero crossings during the high amplitude response is used to compute a period of 1.52 seconds for the El Centro and 1.60 seconds for the Pacoima response. The empirical code expression, $0.5\ h_n/\sqrt{D}$, is not realistic as it does not incorporate the structural system but just the dimensions h_n and D. Furthermore, care should be taken in the use of

the refined code expression to include the total structure in the analysis and not just the walls.

2.2.6.2 Comparison of Supply vs. Demands

In comparing supply vs. demand for a certain design quantity, the code demand, (incorporating the prescribed forces, load factors, and combinations, as well as the strength reduction factors) - and the nominal supplied strength, should be assessed individually. Because of many factors, rounding off of numbers, detailing requirements, strain hardening in reinforcement, etc., the provided strength is generally higher than the code demand. However, the actually supplied strength and the supplied strength based on the computations as prescribed by the code, are often significantly different, either because of simplifying assumptions, or in some cases, because of misconceptions that affect the accuracy of the computations that are based on code expressions.

A possible means of comparing the code demand, supplied strength, the actual (estimated) strength, and the required (estimated from linear and nonlinear analyses) strength in the case of predominant axial-flexural behavior is through the interaction diagram as shown in Fig. 2.38. It is observed that the supplied strength is significantly more than the strength required by the code. One reason for this is that the code required the wall edge columns to provide all the required axial-flexural strength. Consequently, the actually supplied strength, when the complete wall cross section is considered, is significantly more.

The demand obtained through linear analysis by the El Centro spectrum is observed to far exceed the supplied strength. The demands

for the same earthquake, in the case of the nonlinear response, are, however, well within the range of the provided strength. The hysteretic energy dissipation of the coupling girders has resulted in a significant reduction in the axial-flexural demands of the earthquake from the wall cross section.

The demands obtained from nonlinear analysis by the Pacoima Dam record are observed to equal the supplied code strength. A certain reserve strength, on the other hand, can be estimated by considering the fact that the actual material strengths are generally higher than the nominal strengths.

Another means of assessing axial-flexural supply vs. demand is by considering the distribution of tension and compression at the extreme wall edge columns. The code requires all axial-flexural demands to be satisfied through the strength of the edge columns. For coupled walls, the computed demands from the extreme edge columns are significantly larger than the demands from the interior edge members at the base of the walls. The exterior vs. interior edge member demands due to code and nonlinear analysis are shown in Fig. 2.39. It is observed that the demands obtained through nonlinear time history analysis for the ultimate limit earthquake are significantly higher than the code demands, especially for the tension member. Another significant discrepancy between the code and analysis demands is observed for the distribution of these demands along the elevation of the structure.

An assessment of supply vs demand for the extreme edge members is given in Fig. 2.40. It is observed that the code and nonlinear El Centro analysis demands for the tension edge member are almost identical at the base.

The analysis demand at the upper half of the structure, however, is significantly higher in tension. It is also observed that the extreme edge members are severely overstressed during the Pacoima response. The estimated actual strengths of the members are barely sufficient to satisfy the demands as computed from Pacoima analysis.

The demand vs. supply relations for shear are much more significant than for the axial-flexural effects, as the analysis demands for the flexure is related to the supply while this is not the case for shear. In other words, the analysis demand for the axial-flexural effects cannot exceed the supplied strength during nonlinear response as the supply regulates the demand. In the case of the shear, however, the supply and demand are not related, and the comparison becomes significantly more relevant.

The demand vs. supply relations in shear are summarized in Fig. 2.41. The significant problem in the assessment is the computation of actual supply. If both walls are assumed to contribute in the order of "$14\sqrt{f'_c}\, d_\omega t_\omega$", the actual supply appears to be sufficient to restrain shear failure before flexural yielding. However, in the case of the tension wall, this is questionable. It is, therefore, possible that the demand may exceed the supply even in the case of the El Centro response, if the tension wall does not contribute to the shear strength.

It is one of the objectives of this study to investigate the actual shear strength of a set of coupled walls under different axial force magnitudes. The comparison of demand vs. supply in shear strength, computed with presently available knowledge, indicates a significant danger of shear failure of the walls before sufficient energy dissipation may take place. This is especially the case for the Pacoima response.

2.3 The Model Subassemblage

2.3.1 General Information, Dimensions, Detailing

As explained in Section 2.1, a 4-story, 1/3-scale subassemblage of the prototype coupled wall system, designed in accordance with the 1973-UBC provisions, was selected as the first model. The dimensions and detailing of the model subassemblage follow from the dimensions and detailing of the prototype (Figs. 2.1 - 2.7) and are shown in Figs. 2.42 - 2.47. Apart from the slab thicknesses of 3 in., all the dimensions of the model are one-third of the corresponding dimensions of the prototype. Slab stubs were designated as 3 in. rather than 2 in. in order to have sufficient stiffness to accommodate out-of-plane restraints during the test. The transverse beams that were shown in Fig. 2.1 for the prototype were deleted in the subassemblage to simplify the formwork. Although the deletion of the transverse beams and thickening of the slab stubs can affect the contribution of the floor system to the lateral stiffness and strength, particularly that of the coupling girders, this contribution was considered not to be very significant in relating overall model response to the prototype response.

The wall edge members and the fourth-, third- and second-floor beams were detailed with grade 60 #6 and #4 bars. Number three bars were utilized in the first-floor beam. Specially manufactured 0.207 in. and 0.166 in. diameter wire was used as the edge column spiral and beam ties. The stress-strain relations for the #6 and #4 bars, as well as the 0.207 in. diameter wire, are shown in Figs. 2.48. As illustrated in Fig. 2.48, the stress strain for the steel bar #4 shows a very high yielding strength (75 ksi) and very little plastic plateau. Grade 60 #2 deformed steel bars imported from Sweden were used as the wall

reinforcement; test results for these are also shown in Fig. 2.48. A significant difference in the tensile strain capacity of the bars imported from Sweden and those obtained from the West Coast manufacturers are observed. The slabs were reinforced with welded wire fabric with 0.225 in. diameter material in a square mash, 4 in. O.C..

Ready-mixed concrete commercially available from a nearby plant was used in casting the specimen. As a grout pump was used to pump the concrete, a 7 in. slump and 3/8 in. maximum aggregate size, with a minimum 28 day strength of 4000 psi, was specified. The observed 28 day strength was 4900 psi for the first two floors of the specimen. The specimen was constructed in two halves, in an upright position. The foundation and the first two floors of each half were cast first. The top two floors were cast subsequently, approximately 45 days later. These halves were transported into the test bed on rollers, and after prestressing, the two halves were connected at the base and four floors, where special force transducers (Section 2.5) were installed (See photos: Figs. 2.49, 2.50).

The main requirements for successful subassemblage testing were discussed in Section 2.1. Those requirements pertaining to a sufficiently accurate representation of the material, section, element, and joint behavior -- essential for the credibility of any reinforced concrete model study -- are satisfied by the large scale (1/3) of the model and the consequent choice of the materials. The remaining requirements are related to the realistic representations of the (force and geometry) boundary conditions of the subassemblage and the loading program. These are discussed in subsequent sections.

2.3.2 Boundary and Loading Conditions of the Model Subassemblage

The actual distribution of the gravity and seismic forces throughout a structure is known to be complicated. Interaction between forces in orthogonal directions is an added complexity. Testing a coupled wall system in one plane assumes that bi-axial interactions in the response of the system are negligible.

After this initial assumption, the force and geometry boundary conditions of the model subassemblage may be discussed. These conditions are relevant at the top cross section of the subassemblage, at the base of the foundation, and at the cut ends of the slab stubs as shown in Fig. 2.51. Furthermore, the gravity and seismic force distributions within the subassemblage are also extremely complicated functions which affect the response of the subassemblage. For reasons of clarity, these forces are not indicated in Fig. 2.51.

The assumptions and idealizations that were made to simplify the complicated geometry and force boundary conditions and the force distributions within the subassemblage are as follows:

(1) The effects of the continuity of the slabs (Fig. 2.51) were assumed to be negligible in the planar response of the system. The main contribution of the slabs in the planar response will be in confining the wall panel cracks within each story and redistributing the slope of the effective compression struts developed in these panels. Slabs also contribute to the axial strength and stiffness of the beams (restraining growth) significantly, as well as to the flexural response of the beams (coupling effect) to a minor extent. The selected slab stubs (representing a half of the adjacent spans) are assumed to be sufficient for these purposes.

(2) The foundation flexibility is a significant variable of the study. For the first series of tests, however, this parameter will not

be introduced, and the foundation will be prestressed through 14 points to the test floor, resulting in a very large (relatively infinite) foundation stiffness as shown in Fig. 2.52.

(3) The force boundary conditions at the top cross section are represented by six concentrated force sources. These forces are applied to relatively stiff stubs (headpieces) as shown in Fig. 2.52. A certain variation of the lateral and vertical forces applied to these headpieces will occur during transition to the subassemblage. This arrangement of force is assumed to be sufficiently representative in maintaining the force (stress) continuity of the subassemblage at the fourth-floor level. This assumption may not be as valid for the fourth story as it would be for the first three stories. Consequently, the force and deformation history of the fourth-floor beam may not be accurately representative of the histories that would be realized for that beam if the structural continuity was maintained. However, this is not considered to be a significant drawback.

(4) The gravity and seismic forces of the first three floors are lumped together with the lateral and horizontal forces at the fourth-floor level.

(5) The most significant assumption on the force boundary conditions of the subassemblage is related to the history of the four vertical loads that are applied to the edge columns of the walls. These loads represent (1) gravity forces at the base; (2) overturning moment at their level of 4-1/2 application; and (3) axial forces due to the shear forces developed in the coupling girders between the fifth and fifteenth floors of the structure (Fig. 2.52). The magnitude and history of the vertical forces in relation to the magnitude and histories of the lateral forces at the top of the subassemblage should be representative of the actual response of the complete structure.

The relation between the lateral and vertical force magnitudes and histories are assessed through nonlinear dynamic response analysis studies of the prototype and are presented in Section 2.3.4.

2.3.3 Estimation of the Ultimate Force and Displacement Capacities of the Model Subassemblage

An assessment of the ultimate force and displacement capacities of the model subassemblage is required for the design of the test facility and loading systems.

To estimate the ultimate force capcity, calculations will be carried out on the prototype and then converted to the model basis. In Section 2.2.3, the ultimate force (based on an external M/V ratio of 0.68 H) of 3268 kips was obtained for the prototype. The moment of this force at the fourth-floor level is computed as 2.92×10^6 kip-in.

Assuming all the connecting beams have attained their ultimate capacity, the axial coupling forces at this floor level are computed as $\pm$ 47.5 kips. These forces induce a coupling moment of 2.12×10^6 kip-in at this story level, indicating that the walls should develop 0.8×10^6 kip-in. (2.92×10^6 - x 2.12×10^6) for equilibrium.

The gravity loads that will be applied to the columns at this floor level will be those loads computed at the base as 925 kips and 1345 kips for the exterior and interior columns, respectively. The resulting wall axial forces due to coupling and gravity forces become 6985 kips compression for the compression wall and 2445 kips for the tension wall.

To estimate an overbound on the required ram capacities, it is necessary to make an assumption on the relative moment contributions of the two walls. To obtain bounds it may be assumed that the total moment 0.8×10^6 kip-in.

will be provided by either only by the compression wall or equally by both walls, respectively. The resulting equivalent vertical and lateral forces on the prototype and model subassemblages are shown in Fig. 2.53. These maximum forces are based on the assumption that overturning moment to base shear ratio is 0.68. The effects of the change in this ratio on the maximum vertical and horizontal forces of the model are investigated in Sec. 2.3.4.

To estimate the expected levels of displacement that may be attained at the top of the model, the most logical approach would be to estimate an upper bound on lateral interstory drift. A survey of previous tests on isolated shear walls indicates that (under monotonic loading) 7 percent interstory drift may be accepted as an upper bound. [2.10] The resulting upper bound on the top displacement is 13.44 in..

2.3.4 Establishing Relations Between the Vertical and Lateral Forces of the Subassemblage

To achieve a realistic simulation of the internal forces and/or deformations at least at the bottom two stories of the subassemblage, four vertical and two horizontal loads (Fig. 2.52) are planned to be applied to the boundary of the subassemblage model. The boundary forces (displacements) to the model will be introduced by six actuators connected to an electo-hydraulic closed servo system. The relations between the loads applied by these six actuators at any time during the load history of the test were obtained from a synthesis of the time-history of the responses that were presented in Sec. 2.2.5. The relations obtained for different levels of response (serviceability and damageability) were also compared with the relations obtained by assessing the ultimate limit state. The actual loading history for each of the actuators during the tests is explained in Sec. 2.4.4.

The process that was followed in establishing the relations between the six actuator forces is explained in the following.

The first step in relating actuator forces to each other is to establish the relation between the lateral forces of each wall. These forces represent the base shear forces of the walls. The implicit assumption is that the base shear force and the shears at the fourth floor are sufficiently close together that the total shear of the first four floors can be lumped at the fourth floor (Fig. 2.52).

The following options were considered in relating the lateral (shear) actuator forces (Fig. 2.52):

(1) Both actuators may apply the same lateral force.

(2) Both actuators may be controlled to apply the same lateral stroke (displacement).

(3) The force in one of the actuators may be prescribed as a percentage of the force in the other actuator.

(4) The relation between the forces of the two actuators may be changed depending on the direction of load in these actuators (push and pull or pull and push).

An assessment of these options in view of the results of time-history analysis, indicates that the fourth floor shears of the two walls, as well as the base shears of the two walls, were nearly identical in the El Centro response. Therefore, Option (1) may be adapted in a serviceability level (or low damageability level) test.*

Pacoima response, on the other hand, indicates significant differences between the base shears of the two walls at a certain time instance. The fourth floor level shears, however, are similar for both walls.

---

* El Centro response was assessed to represent an upper bound for the serviceability or a lower bound for the damageability level of response in Sec. 2.2.5.

As the fourth floor and base shears are significantly different (Fig. 2.3.1), lumping the shear of the first four floors at the fourth floor level appears to be a questionable idealization for the upper damageability level response. Furthermore, Option (4) appears to be a more representative manner of loading since the left wall base shear is higher than the right wall base shear when the left wall is in compression, and vice versa when the right wall is in compression. In reality, if the analytical model could incorporate the effect of the changes in the axial force on flexural stiffness, a similar trend would have been observed for the El Centro response as well. The difficulty in the application of Option (4) is the time required to update the relation between the lateral forces at each case of force reversal. A significant creep effect is usually observed when a R/C system is loaded in the post-yield range and when the force is sustained even for only short durations of time, as required for data acquisition and observations. Although pseudo-dynamic testing using actuator in line with computer procedure as suggested by the Japanese seems ideal, even if this procedure could be successfully applied, there is a serious drawback due to the fact that actual structural damping is not included and due to the effect of inelastic creep. It is, therefore, a more practical approach to update force relations each time a zero load is reached.

The option that was chosen for the first series of tests, where significant wall damage was not anticipated, was to maintain identical forces in the two lateral (shear) actuators. Subsequent tests for higher wall damage levels are planned where Options (2) or (4) will be applied. The main problem with applying equal forces to both walls is that in the event of premature loss of strength in one wall, if the

actuator loading that wall is the slave to the actuator loading the other wall, it would not release its force accordingly.

Option (2), where the lateral displacements of the walls may be prescribed to be identical, would result in constraining the growth of the walls and the connecting beams. If the axially rigid diaphragm assumption should be a correct one, this will not be a serious drawback. This option is being considered for subsequent tests. The main difficulty associated with this option is in establishing transfers between vertical and lateral forces, as the lateral forces would not be predetermined.

Based on the decision to load both walls with identical shear forces for the first series of tests, where a high level of damage is not expected to be induced on the walls, the relation between the vertical and lateral forces was then established in the following manner:

(1) Relations between the vertical and lateral forces of the subassemblage for the serviceability level response.

The response state where walls remain linear and the connecting beams do not have extensive inelastic deformation, is defined as the serviceability response. The response of the complete prototype structure to the N-S component of the 1940 El Centro record (0.33 g) could be appraised as an upper bound for the serviceability response, or a lower bound for the damageability response. The walls and frames remained linear during the excitation while the connecting beams developed plastic hinges at each end. The plastic rotations, however, did not exceed 0.0026 radians, indicating that the beam inelasticity was not extensive. The moments and shear forces in the two walls were nearly identical, the only difference caused by the differences in the positive and negative moment capacity of the beams.

Another observation is that there are instances when the shears of the fourth floor and the base are different. At times of high base shear, between 4 and 5 seconds, the base shear is almost twice the shear at the fourth floor (Fig. 2.25). In general, however, an average positive shear of 675 kips and an average negative shear of 966 kips at each wall may be considered representative of the peaks for the base and the fourth floor as well. As far as the moments are concerned, I 125000 kip-in. are observed to represent the peak responses for the fourth floor (Fig. 2.26). Similarly, the peaks of the coupling axial forces of the fourth floor are observed to be 2069 kips compression and 3000 kips of tension (Fig. 2.27). As the waveforms for displacement, shear, moment, and axial force indicate that these are all in phase, these established average peak values may be used to relate the shears to the moments and axial forces, as shown in Fig. 2.5.4., and to establish the transfer relations for the serviceability level of response. The transfers obtained in this manner should be considered applicable for up to 90 kips of shear per wall in the model, as this corresponds to the 820 kips of average shear (675 + 966)/2 obtained for the peaks of the El Centro response.

(2) Relations between the vertical and lateral forces of the sub-assemblage for the ultimate limit state.

Another approach to arriving at transfer relations is to consider the vertical and horizontal forces at the state of collapse. The ratio of vertical force to horizontal force (defined as force transfer) is lowest at this state, whereas at any other response state the base shear will be less while the coupling forces will not decrease at the same rate. The basic problem in this approach is to estimate the correct overturning moment to base shear ratio at the state of collapse. The

total base overturning moment resistance of the prototype wall system was computed as 4.8 x 10^6 kip-in. in Sec. 2.2.3. The base shear at the ultimate limit state depends on the assumed moment to shear ratio at this state. As this was observed to change between (approximately) 0.5 H - 0.75 H in linear and nonlinear analysis, transfers are evaluated for these bounds (Figs. 2.55 - 2.57).

Assuming a base overturning moment - shear ratio of 0.5 H, (Fig. 2.55) the shear at collapse is obtained as 4444 kips. The coupling forces at the fourth floor are I4715 kips, computed from the ultimate shear capacities of the beams, as given in Sec. 2.2.3. The overturning moment at the fourth floor is 4444 kips x 504 in. = 2,239,776 kip-in.. As the coupling forces provide 4715 kips x 450 in. = 2,121,750 kip-in, the wall moments are obtained as 59,013 kip-in. at this floor. The results of resolving and transfers are shown in Fig. 2.55. Repeating the same operations for a base overturning moment-shear ratio of 0.75 H, the corresponding transfers are shown in Fig. 2.56.

An assessment of the computed transfer relations, 1.17 V and 2.9 V for the exterior edge members, indicates the significance of the moment to shear ratio in transfer of force. In general, during nonlinear dynamic response of the coupled wall-frame structure, the base overturning moment-shear ratio shifts continuously, as discussed in Sec. 2.2.5. The transfer corresponding to an <u>average</u> moment to shear ratio of 60 percent of H is 1.85V for the exterior columns and 0.69V for the interior columns. These figures are quite close to those derived from the time-history of the responses, and were, therefore, selected to represent the average lateral force - vertical force (excluding gravity) transfer during the initial series of tests. The selected values of transfer and expected maximum lateral and vertical forces are indicated

in Fig. 2.57. For subsequent tests, different transfer histories will be applied to study this variable.

2.4 The Test Facility

2.4.1 General

The test facility for the coupled wall subassemblage testing is located in the Structures Laboratory at the Richmond Field Station of the University. An already existing braced frame system that was at the east end of the laboratory's main bay is the major component of the test facility. The other components were designed to incorporate this existing braced frame system. The design was carried out by Li under the supervision of Bertero [2.7], the working drawings were made, and the execution of the design was completed, by Development Engineer Barry Lotz.

2.4.2 The Test Floor

The test floor of the Structures Laboratory at the location stated above, (Fig. 2.58) has dimensions of 60 ft and 20 ft and is pierced by 2-1/2 in. diameter holes, 3 ft O.C., illustrated in Figs. 2.58. This floor was designed to act as a hollow box girder, prestressed in the longitudinal direction. The system is a vierendeel girder in the shorter direction. The braced frame system that was existing in the laboratory is shown in Fig. 2.59, and a plan view of the east end of the main bay, showing the location of the test facility with respect to the holes on the floor, is given in Fig. 2.60.

The perforated test slab was designed for service loads of 100 kips acting either up or down every 3 ft along the slab. A longitudinal horizontal force of 300 kips, acting 18 in. above and along the top of the box section, was also considered as a possible service load. The box girder, as a whole, was designed for a flexural capacity of 20×10^3

kip-ft and a shear capacity of 1500 kips (distributed equally to three webs).

The main functions of the test slab regarding the test facility were considered to be:

(1) To carry the weight of the specimens and the test frame (estimated to be less than 4 kips every 3 sq ft).

(2) To withstand the local bearing pressures exerted around the perforations due to the prestressing of both the specimens and components of the test frame to the floor (max. 1600 psi).

(3) To withstand the maximum possible vertical force exerted on the locations indicated in Fig. 2.60 due to the vertical loading of the specimen as will be discussed in the next section. The maximum vertical force demand on any of these locations indicated in Fig. 2.60 was calculated to be significantly less than the design service load of 100 kips every 3 sq ft for the slab.

(4) To withstand the lateral friction forces that are generated between the reaction blocks of the braced frame and the test floor, estimated to be insignificant for the floor system.

An assessment of the possible demands from the existing test floor indicates that the supplies are sufficiently adequate.

2.4.3 Loading Frame

The braced frame system that was existing in the laboratory had a lateral load capacity of 4 x 240 kips = 960 kips where the load application points are indicated in Fig. 2.59. This frame was incorporated in the design of the loading system, the mathematical model of which is shown in Fig. 2.61. The major components are labelled as braced frame, cross beams, top grid, and columns. The six load sources are also indicated in

Fig. 2.61.

Comparing the mathematical model with the front view of the specimen and the test frame, shown in Figs. 2.62 - 2.64, the mathematical model and the actual counterparts may be related to each other. The crossbeams are transferring the north side lateral force to the braced frame while the south side lateral force is directly transferred to the middle columns of the braced frame. Both lateral forces are subsequently transferred to the floor in the form of a friction force between the base of the reaction blocks and the floor.

The four vertical forces are applied through the top grid which transfers these forces to the middle columns of the braced frame and the columns at the end, as indicated in Fig. 2.61 and then to the floor, through the foundation grid prestressed to the floor and as shown in Figs. 2.62 and 2.65.

All components and connections, as well as the reaction blocks of the loading frame, were designed and checked against the capacities of the actuators (Fig. 2.67), which were larger than the expected maximum forces on the model subassemblage, discussed in Section 2.3.3 and shown on Fig. 2.53. The possibility of changes in the positioning of the vertical forces to accommodate models of different geometry, was also considered. Detailed drawings of the test frame are given in Figs. 2.62 - 2.66. A parts list for the frame is given in Table 2.5.

2.4.4 Actuators and Loading Control System

Information about the load and displacement requirement from the six load sources was given in Sections 2.3.3 and 2.3.4. The six actuators that were installed in the test frame for the purposes of applying the horizontal and vertical forces of the subassemblage are shown in Fig. 2.67.

Also, included in this figure is relevant data, and, the force and stroke capacities for these actuators. The force and displacement capacities were chosen to be adequate for the corresponding force and displacement bounds estimated for the specimen in Sec. 2.3.3. A main hydraulic power supply, which also provides power to the shaking table at the Richmond Field Station, was tapped for the hydraulic pressure demands of the actuators. The power supply provides an adequate flow of oil at 3000 psi to the actuators when the shaking table is not in operation.

Each actuator was equipped with a servo-valve and a load cell, rated for the capacity of the actuator. Each actuator was linked to a controller, which was capable of commanding the actuator through the servo-valve on either force or stroke control. The force feedback was obtained from the load cell of the actuator while the stroke feedback could be obtained from any selected displacement transducer on the specimen.

The loading system thus consisted of six actuators with servo-valves and load cells, and six independent controllers, one for each actuator. Each controller could be operated manually, by monitoring the force or stroke feedback through a digital voltimeter, and maintaining any desired value for the feedback. Other alternatives were also available; to preset the force or stroke of any actuator, a slave to the force or stroke in a master actuator was possible by wiring between controllers. In this manner, one master actuator could be commanded through either force or stroke feedback while another, or any other slave actuator(s), could apply a force or displacement which is an established percentage of the force or displacement of the master actuator. A further option in the operation of the actuators was the possibility of operating each

actuator either independently or as a slave through two individual control channels in each controller. This option was used to maintain gravity loads in the vertical actuators individually, followed by operating all vertical actuators as slaves to a lateral actuator to simulate overturning and coupling effects at the top of the subassemblage.

Using the control options explained above, the six actuators were programmed to operate in the following manner during the initial period of tests:

(1) The gravity loads were applied by the four vertical actuators (in increments).

(2) The lateral actuators were loaded in force control at small increments until a certain inelastic response state was reached by the specimen.

(3) The force in the lateral actuator at the north end was made a slave to the force in the lateral actuator at the south end at all times.

(4) Lateral loadings after a certain inelastic response state was continued on a displacement feedback. The problem associated with this operation was the possibility of the failure of the wall loaded by the slave actuator, while the wall being loaded by the master actuator retained its capacity. Trying to maintain the same force applied by the master ram, the slave ram would not release its load and could relentlessly destroy the girders and the wall to which it is attached. This possibility was checked by manually and continuously monitoring displacement readouts on rams. Another alternative was to maintain identical strokes by the two lateral actuators. This, however, was not applied during the first series of tests as it would have resulted in involuntarily restraining the growth of the walls and the beams at the top of the specimen, as explained in Section 2.3.4. More significantly, relating vertical forces

to the lateral forces would have been a difficult problem when the lateral force in each wall is not predetermined. One possible solution appears to be relating the vertical forces of each wall to the lateral force that is resisted by that particular wall.

(5) The vertical actuators, after applying the gravity loads, applied forces as a function of the forces in the master lateral actuator. The force transfer relations between the lateral and vertical rams were discussed and derived in Section 2.3.4.

2.5 Instrumentation and Data Acquisition

2.5.1 General

The main external force, internal force, deformation, and strain quantities to be measured were assessed critically with the objective of arriving at an optimum external and internal instrumentation scheme for the specimens. Although it is usually tempting to over-instrument a test specimen, limitations to the speed and capacity of data acquisition systems, as well as data reduction capabilities, limit the amount of data that may be retrieved from a test.

The six external forces (applied by the actuators, Fig. 2.67) were monitored by load cells built specially for each actuator. The internal forces of the four connecting beams were the internal force quantities monitored by force transducers designed and manufactured for this purpose, (Figs. 2.69 - 2.73). Knowing the 6 external and 12 internal force quantities, the internal forces of any other cross section of the structure could be obtained through statics.

The deformations that were decided to be measured (Fig. 2.68) were:

(1) The lateral displacement of each wall at each floor level and the mid-height of the first floor.

(2) The contribution of shear distortion to the lateral deformations of each wall at each floor level.

(3) The axial deformations along each of the four edge members, and the pull-out deformation at their bases.

(4) The average strain in the 0°, 45° and 90° directions, at each corner of both first floor wall panels.

(5) The elongation (growth) of each beam.

(6) The rotations along the critical regions of the beams.

(7) The contribution of the shear distortion to these beam rotations.

The rigid body displacement components at the bases of the walls and any displacement of the reference frame from which specimens' deformations were measured, were also included in the external instrumentation (Fig. 2.68). The internal (strain) instrumentation was designed with the objectives of recording the strain history of and detecting the first yield of the reinforcing bars at the critical regions of the beams (Fig. 2.74) and the walls (Fig. 2.75). Bond stress distribution over a number of the reinforcing bars at the critical regions were also obtained.

2.5.2 Data Acquisition

Special force transducers, load cells, large displacement capacity wire linear potentiometers (wire pots), regular metal core linear potentiometers (stick pots), clip gages and weldable strain gages, as well as dial gages, constituted the force, deformation (displacement), and strain measuring devices used in the experiments. Data from all instrumentation were collected by two identical data acquisition systems

at manually controlled intervals. Each system, incorporating a teletype, scanner boxes, a computer, and a tape device, was capable of reading up to 500 data channels at 2 channels per second, converting this data to engineering units, and storing it on magnetic tape. Due to the large number of data channels (approx. 250), if only one data acquisition system were used, a reading of all the data channels, printing of results on the teletype (requiring a significant amount of time), and writing on magnetic tape, would have required approximately 10 minutes. This would have resulted in acquiring data at infrequent load and/or displacement intervals and would have led to significant inelastic creep problems during the tests. It was decided to consider the data in two groups connected to two different acquisition systems:

(1) Primary (control) data, including basic external force and displacement measurements, required to control the test and immediate diagnosis of behavior, (approx. 50 channels).

(2) Secondary data, including all strain readings and local deformation readings (approx. 200 channels).

The primary data, involving only 50 channels, were retrieved at close intervals and printed for immediate diagnosis; and the secondary data were recorded on tape, which required less time than printing the primary data. At a number of intermediate load or displacement points during the load history, data were scanned and stored by both systems without printing the primary data channels. Using two data acquisition systems in such a manner facilitated the control and execution of the test. The major force and displacement channels were also monitored by two and three channel x-y recorders.

The data stored on magnetic tape are reduced subsequently on a CDC 7600 computer system. Reorganization of, and printing, plotting, and carrying out computations on this data are achieved by writing computer codes for this purpose. A detailed in-house report on these data reduction codes, which also contains detailed technical specifications and other data on instrumentation, is available [2.4]. Brief information is provided on the type, location, and purpose behind installation of the individual force, displacement, or strain sensors in subsequent sections.

2.5.3 External Instrumentation

The external instrumentation consisted of (1) Load cells, (2) Force transducers, (3) Displacement transducers (wire or stick linear potentiometers),(4) Clip gages, (5) Dial gages. These are indicated in Fig. 2.68.

(1) Load Cells: (Fig. 2.68) Each actuator was equipped with a screw-in load cell rated for the capacity of the actuator (Fig. 2.67). The six load cells were connected to the six controllers, and then to both data acquisition systems and recorders.

(2) Force Transducers: (Fig. 2.68) Special force transducers were designed to monitor the axial force, shear force, and bending moment at the midspan of the connecting beams. A detailed in-house report is available on these transducers [2.4]. The basic approach in the design was to idealize a beam segment by various axially-loaded fibers (force-bars) which could be instrumented by strain-gages and wired so that individual internal force channels, which do not interact with each other, could be obtained.

The side view of the force transducer indicating the force bars is shown in Fig. 2.69. A front view, and connection details between the force bars and the end plates, are shown in Figs. 2.70 and 2.71. The wiring diagram for each of the internal force channels is shown in Fig. 2.72. The transducers were calibrated under axial compression, pure bending, and bending with shear, as outlined in Fig. 2.73.

In the transducers, the total number of force channels, twelve altogether, were monitored by the primary data acquisition system. It was possible to compute the internal force at any cross section of any member of the subassemblage with the information obtained from the force transducers and the load cells, as the components of the subassemblage were rendered statically determinate with this information. The force transducers thus yielded vital information to assess the overall behavior of the subassemblage, namely, the shear and flexural redistributions that occurred between the walls, and the axial load in each wall.

(3) Displacement Transducers: The different types of displacement transducers used on the specimens were wire pots, stick pots, LVDT's, clip gages, and dial gages. An instrumentation column was erected at each side of the specimen (Fig. 2.68), on which a wire pot was installed to measure the lateral displacement at each floor level of each wall. The pots at the floors were 30 in. capacity ($\mp$ 15 in.), while mid-height first floor, was instrumented with 12 in. capacity ($\mp$ 6 in.) stick pots. The top of the instrumentation columns were instrumented with wire pots to record displacements of these columns with respect to stationary points in the laboratory. Displacements in the order of 0.025 inches were recorded at the top of the instrumentation columns because of floor rotations at the base. The measured specimen lateral deformations were

corrected to incorporate the displacement column displacements during the data reduction.

The shear distortion of each floor of each wall was measured by diagonally placed stick pots (Fig. 2.68). Elongation of the columns and the pull-out distortion at the foundation level were measured with clip gages (Fig. 2.68). In addition to computing the growth of each edge column, these clip gages were used to compute the distribution of average rotation over the height of the walls. The two first-floor panels were instrumented with clip-gage rosettes at each corner, as shown in Fig. 2.68, to evaluate the direction and magnitude of the principal strains at these locations. Beams were instrumented with clip gages to measure the rotations at the column-beam interface and along the critical sections of the beams, as shown in Fig. 2.74. The diagonally placed clip gages were for measuring the contribution of shear distortions to the overall rotations of the beam critical regions.

The displacements and rigid body rotations of the test specimen foundation were checked with a sufficient number of dial gages. The total number of displacement transducers used during a typical test, follows (Fig. 2.68)

8 - 30 in. capacity wire pots

23 - 12 in. capacity stick pots

2 - 12 in. capacity wire pots

16 - 4 in. long clip gages

96 - 12 in. long clip gages.

Of these instruments, the wire pots and stick pots were connected to the primary data acquisition system. The clip gages were connected to the secondary system. The two top level displacement potentiometers were

also connected to the secondary system in order to relate the readings in both systems. These top level displacement potentiometers were first connected to the controllers to operate the lateral actuators in stroke control; they were then connected to the two data acquisition systems and recorders.

2.5.4 Internal Instrumentation

The internal instrumentation consisted of weldable strain gages with a strain capacity of 0.02. These gages were welded along their lengths on reinforcing bars. The protruding lugs of the deformed bars were ground off at the locations of these gages. The strain gage locations of a typical beam are shown in Fig. 2.74. The gages of the walls and the edge columns are indicated in Fig. 2.75.

A total of 112 strain gages were used in each specimen, with the basic objectives being to: (1) Detect the yield of stirrups and flexural bars; (2) Determine the distribution of strain along the bars instrumented with more than one gage, i.e., bond stress distribution; (3) Obtaining the distribution of strain along cross sections instrumented by gages at different locations, i.e., curvature computations; (4) Record the history of bar strains at the critical regions of the beams, edge columns, and panels. All the strain gages were connected to the secondary data acquisition system.

REFERENCES

2.1 Abrams, D. P., Sozen, M. A., "Experimental Study of Frame-Wall Interaction in Reinforced Concrete Structures Subjected to Strong Ground Motions," Civil Engineering Studies, SRS No. 460, University of Illinois at Urbana-Champaign, May 1979.

2.2 Aristizabal-Ochoa, J.D., Shiu, K. N., and Corley, W. G., "Effects of Beam Strength and Stiffness on Coupled Wall Behavior," Proceedings of the Second U.S. National Conference on Earthquake Engineering, Stanford University, Stanford, California, August 22-24, 1979, pp. 323-332.

2.3 Coull, A., and Choudbury, J. R., "Analysis of Coupled Shear Walls," Journal ACI, September 1967.

2.4 Habib, M., "Response of Coupled Shear Wall Subassemblage Test Specimen," Earthquake Engineering Research Center, In-house Report, University of California, Berkeley, California.

2.5 Iliya, R., and Bertero, V. V., "Effects of Amount and Arrangement of Wall-Panel Reinforcement on Hysteretic Behavior of Reinforced Concrete Walls," Report No. UCB/EERC 80-04, Earthquake Engineering Research Center, University of California, Berkeley, 1980.

2.6 Kanaan, A. E., and Powell, G. H., "DRAIN-2D, A General Purpose Computer Program for Dynamic Analysis of Inelastic Plane Structures," Earthquake Engineering Research Center, Report No. UCB/EERC 73-6, Revised August 1975, University of California, Berkeley, California.

2.7 Li-Hyung and Bertero, V. V., "Testing Facility for Coupled Shear Walls," Earthquake Engineering Research Center, In-House Report, University of California, Berkeley, California.

2.8 Mahin, S. A., and Bertero, V. V., "An Evaluation of Some Methods for Predicting Seismic Behavior of Reinforced Concrete Buildings," Report No. UCB/EERC 75-15, Earthquake Engineering Research Center, University of California, Berkeley, California, 1975.

2.9 Mahin, S. A., Bertero, V. V., Chopra, A. K., and Collins, R., "Response of the Olive View Hospital Main Building during the San Fernando Earthquake," Earthquake Engineering Research Center, Report No. UCB/EERC 76-22, University of California, Berkeley, California, 1976.

2.10 Oesterle, R. G., et al., "Earthquake Resistant Structural Walls - Tests of Isolated Walls - Phase II," Report to NSF submitted by Construction Technology Laboratories, P.C.A., October 1979.

2.11 Paulay, T., "Coupling Beams of Reinforced Concrete Shear Walls," Proceedings of a Workshop on Earthquake Resistant Reinforced Concrete Building Construction (V. V. Bertero, Organizer), July 11-15, University of California, Berkeley, Vol. III - Technical Papers, pp. 1452-1462.

2.12 Piazza, M., Aktan, A. E., and Bertero, V. V., "Time-History Analyses of a 15-Story R/C Coupled Wall - Frame Building," EERC Report in Preparation.

2.13 Recommended Lateral Force Requirements and Commentary, Seismology Committee, Structural Engineers Association of California, 1975.

2.14 Santhakumar, A. R., "Ductility of Coupled Shear Walls," Thesis presented for the degree of Doctor of Philosophy in Civil Engineering, in the University of Canterbury, Chirstchurch, New Zealand, October 1974.

2.15 Tentative provisions for the Development of Seismic Regulations for Buildings prepared by the Applied Technology Council (ATC 3-06), 1978.

2.16 Uniform Building Code, 1973 Edition, International Conference of Building Officials, Whittier, California.

2.17 Uniform Building Code, 1979 Edition, International Conference of Building Officials, Whittier, California.

2.18 Vallenas, J. M., Bertero, V. V., and Popov, E. P., "Hysteretic Behavior of Reinforced Concrete Structural Walls," Report No. UCB/EERC 79-20, Earthquake Engineering Research Center, University of California, Berkeley, California, 1973.

2.19 Wang, T. Y., Bertero, V. V. and Popov, E. P., "Hysteretic Behavior of Reinforced Concrete Frames Walls," Report No. UCB/EERC 75-23, Earthquake Engineering Research Center, University of California, Berkeley, California, 1975.

2.20 Wilson, E. L., Dovey, H. H. and Habibullah, A., "Three Dimensional Analysis of Building Systems - TABS 77," Report No. UCB/EERC 72-8, Revised April 1979, College of Engineering, University of California, Berkeley, California.

TABLES

TABLE 2.1 MAGNITUDE AND DISTRIBUTION OF THE EARTHQUAKE LOADING FOR THE PROTOTYPE COUPLED WALL SYSTEM (INCLUDING TORSION)

	1973 UBC (ZONE 3)	1979 UBC (ZONE 4)
FLOOR	KIPS	KIPS
15	86.76	183.90
14	91.63	108.68
13	85.09	100.92
12	78.54	93.15
11	72.00	85.40
10	65.45	77.63
9	58.91	69.87
8	52.36	62.10
7	45.82	54.34
6	39.27	46.58
5	32.73	38.81
4	26.18	31.05
3	19.64	23.28
2	13.09	15.53
1	6.55	7.76
Total Base Shear, Kips	774	999

* The point of application of the resultant "E" loading, measured from the base of the wall, is: 1478 in. for 1973-UBC loading (0.68 H), and, 1534 in. for 1979-UBC loading (0.71 H).

TABLE 2.2 RESULTS OF NOMINAL ANALYSIS BY NONFACTORED "E," "D" AND "L" LOADING PRESCRIBED BY UBC-73 AND UBC-79

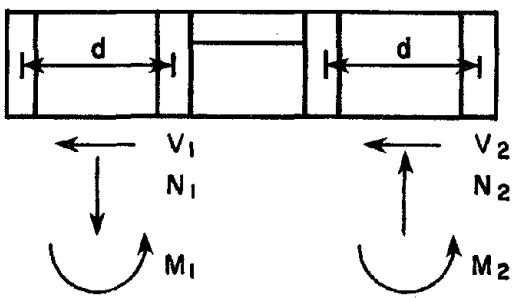

FORCES AT THE BASE RESULTING FROM "E" LOADING ONLY (NO GRAVITY EFFECTS)

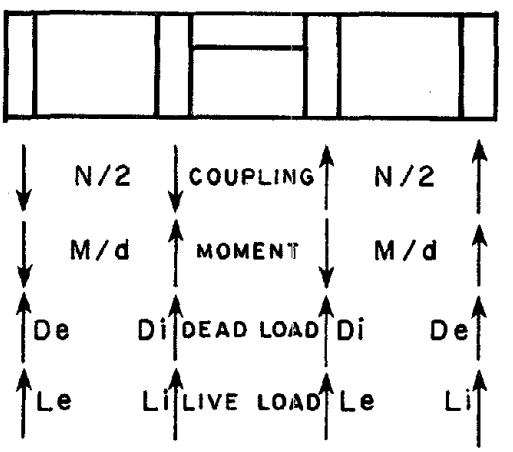

EDGE MEMBER DESIGN FORCES INCLUDING GRAVITY

	"E" LOAD ANALYSIS			EDGE MEMBER DESIGN FORCES (kips)					
	$V_1 = V_2$ (kips)	$M_1 = M_2$ (kip-in.)	$N_1 = N_2$ (kips)	N/2	M/d	De	Di	Le	Li
UBC73	-387.00	191838	1690	845	761	854	1232	71	113
UBC79	499.50	252313	2283	1142	1001	854	1232	71	113

TABLE 2.3 RESULTS OF NOMINAL ANALYSIS;
BEAM DEMANDS FOR "E" LOADING

	BEAM END MOMENTS (KIP-IN.)			
FLOOR	UBC 73	TYPE	UBC 79	TYPE
15	4936		7496	
14	5522	1	8257	1
13	* 6457		* 9407	
12	7567		10749	
11	8732	2	12144	2
10	* 9867		*13493	
9	10905		14717	
8	11788		15745	
7	12456		16504	
6	12839	3	*16907	3
5	*12847		16835	
4	12350		16124	
3	11164		14534	
2	9013	2	11710	2
1	5493	1	7125	1

Beam End Moments for Gravity Loading $\frac{Wl^2}{12}$:

1.4(DL + LL)†	1312 kip-in.
0.9 DL	737 kip-in.

† LL is reduced by 60%

TABLE 2.4 LINEAR DEMANDS FOR ONE SET OF COUPLED WALLS AND ONE TYPICAL FRAME AT THE BASE OF THE PROTOTYPE

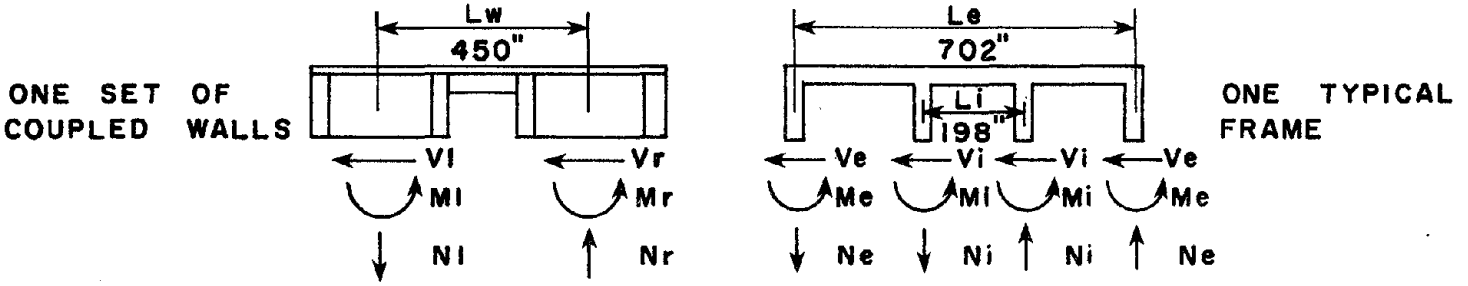

$V_w = V_l + V_r$

$BOM_w^* = M_l + M_r + R_w N$

$V_f = 2V_e + 2V_i$

$BOM_f^* = 2M_e + 2M_i + l_i N_i + l_e N_e$

	WALLS RESIST ALL E/Q EFFECTS INDIVIDUALLY		WALLS AND FRAMES RESIST ALL E/Q EFFECTS TOGETHER			
ANALYSIS	V_w KIPS	BOM_w 10^3 kip-in	V_w kips	BOM_w 10^3 kip-in	V_f kips	BOM_f 10^3 kip-in
UBC 73 "E" LOADING	774	1144.18	656	807.35	30	190.56
EL CENTRO ** 500 E, 0.33 g 5% DAMPING	4418	6188.34	5692	6963.61	257	727.73
DERIVED PACOIMA** S16E, 0.4 g 5% DAMPING	13012	19828.06	11554	14613.28	527	1533.08

* BOM: Base Overturning Moment, which is a measure of flexural demand.

** Modal Spectral Analysis, only the first three Modes of the structure were considered.

TABLE 2.5 PARTS LIST OF THE TEST FRAME

Part	No. of Parts	Rolled Sections[2]			Plates[2]		
		Section[1]	Total Length (in.)	Total Weight (lbs.)	No. per Part	Dimensions (in.)	Total Weight (lbs.)
A	2	W 30x132+	23' 3-1/4"	6,144	1	30-1/4x10-1/2x3/4	138
					2	12x24x1+	334
					4	28-1/4x5x5/8	205
B	4	W 27x177+	25-3/8	1,500	4	24-7/8x6-5/8x3/8	287
		L 4x3x5/8(4)	82	372			
C	1	W 21x142+	67	793	2	21-1/2x13-1/8x3/4	123
					4	19-1/4x6-1/4x3/8	53
D	2	□ 10x10x5/8	31' 6-1/2"	4,667	1	12-5/8x12-5/8x1-3/4	162
					2	7x7-1/2x2	61
E	2	□ 10x10x5/8	31' 5"	4,648	1	12x14x2	195
					2	10x11-1/2x3	400
F	4	C 10x20	94	627	1	7x15x1-1/2	183
					1	20-1/2x15x5/8	223
					2	17-1/2x5x1	203
G	2				1	12x36x2-1/2	626
H	2	EYE			1	12-3/4x12-3/4x1-3/4	165
					1	8x7x4	130

(Cont.)

[1]Total number of various sections given in ( ) if greater than one.

[2]All parts A36 steel except those noted + = A588 steel.

TABLE 2.5 Continued

Part	No. of Parts	Rolled Sections[2]			Plates[2]		
		Section[1]	Total Length (in.)	Total Weight (lbs.)	No. per Part	Dimensions (in.)	Total Weight (lbs.)
I	2	EYE			1	37x18x4	1,545
					1	17-1/2x16x8	1,300
J	2	EYE			1	37x18x4	1,545
					1	10x11-1/2x6	400
K	1	EYE			1	13-1/8x19x2-1/2	181
					1	11-1/2x10x6	200
L	2				1	20-1/2x16-1/2x2-1/2	490
					2	11-3/4x10x3	205
M	2	CLEVIS			1	16x24x3	668
					2	11-1/2x10x3	400
N	2	CLEVIS			1	19x15-1/4x2-1/2	420
					1	11-1/2x10x6	400
O	5	L 5x5x1/2	52-11/16	378			
P	1	C 15x33.9		2,829	1	72x20-/34x1/2	217
					4	3-3/8x15x1/2	29
					4	7x15x1/2	61
					6	13x13x2	588
					2	13x18x2	136

[1]Total number of various sections given in ( ) if greater than one.

[2]All parts A36 steel except those noted + = A588 steel.

(Cont.)

TABLE 2.5 Continued

Part	No. of Parts	Rolled Sections[2]			Plates[2]		
		Section[1]	Total Length (in.)	Total Weight (lbs.)	No. per Part	Dimensions (in.)	Total Weight (lbs.)
Q	1	C 9x15	88-1/2	111			
R	2	CLEVIS			1 2	23x21x3 16x17x2-1/2	
S	2	CLEVIS			1 2	21x17-1/4x2-1/2 11-1/2x10x3	
T	4	W 36x230	N.A.	N.A.			
U	4	W 12x65	N.A.	N.A.			
V*	2	MC 12x35(2) MC 7x19.1(15)	34' 10" 15'	2,438 573	6 6 6	3-3/4x12x1/2 10-5/8x3-1/4x1/2 7x14x1-1/2	78 60 511
W*	2	□ 8x8x1/2	28'2-7/8"	2,674	1	15-1/2x15-1/2x1-1/2	209
X*	2	C 10x25	9' 8"	483			
Y*	4	□ 8x8x1/2	21'	3,977	1	15-1/2x15-1/2x1-1/2	418
Z*	3	C 5x9	9' 6"	257			
a*	4	C 5x9	15' 8"	564			
b*	2	MC 8x18.7	10	32			

[1]Total number of various sections given in ( ) if greater than one.

(Cont.)

[2]All parts A36 steel except those noted + = A588 steel.

*Ancillary frame parts.

TABLE 2.5 Continued

Part	No. of Parts	Rolled Sections[2]			Plates[2]		
		Section[1]	Total Length (in.)	Total Weight (lbs.)	No. per Part	Dimensions (in.)	Total Weight (lbs.)
c	6				1	36-1/2x5x1/2	159
d	4	C 9x20	96				
e	6	C 10x20	40				
f	4	W 6x8.5	15-1/4				
g	2	PIN 5"ϕSTOCK	12	137			
h	2	PIN 3-1/2"ϕSTOCK	10	56			
i	2	PIN 5"ϕSTOCK	14	160			

[1]Total number of various sections given in ( ) if greater than one.

[2]All parts A36 steel except those noted + = A588 steel.

FIGURES

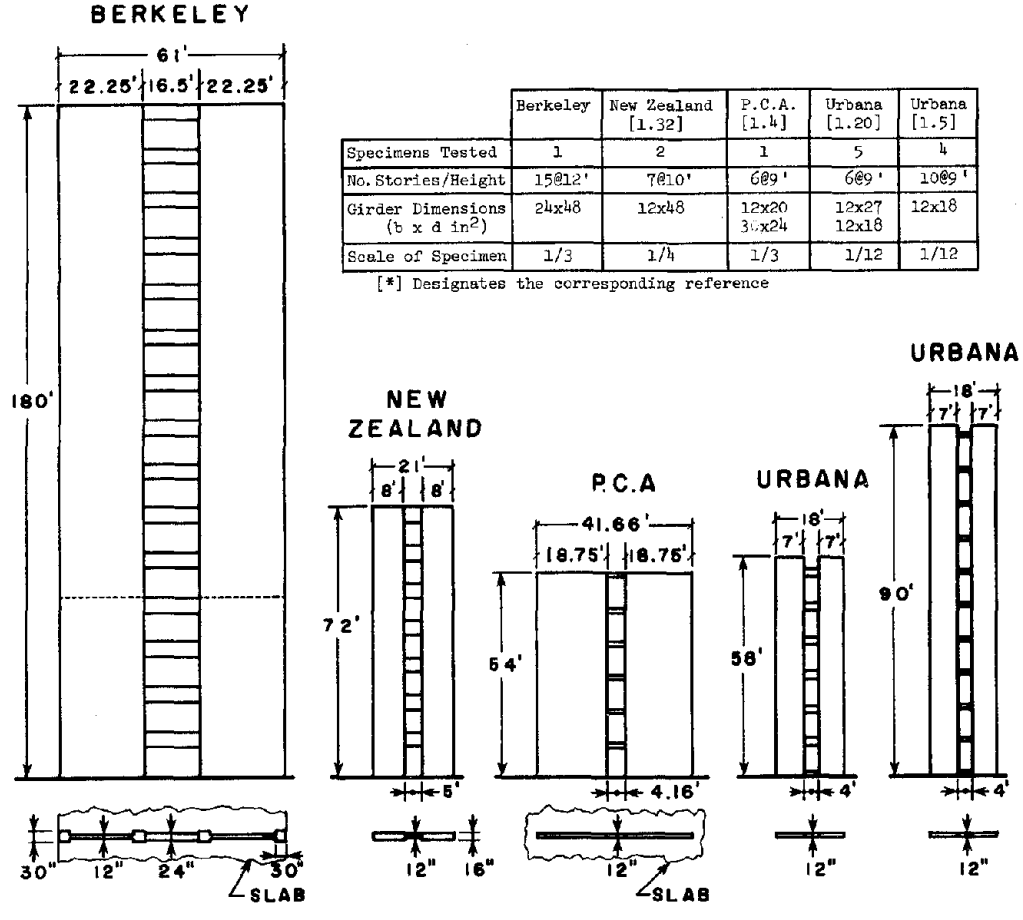

	Berkeley	New Zealand [1.32]	P.C.A. [1.4]	Urbana [1.20]	Urbana [1.5]
Specimens Tested	1	2	1	5	4
No. Stories/Height	15@12'	7@10'	6@9'	6@9'	10@9'
Girder Dimensions (b x d in^2)	24x48	12x48	12x20 30x24	12x27 12x18	12x18
Scale of Specimen	1/3	1/4	1/3	1/12	1/12

[*] Designates the corresponding reference

FIG. 1.1 SAME SCALE PRESENTATION OF THE PROTOTYPES OF PREVIOUSLY TESTED COUPLED WALL SPECIMENS

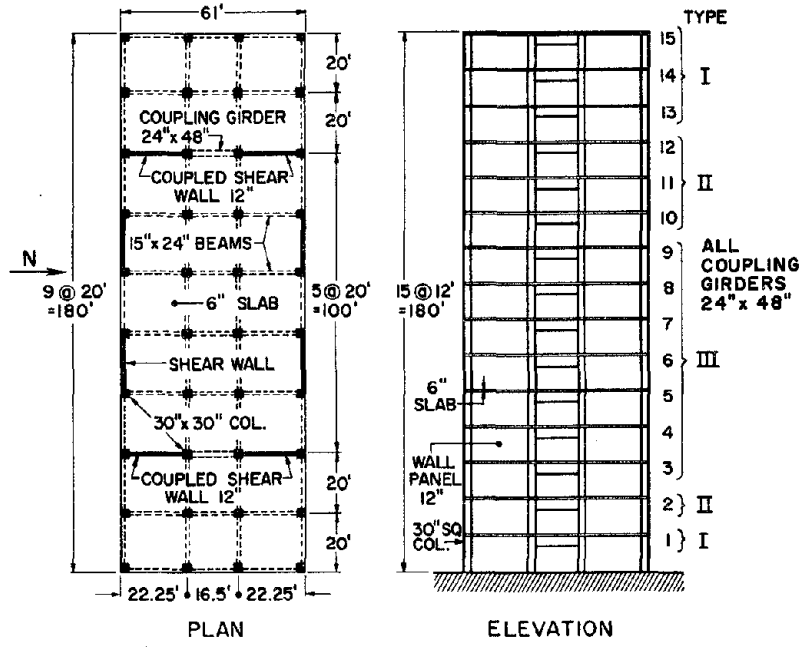

FIG. 2.1 PROTOTYPE STRUCTURE

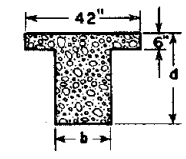

Section (bxd)	$I_p \times 10^3$ in^4	k_{cw}/k_{sw} (%)
21 x 39	134	67
24 x 48	265	79
30 x 48	307	81
30 x 52	388	84
30 x 54	434	85
30 x 60	591	88

k_{cw}: coupled wall stiffness

k_{sw}: solid wall stiffness

I_p: gross section moment of inertia of the connecting beam

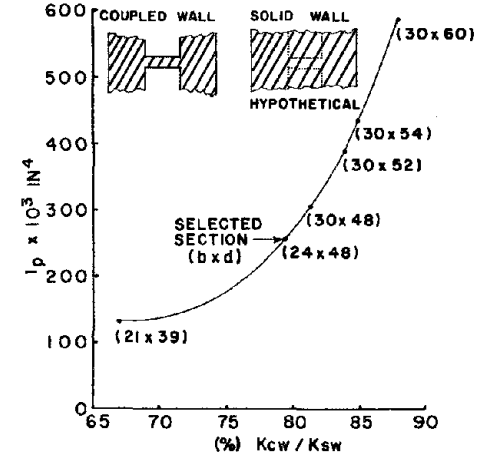

FIG. 2.2 CONTRIBUTION OF BEAM STIFFNESS TO THE STIFFNESS OF COUPLED WALLS

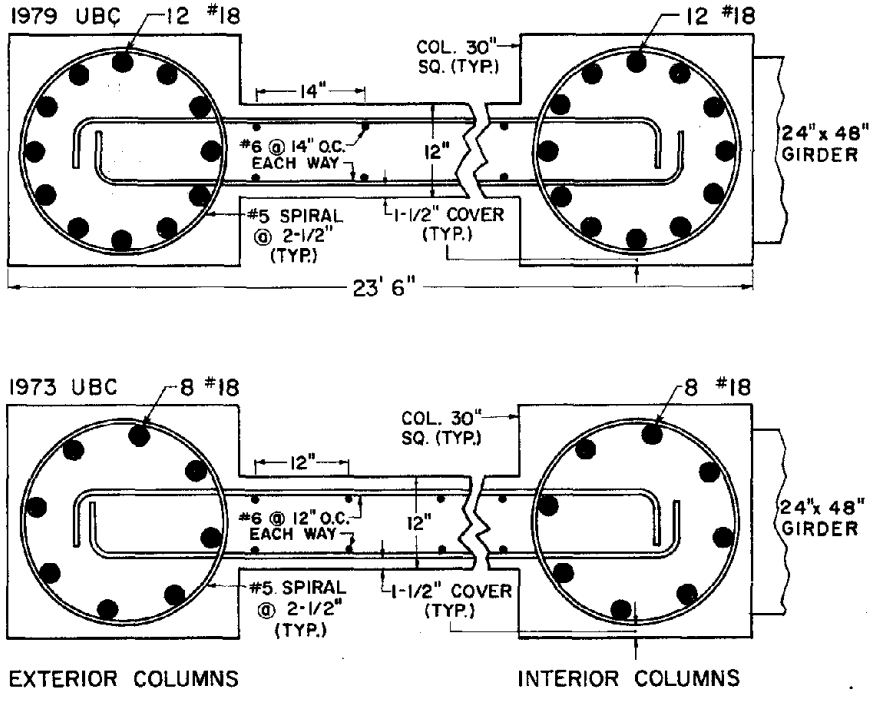

FIG. 2.3 WALL CROSS SECTIONS DESIGNED BY UBC-73 AND UBC-79 PROVISIONS

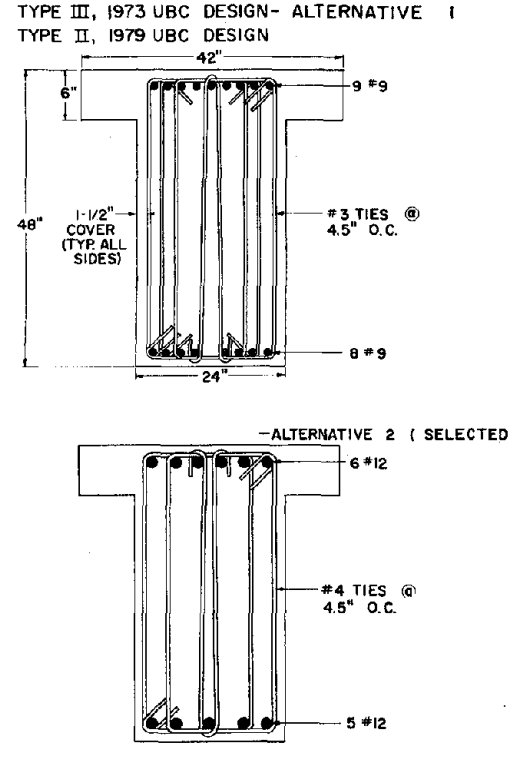

FIG. 2.4 DETAILING OF GIRDER TYPE 3, UBC-73 DESIGN (GIRDER TYPE 2, UBC-79 DESIGN)

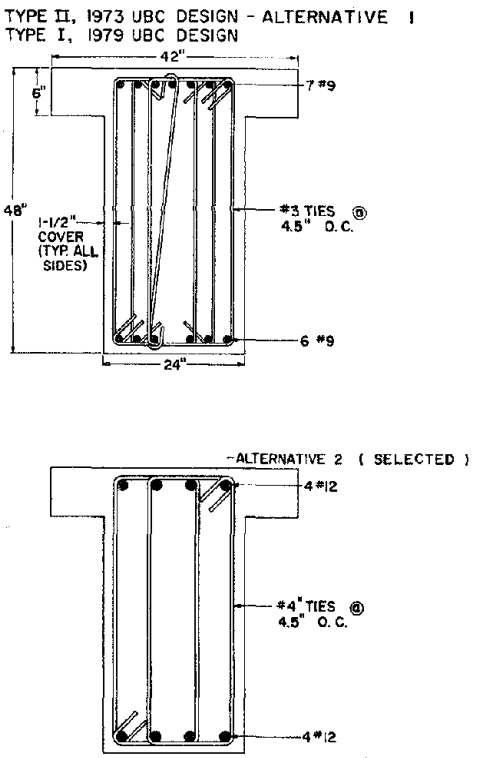

FIG. 2.5 DETAILING OF GIRDER TYPE 2, UBC-73 DESIGN (GIRDER TYPE 1, UBC-79 DESIGN)

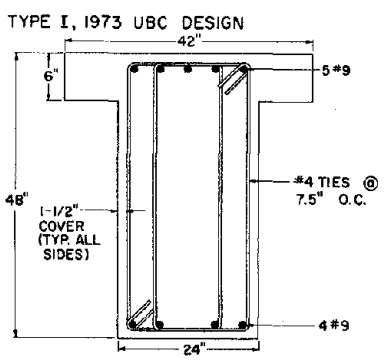

FIG. 2.6 DETAILING OF GIRDER TYPE 1, UBC-73 DESIGN

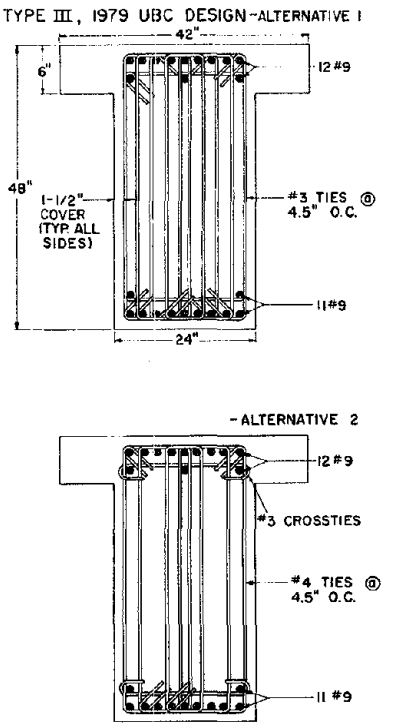

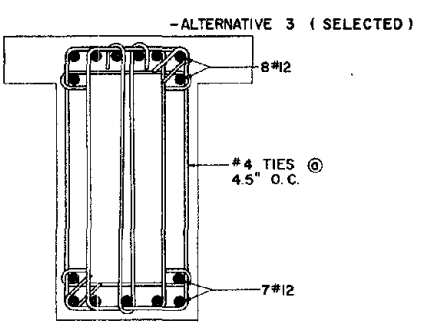

FIG. 2.7 DETAILING OF GIRDER TYPE 3, UBC-79 DESIGN

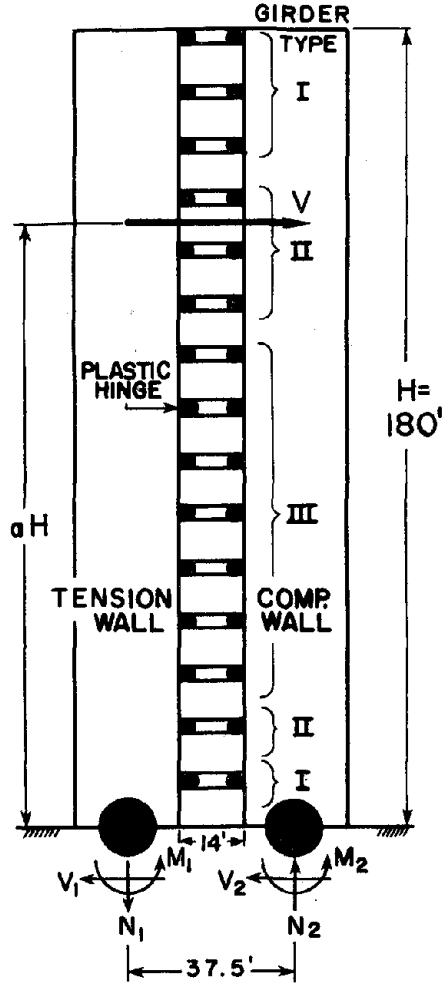

FIG. 2.8 ASSUMED COLLAPSE MECHANISM

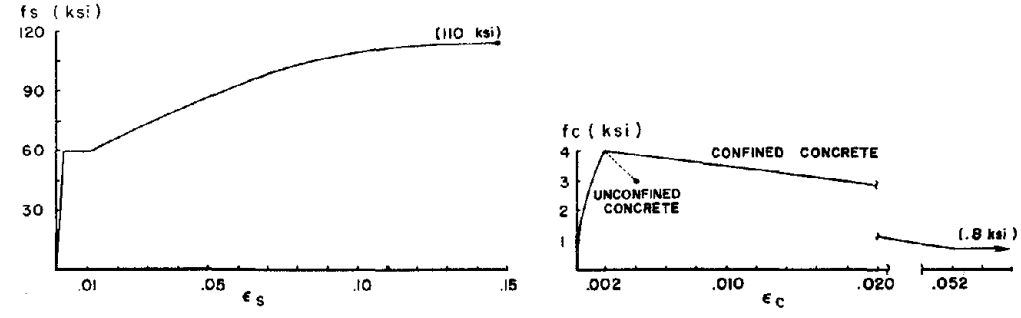

FIG. 2.9 ASSUMED MATERIAL STRESS-STRAIN, CHARACTERISTICS IN GENERATING MOMENT-CURVATURE RESPONSES OF THE BEAMS AND THE WALL CROSS SECTIONS

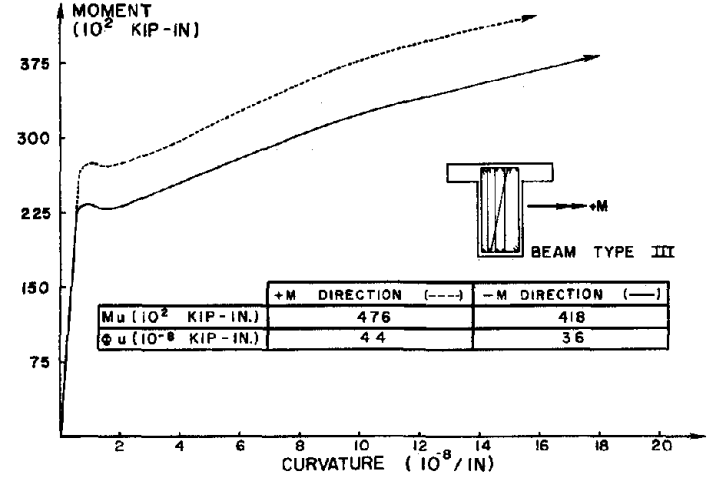

	+M DIRECTION (---)	-M DIRECTION (—)
Mu (10² KIP-IN.)	476	418
Φu (10⁻⁸ KIP-IN.)	44	36

FIG. 2.10 MOMENT-CURVATURE RESPONSES IN BOTH BENDING DIRECTIONS, BEAM TYPE 3, UBC-73 DESIGN

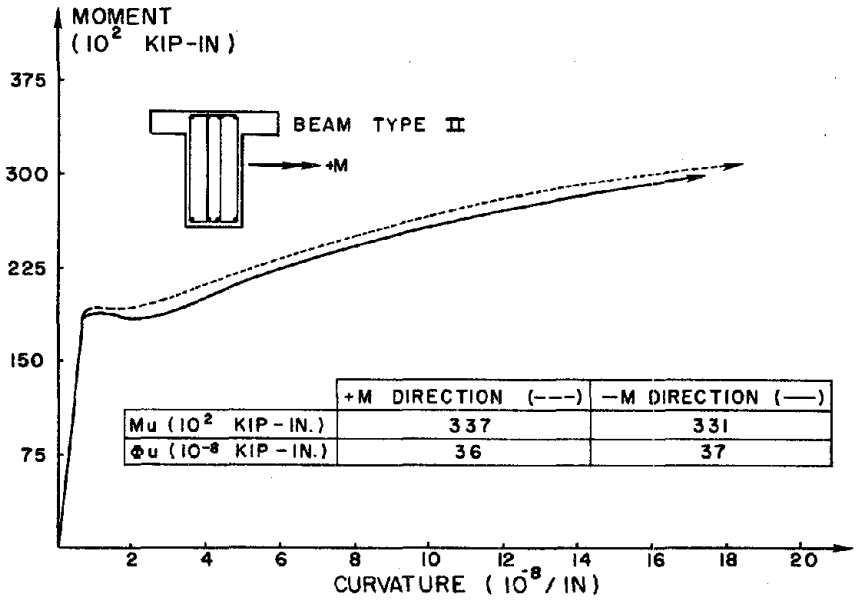

FIG. 2.11 MOMENT-CURVATURE RESPONSES IN BOTH BENDING DIRECTIONS, BEAM TYPE 2, UBC-73 DESIGN

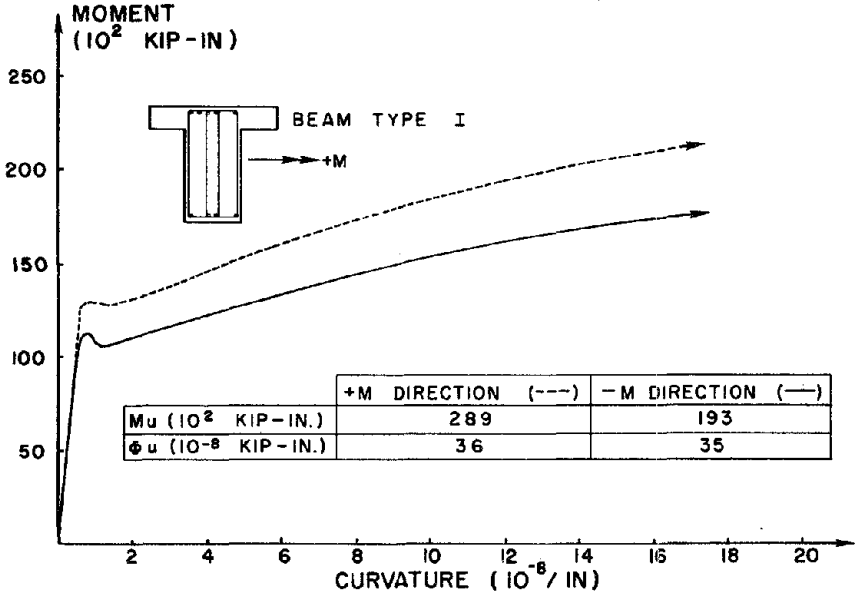

FIG. 2.12 MOMENT-CURVATURE RESPONSES IN BOTH BENDING DIRECTIONS, BEAM TYPE 1, UBC-73 DESIGN

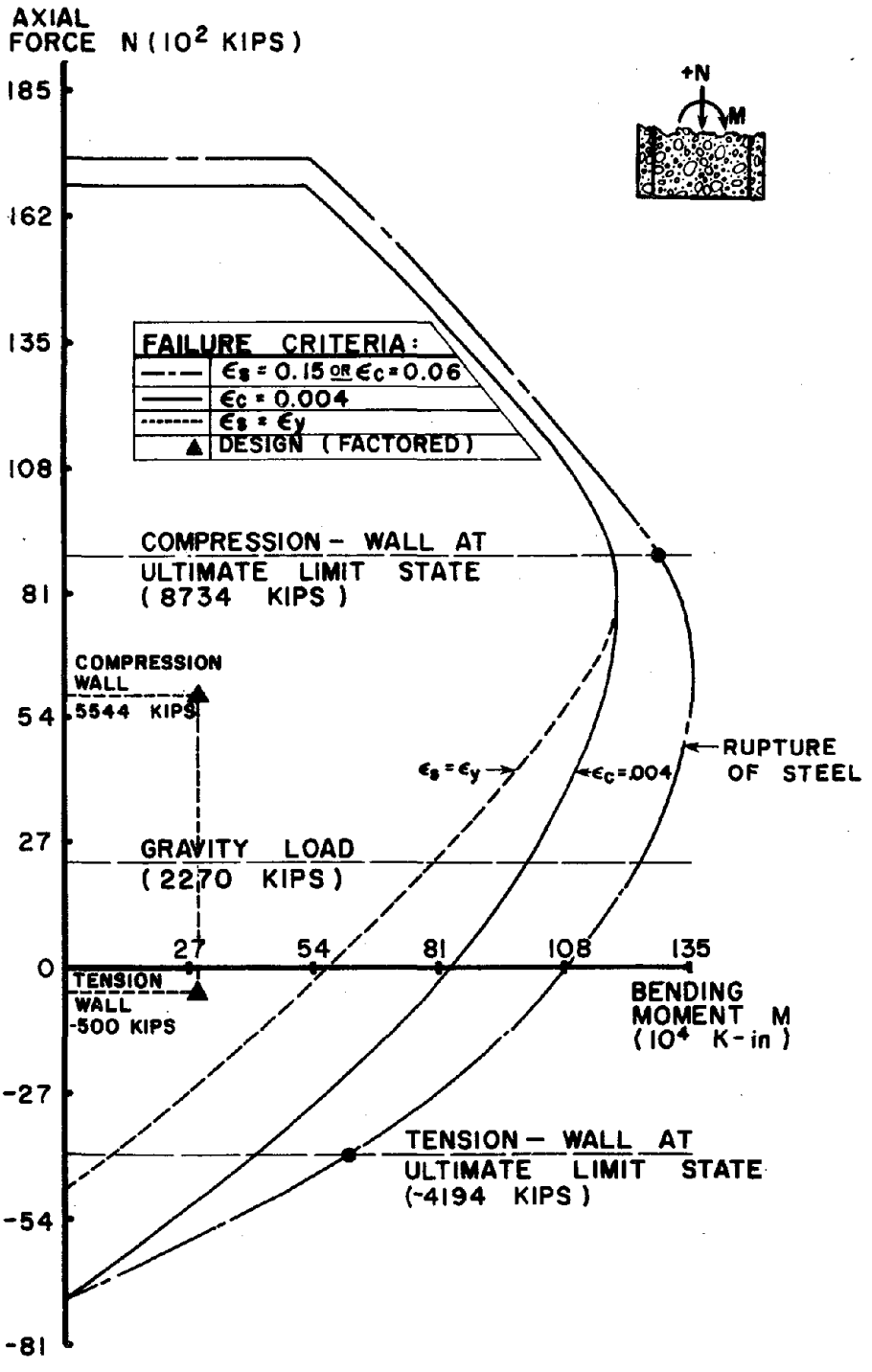

FIG. 2.13 AXIAL FORCE-BENDING MOMENT INTERACTION DIAGRAM FOR THE WALL SECTION DESIGNED BY UBC-73 PROVISIONS

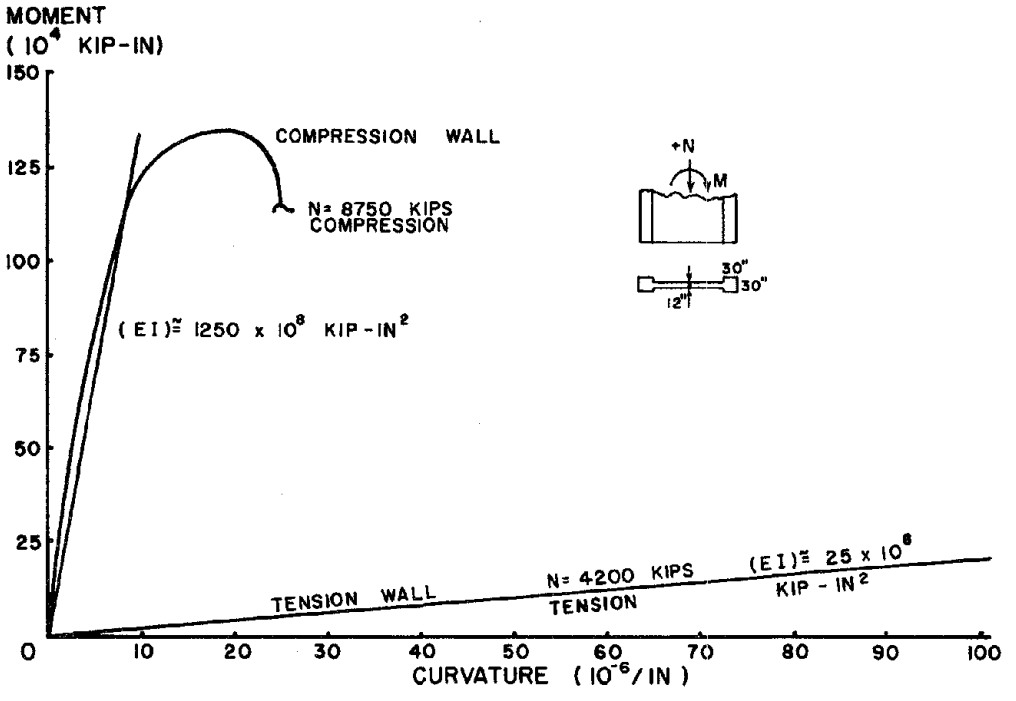

FIG. 2.14 MOMENT-CURVATURE RESPONSES FOR THE WALL SECTION AT AXIAL FORCES CORRESPONDING TO THE ULTIMATE LIMIT STATE

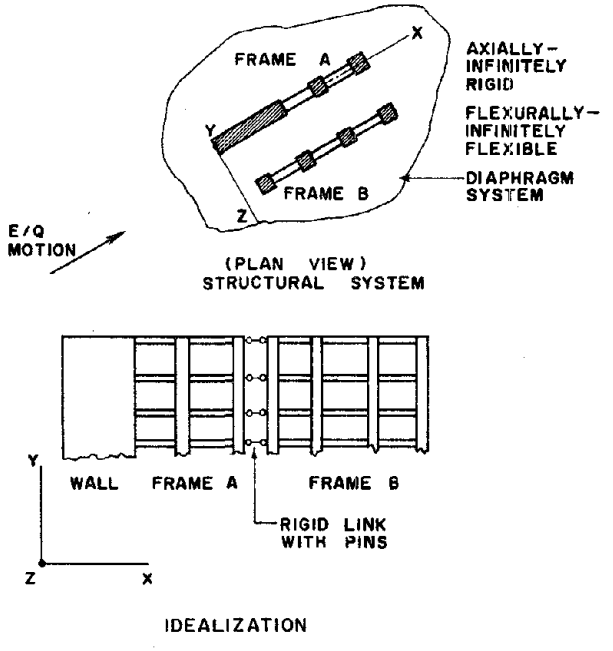

FIG. 2.15 MODELLING FRAME-WALL INTERACTION AS A PLANE PROBLEM

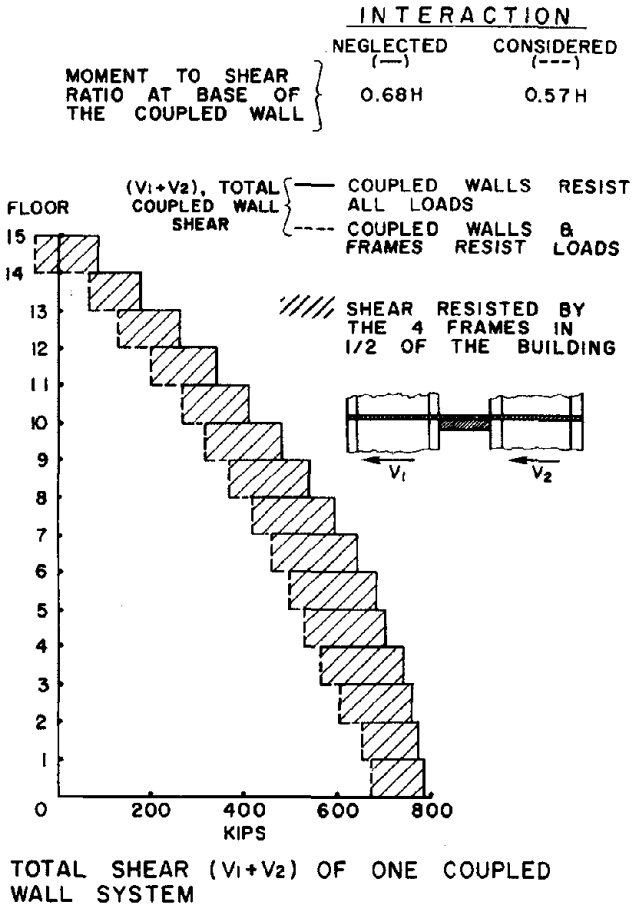

TOTAL SHEAR (V1+V2) OF ONE COUPLED WALL SYSTEM

FIG. 2.16 RESULTS OF STATIC UBC-73 "E" LOAD ANALYSIS, OF ONE-HALF OF THE SYMMETRIC BUILDING

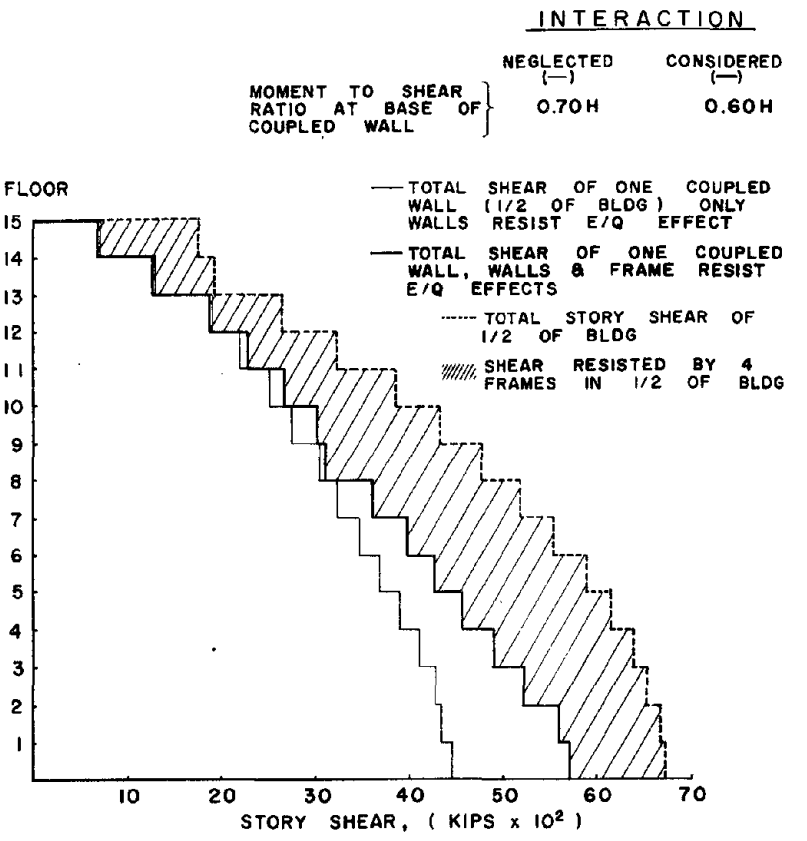

FIG. 2.17 RESULTS OF MODAL SPECTRAL ANALYSIS, WALLS CONSIDERED ACTING ALONE AND WITH FRAMES; EL CENTRO SPECTRUM

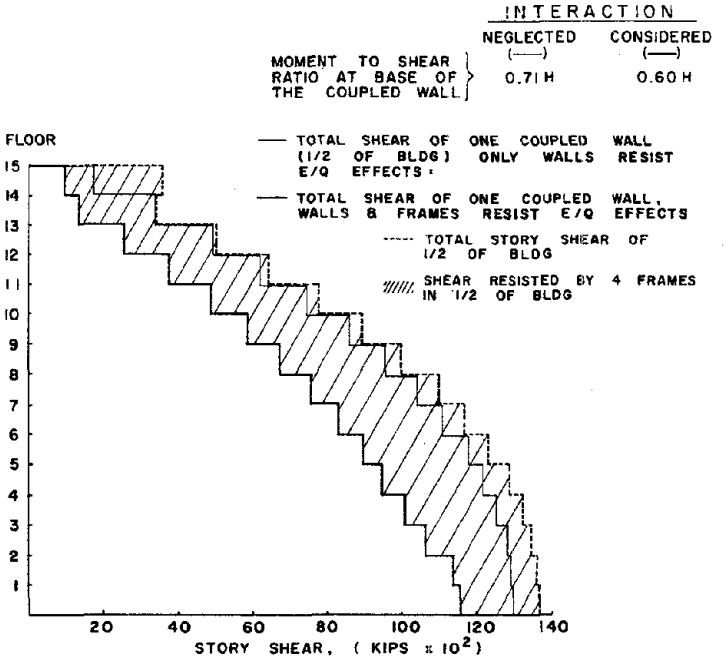

FIG. 2.18 RESULTS OF MODAL SPECTRAL ANALYSIS, WALLS CONSIDERED ACTING ALONE AND WITH FRAMES; PACOIMA SPECTRUM

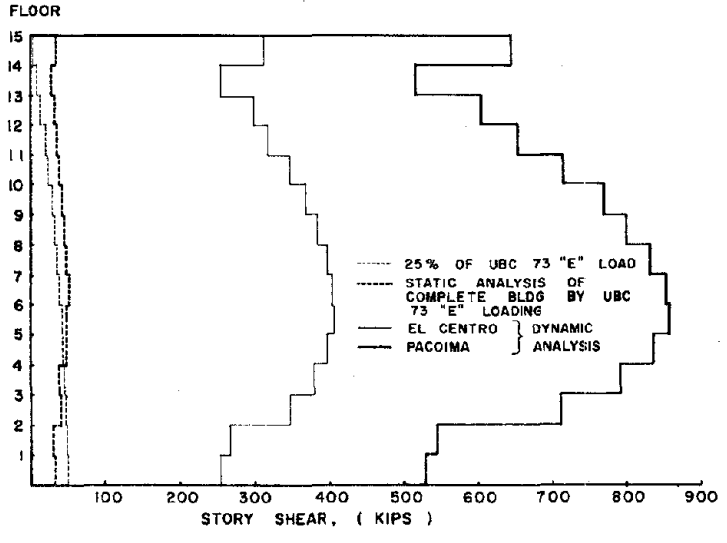

FIG. 2.19 FRAME STORY SHEAR DEMANDS BY CODE AND LINEAR DYNAMIC ANALYSIS FOR ONE TYPICAL FRAME OF THE PROTOTYPE

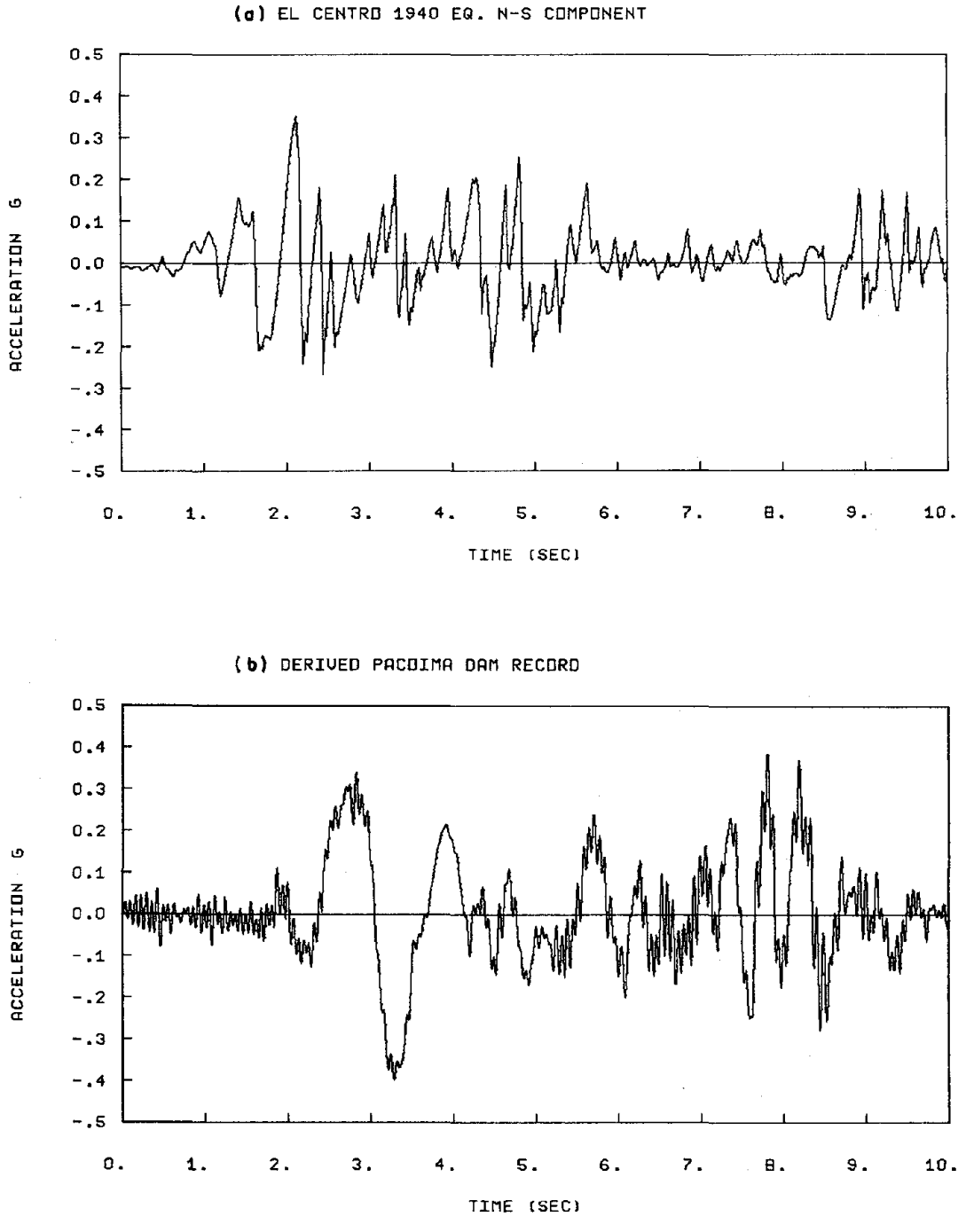

FIG. 2.20 THE ACCELEROGRAMS USED IN THE ANALYSES

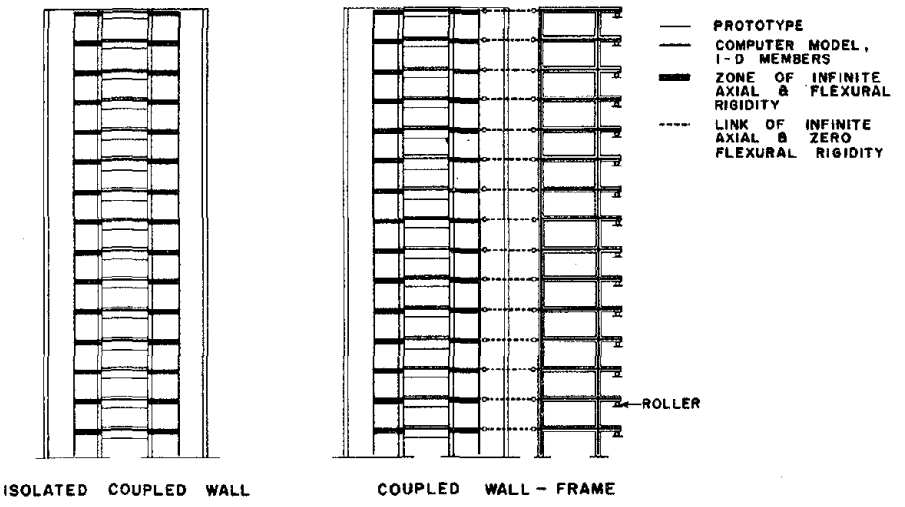

FIG. 2.21 MATHEMATICAL MODELS USED IN NONLINEAR TIME-HISTORY ANALYSES OF THE PROTOTYPE BUILDING

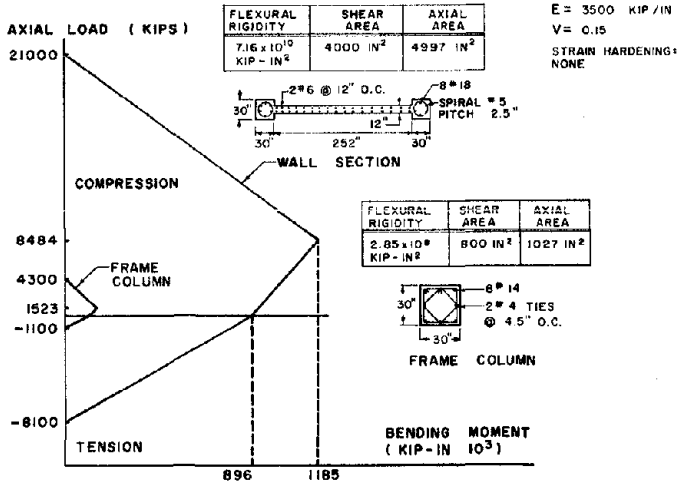

FIG. 2.22 PROPERTIES OF THE BEAM-COLUMN ELEMENTS

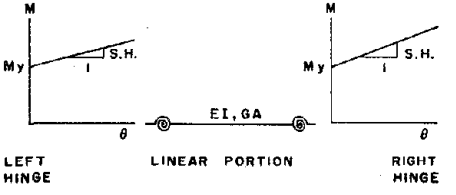

STIFFNESS DEGRADING BEAM ELEMENT

BEAM	YIELD MOMENT POSITIVE	YIELD MOMENT NEGATIVE	EI($\times 10^8$)	SH(% of EI)	GA($\times 10^6$)	EA($\times 10^6$)
GIRDER TY1	10388	12681	2.091	3.9	1.872	5.224
GIRDER TY2	17960	17653	3.069	4	1.872	5.173
GIRDER TY3	22285	26104	3.903	3.9	1.872	5.290
FRAME BEAM	25000	25000	0.246	2.7	1.521	3.500

All Units kips and inches

FIG. 2.23 PROPERTIES OF THE BEAM ELEMENTS

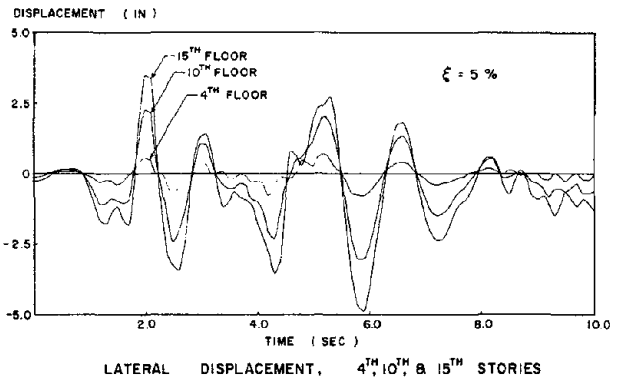

FIG. 2.24 DISPLACEMENT HISTORIES, 4th, 10th AND 15th FLOORS, COUPLED WALL-FRAME MODEL SUBJECTED TO THE 1940 EL CENTRO N.S. GROUND ACCELERATION RECORD

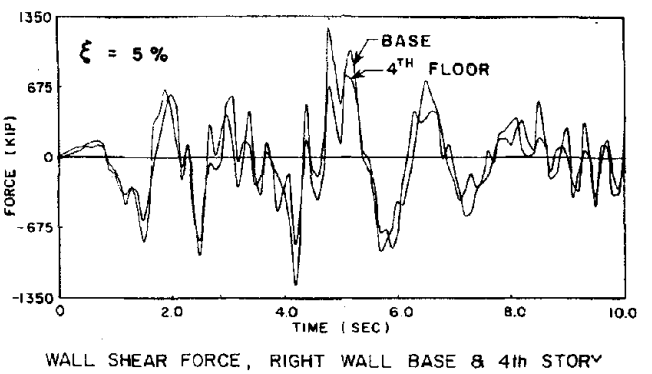

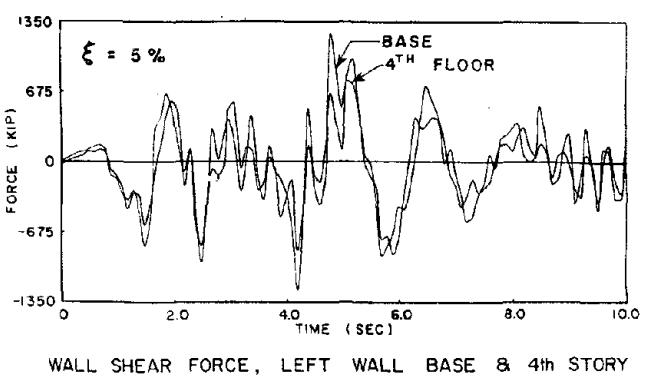

FIG. 2.25 THE SHEAR FORCE HISTORIES AT THE BASE AND FOURTH FLOOR OF THE TWO WALLS, COUPLED WALL-FRAME MODEL SUBJECTED TO THE 1940 EL CENTRO N.S. GROUND ACCELERATION RECORD

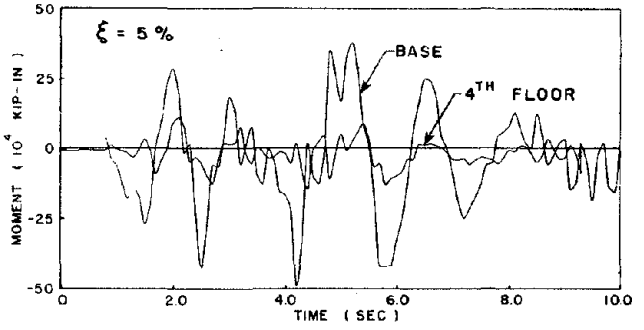

WALL BENDING MOMENT, RIGHT WALL BASE & 4th STORY

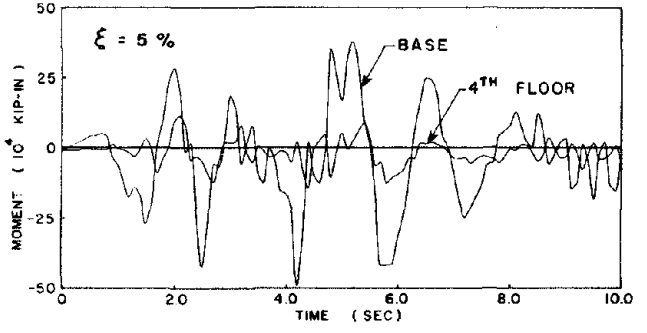

WALL BENDING MOMENT, LEFT WALL BASE & 4th STORY

FIG. 2.26 THE BENDING MOMENT HISTORIES AT THE BASE AND FOURTH FLOOR OF THE TWO WALLS, COUPLED WALL-FRAME MODEL SUBJECTED TO THE 1940 EL CENTRO N.S. GROUND ACCELERATION RECORD

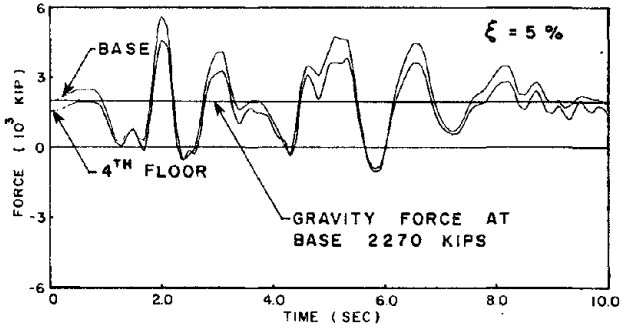

WALL AXIAL FORCE, RIGHT WALL BASE & 4th STORY

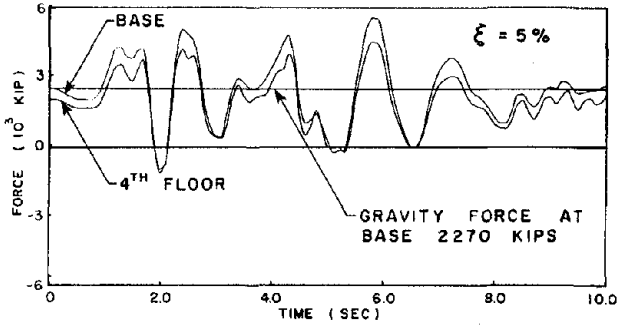

WALL AXIAL FORCE, LEFT WALL BASE & 4th STORY

FIG. 2.27 THE AXIAL FORCE HISTORIES AT THE BASE AND FOURTH FLOOR OF THE TWO WALLS, COUPLED WALL-FRAME MODEL SUBJECTED TO THE 1940 EL CENTRO N.S. GROUND ACCELERATION RECORD

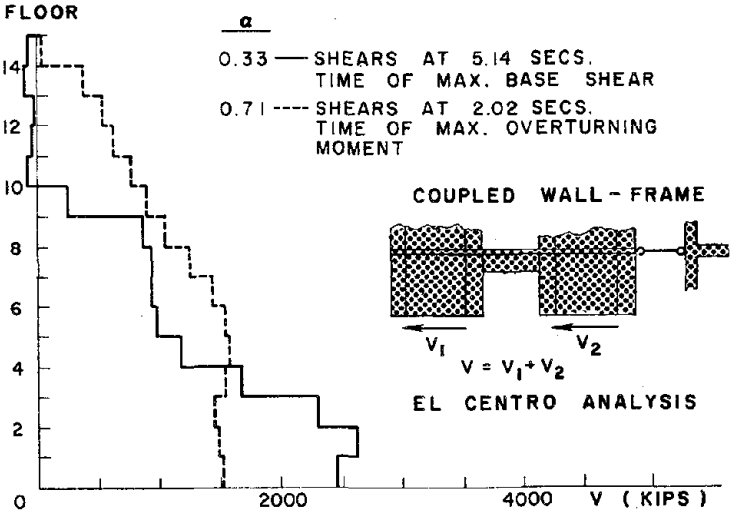

FIG. 2.28 THE SEISMIC FORCE DEMANDS FROM THE COUPLED WALL SYSTEM WHEN THE COMPLETE STRUCTURE IS SUBJECTED TO THE EL CENTRO GROUND MOTION

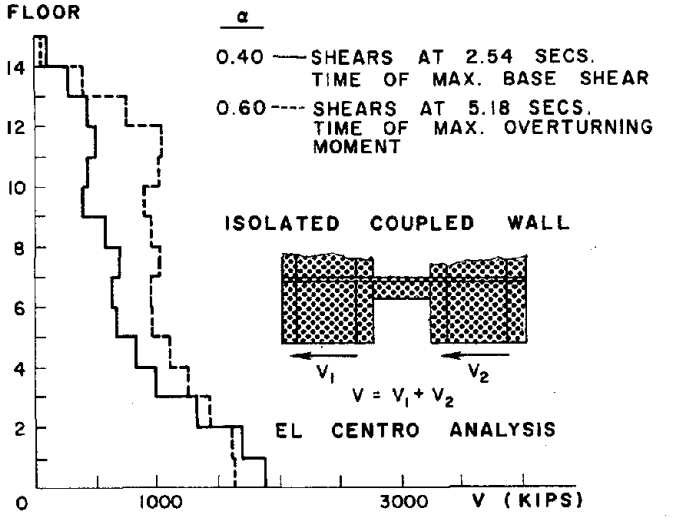

FIG. 2.29 THE SEISMIC FORCE DEMANDS FROM THE COUPLED WALL SYSTEM WHEN THE ISOLATED COUPLED WALL SYSTEM IS SUBJECTED TO THE EL CENTRO GROUND MOTION

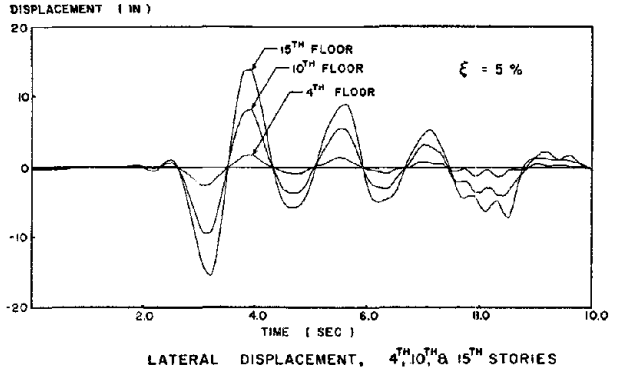

FIG. 2.30 DISPLACEMENT HISTORIES, 4th, 10th, AND 15th FLOORS, COUPLED WALL-FRAME MODEL SUBJECTED TO THE 1971 PACOIMA DAM (DERIVED) RECORD

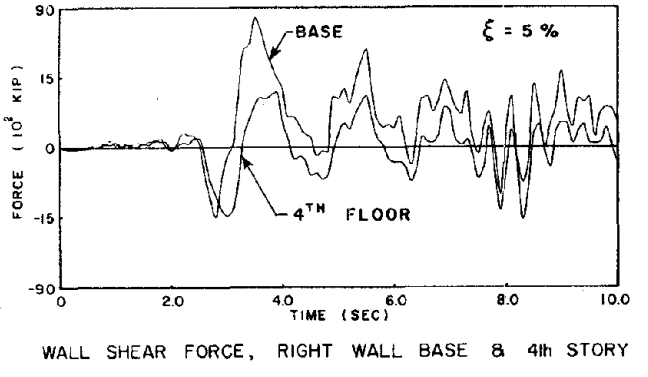

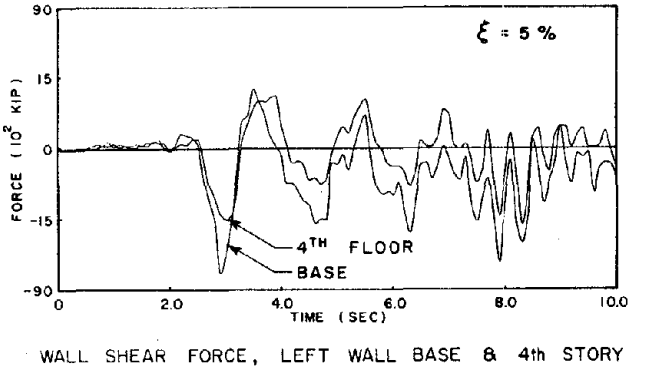

FIG. 2.31 THE SHEAR WALL HISTORIES AT THE BASE AND FOURTH FLOOR OF THE TWO WALLS, COUPLED WALL-FRAME MODEL SUBJECTED TO THE 1971 PACOIMA DAM (DERIVED) S16E GROUND ACCELERATION RECORD

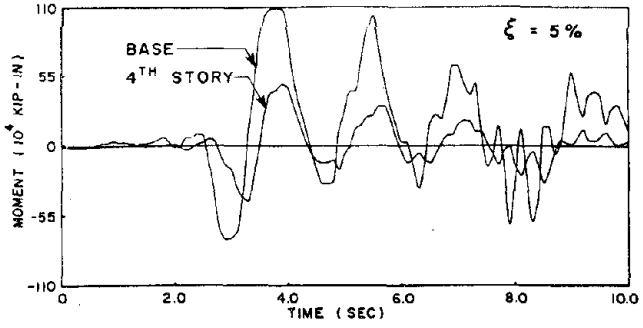

WALL BENDING MOMENT, RIGHT WALL BASE & 4th STORY

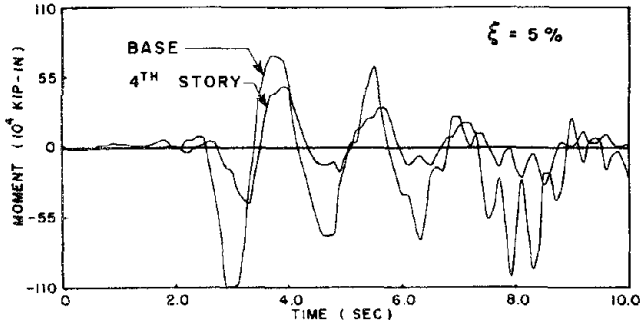

WALL BENDING MOMENT, LEFT WALL BASE & 4th STORY

FIG. 2.32 THE BENDING MOMENT HISTORIES AT THE BASE AND FOURTH FLOOR OF THE TWO WALLS, COUPLED WALL-FRAME MODEL SUBJECTED TO THE 1971 PACOIMA DAM (DERIVED) S16E GROUND ACCELERATION RECORD

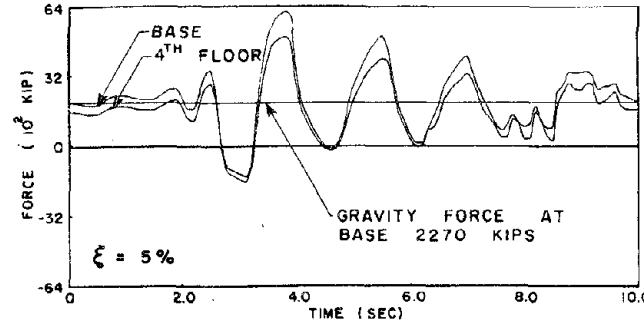

WALL AXIAL FORCE, RIGHT WALL BASE & 4th STORY

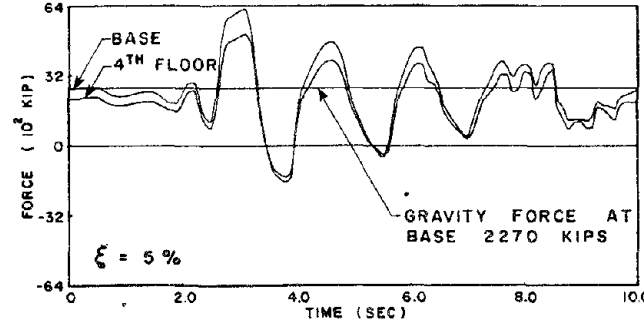

WALL AXIAL FORCE, LEFT WALL BASE & 4th STORY

FIG. 2.33 THE AXIAL FORCE HISTORIES AT THE BASE AND FOURTH FLOOR OF THE TWO WALLS, COUPLED WALL-FRAME MODEL SUBJECTED TO THE 1971 PACOIMA DAM (DERIVED) S16E GROUND ACCELERATION RECORD

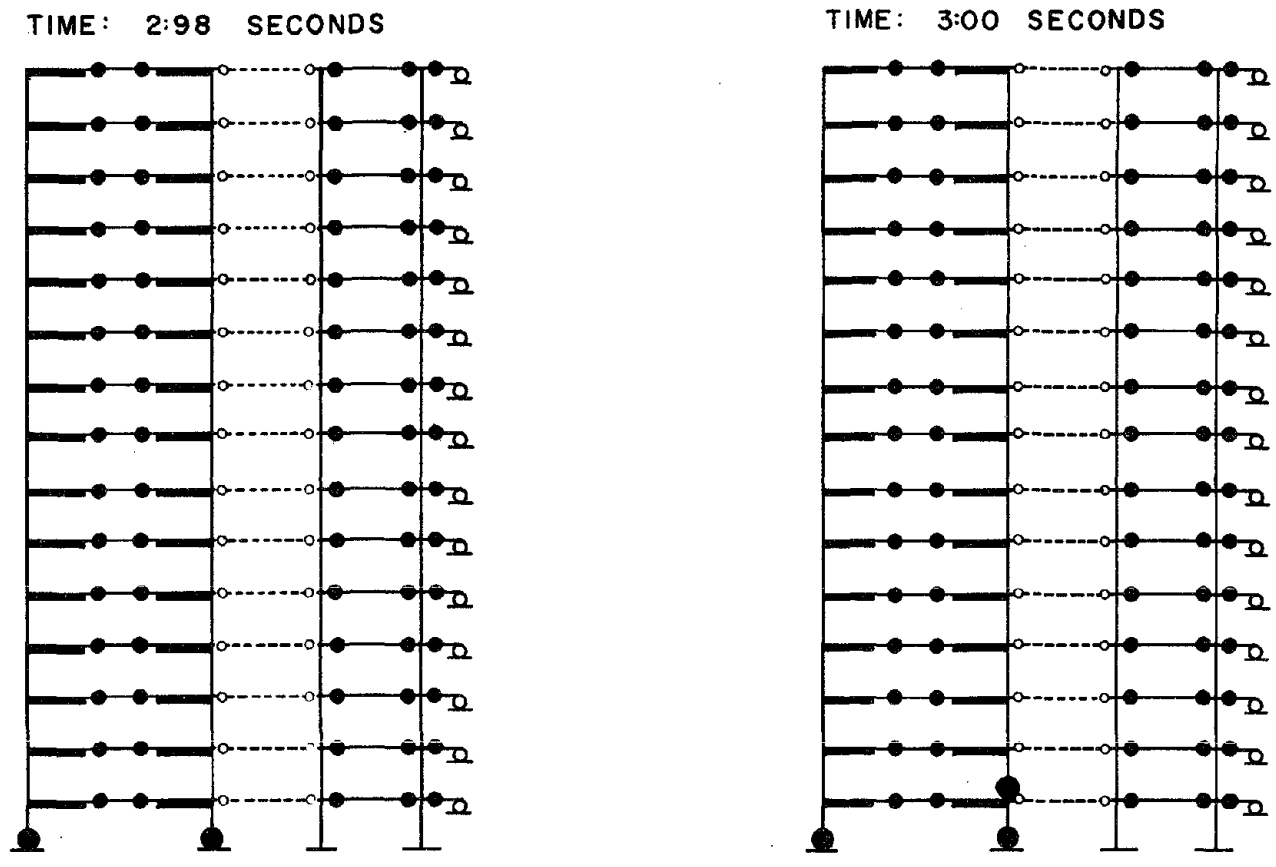

FIG. 2.34 THE PLASTIC HINGE PATTERNS OF THE COUPLED WALL-FRAME MODEL AT 2.98 AND 3.00 SECONDS OF RESPONSE TO THE PACOIMA DAM RECORD

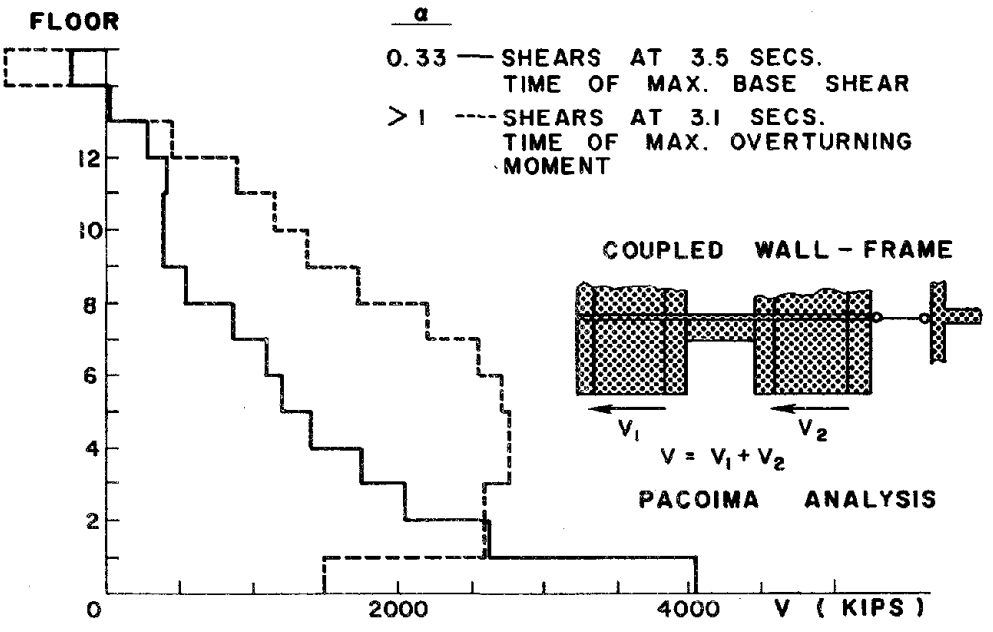

FIG. 2.35 THE SEISMIC FORCE DEMANDS FROM THE COUPLED WALL SYSTEM WHEN THE COUPLED WALL-FRAME SYSTEM IS SUBJECTED TO THE DERIVED PACOIMA DAM GROUND MOTION

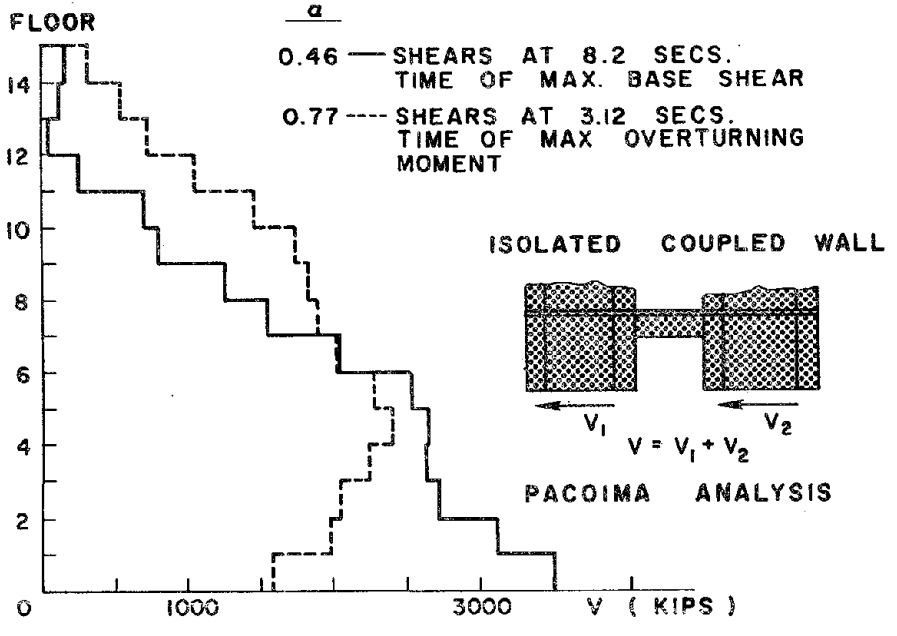

FIG. 2.36 THE SEISMIC FORCE DEMANDS FROM THE COUPLED WALL SYSTEM WHEN THE ISOLATED COUPLED-WALL SYSTEM IS SUBJECTED TO THE DERIVED PACOIMA DAM GROUND MOTION

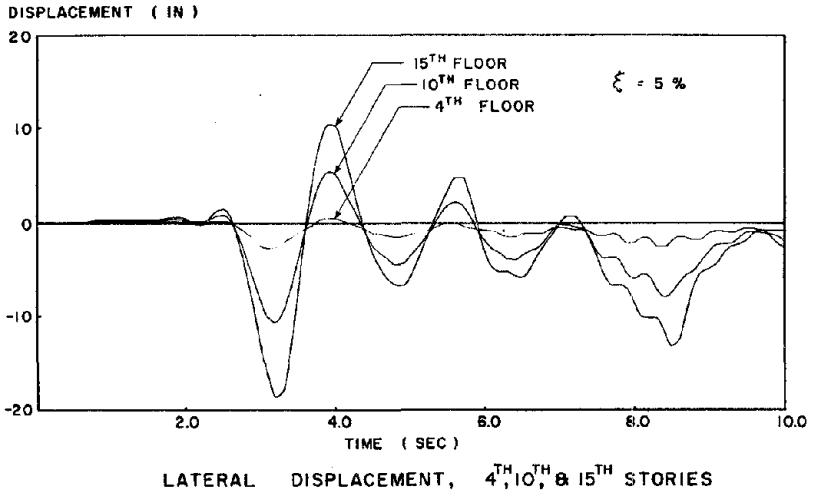

FIG. 2.37 DISPLACEMENT HISTORIES, 4th, 10th AND 15th FLOORS, ISOLATED COUPLED WALL MODEL SUBJECTED TO THE 1971 PACOIMA DAM (DERIVED) S16E GROUND ACCELERATION RECORD

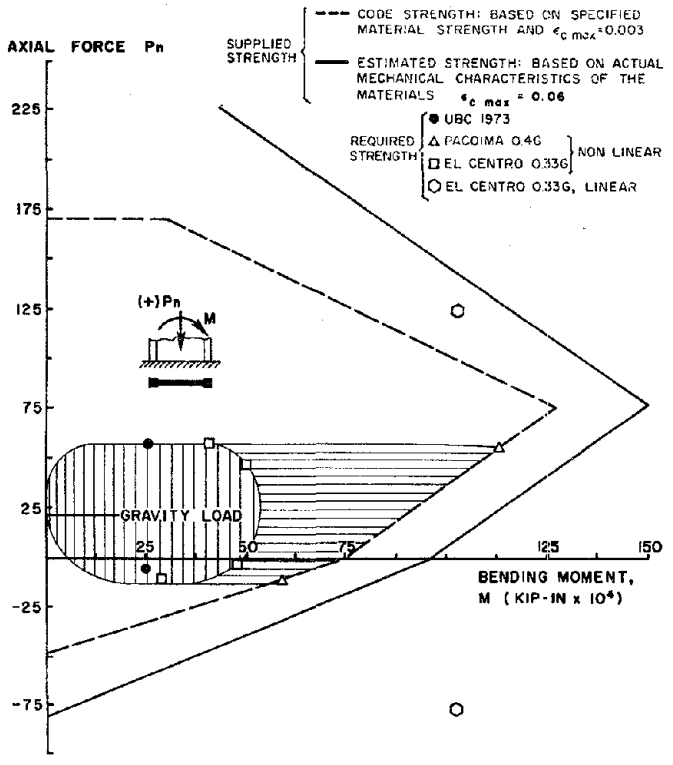

FIG. 2.38 SUPPLIED VS. REQUIRED STRENGTH AT THE BASE OF THE WALL CROSS SECTION

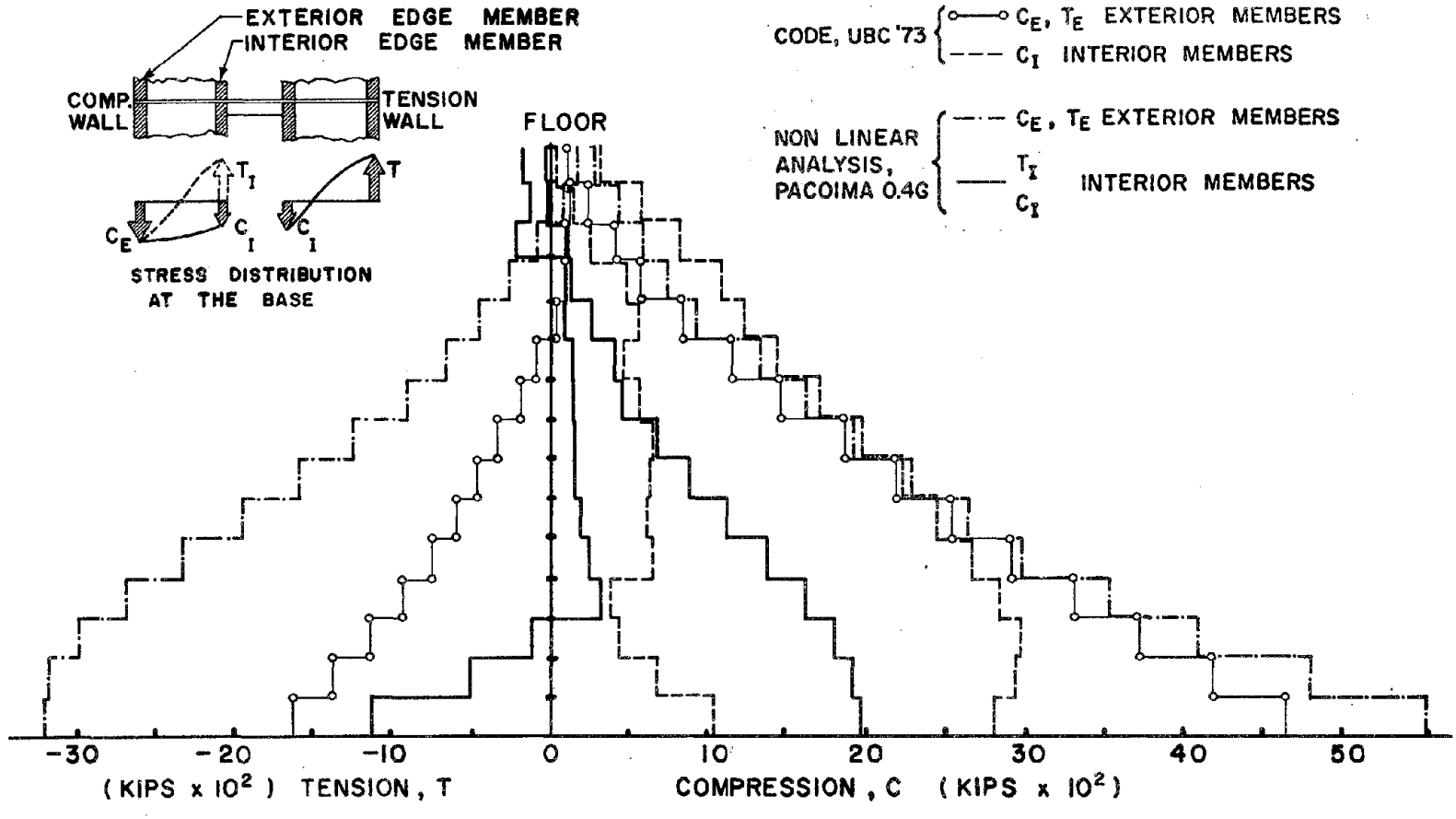

FIG. 2.39 EXTERIOR VS. INTERIOR EDGE MEMBER DEMANDS DUE TO CODE AND ANALYSIS

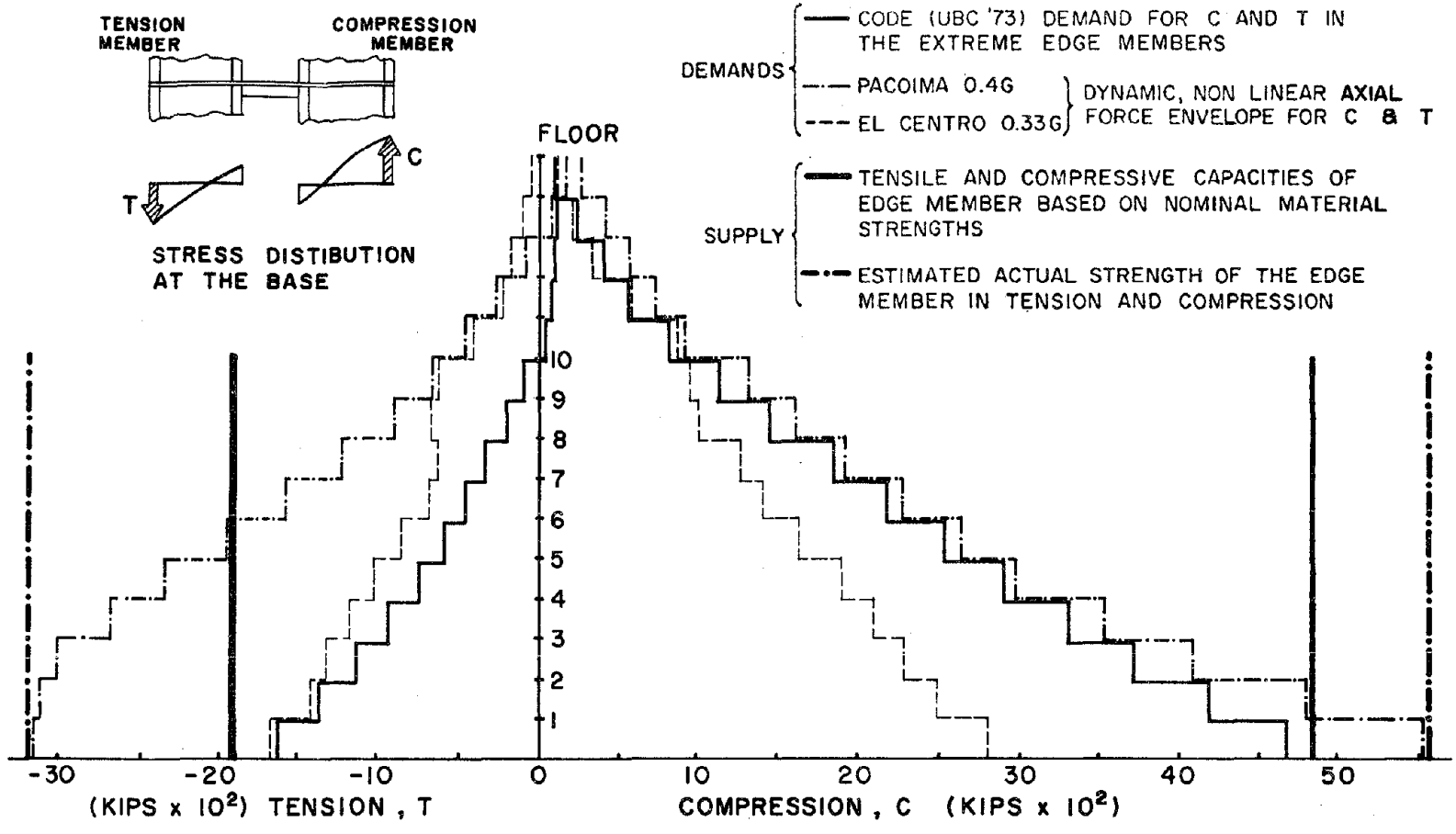

FIG. 2.40 EXTREME EDGE MEMBER AXIAL FORCE DEMAND VS. SUPPLY RELATIONS OF THE COUPLED WALL

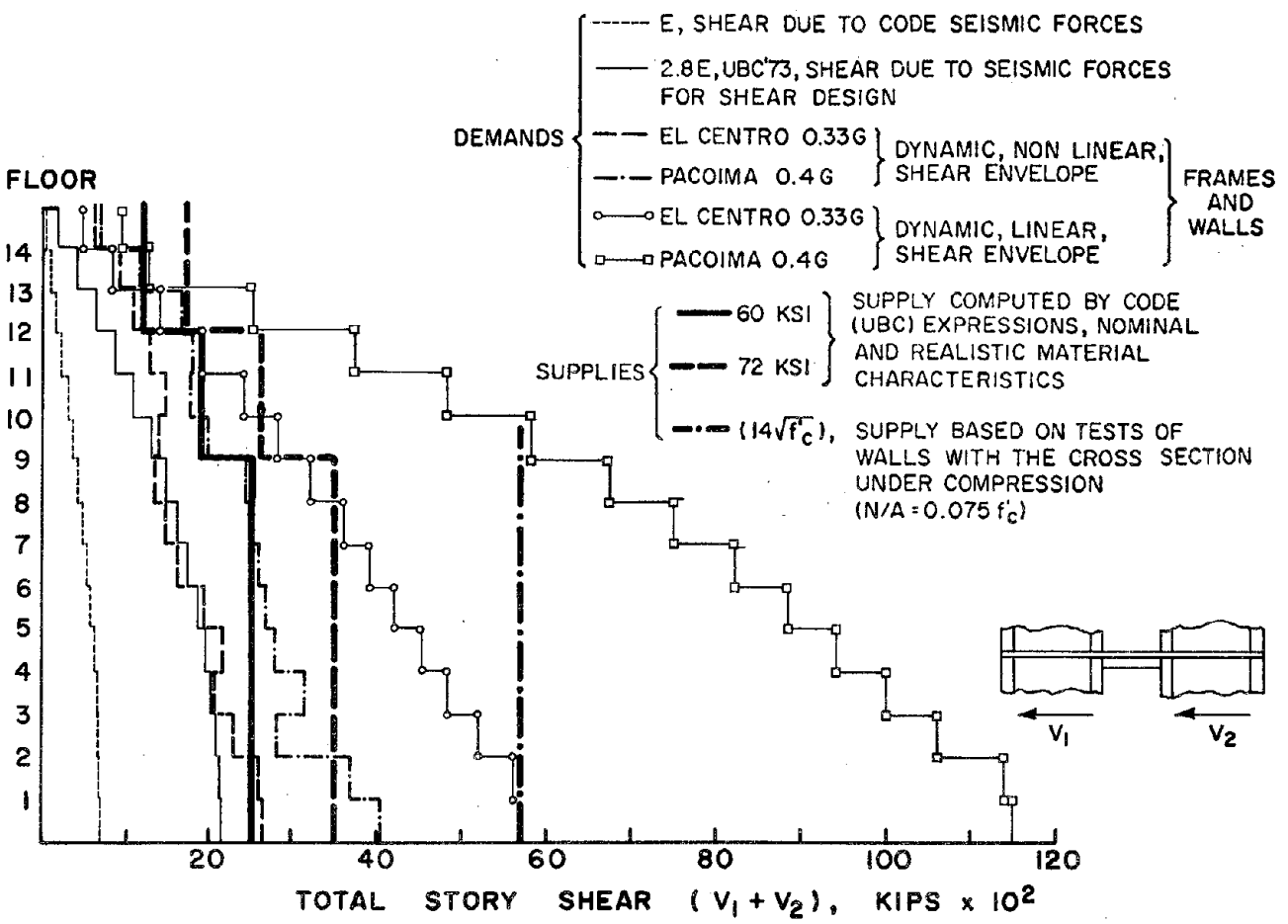

FIG. 2.41 STORY SHEAR DEMANDS (DUE TO CODE, LINEAR AND NONLINEAR ANALYSIS) VS. SUPPLIES (DUE TO CODE AND BASED ON RECENT EXPERIMENTAL DATA) FOR ONE SET OF COUPLED WALLS

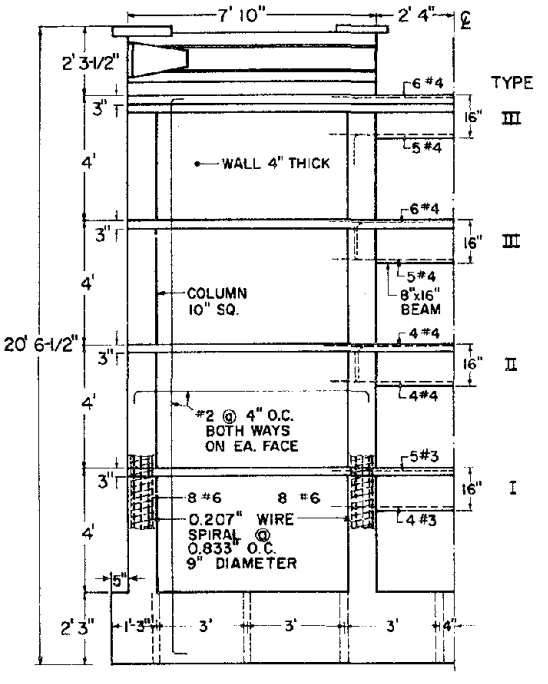

FIG. 2.42 (a) DIMENSIONS AND DETAILING OF THE MODEL SUB-ASSEMBLAGE, FRONT ELEVATION

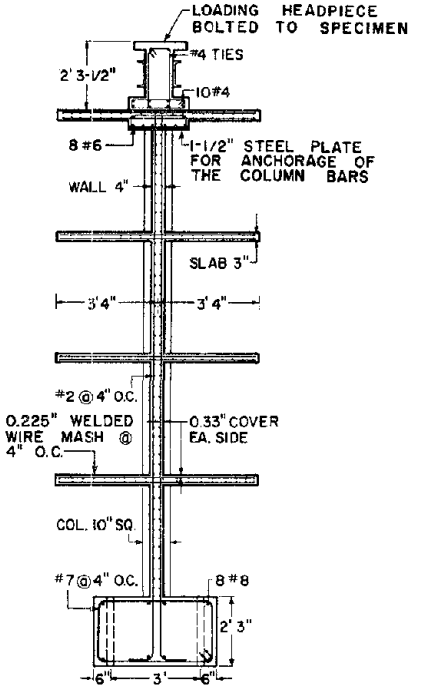

FIG. 2.43 DIMENSIONS AND DETAILING OF THE MODEL SUB-ASSEMBLAGE, SIDE ELEVATION

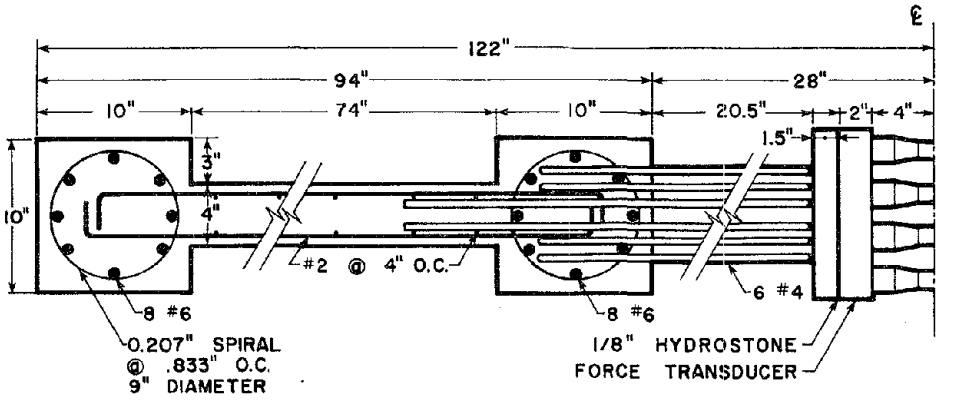

FIG. 2.42 (b) DETAILING OF THE COLUMNS AND THE THIRD FLOOR BEAM-COLUMN INTERFACE

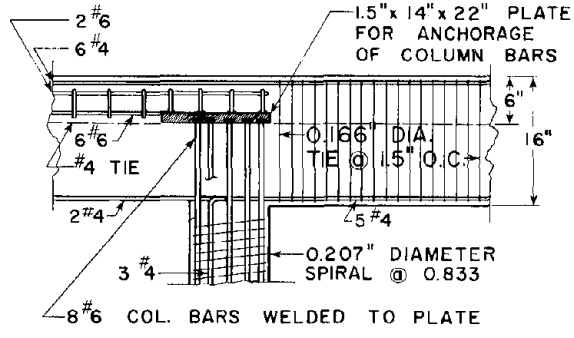

FIG. 2.44 DIMENSIONS AND DETAILING OF THE 4th STORY BEAM OF THE MODEL SUBASSEMBLAGE

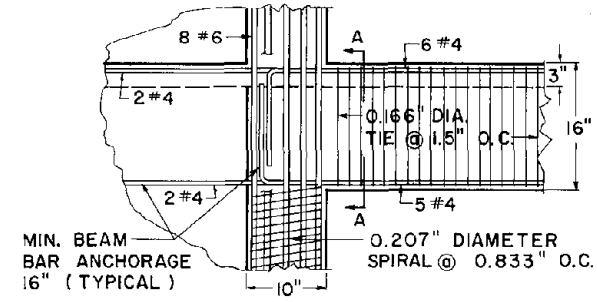

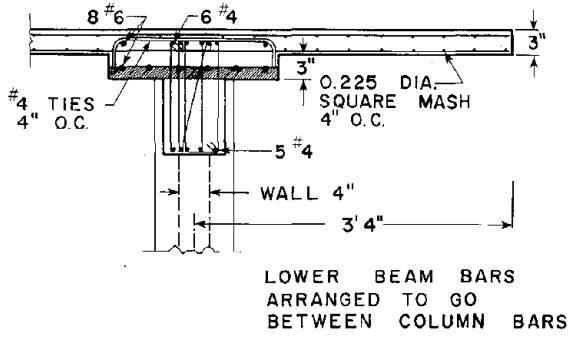

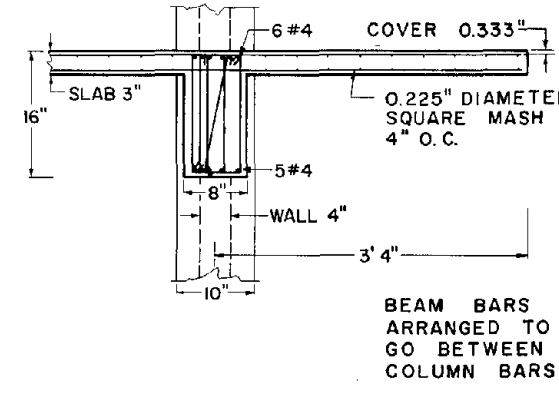

FIG. 2.45 DIMENSIONS AND DETAILING OF THE 3rd STORY BEAM OF THE MODEL SUBASSEMBLAGE

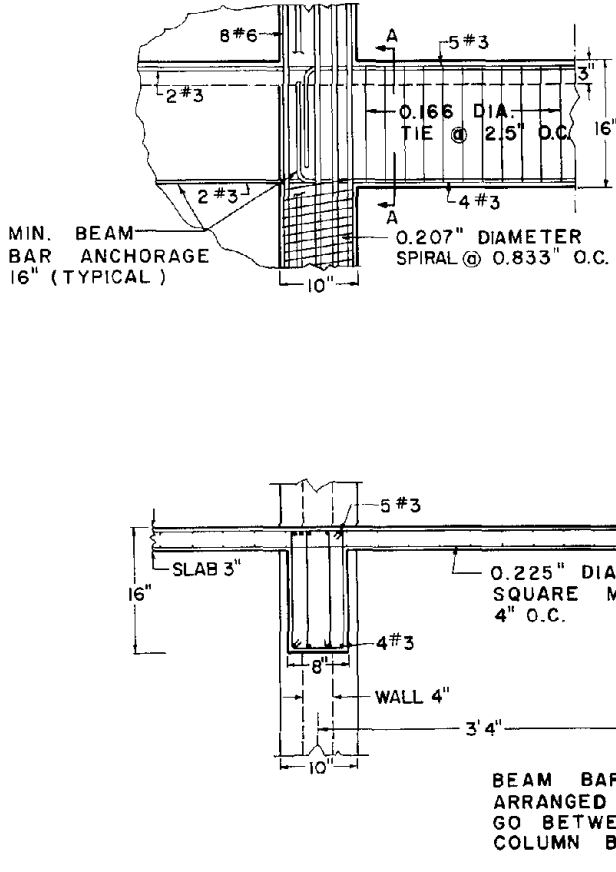

FIG. 2.46 DIMENSIONS AND DETAILING OF THE 2nd STORY BEAM OF THE MODEL SUBASSEMBLAGE

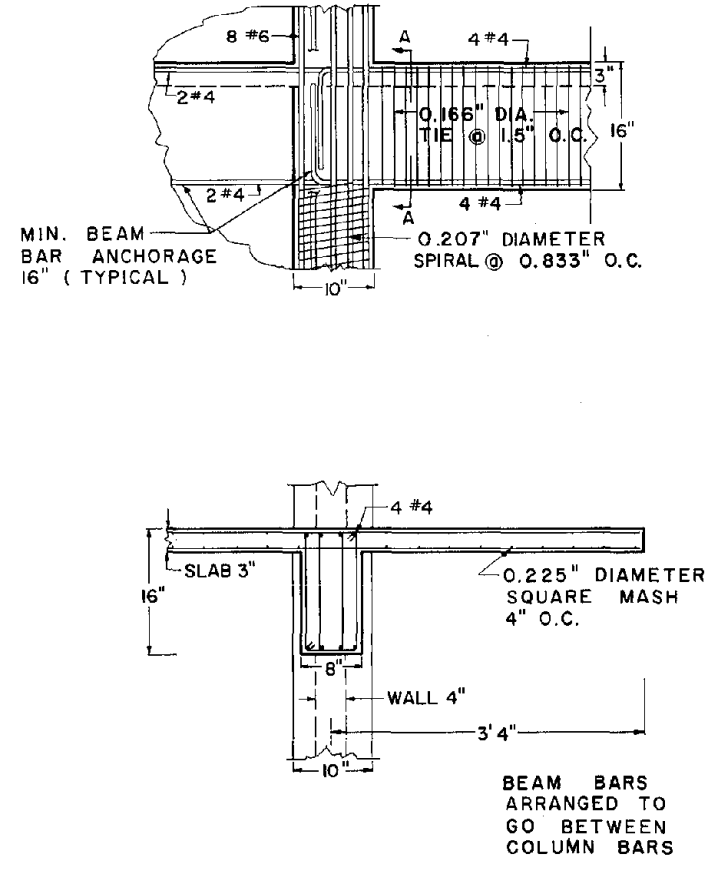

FIG. 2.47 DIMENSIONS AND DETAILING OF THE 1st STORY BEAM OF THE MODEL SUBASSEMBLAGE

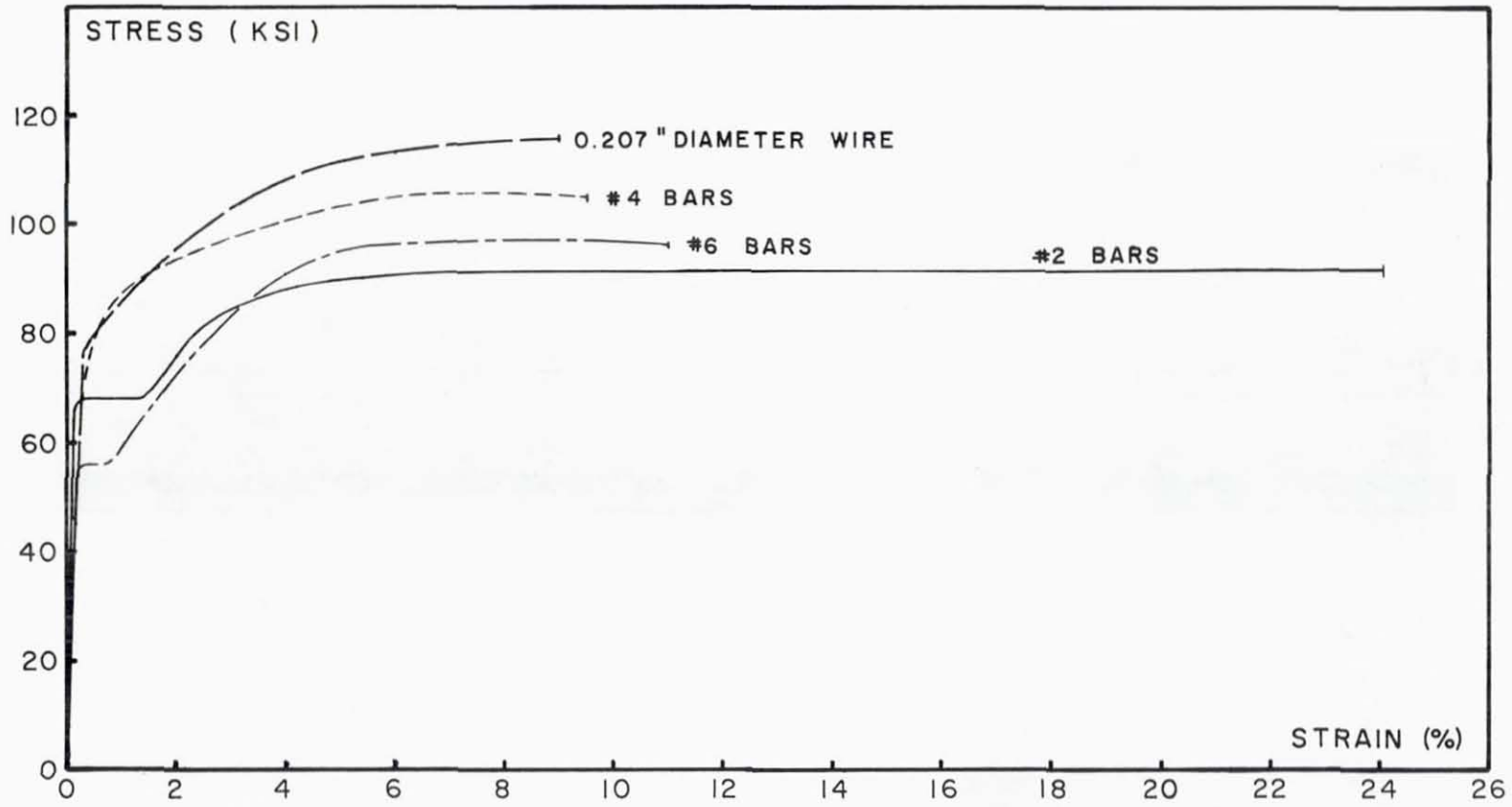

FIG. 2.48 STRESS-STRAIN RELATIONSHIPS OF THE 0.207 IN. DIAMETER WIRE, #2, #4, AND #6 REINFORCING BARS USED IN THE MANUFACTURING OF THE MODEL

FIG. 2.49 CONSTRUCTION OF THE MODEL

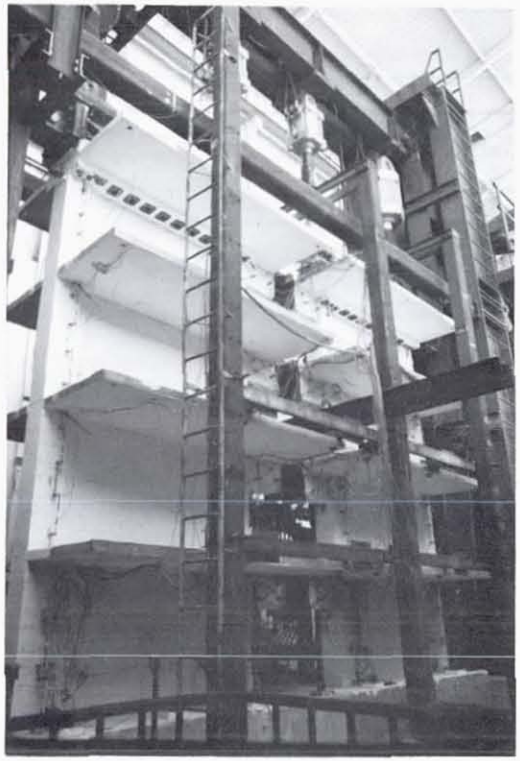

FIG. 2.50 THE MODEL

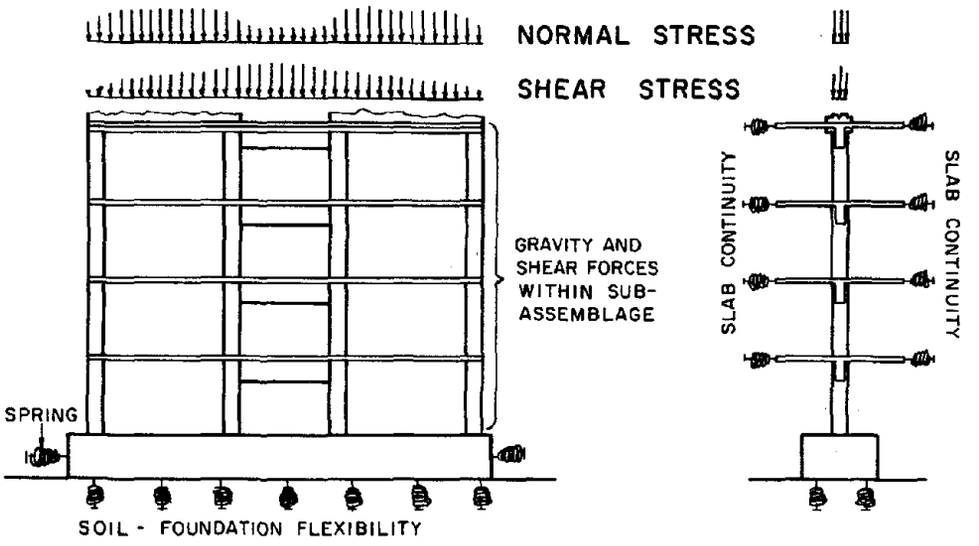

FIG. 2.51 FORCE AND GEOMETRIC BOUNDARY CONDITIONS OF THE SUBASSEMBLAGE

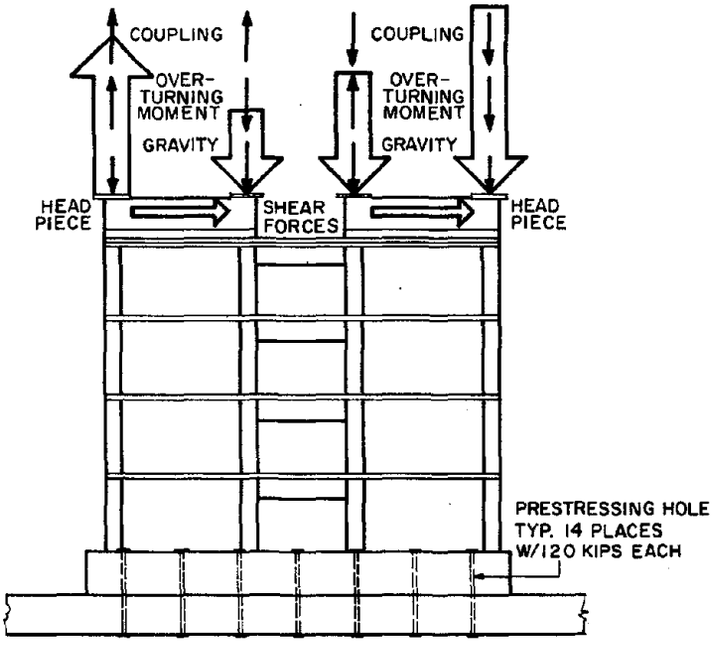

FIG. 2.52 SIMULATION OF FORCE AND GEOMETRIC CONTINUITIES OF THE MODEL SUBASSEMBLAGE

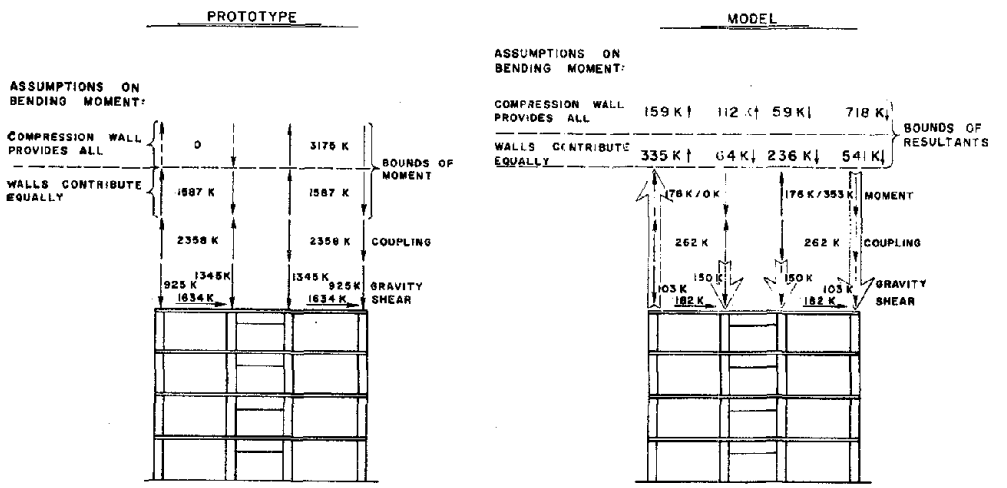

FIG. 2.53 THE EXPECTED MAXIMUM FORCES OF THE SUBASSEMBLAGE

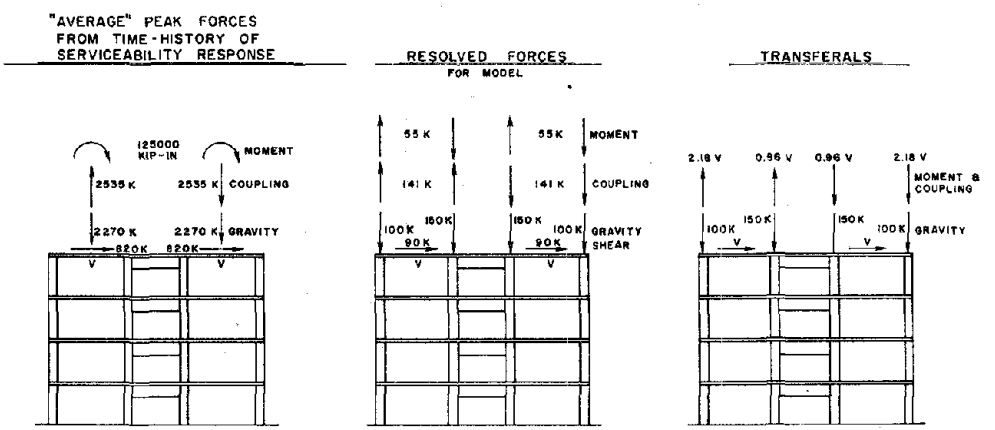

FIG. 2.54 ESTABLISHING LATERAL-VERTICAL FORCE TRANSFERS FROM TIME-HISTORY OF SERVICEABILITY RESPONSE

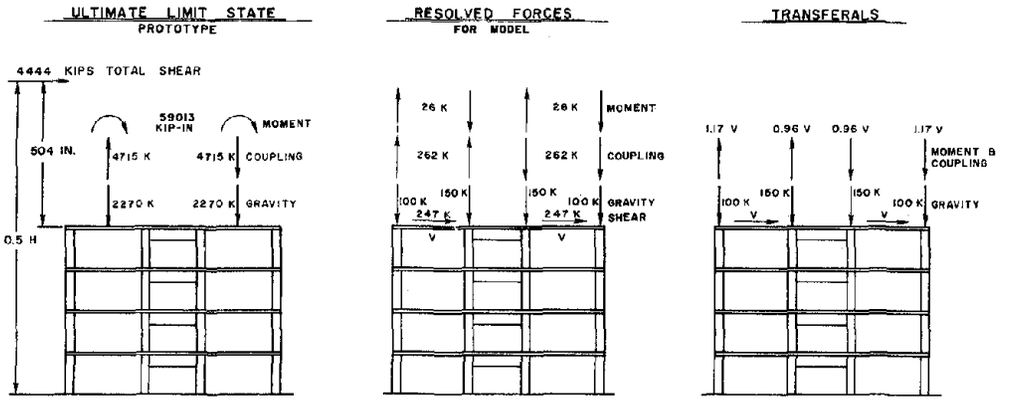

FIG. 2.55 ESTABLISHING LATERAL-VERTICAL FORCE TRANSFERS FOR ULTIMATE LIMIT STATE, $\alpha = 0.5$

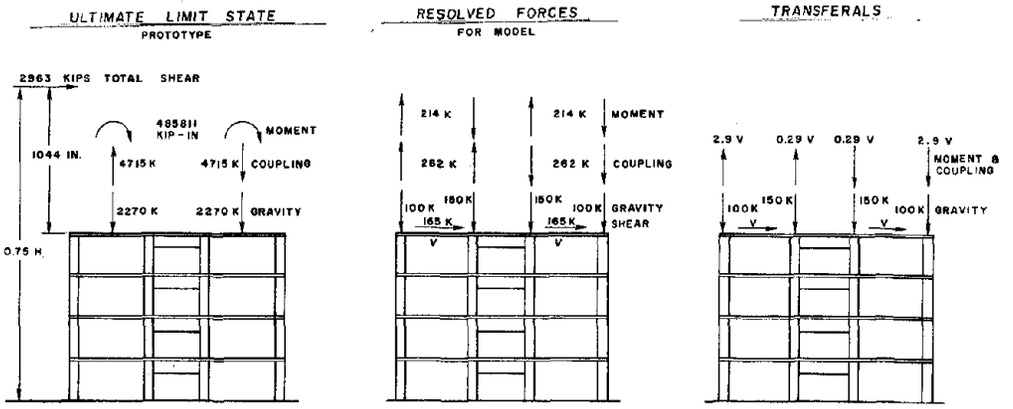

FIG. 2.56 ESTABLISHING LATERAL-VERTICAL FORCE TRANSFERS FOR ULTIMATE LIMIT STATE, $\alpha = 0.75$

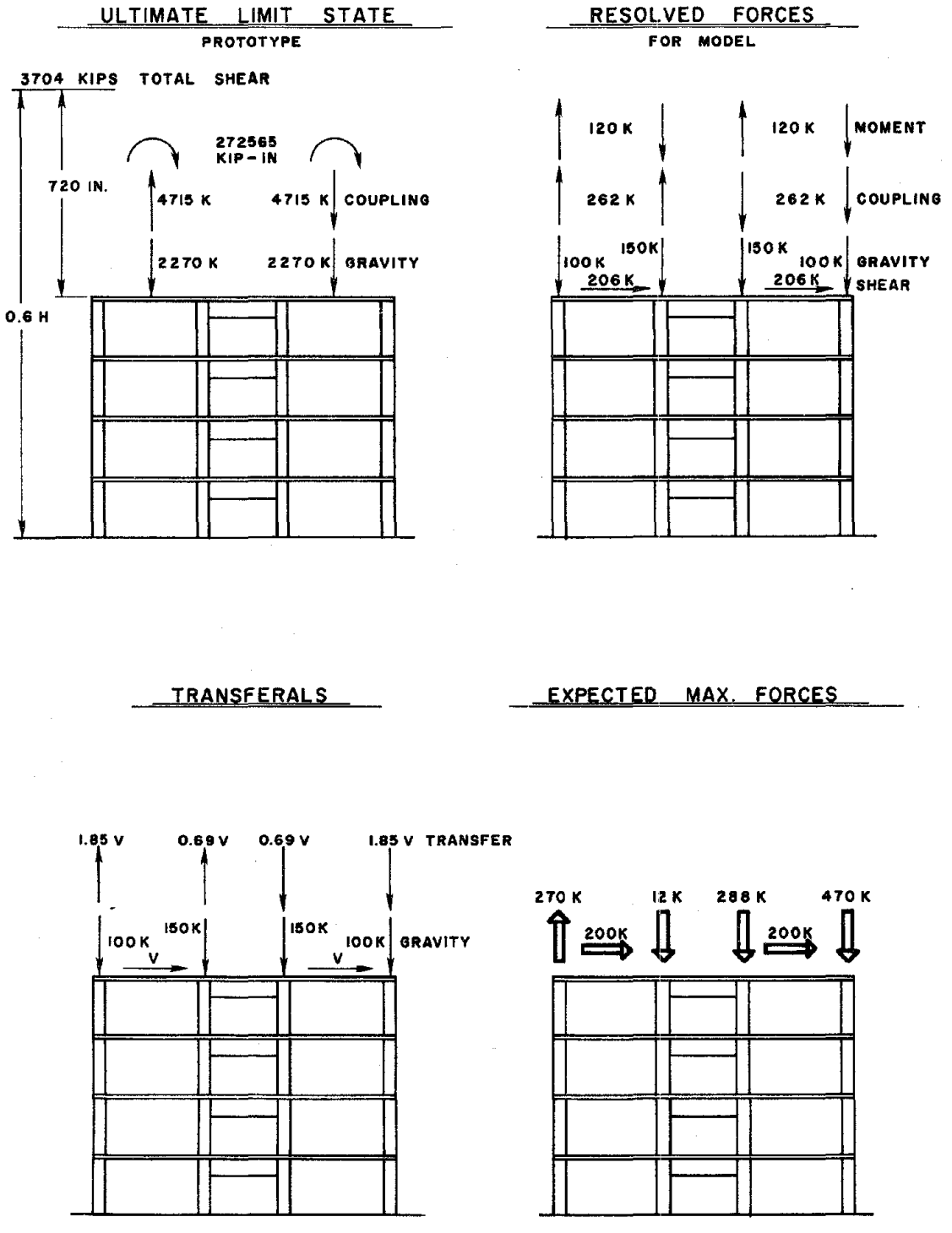

FIG. 2.57 ESTABLISHED LATERAL-VERTICAL FORCE TRANSFERS FOR ULTIMATE LIMIT STATE; $\alpha = 0.60$

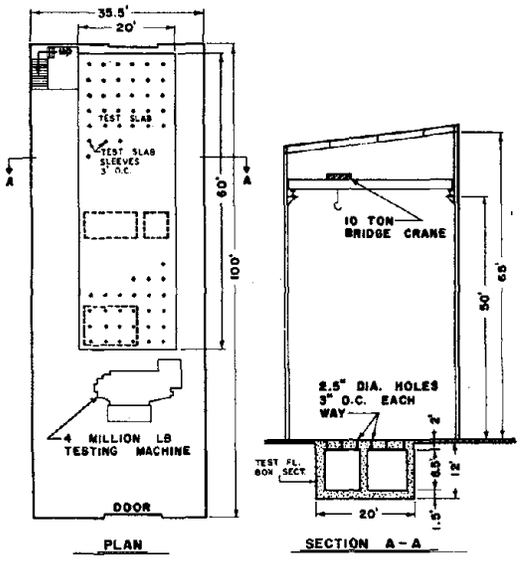

FIG. 2.58 PLAN AND SECTION OF THE MAIN BAY OF THE STRUCTURAL RESEARCH LABORATORY AT RICHMOND FIELD STATION

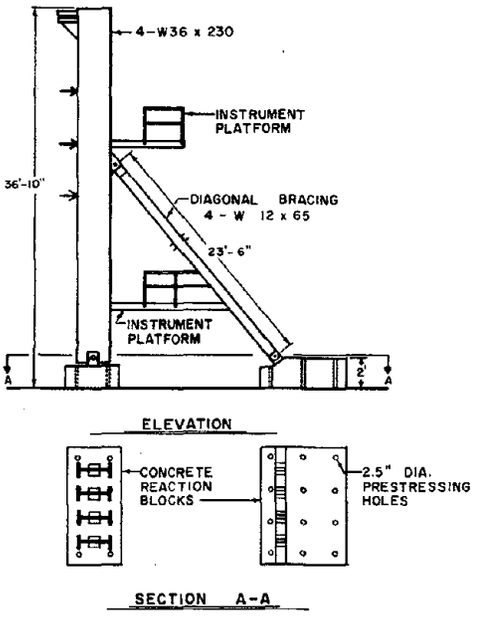

FIG. 2.59 THE BRACED FRAME SYSTEM THAT WAS EXISTING IN THE STRUCTURES LABORATORY

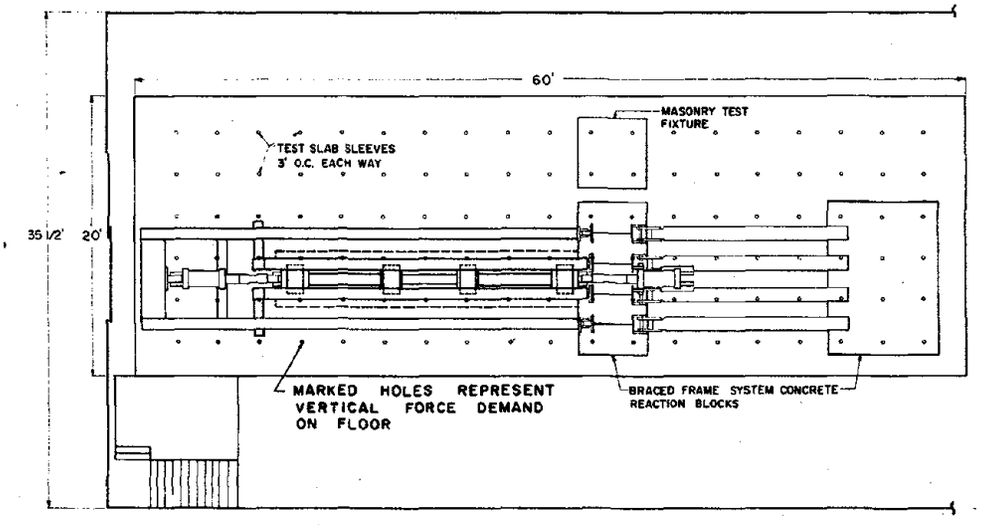

FIG. 2.60 VIEW OF THE EAST END OF THE MAIN BAY OF THE STRUCTURAL RESEARCH LABORATORY, INCLUDING THE PLAN OF THE TEST FACILITY

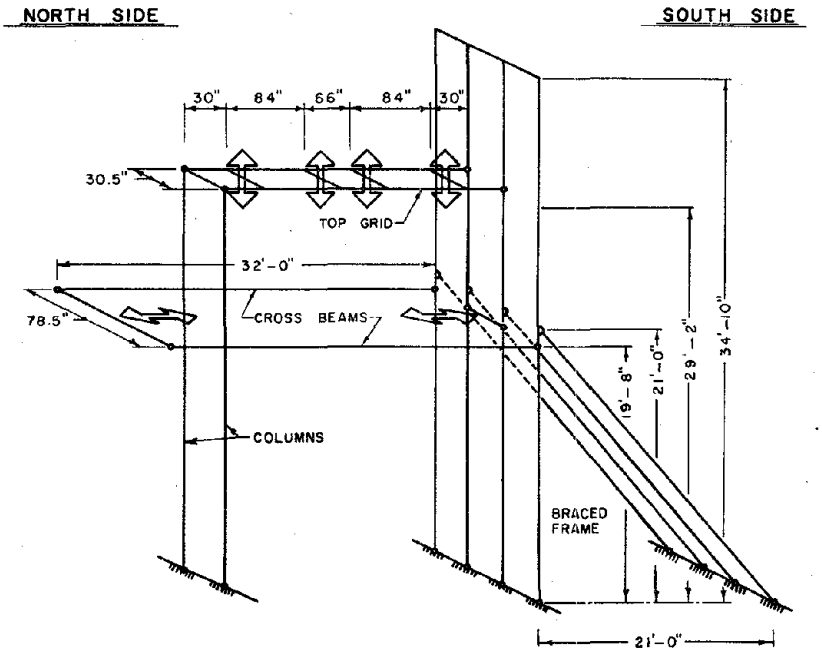

FIG. 2.61 MAJOR COMPONENTS AND MATHEMATICAL IDEALIZATION OF THE LOADING FRAME

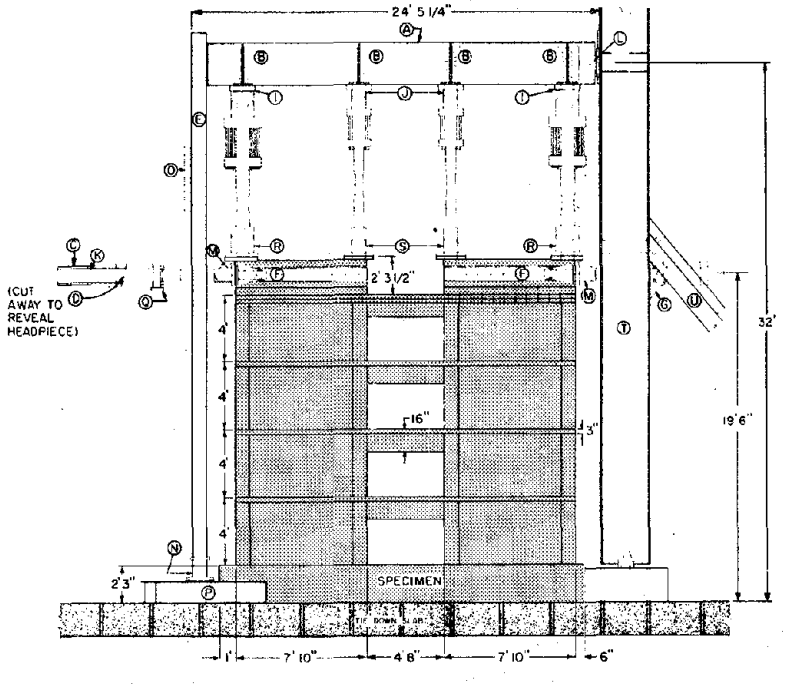

FIG. 2.62 FRONT VIEW OF THE SPECIMEN AND THE TEST FRAME

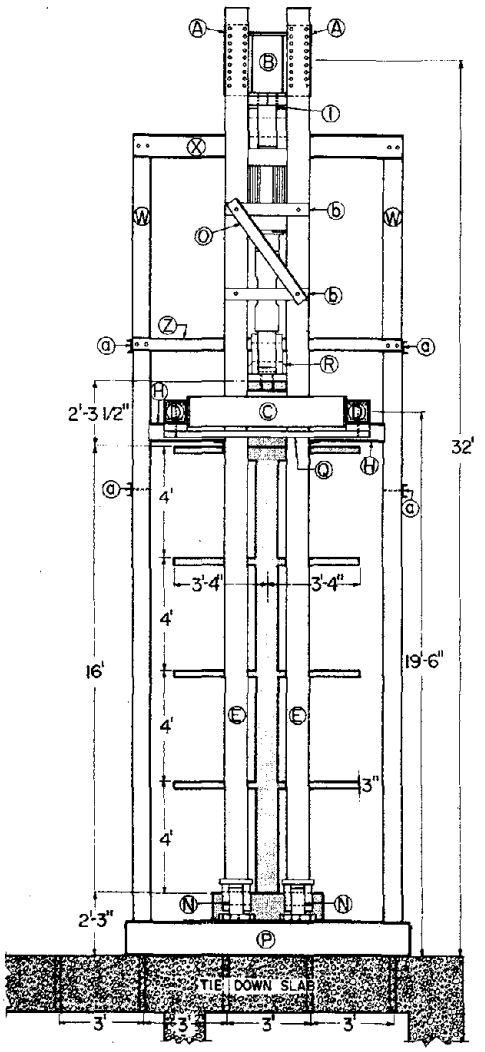

FIG. 2.63 SIDE VIEW OF THE SPECIMEN AND THE TEST FRAME

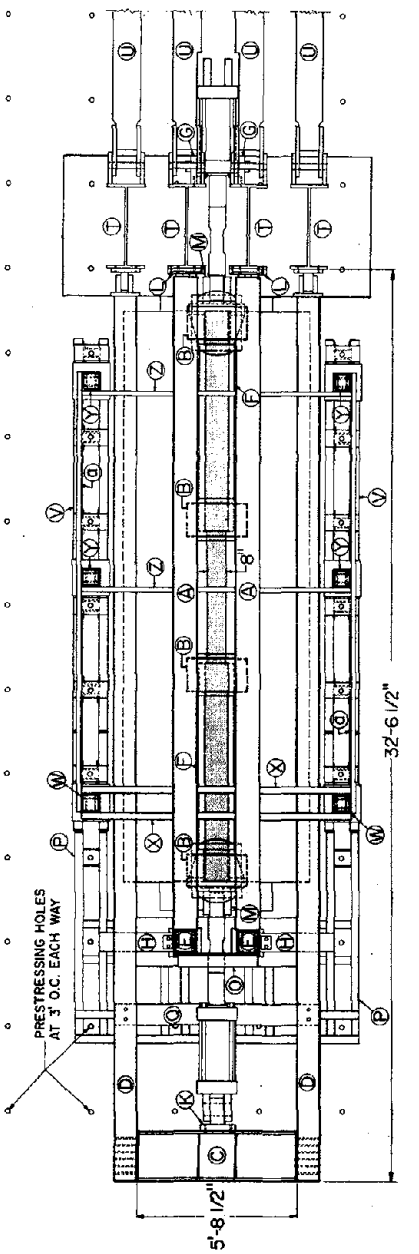

FIG. 2.64 TOP VIEW OF THE SPECIMEN AND THE TEST FRAME

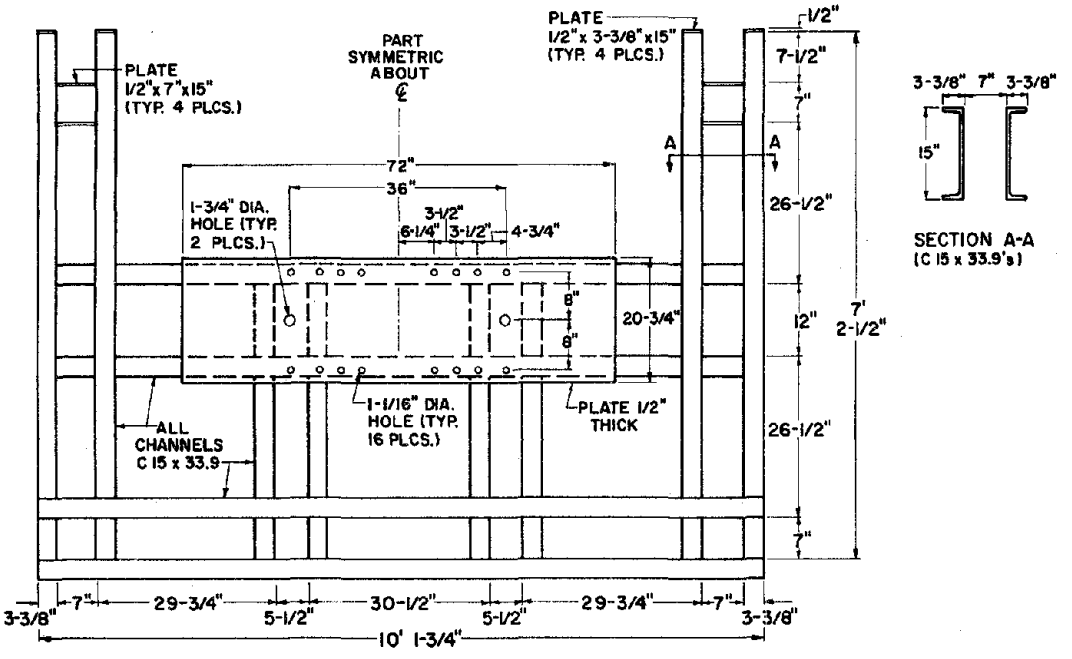

FIG. 2.65 A CLOSE UP DETAIL OF THE BASE OF THE AXIALLY LOADED COLUMNS OF THE TEST FRAME (DESIGNATED AS PART E IN FIGS. 2.62, 2.63)

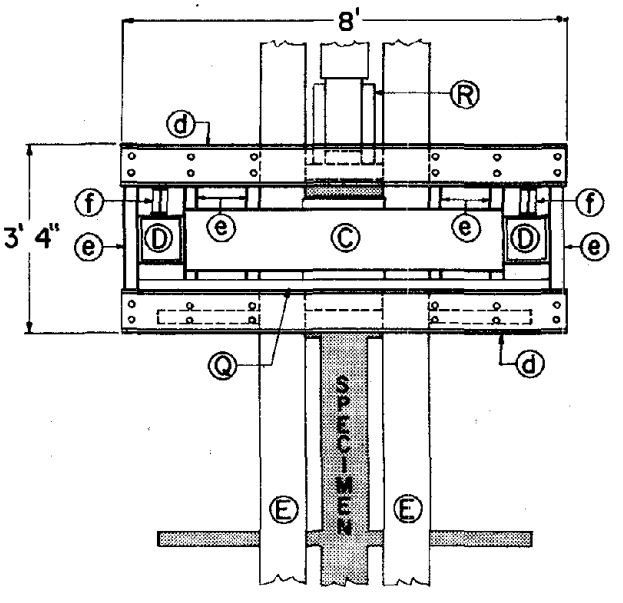

FIG. 2.66 A CLOSE UP DETAIL OF THE INTERFACE OF THE HORIZONTAL AND VERTICAL LOADING SYSTEMS IN THE TEST FRAME

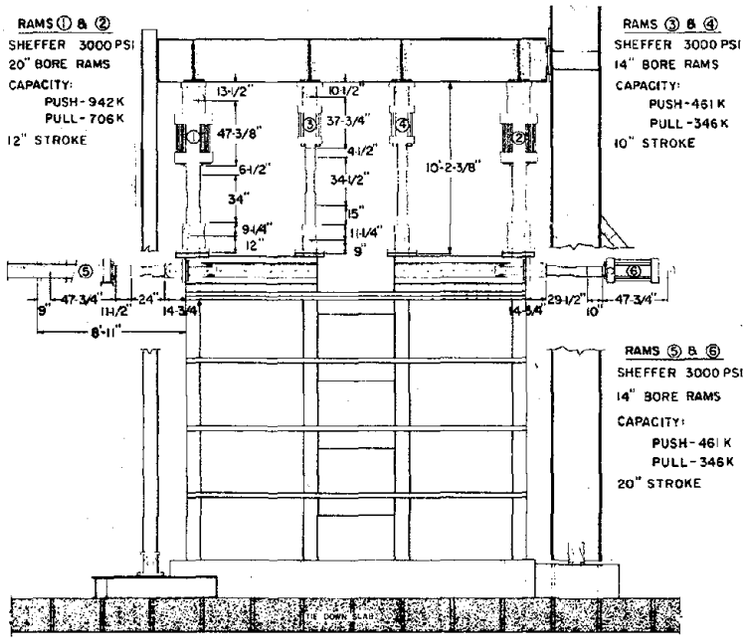

FIG. 2.67 RELEVANT DATA FOR THE ACTUATORS OF THE TEST SET UP

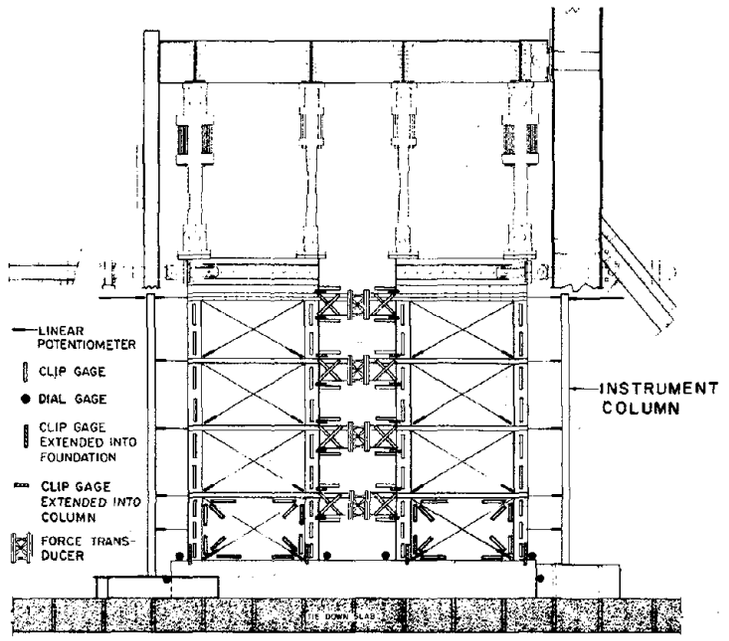

FIG. 2.68 EXTERNAL INSTRUMENTATION OF MODEL SUBASSEMBLAGE

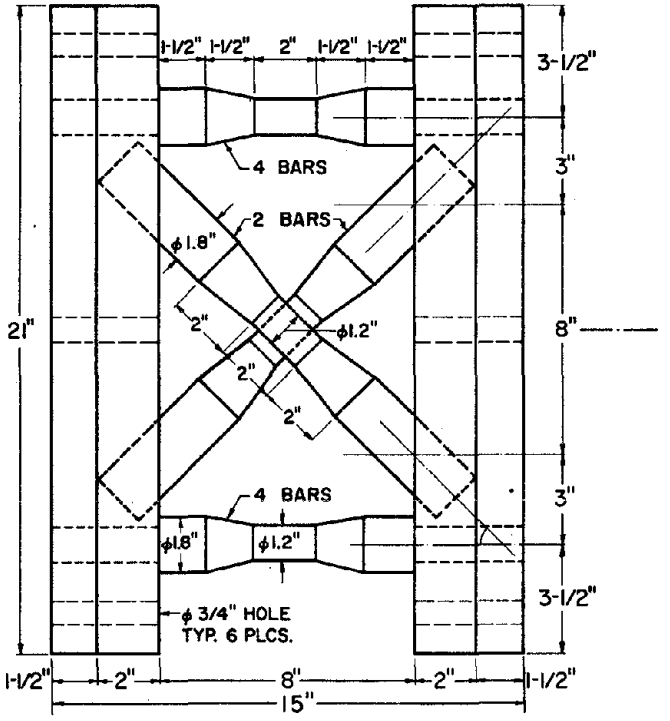

FIG. 2.69 FORCE TRANSDUCER, SIDE VIEW

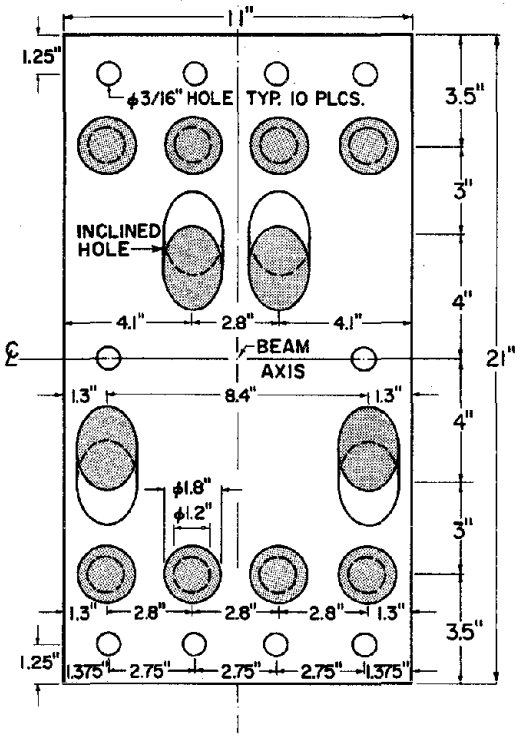

FIG. 2.70 FORCE TRANSDUCER, FRONT VIEW OF THE END PLATE

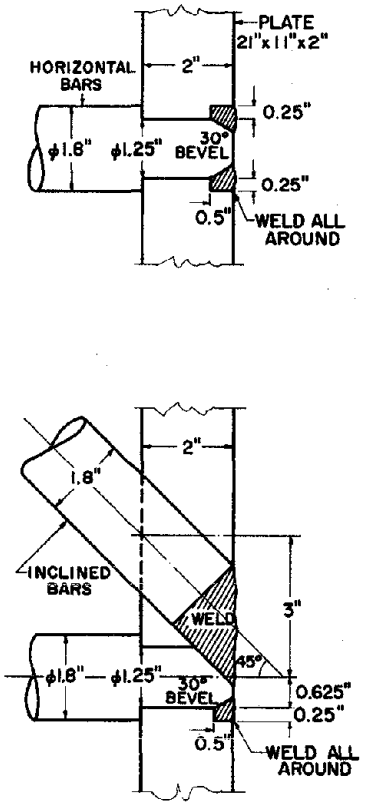

FIG. 2.71 CONNECTING DETAILS FOR THE FORCE BARS AND END PLATES OF THE FORCE TRANSDUCER

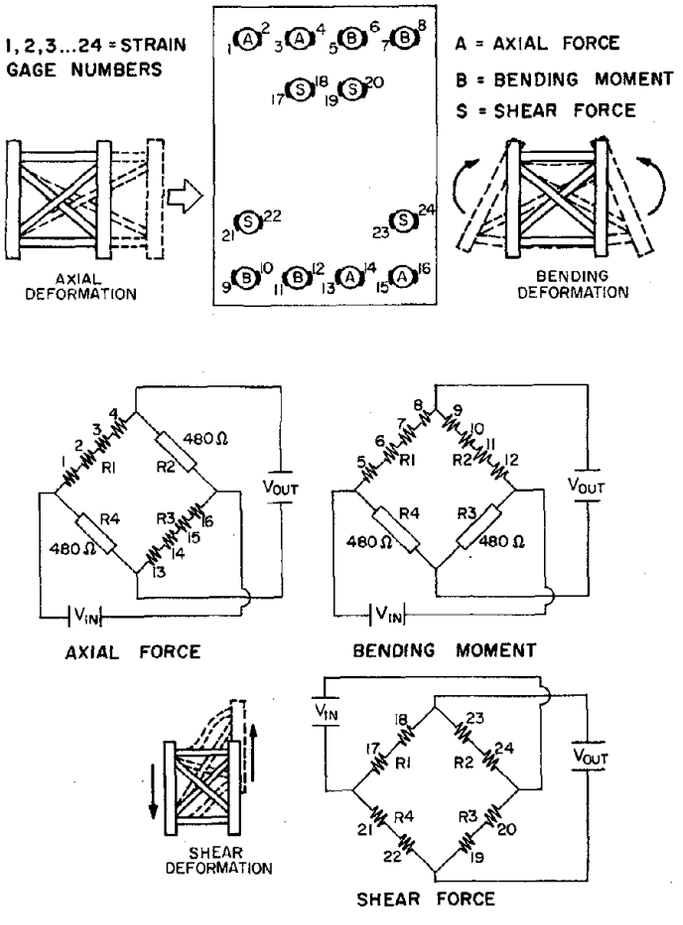

FIG. 2.72 WIRING DIAGRAM FOR THE INTERNAL FORCE CHANNELS

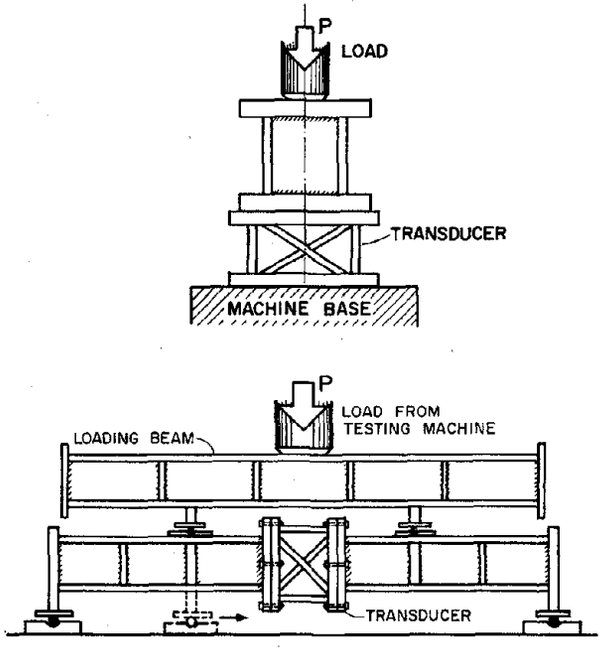

FIG. 2.73 CALIBRATION SCHEME FOR THE FORCE TRANSDUCER

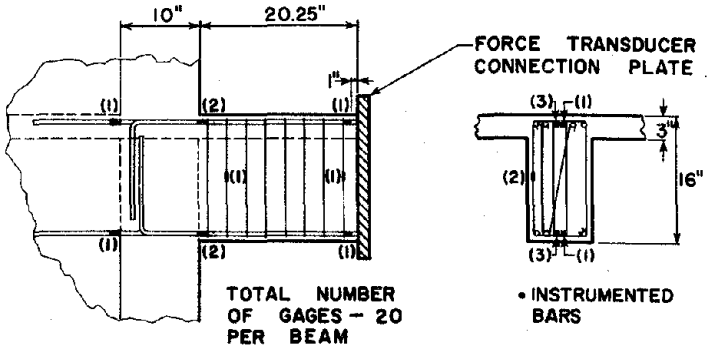

INTERNAL INSTRUMENTATION

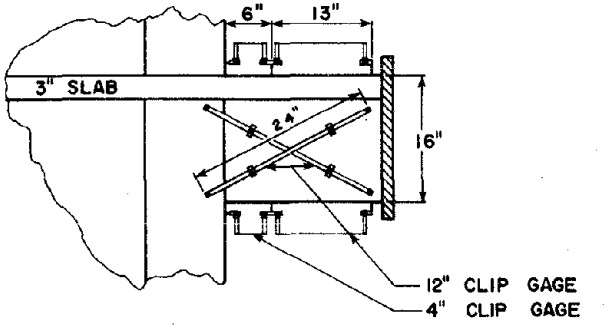

EXTERNAL INSTRUMENTATION

FIG. 2.74 EXTERNAL AND INTERNAL INSTRUMENTATION OF BEAMS

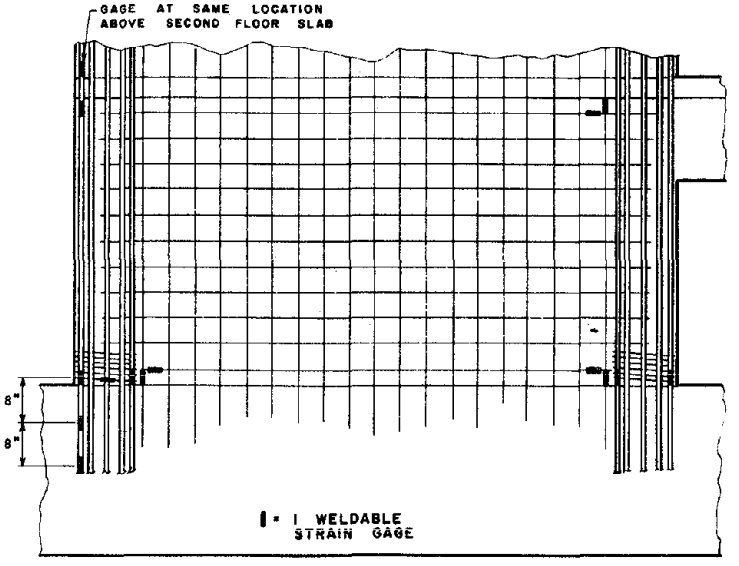

FIG. 2.75 INTERNAL INSTRUMENTATION OF THE WALL PANELS AND EDGE COLUMNS

A2. APPENDIX TO CHAPTER 2

A.2.1 Relating Girder Stiffness to Coupled Wall Stiffness

Using the laminar approach, the top deflection of the coupled wall system subjected to a triangular distributed load (similar to that required by seismic codes [2.16, 2.17]) has been derived as [2.3]:

$$y_{top}(\text{coupled wall}) = \frac{11}{120}\,\frac{\omega H^4}{E(I_1+I_2)}\,K_4$$

where;

$$K_4 = 1 - \frac{1}{\mu} + \frac{120}{11}\,\frac{1}{\mu(\alpha H)^2}\left(\frac{1}{3} - \frac{1 + (\frac{\alpha H}{2} - \frac{1}{\alpha H})\,\text{Sinh}\,\alpha H}{(\alpha H)^2\,\text{Cosh}\,\alpha H}\right)$$

$$\mu = 1 + \frac{(A_1+A_2)(I_1+I_2)}{A_1A_2L^2}$$

$$\alpha = \left(\frac{12\,I_p\,L^2}{hb^3(I_1+I_2)}\,\mu\right)^{\frac{1}{2}}$$

The nomenclature is defined at the end of Section A.2.1. There are a number of assumptions pertaining to the above formulation, namely:

(1) The cross sectional properties of the walls and the beams are constant over the height of the building.

(2) The walls deflect equally, i.e., the connecting elements have zero moment at their midspan.

(3) Material is linear.

(4) Plane sections remain plane.

The top deflection of the coupled wall system, assuming it to be a solid cantilever beam, subjected to triangular load of intensity ω at top, can be obtained as:

$$y_{top}(\text{solid wall}) = \frac{11}{120}\,\frac{\omega H^4}{EI_{sw}}$$

Consequently, the ratio of stiffnesses of the coupled wall and the (hypothetical) solid wall are obtained as:

$$y_{top}(\text{solid wall})/y_{top}(\text{coupled wall}) = \frac{I_1+I_2}{I_{s\omega}} \frac{1}{K_4}$$

For the prototype structure, the quantities I_1, I_2 and $I_{s\omega}$ are computed as follows:

$$I_1 = I_2 = \frac{30 \times 282^3}{12} - \frac{(30-12) \times 222^3}{12} = 39.65 \times 10^6 \text{ in.}^4$$

$$I_{s\omega} = \frac{12 \times 732^3}{12} + 4 \left(\frac{18 \times 30^3}{12}\right) + 2 (18 \times 30 \times 351^2)$$

$$+ 2 (16 \times 30 \times 99^2) = 536 \times 10^6 \text{ in.}^4$$

To evaluate $y_{top}(\text{solid wall})/y_{top}(\text{coupled wall})$, μ is obtained as follows:

$$A_1 = A_2 = 4464 \text{ in.}^2$$

$$\mu = 1 + \frac{2 \times 4464 \times 2 \times 39.65 \times 10^6}{4464^2 \times 450^2} = 1.175$$

The procedure followed in constructing Fig. 2.2, where the ratio $y_{top}(\text{solid wall})/y_{top}(\text{coupled wall})$ is shown for various beam sections, is as follows:

(1) For a given beam dimension, calculate the gross section moment of inertia, I_p, for the beam.

(2) Calculate α, K_4 and $y_{top}(\text{solid wall})/y_{top}(\text{coupled wall})$.

As an example, for the T-beam dimensions of 48" x 24", with 6" flange thickness and 42" flange width,

$$I_p = 265{,}054 \text{ in.}^4$$

$$\alpha = \left(\frac{12 \times 265{,}054 \times 450^2}{144 \times 168^3 \times 2 \times 39.65 \times 10^6} \times 1.175 \right)^{\frac{1}{2}} = 3.74 \times 10^{-3} \text{ 1/in.}$$

$$K_4 = 0.1879$$

$$y_{top}(\text{solid wall})/y_{top}(\text{coupled wall}) = \frac{2 \times 39.65 \times 10^6}{536 \times 10^6} \times \frac{1}{0.1879} = 0.79$$

i.e., the stiffness of the coupled wall, assuming a triangular distribution of external force, is 79 percent of the stiffness of the solid wall.

Notation:

y_{top} = horizontal deflection at the top

ω = intensity of triangularly distributed load at top

H = total height of the system

E = Youngs modulus of elasticity

h = story height

b = clear length of girder

L = distance between wall centroidal axes

A_1, A_2 = cross sectional areas of walls

I_1, I_2 = moments of inertia of walls

I_p = moment of inertia of connecting girder

$I_{s\omega}$ = moment of inertia of solid cantilever wall obtained by assuming the openings do not exist.

$$\mu = 1 + \frac{(A_1+A_2)}{A_1 A_2} \quad \frac{(I_1+I_2)}{L^2}$$

$$\alpha = \left(\frac{12\ I_p\ L^2}{h\ b^3} \quad \frac{\mu}{(I_1+I_2)} \right)^{\frac{1}{2}}$$

A.2.2. Design of the 15-Story Prototype Coupled Wall System with the 1973-UBC [2.16] and 1979-UBC [2.17] Provisions

A.2.2.1 Dead Loads

Based on the floor area and member dimensions in Fig. 2.1, the dead load of the beam and slab system, columns shear walls, and connecting girders, as well as the loads due to partitions, exterior walls, and mechanical equipment, were computed to be a total of 2028 kips for the roof and 2295 kips for the typical floor. The total building dead weight was then computed as 34158 kips.

A.2.2.2 Earthquake Load, 1973-UBC

According to Sec. 2314 of 1973-UBC,

$$T = \frac{0.05\ h_n}{\sqrt{D}} = 1.152 \text{ sec.}$$

$$C = \frac{0.05}{\sqrt[3]{T}} = 0.48$$

$$V = ZKCW = 1 \times 0.8 \times 0.048\ W = 3.84\%\ W$$

$$V = 0.0384 \times 34158 = 1312 \text{ kips.}$$

The structure is assumed to be located in the maximum seismic load zone, Zone 3. Consequently, Z is 1. The horizontal force factor K is taken as 0.8 from Table no. 23-I of the code. According to UBC Sec. 2314 (j) Structural Systems. 1. Design requirements. the structure, which is

over 160 ft tall, is required to have a space frame capable of resisting not less than 25 percent of the required seismic forces for the structure as a whole. Hence, the horizontal force factor, 0.8. Also, in Table 23-I, three criteria for the design of such systems are prescribed as:

(1) The frames and shear walls will resist the total lateral force in accordance with their relative rigidities considering the interaction of the shear walls and frames;

(2) The shear walls, acting independently of the ductile moment resisting portions of the space frame, will resist the total required lateral forces;

(3) The ductile moment resisting space frame will have the capacity to resist not less than 25 percent of the required lateral force.

By virtue of the second criterion above, the shear walls will be designed to resist all the total required lateral forces for the building, as this appears to be the most critical of the above criteria for the design of these walls. However, criterion (1), which prescribes design with proper incorporation of the frame-wall interaction, may result in a design with a more favorable ultimate limit state behavior. This is discussed more thoroughly in Section 2.2.4. According to UBC Sec. 2314 (g), a 5 percent eccentricity between the centers of mass and rigidity should be incorporated. This eccentricity results in a torque of 11808 kip-ft (0.05 x 180 ft x 1312 kips) for the N-S direction of the building. By virtue of criterion (2) in Table 23-I of UBC the two coupled wall systems are assumed to resist this torque completely, by developing shears equal to 118 kips (11808 kip-ft/100 ft) in addition to the base shear obtained from Sec. 2314 (d), eq. (14-1).

The base shear that is resisted by each coupled wall, therefore, becomes 774 kips (1312 kips/2 + 118 kips). The distribution of this total base shear, including the effect of torsion, is shown in Table 2.1. The coupled wall system was analyzed under this distribution with the program TABS [2.20]. The results of analysis are given in Tables 2.2 and 2.3.

A.2.2.3 Earthquake Load, 1979-UBC

According to Sec. 2312 of 1979-UBC,

$$T = \frac{0.05\ h_n}{\sqrt{D}} = 1.152 \text{ sec.}$$

$$C = \frac{1}{15\sqrt{T}} = 0.062 \text{ (was 0.048 for 1973-UBC)}$$

$$V = ZIKCSW = 1 \times 1 \times 0.8 \times 0.062 \times 1\ W = 4.96\%\ W$$

$$V = 0.0496 \times 34158 = 1694 \text{ kips}$$

The assumptions implicit in the above computation are: (1) The structure is located in Zone 4, Zone of the highest seismic risk; (2) Occupancy importance factor I is 1; (3) Site-structure resonance coefficient S is 1. The assumptions were made to obtain the earthquake load that may be as near as possible to the load prescribed by the 1973-UBC. There is, regardless, a 29 percent increase in the base shear as compared to the base shear computed by the 1973-UBC, due to the difference in the coefficient C. In general, the coefficient S will be larger than 1, accentuating the increase in base shear.

The provisions in UBC-1979 regarding the horizontal force factor K are unchanged from UBC-1973. The discussion pertaining to this factor in

Sec. A.2.2.2 will be valid here as well. The design earthquake base shear of one coupled wall system, incorporating the provision 2312 (e) 5, regarding the Horizontal Torsional Moment, in a similar manner as in Sec. A.2.2.2, becomes 999 kips (1694 kips/2 + 0.05 x 180 ft x 1694 kips/100 ft).

Provisions regarding the distribution of this base shear, specifically the expression for the concentrated force at the top of the structure, are different than in 1973-UBC. The computed distribution is shown in Table 2.1. The moment to shear ratio at the base is 71 percent of height, as compared to 68 percent of height, which was obtained for the 1973-UBC prescribed distribution. It is concluded that the lateral force and the moment to shear ratio resulting from this distribution are significantly more in the 1979-UBC provisions.

The results of analysis of the coupled wall system by the 1979-UBC prescribed loading using the program TABS [2.20] are given in Tables 2.2 and 2.3. Comparing nominal analysis results, wall base moment, and base shear demands and beam flexural demands are approximately 30 percent to 35 percent more with 1979-UBC prescribed loading as compared to 1973-UBC prescribed loading.

A.2.2.4 Gravity Loads of the Coupled Wall System

The gravity loads of the edge members of the coupled wall system were based on tributary areas of 235 sq ft for the exterior and 375 sq ft for the interior edge member (Table 2.2). The live load was reduced by 60 percent as permitted by Sec. 2306 of UBC (73 and 79), to 20 psf. The dead and live loads, thus computed, were 854 kips and 71 kips at the foundation of the exterior edge columns, respectively. The interior columns were computed to have 1232 kips and 113 kips as dead and live loading at the foundation, respectively. These loads are indicated on Table 2.2.

A.2.2.5 Design of the Wall Edge Columns with the 1973-UBC Provisions

The unfactored earthquake and gravity load demands from the edge columns of the coupled shear wall are indicated in Table 2.2. The exterior columns are observed to be critical members, as the forces due to the overturning moment and coupling action cancel each other at the interior columns. The edge columns are designed as members under pure axial load (Sec. 2627). Tension column (Table 2.2) demand: $\frac{1.4E + 0.9\ D}{\phi}$ = 1644 kips, where ϕ = 0.9. With 8#18 bars (ρ = 3.56%), supply is 1920 kips. Compression column (Table 2.2) demand: $\frac{1.4\ (E + D + L)}{\phi}$ = 4725 kips, where ϕ = 0.75. With 8#18 bars, supply is: $0.85 \times 4\ (30^2 - 4 \times 8) + 60 \times 8 \times 4$ = 4821 kips. In these computations the biaxial moments are not considered as the lateral earthquake forces are assumed to act nonconcurrently according to UBC [2.16, 2.17]. ATC-3[2.15] recommends the incorporation in design of 30 percent of the effects caused by the lateral seismic forces acting in the orthogonal direction. Slenderness effects are also neglected in the edge member design as the wall panel fully restrains the edge columns in the plane of the wall, and the floor slab offers sufficient restraint to avoid buckling of the column in the plane perpendicular to the wall.

The inner column demands require only minimum reinforcement, nine #9 bars, ρ = 1%. However, due to reasons explained in Section 2.2.2 of this report, these columns were provided with the same reinforcement as the exterior columns (Fig. 2.3). The reinforcement demands of the inner edge columns of the coupled walls were also checked by considering the design of these columns as part of the frames along the long direction of the building. The demands, computed in this manner, still required only minimum reinforcement.

By virtue of Sec. 2627(c), the edge columns should be provided by

special transverse reinforcement. It was decided to use spiral reinforcement for this purpose. According to Sec. 2626(e) - 4, the minimum percentage for spiral reinforcement is $0.45\ (A_g/A_c-1)f'_c/f_y = 0.172$. This is larger than $0.12\ f'_c/f_{yh}$. Using Gr. 60 #5 bar for spiral with a pitch of 2.5 in., $\rho_s = 0.018$. The column with this lateral reinforcement is capable of resisting a shear of:

$$V_u = (2A_v/3)f_y d_c/\phi s) = (2 \times 2 \times 0.3/3)\ 60 \times 26/(0.85 \times 2.5) = 294 \text{ kips}$$

by virtue of expression (26-7), Sec. 2626 of UBC, where the concrete contribution is neglected. The contribution of the four edge columns to the shear resistance of the walls, based on this computation, is 4 x 294 = 1176 kips.

An important shortcoming of the code (1973-UBC, 1979-UBC) provisions in the design of frame-wall (dual) structural systems is observed when the design of the walls in the longer direction of the building is considered. The period of the building in this direction is computed as:

$$T = \frac{0.05h_n}{\sqrt{D}} = \frac{0.05 \times 130}{\sqrt{180}} = 0.67 \text{ secs.}$$

and the spectral coefficient C is:

$$C = \frac{0.05}{\sqrt[3]{T}} = \frac{0.05}{\sqrt[3]{0.67}} = 0.057$$

which is 19 percent larger than the value of C for the short direction. The corresponding earthquake base shear for the building is V = 1558 kips, as compared to the 1312 kips for the shorter direction. By virtue of the provision requiring that "the shear walls, acting independently of the ductile moment resisting protions of the space frame shall resist the total required lateral forces," the four shear walls in the longer direction of the building (Fig. 2.1) should be designed for higher demands than the walls in the shorter direction.

The relative contribution of these walls to the overall strength

and stiffness of the building in the longer direction is significantly less than the corresponding contribution of the walls in the shorter direction. Consequently, when the designer incorporates walls in a certain direction of a building frame, when the frame stiffness and strength along that direction is high, the wall demands are severely and unjustifiably increased when all the earthquake force attracted in that direction is assigned to the walls. ATC-3 [2.15] requires the total seismic force to be distributed to the components of the seismic resisting system with due consideration of the relative stiffnesses of the components and the diaphragm. This is a more realistic approach.

A.2.2.6 Shear Design of the Walls in Accordance with 1973-UBC Provisions

Results of Analysis with 1973-UBC "E" loading (Table 2.2) indicate a base shear force of 387 kips for each wall and one coupled shear wall system in the building. According to Section 2627.(a), the demand is either 1.4(D+L) + 1.4E or 0.9D+1.4E, but 2.8E instead of 1.4E should be used in calculating shear and diagonal tension stresses. As 0.9D+1.4E results in a tension N_u in the wall of (-)489 kips, this axial force is selected acting together with V-387 kips in designing against shear. The moment M_u corresponding to this combination is 2.7×10^5 kip-in. (The value of unfactored internal forces corresponding to D, L and E are given in Table 2.2). The design shear is computed from 2.8 x 387/0.85 = 1275 kips where 0.85 is the ϕ factor. The corresponding shear stress is computed as 1275/(0.8 x 282 x 12) = 0.470 ksi, from eq (11-31), Section 2611.(q). This is less than $10\sqrt{f'_c}$, which is 0.632 ksi for a nominal concrete stress of 4000 psi. Section 2611.(q) permits the use of expression (11-8), $v_c = 2(1+0.002\ N_u/A_g)\sqrt{f'_c}$, to compute a concrete contribution. This contribution is considered zero for columns when the axial compressive stress is less than

0.12 f'_c (Sec. 2626.). The concrete contribution corresponding to expression (11-8) is $2(1-0.002 \times 489000/4464)\sqrt{4000}$ = 100 psi. UBC-1973, therefore, acknowledges a concrete contribution in the shear design of a wall which is subjected to a tensile stress.

The same code does not permit concrete contribution in the shear design of the columns of DMRSF's when the "compressive" stress is less than 0.12 f'_c.

The wall steel, finally, is computed by the following expression, incorporating concrete contribution:

$$A_v = (v_u - v_c)b_\omega \, s/f_y \text{ (expression 11-13).}$$

Assuming a 12 in. spacing,

$$A_v = (470-100) \times 12 \times 12/60000 = 0.88 \text{ in.}^2$$

Using two #6 bars (12 in. O.C.), A_v = 0.88 in.^{2}. The corresponding $\rho_h = 0.88/(12 \times 12) = 0.0061$, which is larger than 0.0025. The vertical wall reinforcement, according to Section 2611.(q), is computed from $\rho_n = 0.0025 + 0.5\,(2.5 - h_\omega/h_\omega)(\rho_h - 0.0025)$, which is less than 0.0025. It was decided to use ρ_n equal to ρ_h as suggested by the SEAOC, [2.13] that is, two #6 bars at 12 in. O.C. The wall, therefore, was designed with two curtains of #6 Gr. 60 reinforcement at 12 in. O.C. both ways. If the concrete contribution is neglected, the spacing becomes 9 in. Such a closer spacing was not chosen because the actual shear carrying mechanism of walls with confined edge members is quite different from the shear carrying mechanism of beams, on which these design provisions were based. The walls with confined edge columns are capable of developing shear strengths significantly larger than those computed from beam (truss) analogy. Furthermore, the contribution of web steel to the

shear strength of such walls were observed to be not as significant as this contribution in the case of beams. Note that the edge members acting as separate columns are capable of resisting a shear inducing diagonal tension type of shear failure of 294 kips each, as computed in A 2.2.5. This contribution is 588 kips for each wall, which constitutes 46 percent of the required supply of shear strength from the wall. This contribution, however significant, is completely neglected when the wall shear reinforcement is computed based on UBC expressions [2.16, 2.17].

A.2.2.7 Design of the Connecting Beams with the 1973-UBC Provisions

The connecting beams were considered in three groups for design purposes, as shown in Table 2.3., as there was a significant change in demands along the height of the structure. These demands were obtained through linear analysis with the code prescribed loading.

Design for type 3 beam (3rd - 9th floors): The design of the type 3 beam was based on the demands of the fifth floor. (Table 2.3). The negative moment demand, $1.4(D + L + E)/\phi$ was computed as 21442 kip-in. ({1312 + 1.4 x 12847}/0.9). The positive moment demand was computed by (0.9D + 1.4E)/0.9, as 19166 kip-in ({-737 + 1.4 x 12847}/0.9). Using nine #9 bars top and eight #9 bars bottom, the positive and negative moment supplies were computed as 21033 kip-in. and 23356 kip-in., respectively, with established ultimate strength procedures.

The design shear force was then obtained as 377 kips (1.25{21033 + 23356}/168 + 47), incorporating a simple span shear of 47 kips for the load combination of 1.4 (D + L). This results in a nominal shear stress demand of 406 psi (377/{0.85 x 24 x 45.5}). This is a significantly high nominal shear stress equivalent to $6.42\sqrt{f'_c}$. The corresponding area of web reinforcement, for a center to center spacing of 4-1/2 inches, is computed as 0.5 $in.^2$ (4.5 x 24{406 - $2\sqrt{4000}$}/60000). According to the code

provisions, a tie spacing of 9 in. is permitted (Sec. 2626(e) 5-c) as d/4, 8 bar diameters, 24 stirrup tie diameters or 12 inches, whichever is less, is specified for the maximum spacing at member ends. Using #4 bars for ties, the critical constraint is 8 bar diameters, which is 9 inches. To have a tie spacing of 9 inches for a beam which is expected to develop a shear stress of $6.42\sqrt{f'_c}$, although permitted by the code, is known to be an extremely deficient design (Sec. 1.2.3) considering the post yield cyclic behavior of the beam. Consequently, a spacing of 4-1/2 inches corresponding to half of the spacing permitted by the code, was selected.

The amount of web reinforcement is another factor requiring careful consideration in design. Three #4 bars (0.6 $in.^2$) are sufficient for the calculated demand of 0.5 $in.^2$, based on the 4-1/2 in. spacing. However, as explained in Sec. 2.2.2, when the need to provide effective lateral restraints to all the main bars is considered, eight #4 bars had to be provided, as shown in Fig. 2.4.

A simpler scheme is possible if #12 bars are used to replace #9 bars as the main flexural reinforcement, as shown in Fig. 2.4, alternative 2. Although a #12 bar does not exist, this would correspond to a #4 bar in the 1/3-scale model, which is available. In this case six #4 bars - two ties and a crosstie are adequate for lateral support of the flexural bars.

In each of the two alternatives, Fig. 2.4, the amount of lateral reinforcement is significantly more than the demand due to shear. Alternative 2 was selected as it was simpler, although larger bars, in general, lead to anchorage problems. The supply of shear reinforcement in this alternative is 1.14 $in.^2$, compared to 0.5 $in.^2$ of demand. On the other hand, using #12 bars rather than #9 bars results in a slight increase

in the demand as the area of six #12 bars is 19 percent larger than the area of nine #9 bars.

Design for type 2 beam (2nd, 10 - 12th floors): The demands of this type of beam were based on the demands of the tenth-floor beam (Table 2.3). Negative moment demand was computed as 16807 kip-in. ({1.4 x 9867 + 1312}/ 0.9). The positive moment demand was 14530 kip-in.{1.4x9867-737)/0.9}. Using seven #9 bars top and six #9 bars bottom, the supplied flexural strengths were computed as 15926 kip-in. and 18171 kip-in. for the positive and negative moment directions, respectively.

The design shear force for this beam was obtained as 301 kips (1.25{15926 + 18171}/168 + 47). The resulting nominal shear stress demand is 324 psi ($5.12\sqrt{f'_c}$), incorporating the ϕ factor of 0.85. Demand for tie area, based on a tie spacing of 4-1/2 in., is computed as 0.36 in.^{2} ({324 - $2\sqrt{4000}$} 24 x 4.5/60000). Using three #3 ties and one #3 crosstie for the purpose of restraining the main flexural bars, as shown in Fig. 2.5, as alternative 1, the supply becomes 0.77 in.^{2}. A simpler scheme is possible if four #12 (7.06 in.^{2}) bars are used to replace the seven #9 (7 in.^{2}) and six #9 (6 in.^{2}) bars top and bottom and using two #4 ties. In this case the supply is 0.8 in.^{2}(Fig. 2.5).

Design for type 1 beam (1st, 13-15th floors): Demands are based on the analysis results for the 13th-floor beam. These were computed as 9226 kip-in. and 11502 kip-in. for the positive and negative bending directions, respectively. Using four #9 and five #9, the supplied strengths were computed as 10718 kip-in. and 13402 kip-in. for the same bending directions, respectively. The design shear force is computed as 226 kips, and the corresponding nominal shear stress demand is 243 psi ($3.84\sqrt{f'_c}$). The demand for tie area, based on a 7-1/2 in. spacing, was computed as 0.35 in.^{2}. Using two #4 ties, supply is 0.79 in.^{2}. As the demand from

this type of beam is significantly lower than the others, a 7-1/2 in. spacing was used (Fig. 2.6).

A.2.2.8 Design of the Wall Edge Columns with 1979-UBC Provisions

The procedure for design is similar to the 1973-UBC design. The unfactored earthquake and gravity load demands are indicated in Table 2.2. The nominal design demands for the tension and compression columns were obtained as 2480 kips and 5727 kips, respectively. Using twelve #18 bars in these columns (ρ = 5.3%), the supplies in tension and compression become 2880 kips and 5777 kips, respectively. The spiral requirements of the 1979-UBC code are similar to these requirements of the 1973-UBC, and hence, #5 spiral with 2-1/2 in. pitch was selected. The resulting edge column design is shown in Fig. 2.3. The flexural steel in the edge columns of the wall designed with 1979-UBC provisions is 50 percent more than the steel in the edge columns of the wall designed with 1973-UBC provisions.

A.2.2.9 Shear Design of the Walls in Accordance with 1979-UBC Provisions

Unfactored "E" loading results in a base shear of 499.5 kips for each wall (Table 2.2). The demands are expressed as either 1.4 (D+L)+1.4E or 0.9D+1.4E where 2E instead of 1.4E will be used in computing shear stress. As both combinations result in compression in the walls, a concrete contribution of $2\sqrt{f'_c}$ is permitted. The design shear force is calculated as 1175 kips (2 x 499.5/0.85). The corresponding nominal stress is 434 psi (1175000/{0.8 x 282 x 12}), where 0.8 times total depth of the wall section is used to compute the effective depth. The nominal stress is equivalent to $6.86\sqrt{f'_c}$, less than $10\sqrt{f'_c}$. Horizontal wall reinforcement is established as two #6 bars at 14 in. O.C., resulting in a ρ_h of 0.0052 (2 x 0.44/12 x 14). The demand, for the nominal shear stress of

434 psi, is computed from (434 - $2\sqrt{4000}$)/60000 as 0.0051. The horizontal wall reinforcement is made equal to the vertical reinforcement (Fig. 2.3). It is observed that the 1979-UBC design results in 50 percent more edge column flexural steel and 17 percent less horizontal and vertical wall steel, as compared to the 1973-UBC design. The actual shear demand of the 1979-UBC designed wall is expected to be significantly higher than that of 1973-UBC design, due to the increased yield strength at the base. The shear design of this wall, however, is carried out for less shear than the 1973-UBC design.

A.2.2.10 Design of the Connecting Beams with 1979-UBC Provisions

The design procedure is similar to that followed in the 1973-UBC design. The "E" load demands of the beams are shown in Table 2.3, and the beams are designed in three types, as indicated in this Table.

Design for type 3 beam (3rd - 9th floors): The sixth-floor beam has the largest demands for positive and negative moment (Table 2.3). The nominal demands were computed as 25481 kip-in. and 27758 kip-in. for the positive and negative bending directions. Using twelve #9 bars top and eleven #9 bars bottom, the supplies for the positive and negative bending directions are obtained as 27845 kip-in. and 30332 kip-in., respectively. An alternative is using eight #12 bars top and seven #12 bars bottom, as shown in Fig. 2.7, increasing the supplies by approximately 20 percent. The design shear force was obtained as 480 kips for this beam (1.25{30332 + 27845}/168 + 47). The corresponding nominal stress is 529 psi (480000/{0.85 x 24 x 44.5}) = $8.4\sqrt{f'_c}$. The tie stress is computed as 403 psi (529 - $2\sqrt{4000}$) which satisfies the code as this is $6.4\sqrt{f'_c}$, less than $8\sqrt{f'_c}$. The amount of total nominal shear stress, $8.4\sqrt{f'_c}$, although permitted by the code, is an extremely high shear stress to expect an

adequate hysteretic response with the conventional detailing used. Using a 4-1/2 in. tie spacing, the required area of ties is obtained as 1.21 in.^{2} (403 x 4.5 x 24/60000). Each of the three alternatives in Fig. 2.7 provide adequate supplies according to code requirements.

Design for type 2 and type 1 beams: As indicated in Table 2.3, the demands for the type 2 and type 1 beams, 1979-UBC design, are quite close to the demands for the type 3 and type 2 beams, 1973-UBC design. Consequently, beam types 3 and 2 of the 1973-UBC design are adapted for beam types 2 and 1 of the 1979-UBC design, shown in Figs. 2.4 and 2.5.

EARTHQUAKE ENGINEERING RESEARCH CENTER REPORTS

NOTE: Numbers in parenthesis are Accession Numbers assigned by the National Technical Information Service; these are followed by a price code. Copies of the reports may be ordered from the National Technical Information Service, 5285 Port Royal Road, Springfield, Virginia, 22161. Accession Numbers should be quoted on orders for reports (PB --- ---) and remittance must accompany each order. Reports without this information were not available at time of printing. Upon request, EERC will mail inquirers this information when it becomes available.

EERC 67-1 "Feasibility Study Large-Scale Earthquake Simulator Facility," by J. Penzien, J.G. Bouwkamp, R.W. Clough and D. Rea - 1967 (PB 187 905)A07

EERC 68-1 Unassigned

EERC 68-2 "Inelastic Behavior of Beam-to-Column Subassemblages Under Repeated Loading," by V.V. Bertero - 1968 (PB 184 888)A05

EERC 68-3 "A Graphical Method for Solving the Wave Reflection-Refraction Problem," by H.D. McNiven and Y. Mengi - 1968 (PB 187 943)A03

EERC 68-4 "Dynamic Properties of McKinley School Buildings," by D. Rea, J.G. Bouwkamp and R.W. Clough - 1968 (PB 187 902)A07

EERC 68-5 "Characteristics of Rock Motions During Earthquakes," by H.B. Seed, I.M. Idriss and F.W. Kiefer - 1968 (PB 188 338)A03

EERC 69-1 "Earthquake Engineering Research at Berkeley," - 1969 (PB 187 906)A11

EERC 69-2 "Nonlinear Seismic Response of Earth Structures," by M. Dibaj and J. Penzien - 1969 (PB 187 904)A08

EERC 69-3 "Probabilistic Study of the Behavior of Structures During Earthquakes," by R. Ruiz and J. Penzien - 1969 (PB 187 886)A06

EERC 69-4 "Numerical Solution of Boundary Value Problems in Structural Mechanics by Reduction to an Initial Value Formulation," by N. Distefano and J. Schujman - 1969 (PB 187 942)A02

EERC 69-5 "Dynamic Programming and the Solution of the Biharmonic Equation," by N. Distefano - 1969 (PB 187 941)A03

EERC 69-6 "Stochastic Analysis of Offshore Tower Structures," by A.K. Malhotra and J. Penzien - 1969 (PB 187 903)A09

EERC 69-7 "Rock Motion Accelerograms for High Magnitude Earthquakes," by H.B. Seed and I.M. Idriss - 1969 (PB 187 940)A02

EERC 69-8 "Structural Dynamics Testing Facilities at the University of California, Berkeley," by R.M. Stephen, J.G. Bouwkamp, R.W. Clough and J. Penzien - 1969 (PB 189 111)A04

EERC 69-9 "Seismic Response of Soil Deposits Underlain by Sloping Rock Boundaries," by H. Dezfulian and H.B. Seed 1969 (PB 189 114)A03

EERC 69-10 "Dynamic Stress Analysis of Axisymmetric Structures Under Arbitrary Loading," by S. Ghosh and E.L. Wilson 1969 (PB 189 026)A10

EERC 69-11 "Seismic Behavior of Multistory Frames Designed by Different Philosophies," by J.C. Anderson and V. V. Bertero - 1969 (PB 190 662)A10

EERC 69-12 "Stiffness Degradation of Reinforcing Concrete Members Subjected to Cyclic Flexural Moments," by V.V. Bertero, B. Bresler and H. Ming Liao - 1969 (PB 202 942)A07

EERC 69-13 "Response of Non-Uniform Soil Deposits to Travelling Seismic Waves," by H. Dezfulian and H.B. Seed - 1969 (PB 191 023)A03

EERC 69-14 "Damping Capacity of a Model Steel Structure," by D. Rea, R.W. Clough and J.G. Bouwkamp - 1969 (PB 190 663)A06

EERC 69-15 "Influence of Local Soil Conditions on Building Damage Potential during Earthquakes," by H.B. Seed and I.M. Idriss - 1969 (PB 191 036)A03

EERC 69-16 "The Behavior of Sands Under Seismic Loading Conditions," by M.L. Silver and H.B. Seed - 1969 (AD 714 982)A07

EERC 70-1 "Earthquake Response of Gravity Dams," by A.K. Chopra - 1970 (AD 709 640)A03

EERC 70-2 "Relationships between Soil Conditions and Building Damage in the Caracas Earthquake of July 29, 1967," by H.B. Seed, I.M. Idriss and H. Dezfulian - 1970 (PB 195 762)A05

EERC 70-3 "Cyclic Loading of Full Size Steel Connections," by E.P. Popov and R.M. Stephen - 1970 (PB 213 545)A04

EERC 70-4 "Seismic Analysis of the Charaima Building, Caraballeda, Venezuela," by Subcommittee of the SEAONC Research Committee: V.V. Bertero, P.F. Fratessa, S.A. Mahin, J.H. Sexton, A.C. Scordelis, E.L. Wilson, L.A. Wyllie, H.B. Seed and J. Penzien, Chairman - 1970 (PB 201 455)A06

EERC 70-5 "A Computer Program for Earthquake Analysis of Dams," by A.K. Chopra and P. Chakrabarti - 1970 (AD 723 994)A05

EERC 70-6 "The Propagation of Love Waves Across Non-Horizontally Layered Structures," by J. Lysmer and L.A. Drake 1970 (PB 197 896)A03

EERC 70-7 "Influence of Base Rock Characteristics on Ground Response," by J. Lysmer, H.B. Seed and P.B. Schnabel 1970 (PB 197 897)A03

EERC 70-8 "Applicability of Laboratory Test Procedures for Measuring Soil Liquefaction Characteristics under Cyclic Loading," by H.B. Seed and W.H. Peacock - 1970 (PB 198 016)A03

EERC 70-9 "A Simplified Procedure for Evaluating Soil Liquefaction Potential," by H.B. Seed and I.M. Idriss - 1970 (PB 198 009)A03

EERC 70-10 "Soil Moduli and Damping Factors for Dynamic Response Analysis," by H.B. Seed and I.M. Idriss - 1970 (PB 197 869)A03

EERC 71-1 "Koyna Earthquake of December 11, 1967 and the Performance of Koyna Dam," by A.K. Chopra and P. Chakrabarti 1971 (AD 731 496)A06

EERC 71-2 "Preliminary In-Situ Measurements of Anelastic Absorption in Soils Using a Prototype Earthquake Simulator," by R.D. Borcherdt and P.W. Rodgers - 1971 (PB 201 454)A03

EERC 71-3 "Static and Dynamic Analysis of Inelastic Frame Structures," by F.L. Porter and G.H. Powell - 1971 (PB 210 135)A06

EERC 71-4 "Research Needs in Limit Design of Reinforced Concrete Structures," by V.V. Bertero - 1971 (PB 202 943)A04

EERC 71-5 "Dynamic Behavior of a High-Rise Diagonally Braced Steel Building," by D. Rea, A.A. Shah and J.G. Bouwkamp 1971 (PB 203 584)A06

EERC 71-6 "Dynamic Stress Analysis of Porous Elastic Solids Saturated with Compressible Fluids," by J. Ghaboussi and E. L. Wilson - 1971 (PB 211 396)A06

EERC 71-7 "Inelastic Behavior of Steel Beam-to-Column Subassemblages," by H. Krawinkler, V.V. Bertero and E.P. Popov 1971 (PB 211 335)A14

EERC 71-8 "Modification of Seismograph Records for Effects of Local Soil Conditions," by P. Schnabel, H.B. Seed and J. Lysmer - 1971 (PB 214 450)A03

EERC 72-1 "Static and Earthquake Analysis of Three Dimensional Frame and Shear Wall Buildings," by E.L. Wilson and H.H. Dovey - 1972 (PB 212 904)A05

EERC 72-2 "Accelerations in Rock for Earthquakes in the Western United States," by P.B. Schnabel and H.B. Seed - 1972 (PB 213 100)A03

EERC 72-3 "Elastic-Plastic Earthquake Response of Soil-Building Systems," by T. Minami - 1972 (PB 214 868)A08

EERC 72-4 "Stochastic Inelastic Response of Offshore Towers to Strong Motion Earthquakes," by M.K. Kaul - 1972 (PB 215 713)A05

EERC 72-5 "Cyclic Behavior of Three Reinforced Concrete Flexural Members with High Shear," by E.P. Popov, V.V. Bertero and H. Krawinkler - 1972 (PB 214 555)A05

EERC 72-6 "Earthquake Response of Gravity Dams Including Reservoir Interaction Effects," by P. Chakrabarti and A.K. Chopra - 1972 (AD 762 330)A08

EERC 72-7 "Dynamic Properties of Pine Flat Dam," by D. Rea, C.Y. Liaw and A.K. Chopra - 1972 (AD 763 928)A05

EERC 72-8 "Three Dimensional Analysis of Building Systems," by E.L. Wilson and H.H. Dovey - 1972 (PB 222 438)A06

EERC 72-9 "Rate of Loading Effects on Uncracked and Repaired Reinforced Concrete Members," by S. Mahin, V.V. Bertero, D. Rea and M. Atalay - 1972 (PB 224 520)A08

EERC 72-10 "Computer Program for Static and Dynamic Analysis of Linear Structural Systems," by E.L. Wilson, K.-J. Bathe, J.E. Peterson and H.H. Dovey - 1972 (PB 220 437)A04

EERC 72-11 "Literature Survey - Seismic Effects on Highway Bridges," by T. Iwasaki, J. Penzien and R.W. Clough - 1972 (PB 215 613)A19

EERC 72-12 "SHAKE-A Computer Program for Earthquake Response Analysis of Horizontally Layered Sites," by P.B. Schnabel and J. Lysmer - 1972 (PB 220 207)A06

EERC 73-1 "Optimal Seismic Design of Multistory Frames," by V.V. Bertero and H. Kamil - 1973

EERC 73-2 "Analysis of the Slides in the San Fernando Dams During the Earthquake of February 9, 1971," by H.B. Seed, K.L. Lee, I.M. Idriss and F. Makdisi - 1973 (PB 223 402)A14

EERC 73-3 "Computer Aided Ultimate Load Design of Unbraced Multistory Steel Frames," by M.B. El-Hafez and G.H. Powell 1973 (PB 248 315)A09

EERC 73-4 "Experimental Investigation into the Seismic Behavior of Critical Regions of Reinforced Concrete Components as Influenced by Moment and Shear," by M. Celebi and J. Penzien - 1973 (PB 215 884)A09

EERC 73-5 "Hysteretic Behavior of Epoxy-Repaired Reinforced Concrete Beams," by M. Celebi and J. Penzien - 1973 (PB 239 568)A03

EERC 73-6 "General Purpose Computer Program for Inelastic Dynamic Response of Plane Structures," by A. Kanaan and G.H. Powell - 1973 (PB 221 260)A08

EERC 73-7 "A Computer Program for Earthquake Analysis of Gravity Dams Including Reservoir Interaction," by P. Chakrabarti and A.K. Chopra - 1973 (AD 766 271)A04

EERC 73-8 "Behavior of Reinforced Concrete Deep Beam-Column Subassemblages Under Cyclic Loads," by O. Küstü and J.G. Bouwkamp - 1973 (PB 246 117)A12

EERC 73-9 "Earthquake Analysis of Structure-Foundation Systems," by A.K. Vaish and A.K. Chopra - 1973 (AD 766 272)A07

EERC 73-10 "Deconvolution of Seismic Response for Linear Systems," by R.B. Reimer - 1973 (PB 227 179)A08

EERC 73-11 "SAP IV: A Structural Analysis Program for Static and Dynamic Response of Linear Systems," by K.-J. Bathe, E.L. Wilson and F.E. Peterson - 1973 (PB 221 967)A09

EERC 73-12 "Analytical Investigations of the Seismic Response of Long, Multiple Span Highway Bridges," by W.S. Tseng and J. Penzien - 1973 (PB 227 816)A10

EERC 73-13 "Earthquake Analysis of Multi-Story Buildings Including Foundation Interaction," by A.K. Chopra and J.A. Gutierrez - 1973 (PB 222 970)A03

EERC 73-14 "ADAP: A Computer Program for Static and Dynamic Analysis of Arch Dams," by R.W. Clough, J.M. Raphael and S. Mojtahedi - 1973 (PB 223 763)A09

EERC 73-15 "Cyclic Plastic Analysis of Structural Steel Joints," by R.B. Pinkney and R.W. Clough - 1973 (PB 226 843)A08

EERC 73-16 "QUAD-4: A Computer Program for Evaluating the Seismic Response of Soil Structures by Variable Damping Finite Element Procedures," by I.M. Idriss, J. Lysmer, R. Hwang and H.B. Seed - 1973 (PB 229 424)A05

EERC 73-17 "Dynamic Behavior of a Multi-Story Pyramid Shaped Building," by R.M. Stephen, J.P. Hollings and J.G. Bouwkamp - 1973 (PB 240 718)A06

EERC 73-18 "Effect of Different Types of Reinforcing on Seismic Behavior of Short Concrete Columns," by V.V. Bertero, J. Hollings, O. Küstü, R.M. Stephen and J.G. Bouwkamp - 1973

EERC 73-19 "Olive View Medical Center Materials Studies, Phase I," by B. Bresler and V.V. Bertero - 1973 (PB 235 986)A06

EERC 73-20 "Linear and Nonlinear Seismic Analysis Computer Programs for Long Multiple-Span Highway Bridges," by W.S. Tseng and J. Penzien - 1973

EERC 73-21 "Constitutive Models for Cyclic Plastic Deformation of Engineering Materials," by J.M. Kelly and P.P. Gillis 1973 (PB 226 024)A03

EERC 73-22 "DRAIN - 2D User's Guide," by G.H. Powell - 1973 (PB 227 016)A05

EERC 73-23 "Earthquake Engineering at Berkeley - 1973," (PB 226 033)A11

EERC 73-24 Unassigned

EERC 73-25 "Earthquake Response of Axisymmetric Tower Structures Surrounded by Water," by C.Y. Liaw and A.K. Chopra 1973 (AD 773 052)A09

EERC 73-26 "Investigation of the Failures of the Olive View Stairtowers During the San Fernando Earthquake and Their Implications on Seismic Design," by V.V. Bertero and R.G. Collins - 1973 (PB 235 106)A13

EERC 73-27 "Further Studies on Seismic Behavior of Steel Beam-Column Subassemblages," by V.V. Bertero, H. Krawinkler and E.P. Popov - 1973 (PB 234 172)A06

EERC 74-1 "Seismic Risk Analysis," by C.S. Oliveira - 1974 (PB 235 920)A06

EERC 74-2 "Settlement and Liquefaction of Sands Under Multi-Directional Shaking," by R. Pyke, C.K. Chan and H.B. Seed 1974

EERC 74-3 "Optimum Design of Earthquake Resistant Shear Buildings," by D. Ray, K.S. Pister and A.K. Chopra - 1974 (PB 231 172)A06

EERC 74-4 "LUSH - A Computer Program for Complex Response Analysis of Soil-Structure Systems," by J. Lysmer, T. Udaka, H.B. Seed and R. Hwang - 1974 (PB 236 796)A05

EERC 74-5 "Sensitivity Analysis for Hysteretic Dynamic Systems: Applications to Earthquake Engineering," by D. Ray 1974 (PB 233 213)A06

EERC 74-6 "Soil Structure Interaction Analyses for Evaluating Seismic Response," by H.B. Seed, J. Lysmer and R. Hwang 1974 (PB 236 519)A04

EERC 74-7 Unassigned

EERC 74-8 "Shaking Table Tests of a Steel Frame - A Progress Report," by R.W. Clough and D. Tang - 1974 (PB 240 869)A03

EERC 74-9 "Hysteretic Behavior of Reinforced Concrete Flexural Members with Special Web Reinforcement," by V.V. Bertero, E.P. Popov and T.Y. Wang - 1974 (PB 236 797)A07

EERC 74-10 "Applications of Reliability-Based, Global Cost Optimization to Design of Earthquake Resistant Structures," by E. Vitiello and K.S. Pister - 1974 (PB 237 231)A06

EERC 74-11 "Liquefaction of Gravelly Soils Under Cyclic Loading Conditions," by R.T. Wong, H.B. Seed and C.K. Chan 1974 (PB 242 042)A03

EERC 74-12 "Site-Dependent Spectra for Earthquake-Resistant Design," by H.B. Seed, C. Ugas and J. Lysmer - 1974 (PB 240 953)A03

EERC 74-13 "Earthquake Simulator Study of a Reinforced Concrete Frame," by P. Hidalgo and R.W. Clough - 1974 (PB 241 944)A13

EERC 74-14 "Nonlinear Earthquake Response of Concrete Gravity Dams," by N. Pal - 1974 (AD/A 006 583)A06

EERC 74-15 "Modeling and Identification in Nonlinear Structural Dynamics - I. One Degree of Freedom Models," by N. Distefano and A. Rath - 1974 (PB 241 548)A06

EERC 75-1 "Determination of Seismic Design Criteria for the Dumbarton Bridge Replacement Structure, Vol. I: Description, Theory and Analytical Modeling of Bridge and Parameters," by F. Baron and S.-H. Pang - 1975 (PB 259 407)A15

EERC 75-2 "Determination of Seismic Design Criteria for the Dumbarton Bridge Replacement Structure, Vol. II: Numerical Studies and Establishment of Seismic Design Criteria," by F. Baron and S.-H. Pang - 1975 (PB 259 408)A11 (For set of EERC 75-1 and 75-2 (PB 259 406))

EERC 75-3 "Seismic Risk Analysis for a Site and a Metropolitan Area," by C.S. Oliveira - 1975 (PB 248 134)A09

EERC 75-4 "Analytical Investigations of Seismic Response of Short, Single or Multiple-Span Highway Bridges," by M.-C. Chen and J. Penzien - 1975 (PB 241 454)A09

EERC 75-5 "An Evaluation of Some Methods for Predicting Seismic Behavior of Reinforced Concrete Buildings," by S.A. Mahin and V.V. Bertero - 1975 (PB 246 306)A16

EERC 75-6 "Earthquake Simulator Study of a Steel Frame Structure, Vol. I: Experimental Results," by R.W. Clough and D.T. Tang - 1975 (PB 243 981)A13

EERC 75-7 "Dynamic Properties of San Bernardino Intake Tower," by D. Rea, C.-Y. Liaw and A.K. Chopra - 1975 (AD/A008 406) A05

EERC 75-8 "Seismic Studies of the Articulation for the Dumbarton Bridge Replacement Structure, Vol. I: Description, Theory and Analytical Modeling of Bridge Components," by F. Baron and R.E. Hamati - 1975 (PB 251 539)A07

EERC 75-9 "Seismic Studies of the Articulation for the Dumbarton Bridge Replacement Structure, Vol. 2: Numerical Studies of Steel and Concrete Girder Alternates," by F. Baron and R.E. Hamati - 1975 (PB 251 540)A10

EERC 75-10 "Static and Dynamic Analysis of Nonlinear Structures," by D.P. Mondkar and G.H. Powell - 1975 (PB 242 434)A08

EERC 75-11 "Hysteretic Behavior of Steel Columns," by E.P. Popov, V.V. Bertero and S. Chandramouli - 1975 (PB 252 365)A11

EERC 75-12 "Earthquake Engineering Research Center Library Printed Catalog," - 1975 (PB 243 711)A26

EERC 75-13 "Three Dimensional Analysis of Building Systems (Extended Version)," by E.L. Wilson, J.P. Hollings and H.H. Dovey - 1975 (PB 243 989)A07

EERC 75-14 "Determination of Soil Liquefaction Characteristics by Large-Scale Laboratory Tests," by P. De Alba, C.K. Chan and H.B. Seed - 1975 (NUREG 0027)A08

EERC 75-15 "A Literature Survey - Compressive, Tensile, Bond and Shear Strength of Masonry," by R.L. Mayes and R.W. Clough - 1975 (PB 246 292)A10

EERC 75-16 "Hysteretic Behavior of Ductile Moment Resisting Reinforced Concrete Frame Components," by V.V. Bertero and E.P. Popov - 1975 (PB 246 388)A05

EERC 75-17 "Relationships Between Maximum Acceleration, Maximum Velocity, Distance from Source, Local Site Conditions for Moderately Strong Earthquakes," by H.B. Seed, R. Murarka, J. Lysmer and I.M. Idriss - 1975 (PB 248 172)A03

EERC 75-18 "The Effects of Method of Sample Preparation on the Cyclic Stress-Strain Behavior of Sands," by J. Mulilis, C.K. Chan and H.B. Seed - 1975 (Summarized in EERC 75-28)

EERC 75-19 "The Seismic Behavior of Critical Regions of Reinforced Concrete Components as Influenced by Moment, Shear and Axial Force," by M.B. Atalay and J. Penzien - 1975 (PB 258 842)A11

EERC 75-20 "Dynamic Properties of an Eleven Story Masonry Building," by R.M. Stephen, J.P. Hollings, J.G. Bouwkamp and D. Jurukovski - 1975 (PB 246 945)A04

EERC 75-21 "State-of-the-Art in Seismic Strength of Masonry - An Evaluation and Review," by R.L. Mayes and R.W. Clough 1975 (PB 249 040)A07

EERC 75-22 "Frequency Dependent Stiffness Matrices for Viscoelastic Half-Plane Foundations," by A.K. Chopra, P. Chakrabarti and G. Dasgupta - 1975 (PB 248 121)A07

EERC 75-23 "Hysteretic Behavior of Reinforced Concrete Framed Walls," by T.Y. Wong, V.V. Bertero and E.P. Popov - 1975

EERC 75-24 "Testing Facility for Subassemblages of Frame-Wall Structural Systems," by V.V. Bertero, E.P. Popov and T. Endo - 1975

EERC 75-25 "Influence of Seismic History on the Liquefaction Characteristics of Sands," by H.B. Seed, K. Mori and C.K. Chan - 1975 (Summarized in EERC 75-28)

EERC 75-26 "The Generation and Dissipation of Pore Water Pressures during Soil Liquefaction," by H.B. Seed, P.P. Martin and J. Lysmer - 1975 (PB 252 648)A03

EERC 75-27 "Identification of Research Needs for Improving Aseismic Design of Building Structures," by V.V. Bertero 1975 (PB 248 136)A05

EERC 75-28 "Evaluation of Soil Liquefaction Potential during Earthquakes," by H.B. Seed, I. Arango and C.K. Chan - 1975 (NUREG 0026)A13

EERC 75-29 "Representation of Irregular Stress Time Histories by Equivalent Uniform Stress Series in Liquefaction Analyses," by H.B. Seed, I.M. Idriss, F. Makdisi and N. Banerjee - 1975 (PB 252 635)A03

EERC 75-30 "FLUSH - A Computer Program for Approximate 3-D Analysis of Soil-Structure Interaction Problems," by J. Lysmer, T. Udaka, C.-F. Tsai and H.B. Seed - 1975 (PB 259 332)A07

EERC 75-31 "ALUSH - A Computer Program for Seismic Response Analysis of Axisymmetric Soil-Structure Systems," by E. Berger, J. Lysmer and H.B. Seed - 1975

EERC 75-32 "TRIP and TRAVEL - Computer Programs for Soil-Structure Interaction Analysis with Horizontally Travelling Waves," by T. Udaka, J. Lysmer and H.B. Seed - 1975

EERC 75-33 "Predicting the Performance of Structures in Regions of High Seismicity," by J. Penzien - 1975 (PB 248 130)A03

EERC 75-34 "Efficient Finite Element Analysis of Seismic Structure - Soil - Direction," by J. Lysmer, H.B. Seed, T. Udaka, R.N. Hwang and C.-F. Tsai - 1975 (PB 253 570)A03

EERC 75-35 "The Dynamic Behavior of a First Story Girder of a Three-Story Steel Frame Subjected to Earthquake Loading," by R.W. Clough and L.-Y. Li - 1975 (PB 248 841)A05

EERC 75-36 "Earthquake Simulator Study of a Steel Frame Structure, Volume II - Analytical Results," by D.T. Tang - 1975 (PB 252 926)A10

EERC 75-37 "ANSR-I General Purpose Computer Program for Analysis of Non-Linear Structural Response," by D.P. Mondkar and G.H. Powell - 1975 (PB 252 386)A08

EERC 75-38 "Nonlinear Response Spectra for Probabilistic Seismic Design and Damage Assessment of Reinforced Concrete Structures," by M. Murakami and J. Penzien - 1975 (PB 259 530)A05

EERC 75-39 "Study of a Method of Feasible Directions for Optimal Elastic Design of Frame Structures Subjected to Earthquake Loading," by N.D. Walker and K.S. Pister - 1975 (PB 257 781)A06

EERC 75-40 "An Alternative Representation of the Elastic-Viscoelastic Analogy," by G. Dasgupta and J.L. Sackman - 1975 (PB 252 173)A03

EERC 75-41 "Effect of Multi-Directional Shaking on Liquefaction of Sands," by H.B. Seed, R. Pyke and G.R. Martin - 1975 (PB 258 781)A03

EERC 76-1 "Strength and Ductility Evaluation of Existing Low-Rise Reinforced Concrete Buildings - Screening Method," by T. Okada and B. Bresler - 1976 (PB 257 906)A11

EERC 76-2 "Experimental and Analytical Studies on the Hysteretic Behavior of Reinforced Concrete Rectangular and T-Beams," by S.-Y.M. Ma, E.P. Popov and V.V. Bertero - 1976 (PB 260 843)A12

EERC 76-3 "Dynamic Behavior of a Multistory Triangular-Shaped Building," by J. Petrovski, R.M. Stephen, E. Gartenbaum and J.G. Bouwkamp - 1976 (PB 273 279)A07

EERC 76-4 "Earthquake Induced Deformations of Earth Dams," by N. Serff, H.B. Seed, F.I. Makdisi & C.-Y. Chang - 1976 (PB 292 065)A08

EERC 76-5 "Analysis and Design of Tube-Type Tall Building Structures," by H. de Clercq and G.H. Powell - 1976 (PB 252 220) A10

EERC 76-6 "Time and Frequency Domain Analysis of Three-Dimensional Ground Motions, San Fernando Earthquake," by T. Kubo and J. Penzien (PB 260 556)A11

EERC 76-7 "Expected Performance of Uniform Building Code Design Masonry Structures," by R.L. Mayes, Y. Omote, S.W. Chen and R.W. Clough - 1976 (PB 270 098)A05

EERC 76-8 "Cyclic Shear Tests of Masonry Piers, Volume 1 - Test Results," by R.L. Mayes, Y. Omote, R.W. Clough - 1976 (PB 264 424)A06

EERC 76-9 "A Substructure Method for Earthquake Analysis of Structure - Soil Interaction," by J.A. Gutierrez and A.K. Chopra - 1976 (PB 257 783)A08

EERC 76-10 "Stabilization of Potentially Liquefiable Sand Deposits using Gravel Drain Systems," by H.B. Seed and J.R. Booker - 1976 (PB 258 820)A04

EERC 76-11 "Influence of Design and Analysis Assumptions on Computed Inelastic Response of Moderately Tall Frames," by G.H. Powell and D.G. Row - 1976 (PB 271 409)A06

EERC 76-12 "Sensitivity Analysis for Hysteretic Dynamic Systems: Theory and Applications," by D. Ray, K.S. Pister and E. Polak - 1976 (PB 262 859)A04

EERC 76-13 "Coupled Lateral Torsional Response of Buildings to Ground Shaking," by C.L. Kan and A.K. Chopra - 1976 (PB 257 907)A09

EERC 76-14 "Seismic Analyses of the Banco de America," by V.V. Bertero, S.A. Mahin and J.A. Hollings - 1976

EERC 76-15 "Reinforced Concrete Frame 2: Seismic Testing and Analytical Correlation," by R.W. Clough and J. Gidwani - 1976 (PB 261 323)A08

EERC 76-16 "Cyclic Shear Tests of Masonry Piers, Volume 2 - Analysis of Test Results," by R.L. Mayes, Y. Omote and R.W. Clough - 1976

EERC 76-17 "Structural Steel Bracing Systems: Behavior Under Cyclic Loading," by E.P. Popov, K. Takanashi and C.W. Roeder - 1976 (PB 260 715)A05

EERC 76-18 "Experimental Model Studies on Seismic Response of High Curved Overcrossings," by D. Williams and W.G. Godden - 1976 (PB 269 548)A08

EERC 76-19 "Effects of Non-Uniform Seismic Disturbances on the Dumbarton Bridge Replacement Structure," by F. Baron and R.E. Hamati - 1976 (PB 282 981)A16

EERC 76-20 "Investigation of the Inelastic Characteristics of a Single Story Steel Structure Using System Identification and Shaking Table Experiments," by V.C. Matzen and H.D. McNiven - 1976 (PB 258 453)A07

EERC 76-21 "Capacity of Columns with Splice Imperfections," by E.P. Popov, R.M. Stephen and R. Philbrick - 1976 (PB 260 378)A04

EERC 76-22 "Response of the Olive View Hospital Main Building during the San Fernando Earthquake," by S. A. Mahin, V.V. Bertero, A.K. Chopra and R. Collins - 1976 (PB 271 425)A14

EERC 76-23 "A Study on the Major Factors Influencing the Strength of Masonry Prisms," by N.M. Mostaghel, R.L. Mayes, R. W. Clough and S.W. Chen - 1976 (Not published)

EERC 76-24 "GADFLEA - A Computer Program for the Analysis of Pore Pressure Generation and Dissipation during Cyclic or Earthquake Loading," by J.R. Booker, M.S. Rahman and H.B. Seed - 1976 (PB 263 947)A04

EERC 76-25 "Seismic Safety Evaluation of a R/C School Building," by B. Bresler and J. Axley - 1976

EERC 76-26 "Correlative Investigations on Theoretical and Experimental Dynamic Behavior of a Model Bridge Structure," by K. Kawashima and J. Penzien - 1976 (PB 263 388)A11

EERC 76-27 "Earthquake Response of Coupled Shear Wall Buildings," by T. Srichatrapimuk - 1976 (PB 265 157)A07

EERC 76-28 "Tensile Capacity of Partial Penetration Welds," by E.P. Popov and R.M. Stephen - 1976 (PB 262 899)A03

EERC 76-29 "Analysis and Design of Numerical Integration Methods in Structural Dynamics," by H.M. Hilber - 1976 (PB 264 410)A06

EERC 76-30 "Contribution of a Floor System to the Dynamic Characteristics of Reinforced Concrete Buildings," by L.E. Malik and V.V. Bertero - 1976 (PB 272 247)A13

EERC 76-31 "The Effects of Seismic Disturbances on the Golden Gate Bridge," by F. Baron, M. Arikan and R.E. Hamati - 1976 (PB 272 279)A09

EERC 76-32 "Infilled Frames in Earthquake Resistant Construction," by R.E. Klingner and V.V. Bertero - 1976 (PB 265 892)A13

UCB/EERC-77/01 "PLUSH - A Computer Program for Probabilistic Finite Element Analysis of Seismic Soil-Structure Interaction," by M.P. Romo Organista, J. Lysmer and H.B. Seed - 1977

UCB/EERC-77/02 "Soil-Structure Interaction Effects at the Humboldt Bay Power Plant in the Ferndale Earthquake of June 7, 1975," by J.E. Valera, H.B. Seed, C.F. Tsai and J. Lysmer - 1977 (PB 265 795)A04

UCB/EERC-77/03 "Influence of Sample Disturbance on Sand Response to Cyclic Loading," by K. Mori, H.B. Seed and C.K. Chan - 1977 (PB 267 352)A04

UCB/EERC-77/04 "Seismological Studies of Strong Motion Records," by J. Shoja-Taheri - 1977 (PB 269 655)A10

UCB/EERC-77/05 "Testing Facility for Coupled-Shear Walls," by L. Li-Hyung, V.V. Bertero and E.P. Popov - 1977

UCB/EERC-77/06 "Developing Methodologies for Evaluating the Earthquake Safety of Existing Buildings," by No. 1 - B. Bresler; No. 2 - B. Bresler, T. Okada and D. Zisling; No. 3 - T. Okada and B. Bresler; No. 4 - V.V. Bertero and B. Bresler - 1977 (PB 267 354)A08

UCB/EERC-77/07 "A Literature Survey - Transverse Strength of Masonry Walls," by Y. Omote, R.L. Mayes, S.W. Chen and R.W. Clough - 1977 (PB 277 933)A07

UCB/EERC-77/08 "DRAIN-TABS: A Computer Program for Inelastic Earthquake Response of Three Dimensional Buildings," by R. Guendelman-Israel and G.H. Powell - 1977 (PB 270 693)A07

UCB/EERC-77/09 "SUBWALL: A Special Purpose Finite Element Computer Program for Practical Elastic Analysis and Design of Structural Walls with Substructure Option," by D.Q. Le, H. Peterson and E.P. Popov - 1977 (PB 270 567)A05

UCB/EERC-77/10 "Experimental Evaluation of Seismic Design Methods for Broad Cylindrical Tanks," by D.P. Clough (PB 272 280)A13

UCB/EERC-77/11 "Earthquake Engineering Research at Berkeley - 1976," - 1977 (PB 273 507)A09

UCB/EERC-77/12 "Automated Design of Earthquake Resistant Multistory Steel Building Frames," by N.D. Walker, Jr. - 1977 (PB 276 526)A09

UCB/EERC-77/13 "Concrete Confined by Rectangular Hoops Subjected to Axial Loads," by J. Vallenas, V.V. Bertero and E.P. Popov - 1977 (PB 275 165)A06

UCB/EERC-77/14 "Seismic Strain Induced in the Ground During Earthquakes," by Y. Sugimura - 1977 (PB 284 201)A04

UCB/EERC-77/15 "Bond Deterioration under Generalized Loading," by V.V. Bertero, E.P. Popov and S. Viwathanatepa - 1977

UCB/EERC-77/16 "Computer Aided Optimum Design of Ductile Reinforced Concrete Moment Resisting Frames," by S.W. Zagajeski and V.V. Bertero - 1977 (PB 280 137)A07

UCB/EERC-77/17 "Earthquake Simulation Testing of a Stepping Frame with Energy-Absorbing Devices," by J.M. Kelly and D.F. Tsztoo - 1977 (PB 273 506)A04

UCB/EERC-77/18 "Inelastic Behavior of Eccentrically Braced Steel Frames under Cyclic Loadings," by C.W. Roeder and E.P. Popov - 1977 (PB 275 526)A15

UCB/EERC-77/19 "A Simplified Procedure for Estimating Earthquake-Induced Deformations in Dams and Embankments," by F.I. Makdisi and H.B. Seed - 1977 (PB 276 820)A04

UCB/EERC-77/20 "The Performance of Earth Dams during Earthquakes," by H.B. Seed, F.I. Makdisi and P. de Alba - 1977 (PB 276 821)A04

UCB/EERC-77/21 "Dynamic Plastic Analysis Using Stress Resultant Finite Element Formulation," by P. Lukkunapvasit and J.M. Kelly - 1977 (PB 275 453)A04

UCB/EERC-77/22 "Preliminary Experimental Study of Seismic Uplift of a Steel Frame," by R.W. Clough and A.A. Huckelbridge 1977 (PB 278 769)A08

UCB/EERC-77/23 "Earthquake Simulator Tests of a Nine-Story Steel Frame with Columns Allowed to Uplift," by A.A. Huckelbridge - 1977 (PB 277 944)A09

UCB/EERC-77/24 "Nonlinear Soil-Structure Interaction of Skew Highway Bridges," by M.-C. Chen and J. Penzien - 1977 (PB 276 176)A07

UCB/EERC-77/25 "Seismic Analysis of an Offshore Structure Supported on Pile Foundations," by D.D.-N. Liou and J. Penzien 1977 (PB 283 180)A06

UCB/EERC-77/26 "Dynamic Stiffness Matrices for Homogeneous Viscoelastic Half-Planes," by G. Dasgupta and A.K. Chopra - 1977 (PB 279 654)A06

UCB/EERC-77/27 "A Practical Soft Story Earthquake Isolation System," by J.M. Kelly, J.M. Eidinger and C.J. Derham - 1977 (PB 276 814)A07

UCB/EERC-77/28 "Seismic Safety of Existing Buildings and Incentives for Hazard Mitigation in San Francisco: An Exploratory Study," by A.J. Meltsner - 1977 (PB 281 970)A05

UCD/EERC-77/29 "Dynamic Analysis of Electrohydraulic Shaking Tables," by D. Rea, S. Abedi-Hayati and Y. Takahashi 1977 (PB 282 569)A04

UCB/EERC-77/30 "An Approach for Improving Seismic - Resistant Behavior of Reinforced Concrete Interior Joints," by B. Galunic, V.V. Bertero and E.P. Popov - 1977 (PB 290 870)A06

UCB/EERC-78/01 "The Development of Energy-Absorbing Devices for Aseismic Base Isolation Systems," by J.M. Kelly and D.F. Tsztoo - 1978 (PB 284 978)A04

UCB/EERC-78/02 "Effect of Tensile Prestrain on the Cyclic Response of Structural Steel Connections, by J.G. Bouwkamp and A. Mukhopadhyay - 1978

UCB/EERC-78/03 "Experimental Results of an Earthquake Isolation System using Natural Rubber Bearings," by J.M. Eidinger and J.M. Kelly - 1978 (PB 281 686)A04

UCB/EERC-78/04 "Seismic Behavior of Tall Liquid Storage Tanks," by A. Niwa - 1978 (PB 284 017)A14

UCB/EERC-78/05 "Hysteretic Behavior of Reinforced Concrete Columns Subjected to High Axial and Cyclic Shear Forces," by S.W. Zagajeski, V.V. Bertero and J.G. Bouwkamp - 1978 (PB 283 858)A13

UCB/EERC-78/06 "Inelastic Beam-Column Elements for the ANSR-I Program," by A. Riahi, D.G. Row and G.H. Powell - 1978

UCB/EERC-78/07 "Studies of Structural Response to Earthquake Ground Motion," by O.A. Lopez and A.K. Chopra - 1978 (PB 282 790)A05

UCB/EERC-78/08 "A Laboratory Study of the Fluid-Structure Interaction of Submerged Tanks and Caissons in Earthquakes," by R.C. Byrd - 1978 (PB 284 957)A08

UCB/EERC-78/09 "Model for Evaluating Damageability of Structures," by I. Sakamoto and B. Bresler - 1978

UCB/EERC-78/10 "Seismic Performance of Nonstructural and Secondary Structural Elements," by I. Sakamoto - 1978

UCB/EERC-78/11 "Mathematical Modelling of Hysteresis Loops for Reinforced Concrete Columns," by S. Nakata, T. Sproul and J. Penzien - 1978

UCB/EERC-78/12 "Damageability in Existing Buildings," by T. Blejwas and B. Bresler - 1978

UCB/EERC-78/13 "Dynamic Behavior of a Pedestal Base Multistory Building," by R.M. Stephen, E.L. Wilson, J.G. Bouwkamp and M. Button - 1978 (PB 286 650)A08

UCB/EERC-78/14 "Seismic Response of Bridges - Case Studies," by R.A. Imbsen, V. Nutt and J. Penzien - 1978 (PB 286 503)A10

UCB/EERC-78/15 "A Substructure Technique for Nonlinear Static and Dynamic Analysis," by D.G. Row and G.H. Powell - 1978 (PB 288 077)A10

UCB/EERC-78/16 "Seismic Risk Studies for San Francisco and for the Greater San Francisco Bay Area," by C.S. Oliveira - 1978

UCB/EERC-78/17 "Strength of Timber Roof Connections Subjected to Cyclic Loads," by P. Gülkan, R.L. Mayes and R.W. Clough - 1978

UCB/EERC-78/18 "Response of K-Braced Steel Frame Models to Lateral Loads," by J.G. Bouwkamp, R.M. Stephen and E.P. Popov - 1978

UCB/EERC-78/19 "Rational Design Methods for Light Equipment in Structures Subjected to Ground Motion," by J.L. Sackman and J.M. Kelly - 1978 (PB 292 357)A04

UCB/EERC-78/20 "Testing of a Wind Restraint for Aseismic Base Isolation," by J.M. Kelly and D.E. Chitty - 1978 (PB 292 833)A03

UCB/EERC-78/21 "APOLLO - A Computer Program for the Analysis of Pore Pressure Generation and Dissipation in Horizontal Sand Layers During Cyclic or Earthquake Loading," by P.P. Martin and H.B. Seed - 1978 (PB 292 835)A04

UCB/EERC-78/22 "Optimal Design of an Earthquake Isolation System," by M.A. Bhatti, K.S. Pister and E. Polak - 1978 (PB 294 735)A06

UCB/EERC-78/23 "MASH - A Computer Program for the Non-Linear Analysis of Vertically Propagating Shear Waves in Horizontally Layered Deposits," by P.P. Martin and H.B. Seed - 1978 (PB 293 101)A05

UCB/EERC-78/24 "Investigation of the Elastic Characteristics of a Three Story Steel Frame Using System Identification," by I. Kaya and H.D. McNiven - 1978

UCB/EERC-78/25 "Investigation of the Nonlinear Characteristics of a Three-Story Steel Frame Using System Identification," by I. Kaya and H.D. McNiven - 1978

UCB/EERC-78/26 "Studies of Strong Ground Motion in Taiwan," by Y.M. Hsiung, B.A. Bolt and J. Penzien - 1978

UCB/EERC-78/27 "Cyclic Loading Tests of Masonry Single Piers: Volume 1 - Height to Width Ratio of 2," by P.A. Hidalgo, R.L. Mayes, H.D. McNiven and R.W. Clough - 1978

UCB/EERC-78/28 "Cyclic Loading Tests of Masonry Single Piers: Volume 2 - Height to Width Ratio of 1," by S.-W.J. Chen, P.A. Hidalgo, R.L. Mayes, R.W. Clough and H.D. McNiven - 1978

UCB/EERC-78/29 "Analytical Procedures in Soil Dynamics," by J. Lysmer - 1978

UCB/EERC-79/01 "Hysteretic Behavior of Lightweight Reinforced Concrete Beam-Column Subassemblages," by B. Forzani, E.P. Popov and V.V. Bertero - April 1979(PB 298 267)A06

UCB/EERC-79/02 "The Development of a Mathematical Model to Predict the Flexural Response of Reinforced Concrete Beams to Cyclic Loads, Using System Identification," by J. Stanton & H. McNiven - Jan. 1979(PB 295 875)A10

UCB/EERC-79/03 "Linear and Nonlinear Earthquake Response of Simple Torsionally Coupled Systems," by C.L. Kan and A.K. Chopra - Feb. 1979(PB 298 262)A06

UCB/EERC-79/04 "A Mathematical Model of Masonry for Predicting its Linear Seismic Response Characteristics," by Y. Mengi and H.D. McNiven - Feb. 1979(PB 298 266)A06

UCB/EERC-79/05 "Mechanical Behavior of Lightweight Concrete Confined by Different Types of Lateral Reinforcement," by M.A. Manrique, V.V. Bertero and E.P. Popov - May 1979(PB 301 114)A06

UCB/EERC-79/06 "Static Tilt Tests of a Tall Cylindrical Liquid Storage Tank," by R.W. Clough and A. Niwa - Feb. 1979 (PB 301 167)A06

UCB/EERC-79/07 "The Design of Steel Energy Absorbing Restrainers and Their Incorporation into Nuclear Power Plants for Enhanced Safety: Volume 1 - Summary Report," by P.N. Spencer, V.F. Zackay, and E.R. Parker - Feb. 1979(UCB/EERC-79/07)A09

UCB/EERC-79/08 "The Design of Steel Energy Absorbing Restrainers and Their Incorporation into Nuclear Power Plants for Enhanced Safety: Volume 2 - The Development of Analyses for Reactor System Piping,""Simple Systems" by M.C. Lee, J. Penzien, A.K. Chopra and K. Suzuki "Complex Systems" by G.H. Powell, E.L. Wilson, R.W. Clough and D.G. Row - Feb. 1979(UCB/EERC-79/08)A10

UCB/EERC-79/09 "The Design of Steel Energy Absorbing Restrainers and Their Incorporation into Nuclear Power Plants for Enhanced Safety: Volume 3 - Evaluation of Commercial Steels," by W.S. Owen, R.M.N. Pelloux, R.O. Ritchie, M. Faral, T. Ohhashi, J. Toplosky, S.J. Hartman, V.F. Zackay and E.R. Parker - Feb. 1979(UCB/EERC-79/09)A04

UCB/EERC-79/10 "The Design of Steel Energy Absorbing Restrainers and Their Incorporation into Nuclear Power Plants for Enhanced Safety: Volume 4 - A Review of Energy-Absorbing Devices," by J.M. Kelly and M.S. Skinner - Feb. 1979(UCB/EERC-79/10)A04

UCB/EERC-79/11 "Conservatism In Summation Rules for Closely Spaced Modes," by J.M. Kelly and J.L. Sackman - May 1979(PB 301 328)A03

UCB/EERC-79/12 "Cyclic Loading Tests of Masonry Single Piers; Volume 3 - Height to Width Ratio of 0.5," by P.A. Hidalgo, R.L. Mayes, H.D. McNiven and R.W. Clough - May 1979(PB 301 321)A08

UCB/EERC-79/13 "Cyclic Behavior of Dense Course-Grained Materials in Relation to the Seismic Stability of Dams," by N.G. Banerjee, H.B. Seed and C.K. Chan - June 1979(PB 301 373)A13

UCB/EERC-79/14 "Seismic Behavior of Reinforced Concrete Interior Beam-Column Subassemblages," by S. Viwathanatepa, E.P. Popov and V.V. Bertero - June 1979(PB 301 326)A10

UCB/EERC-79/15 "Optimal Design of Localized Nonlinear Systems with Dual Performance Criteria Under Earthquake Excitations," by M.A. Bhatti - July 1979(PB 80 167 109)A06

UCB/EERC-79/16 "OPTDYN - A General Purpose Optimization Program for Problems with or without Dynamic Constraints," by M.A. Bhatti, E. Polak and K.S. Pister - July 1979(PB 80 167 091)A05

UCB/EERC-79/17 "ANSR-II, Analysis of Nonlinear Structural Response, Users Manual," by D.P. Mondkar and G.H. Powell - July 1979(PB 80 113 301)A05

UCB/EERC-79/18 "Soil Structure Interaction in Different Seismic Environments," A. Gomez-Masso, J. Lysmer, J.-C. Chen and H.B. Seed - August 1979(PB 80 101 520)A04

UCB/EERC-79/19 "ARMA Models for Earthquake Ground Motions," by M.K. Chang, J.W. Kwiatkowski, R.F. Nau, R.M. Oliver and K.S. Pister - July 1979(PB 301 166)A05

UCB/EERC-79/20 "Hysteretic Behavior of Reinforced Concrete Structural Walls," by J.M. Vallenas, V.V. Bertero and E.P. Popov - August 1979(PB 80 165 905)A12

UCB/EERC-79/21 "Studies on High-Frequency Vibrations of Buildings - 1: The Column Effect," by J. Lubliner - August 1979 (PB 80 158 553)A03

UCB/EERC-79/22 "Effects of Generalized Loadings on Bond Reinforcing Bars Embedded in Confined Concrete Blocks," by S. Viwathanatepa, E.P. Popov and V.V. Bertero - August 1979

UCB/EERC-79/23 "Shaking Table Study of Single-Story Masonry Houses, Volume 1: Test Structures 1 and 2," by P. Gülkan, R.L. Mayes and R.W. Clough - Sept. 1979

UCB/EERC-79/24 "Shaking Table Study of Single-Story Masonry Houses, Volume 2: Test Structures 3 and 4," by P. Gülkan, R.L. Mayes and R.W. Clough - Sept. 1979

UCB/EERC-79/25 "Shaking Table Study of Single-Story Masonry Houses, Volume 3: Summary, Conclusions and Recommendations," by R.W. Clough, R.L. Mayes and P. Gülkan - Sept. 1979

UCB/EERC-79/26 "Recommendations for a U.S.-Japan Cooperative Research Program Utilizing Large-Scale Testing Facilities," by U.S.-Japan Planning Group - Sept. 1979(PB 301 407)A06

UCB/EERC-79/27 "Earthquake-Induced Liquefaction Near Lake Amatitlan, Guatemala," by H.B. Seed, I. Arango, C.K. Chan, A. Gomez-Masso and R. Grant de Ascoli - Sept. 1979(NUREG-CR1341)A03

UCB/EERC-79/28 "Infill Panels: Their Influence on Seismic Response of Buildings," by J.W. Axley and V.V. Bertero - Sept. 1979(PB 80 163 371)A10

UCB/EERC-79/29 "3D Truss Bar Element (Type 1) for the ANSR-II Program," by D.P. Mondkar and G.H. Powell - Nov. 1979 (PB 80 169 709)A02

UCB/EERC-79/30 "2D Beam-Column Element (Type 5 - Parallel Element Theory) for the ANSR-II Program," by D.G. Row, G.H. Powell and D.P. Mondkar - Dec. 1979(PB 80 167 224)A03

UCB/EERC-79/31 "3D Beam-Column Element (Type 2 - Parallel Element Theory) for the ANSR-II Program," by A. Riahi, G.H. Powell and D.P. Mondkar - Dec. 1979(PB 80 167 216)A03

UCB/EERC-79/32 "On Response of Structures to Stationary Excitation," by A. Der Kiureghian - Dec. 1979(PB 80166 929)A03

UCB/EERC-79/33 "Undisturbed Sampling and Cyclic Load Testing of Sands," by S. Singh, H.B. Seed and C.K. Chan - Dec. 1979(

UCB/EERC-79/34 "Interaction Effects of Simultaneous Torsional and Compressional Cyclic Loading of Sand," by P.M. Griffin and W.N. Houston - Dec. 1979

UCB/EERC-80/01 "Earthquake Response of Concrete Gravity Dams Including Hydrodynamic and Foundation Interaction Effects," by A.K. Chopra, P. Chakrabarti and S. Gupta - Jan. 1980(AD-A087297)A10

UCB/EERC-80/02 "Rocking Response of Rigid Blocks to Earthquakes," by C.S. Yim, A.K. Chopra and J. Penzien - Jan. 1980 (PB80 166 002)A04

UCB/EERC-80/03 "Optimum Inelastic Design of Seismic-Resistant Reinforced Concrete Frame Structures," by S.W. Zagajeski and V.V. Bertero - Jan. 1980(PB80 164 635)A06

UCB/EERC-80/04 "Effects of Amount and Arrangement of Wall-Panel Reinforcement on Hysteretic Behavior of Reinforced Concrete Walls," by R. Iliya and V.V. Bertero - Feb. 1980(PB81 122 525)A09

UCB/EERC-80/05 "Shaking Table Research on Concrete Dam Models," by A. Niwa and R.W. Clough - Sept. 1980(PB81 122 368)A06

UCB/EERC-80/06 "The Design of Steel Energy-Absorbing Restrainers and their Incorporation into Nuclear Power Plants for Enhanced Safety (Vol 1A): Piping with Energy Absorbing Restrainers: Parameter Study on Small Systems," by G.H. Powell, C. Oughourlian and J. Simons - June 1980

UCB/EERC-80/07 "Inelastic Torsional Response of Structures Subjected to Earthquake Ground Motions," by Y. Yamazaki April 1980(PB81 122 327)A08

UCB/EERC-80/08 "Study of X-Braced Steel Frame Structures Under Earthquake Simulation," by Y. Ghanaat - April 1980 (PB81 122 335)A11

UCB/EERC-80/09 "Hybrid Modelling of Soil-Structure Interaction," by S. Gupta, T.W. Lin, J. Penzien and C.S. Yeh May 1980(PB81 122 319)A07

UCB/EERC-80/10 "General Applicability of a Nonlinear Model of a One Story Steel Frame," by B.I. Sveinsson and H.D. McNiven - May 1980(PB81 124 877)A06

UCB/EERC-80/11 "A Green-Function Method for Wave Interaction with a Submerged Body," by W. Kioka - April 1980 (PB81 122 269)A07

UCB/EERC-80/12 "Hydrodynamic Pressure and Added Mass for Axisymmetric Bodies," by F. Nilrat - May 1980(PB81 122 343)A08

UCB/EERC-80/13 "Treatment of Non-Linear Drag Forces Acting on Offshore Platforms," by B.V. Dao and J. Penzien May 1980(PB81 153 413)A07

UCB/EERC-80/14 "2D Plane/Axisymmetric Solid Element (Type 3 - Elastic or Elastic-Perfectly Plastic) for the ANSR-II Program," by D.P. Mondkar and G.H. Powell - July 1980(PB81 122 350)A03

UCB/EERC-80/15 "A Response Spectrum Method for Random Vibrations," by A. Der Kiureghian - June 1980(PB81 122 301)A03

UCB/EERC-80/16 "Cyclic Inelastic Buckling of Tubular Steel Braces," by V.A. Zayas, E.P. Popov and S.A. Mahin June 1980(PB81 124 885)A10

UCB/EERC-80/17 "Dynamic Response of Simple Arch Dams Including Hydrodynamic Interaction," by C.S. Porter and A.K. Chopra - July 1980(PB81 124 000)A13

UCB/EERC-80/18 "Experimental Testing of a Friction Damped Aseismic Base Isolation System with Fail-Safe Characteristics," by J.M. Kelly, K.E. Beucke and M.S. Skinner - July 1980(PB81 148 595)A04

UCB/EERC-80/19 "The Design of Steel Energy-Absorbing Restrainers and their Incorporation into Nuclear Power Plants for Enhanced Safety (Vol 1B): Stochastic Seismic Analyses of Nuclear Power Plant Structures and Piping Systems Subjected to Multiple Support Excitations," by M.C. Lee and J. Penzien - June 1980

UCB/EERC-80/20 "The Design of Steel Energy-Absorbing Restrainers and their Incorporation into Nuclear Power Plants for Enhanced Safety (Vol 1C): Numerical Method for Dynamic Substructure Analysis," by J.M. Dickens and E.L. Wilson - June 1980

UCB/EERC-80/21 "The Design of Steel Energy-Absorbing Restrainers and their Incorporation into Nuclear Power Plants for Enhanced Safety (Vol 2): Development and Testing of Restraints for Nuclear Piping Systems," by J.M. Kelly and M.S. Skinner - June 1980

UCB/EERC-80/22 "3D Solid Element (Type 4-Elastic or Elastic-Perfectly-Plastic) for the ANSR-II Program," by D.P. Mondkar and G.H. Powell - July 1980(PB81 123 242)A03

UCB/EERC-80/23 "Gap-Friction Element (Type 5) for the ANSR-II Program," by D.P. Mondkar and G.H. Powell - July 1980 (PB81 122 285)A03

UCB/EERC-80/24 "U-Bar Restraint Element (Type 11) for the ANSR-II Program," by C. Oughourlian and G.H. Powell July 1980(PB81 122 293)A03

UCB/EERC-80/25 "Testing of a Natural Rubber Base Isolation System by an Explosively Simulated Earthquake," by J.M. Kelly - August 1980

UCB/EERC-80/26 "Input Identification from Structural Vibrational Response," by Y. Hu - August 1980(PB81 152 308)A05

UCB/EERC-80/27 "Cyclic Inelastic Behavior of Steel Offshore Structures," by V.A. Zayas, S.A. Mahin and E.P. Popov August 1980

UCB/EERC-80/28 "Shaking Table Testing of a Reinforced Concrete Frame with Biaxial Response," by M.G. Oliva October 1980(PB81 154 304)A10

UCB/EERC-80/29 "Dynamic Properties of a Twelve-Story Prefabricated Panel Building," by J.G. Bouwkamp, J.P. Kollegger and R.M. Stephen - October 1980

UCB/EERC-80/30 "Dynamic Properties of an Eight-Story Prefabricated Panel Building," by J.G. Bouwkamp, J.P. Kollegger and R.M. Stephen - October 1980

UCB/EERC-80/31 "Predictive Dynamic Response of Panel Type Structures Under Earthquakes," by J.P. Kollegger and J.G. Bouwkamp - October 1980(PB81 152 316)A04

UCB/EERC-80/32 "The Design of Steel Energy-Absorbing Restrainers and their Incorporation into Nuclear Power Plants for Enhanced Safety (Vol 3): Testing of Commercial Steels in Low-Cycle Torsional Fatigue," by P. Spencer, E.R. Parker, E. Jongewaard and M. Drory

UCB/EERC-80/33 "The Design of Steel Energy-Absorbing Restrainers and their Incorporation into Nuclear Power Plants for Enhanced Safety (Vol 4): Shaking Table Tests of Piping Systems with Energy-Absorbing Restrainers," by S.F. Stiemer and W.G. Godden - Sept. 1980

UCB/EERC-80/34 "The Design of Steel Energy-Absorbing Restrainers and their Incorporation into Nuclear Power Plants for Enhanced Safety (Vol 5): Summary Report," by P. Spencer

UCB/EERC-80/35 "Experimental Testing of an Energy-Absorbing Base Isolation System," by J.M. Kelly, M.S. Skinner and K.E. Beucke - October 1980(PB81 154 072)A04

UCB/EERC-80/36 "Simulating and Analyzing Artificial Non-Stationary Earthquake Ground Motions," by R.F. Nau, R.M. Oliver and K.S. Pister - October 1980(PB81 153 397)A04

UCB/EERC-80/37 "Earthquake Engineering at Berkeley - 1980," - Sept. 1980

UCB/EERC-80/38 "Inelastic Seismic Analysis of Large Panel Buildings," by V. Schricker and G.H. Powell - Sept. 1980 (PB81 154 338)A13

UCB/EERC-80/39 "Dynamic Response of Embankment, Concrete-Gravity and Arch Dams Including Hydrodynamic Interaction," by J.F. Hall and A.K. Chopra - October 1980(PB81 152 324)A11

UCB/EERC-80/40 "Inelastic Buckling of Steel Struts Under Cyclic Load Reversal," by R.G. Black, W.A. Wenger and E.P. Popov - October 1980(PB81 154 312)A08

UCB/EERC-80/41 "Influence of Site Characteristics on Building Damage During the October 3, 1974 Lima Earthquake," by P. Repetto, I. Arango and H.B. Seed - Sept. 1980(PB81 161 739)A05

UCB/EERC-80/42 "Evaluation of a Shaking Table Test Program on Response Behavior of a Two Story Reinforced Concrete Frame," by J.M. Blondet, R.W. Clough and S.A. Mahin

UCB/EERC-80/43 "Modelling of Soil-Structure Interaction by Finite and Infinite Elements," by F. Medina

UCB/EERC-81/01 "Control of Seismic Response of Piping Systems and Other Structures by Base Isolation," edited by J.M. Kelly - 1981 (PB81 200 735)

UCB/EERC-81/02 "OPTNSR - An Interactive Software System for Optimal Design of Statically and Dynamically Loaded Structures with Nonlinear Response," by M.A. Bhatti, V. Ciampi and K.S. Pister - 1981

UCB/EERC-81/03 "Analysis of Local Variations in Free Field Seismic Ground Motion," by J.-C. Chen, J. Lysmer and H.B. Seed 1981

UCB/EERC-81/04 "Inelastic Offshore Platforms for Seismic Loading," by V.A. Zayas, P. Shum, B. Shing, S.A. Mahin and E.P. Popov 1981

UCB/EERC-81/05 "Dynamic Response of Light Equipment in Structures," by A. Der Kiureghian, J.L. Sackman and B. Nour-Omid - 1981

UCB/EERC-81/06 "Preliminary Experimental Investigation of a Broad Base Liquid Storage Tank," by J.G. Bouwkamp, J.P. Kollegger and R.M. Stephen - 1981